POLYMERS FROM CELLULOSE FOR ENCAPSULATION

A THESIS
SUBMITTED TO THE
UNIVERSITY OF POONA
FOR THE DEGREE OF
DOCTOR OF PHILOSOPHY
(IN CHEMISTRY)

BY

Mrs. ARUNA NARAYAN BOTE

M. Sc.

DIVISION OF POLYMER CHEMISTRY
NATIONAL CHEMICAL LABORATORY
PUNE - 411 008 (INDIA)

FEBRUARY 1993

DEDICATED

TO

MY MOTHER

DECLARATION

Certified that the work incorporated in the thesis "**Polymers from Cellulose for Encapsulation**" submitted by **Mrs. A.N. Bote** for the degree of Doctor of Philosophy, was carried out by the candidate under my supervision in the National Chemical Laboratory, Pune. Such material as has been obtained from other sources has been duly acknowledged in the thesis.

February, 1993.

(V.M. Nadkarni)
Reserach Guide

Head
Chemical Engineering Division
National Chemical Laboratory,
Pune—411008

ACKNOWLEDGEMENT

It is with a deep sense of gratitude that I wish to express my sincere thanks to Dr. V.M. Nadkarni, Dy. Director and Head, Chemical Engineering Division, National Chemical Laboratory, Pune, for his invaluable guidance, inspiration and encouragement during the course of this investigation.

I am highly grateful to Mr. N. Rajagopalan, Scientist, Division of Polymer Chemistry, NCL, Pune for his constant help, valuable suggestions and useful discussions.

I am also thankful to Dr. P.G. Sharma and Dr. S. Gundiah for their encouragement and help during the course of this investigation.

I thank Dr. S. Ganapathy and Dr. P.R. Rajamohan for many useful discussions and NMR measurements.

Assistance rendered by Dr. B.B. Idage, Dr.(Mrs.) S.B. Idage, Mrs. S.D. Advanthaya, Mrs. U D. Phalgune and Mr. Vinod De from time to time is gratefully acknowledged.

I am highly indebted to Dr. S. Sivaram, Head, Division of Polymer Chemistry, for providing all necessary facilities and unflinching support during the work.

Last but not the least, I express my sincere thanks to the Director, National Chemical Laboratory, Pune, for his kind permission to submit this work in the form of a thesis.

A.N.Bote

February, 1993.

(Mrs. A.N. Bote)

CONTENTS

GLOSSARY

A : Total concentration of active agent per unit volume

A_p : Available surface area for diffusion of active agent through pores

A_s : Available surface area for diffusion of active agent through polymer

B_o : Magnetic field

B_1 : r-f magnetic field

C : Concentration

C_a : Solubility of active agent in eluting solvent

C_e : Concentration of released active agent in eluting medium

C_i : Concentration of dissolved active agent in penetrant

C_o : Active agent loading in the erodible matrix

C_p : Saturation solubility of active agent in polymer

D : Diffusion coefficient

D_a : Diffusion coefficient of active agent in the eluting solvent

D_s : Diffusion coefficient of active agent in the polymer

$D_{s,s}$: Diffusion of coefficient of active agent in the swollen polymer

D_{iw} : Diffusion of coefficient of active agent in water

D_{eff} : Effective diffusion coefficient of active agent in penetrant filled pores

D_{ip} : Diffusion coefficient of active agent through swollen polymer

h : Thickness

I : Spin number

k : Release rate constant

k_s : Swelling rate constant

K : Partition coefficient

K_e : Erosion rate constant

M_t : Amount of active agent released per unit area at time t

M_c : Molecular weight between crosslinks

M_e : Minimum effective level of active agent

M_∞ : The amount of active agent present in the matrix at time O

$M_{t,p}$: Amount of active agent released through pores at time t

$M_{t,s}$: Amount of active agent released through polymer at time t

(M_t/M_∞) : Fractional up take of penetrant by polymer

(M_t/M_∞) : Fraction of active agent released

n : Diffusional exponent

r_o : Outer radius of spherical microcapsule

r_1 : Inner radius of spherical microcapsule

S : Surface area

t : time

t_e : Effective duration of time

T_1 : Spin-lattice relaxation time

T_2 : Spin-spin relaxation time

x : Distance

ϵ : Porosity

τ : Tortuosity

λ : Characteristic relaxation time

θ : Characteristic diffusion time

ν : Larmor frequency

ΔE : Energy difference between magnetic energy levels

CHAPTER - I

INTRODUCTION

1.1. GENERAL INTRODUCTION

Controlled Release technique has rapidly emerged over the past decade as a new interdisciplinary science that offers novel approaches to the delivery of bioactive agents. Inspite of the emergence of many novel biologically active compounds applied successfully in many different disciplines, it has become clear that significant improvements in their efficacy can be made by optimizing the delivery. Such optimization can often be achieved by manipulation of the site and timing of action of the agent, generally referred to as controlled delivery or controlled release. Along with the invention of a constant stream of new and more active crop protection agents, were perceived problems of toxicity, ground water contamination and damage to desirable aquatic life forms. For these reasons several excellent pesticides have lost approval by Government agencies.[1] This encouraged the scientists to develop safer, biologically degradable agrochemicals as well as formulations to avoid off-target contamination and maximise performance. An ideal pesticide is one which is safe, i.e. would have low toxicity to nontarget organisms including humans, has high efficiency i.e. should show good initial and residual efficacy at low dosage and is cost effective. However, it is difficult to achieve a pesticide with all the desirable characteristics. Thus, the chemical manufacturers' attempt will be to optimize the usefulness of pesticide, through performance i.e. by reducing misuse or over use and thereby improving safety to the crop environment as well as users. This

can be achieved by use of controlled release technology.

Controlled release (CR) can be defined as a method or technique by which an active agent is delivered to an intended target at a concentration and for a duration designed to accomplish the desired effect while avoiding other responses or side effects this might cause.

Controlled release formulations (CRF) were first used in the agricultural industries for low molecular weight fertilizers, pesticides and antifoulants in the 1950s[2]. In the 1960s these approaches extended into the medicinal field[2]. By the mid 1970s, controlled release formulations for large molecular weight drugs (e.g. polypeptides)[2] were designed. Developments in this field have been numerous in the past decade. This is evidenced by the number of publications, patents and actual applications emerging in the field as well as establishment of a scientific forum such as Controlled Release Society to meet the professional needs of scientists working in this area[3-12]. This technology has application in diverse fields including medicine, agriculture and biotechnology[9].

1.2 Rationale for controlled release

Increasing awareness of excessive toxicity and some times ineffectiveness of the drugs and agricultural chemicals, when administered or applied by conventional means has led to greater attention being directed towards controlled release technology.

The process of molecular diffusion through polymers and synthetic membranes has been used as an effective and reliable

means of attaining not only the controlled release of drugs and pharmacologically active agents, but also of fertilizers, pesticides and herbicides.

In drug delivery, pharmaco kinetics is an important consideration because target tissues are seldom directly accessible and drugs must be transported from the portal of entry in the body through a variety of biological interfaces to reach the desired receptor site. During the transport process, the drug can undergo severe biochemical degradation and thereby produce a delivery pattern at the receptor site that differs markedly from the pattern of drug release into the system. For agricultural chemicals, concentration, persistence and transport in the soil are decreased by biodegradation, chemical degradation, photolysis, evaporation, surface run off and ground water leaching.

1.2.1 Conventional delivery vs controlled release of active agents

1.2.1.1 Drug Delivery

In the conventional treatment, drugs are administered at periodic intervals by ingestion of pills and liquids or by injection. These are then distributed throughout the body. In such cases the concentration of the drug in the blood initially rises to the "therapeutic level" which is the level at which the concentration of the drug in the plasma is sufficient to produce the desired therapeutic effect. Above a certain level the drug is toxic and can cause side effects. Subsequently, the drug concentration in the blood remains within the range for quite some

time. Finally the drug concentration drops below the therapeutic range. The drug is then ineffective (Fig.1.1). The cycle repeats when a new dose is administered.

A more desirable way would be to release the drug in such a way that its concentration is maintained within the therapeutic limits for extended time and it is released directly to the target.

In Fig.1.1, the ideal controlled release rate (d) is illustrated; i.e. a constant concentration, which is effective but not toxic, is maintained for the desired time. Advantages of this system for therapeutic agents are : (1) reproducible and prolonged constant delivery rate (2) reduction of frequency of dosing and (3) reduced side effects because the dose does not exceed the toxic level.

1.2.1.2 Pesticide delivery

Conventionally insecticides, fertilizers and other pesticides are applied periodically to crops by broad casting, spraying etc. Thus, initially very high and possibly toxic concentrations ensue with subsequent rapid diminution below the minimum effective level. The agricultural chemicals must be biodegradable or non-persistent in the environment which result in the need of repeated application to maintain control.

The principal advantage of CRF is that they allow much less pesticide to be used more effectively for a given time interval, specifically designed to face severe environmental degradation process. In most instances the rate of removal of pesticide

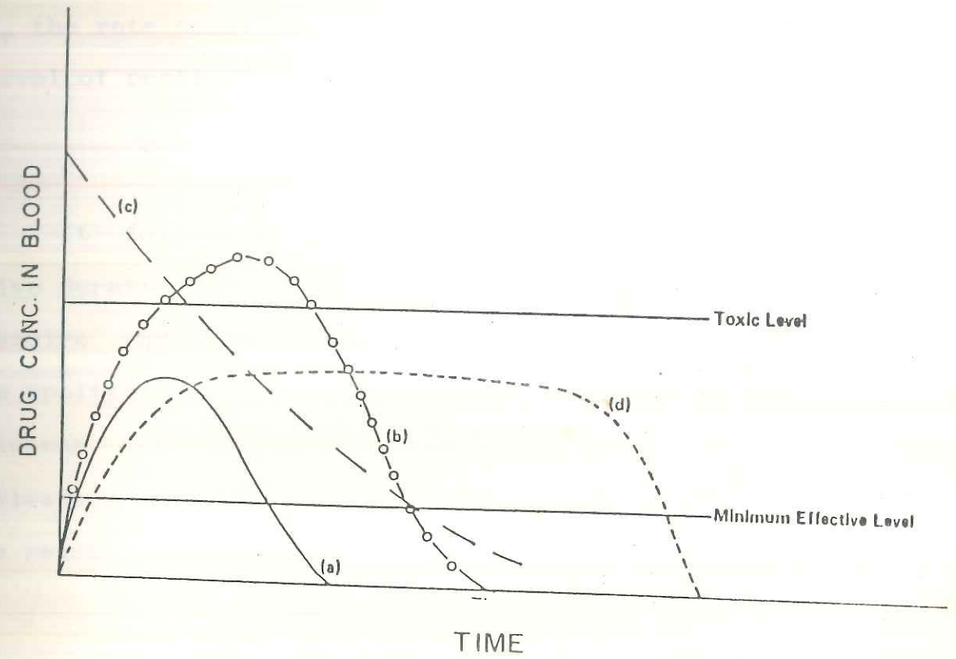

FIG. 1.1 : TYPICAL DRUG LEVEL VERSUS TIME PROFILE .

ⓐ STANDARD ORAL DOSE

ⓑ ORAL OVER DOSE

ⓒ i.v. INJECTION

ⓓ CONTROLLED RELEASE IDEAL DOSE

follows first order kinetics. Thus if M_e, is the minimum effective level: M_∞, the amount of agent applied initially and k_r the rate constant, then t_e, the time during which an effective level of pesticide is present after a single application,would be

$$t_e = \frac{1}{k_r} \ln \frac{M_\infty}{M_e} \qquad .....(1)$$

It follows from equation (1) that an increase in the effective duration of action of conventionally applied pesticide would require that an exponentially greater quantity of the pesticide be applied. If however, the pesticide could be maintained at the minimum effective level by a continuous supply from controlled release system, then optimum performance of the insecticide would be realised and this duration of action. t_e would be

$$t_e = \frac{M_\infty - M_e}{k_d M_e} \qquad .....(2)$$

where, k_d is the rate constant for pesticide delivery from the controlled release device.

Fig.1.2 shows the relationship between the level of application and the duration of action for conventional formulations with first order release rate (equation 2). For Fig.1.2, assumption is made that the half life of the pesticide is 15 days and the minimum effective level is 1g/acre. The area between curves A and B represents the amount of pesticide that is being wasted. For a short duration of effectiveness e.g. one week or less, the conventional method is adequately efficient. As the duration of effectiveness increases, the efficiency of conventional system

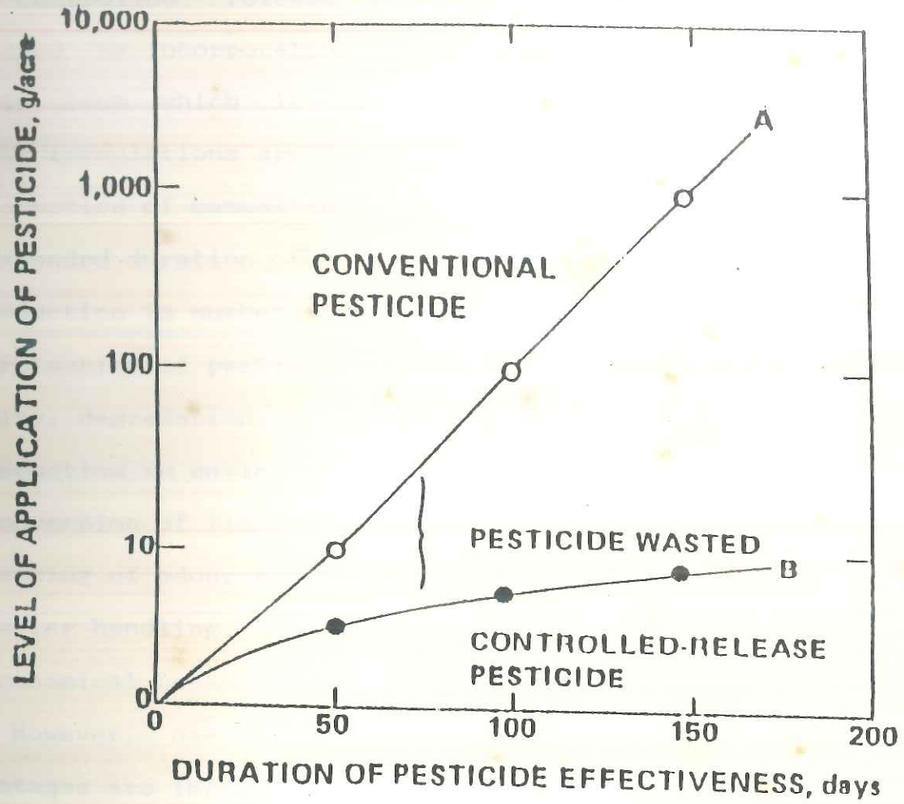

FIG 1·2: RELATIONSHIP BETWEEN THE LEVEL OF APPLICATION AND DURATION OF ACTION FOR CONVENTIONAL AND CONTROLLED RELEASE FORMULATIONS.

decreases.

1.3 Advantages

Controlled release pesticide formulation is generally obtained by incorporating an active agent in a suitable polymer matrix from which it is slowly released. The advantages of CR formulations are :

1. Reduction of mammalian toxicity of highly toxic substances.
2. Extended duration of activity.
3. Reduction in number of applications.
4. Protection of pesticide from environmental forces, phytotoxicity, degradation, leaching, evaporation, flammability etc.
5. Reduction in environmental pollution.
6. Conversion of liquids to solids and flowable powders.
7. Masking of odour and taste of bitter material.
8. Easier handling.
9. Economical because less active material is needed.

However, careful study shows some limitations though the advantages are impressive.

1.4 Limitations

1. Cost of controlled release preparation and processing may be substantially higher than the cost of standard formulations.
2. Fate of the polymer matrix and its effect on environment.
3. Fate of polymer additives, such as plasticizers, stabilizers, antioxidants, fillers etc.
4. Environmental impact of the polymer degradation products following heat, hydrolysis, oxidation, solar radiation

and biological degradation.

5. Cost, time and probability of success in securing government registration of the product, if this is required.

1.5 Design criteria

A controlled release system is a combination of bioactive agent and excipient, commonly a polymeric material, arranged to allow delivery of the bioactive agent to the target at controlled rates over a specified period of time. In selecting the polymer matrix, the following design criteria are important.

1. Molecular weight, glass transition temperature (Tg) and chemical functionality of the polymer must allow proper diffusion and release of the specific agent.
2. Polymer functional groups should not react chemically with the active agent.
3. The polymer and its degradation products must be non-toxic to the environment and in medical applications, nontoxic or antagonistic to the host.
4. The polymer must not decompose in storage and generally not during the useful life of the device.
5. The polymer should be easily manufactured or fabricated into the desired product and should allow incorporation of large amounts of active agent in the product without excessively deteriorating its mechanical properties.

Other factors that must be considered by designers of controlled release systems are :

1. The optimum level of the agent necessary for the desired

biological response.

2. The mechanisms and rates of all agent removal systems operating in a given biological environments.
3. The influence of the biological environment on the mechanism and bioactive agent release kinetics.
4. Inherent restrictions on the physico-chemical properties of delivery materials dictated by particular applications.

A useful classification of controlled release polymeric system is based on the mechanism controlling the release of the incorporated drug.

The rapidly growing interest in the use of biodegradable polymers[13-15] as carrier systems for the controlled release of various bioactive agents is due to advance in polymer science leading to polymers of tailor made properties.

Apart from the proceedings of annual symposia on CR of bioactive materials, being published every year since 1974, CR pesticides formulations have been well documented in the literature[7,9,10].

1.6 Classification

Controlled release systems can be classified according to their major rate controlling mechanism (Fig.1.3) which broadly divides the systems as follows :

1. Diffusion controlled
   a) Reservoirs (Membranes)
   b) Matrices (Monoliths)
2. Chemically controlled

DIFFUSION CONTROLLED

Diffusion-controlled reservoir system

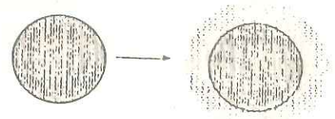

Diffusion-controlled matrix system

CHEMICALLY CONTROLLED

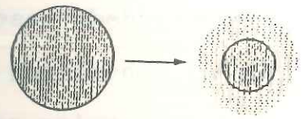

Biodegradable system

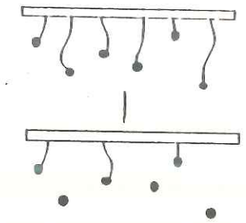

Pendant chain system

SOLVENT ACTIVATED

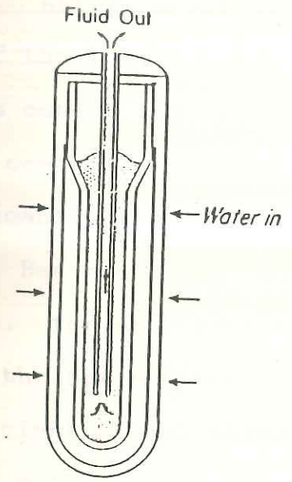

MINI OSMOTIC PUMP

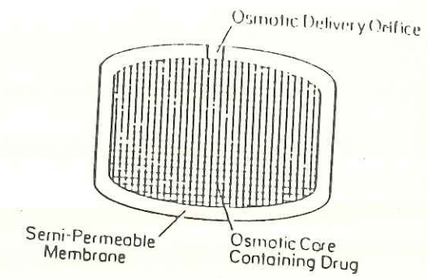

ELEMENTARY OSMOTIC PUMP

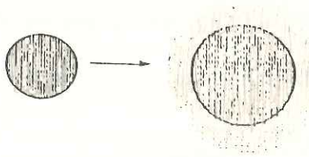

Swelling-controlled system

FIG. 1·3 : CLASSIFICATION OF CONTROLLED RELEASE SYSTEMS ACCORDING TO MECHANISM OF RELEASE

a) Erosion

b) Pendant chain

3. Solvent activated

a) Osmotic pressure

b) Swelling

4. Magnetically controlled

The release behaviour of bioactive agent is the result of diffusional phenomenon in the polymer and mass transfer limitations at the polymer/liquid interface. Therefore, design of controlled release systems requires understanding of mechanism of active agent diffusion through polymeric materials [16]. Irrespective of the CR system, the diffusion coefficient of the bioactive agent through the polymer depends on structural and morphological parameters[17,18]. Active agent diffusivity may also depend on the concentration of the active agent in the polymer [19].

1.6.1 Diffusion controlled systems

Diffusion controlled systems are the most widely used for delivery of bioactive agent and can be divided into two main categories : a) Reservoir and b) Matrix systems. Two cases of diffusion exist, for each type of system. Diffusion occurs either through the space between the macromolecular chains with diffusion coefficient D_{ip} or through a porous network filled with aqueous medium with an effective diffusion coefficient D_{eff} incorporating both porosity and tortuosity. Release of active agent through macromolecular chains may be described in terms of the Fickian diffusion theory by equation :

$$J = dM/dt = - D\, dC/dx \qquad .....(3)$$

where, dM/dt is the rate of active agent transfer across a plane of unit area,

dC/dx is the change in concentration (C) with respect to distance (x) and

D is the diffusion coefficient.

When the law is applied to controlled release device as shown in equation (4) it is found that diffusion of active agent depends on five factors [20].

$$dM_t/dt = \frac{S}{h} D_s (C_p - KC_e) \qquad .....(4)$$

Two factors depend upon the geometry (or dimensions) of the device such as S - surface area of the membrane and h - thickness through which diffusion occurs. Other three factors involve active agent-polymer interactions such as diffusion of active agent in the polymer (D_s), saturation solubility of active agent in the polymer C_p and partition coefficient (K) of active agent between polymer and medium surrounding the device, C_e is the concentration of released active agent in the environment.

1.6.1.1 Reservoir system

Reservoir system consists of a thin inert membrane enclosing a core of bioactive agent. To maintain constant release, constant active agent concentration is maintained in the internal phase by placing an excess solid active agent inside the reservoir system which will maintain a saturated solution of active agent even as diffusion progresses. Application of Ficks

law predicts that a steady state will be established or reservoir system will exhibit nearly zero order or time independent diffusional active agent release behaviour.

Diffusional release problems observed with reservoir systems include time lag and burst effect. The release rate equations (5) and (6) are derived for slab or laminate device and for the sphere or microcapsule respectively[21,22].

$$dM_t/dt = 2SD_s (C_p - C_e)/h \qquad .....(5)$$

$$dM_t/dt = 4\pi r_o r_i D_s(C_p - C_e K)/(r_o - r_i) \qquad .....(6)$$

where, r_o is the radius of the sphere (microcapsule) and

$(r_o - r_i)$ is the thickness of a capsule wall.

Thus, rate of release is independent of time, giving 'zero order' release kinetics. Microcapsules are made with very thin walls and very often the polymer phase is not homogeneous, but cracks and pores are produced. In such cases microcapsules are found to follow '$\sqrt{t}$ order' release kinetics.

1.6.1.2 Monolith systems

Monolith systems are also known as matrix systems in which the active agent, either in dissolved or dispersed form is incorporated in the polymer phase[23]. Therefore, the solubility of the active agent in the polymer becomes a controlling factor in the release from these systems. Based on application of Ficks 2nd law :

$$\delta C/\delta t = D\, \delta^2 C/\delta x^2 \qquad .....(7)$$

on a diffusion dissolution model, release of an active agent from a non-porous slab, monolith is given by a Higuchi equation[24]

where, A >> C_p and pseudosteady state assumption is made.

$$M_t = [2C_pD_s(A-C_p/2)t]^{1/2} \quad .....(8)$$

where, M_t is the amount of agent released per unit area at time t and

A is the total concentration of agent per unit volume in the matrix.

Higuchi equation for a porous monolith, where release occurs through connecting capillaries or pores, is given by,

$$M_t = [C_aD_a\epsilon/\tau(2A - C_a)t]^{1/2} \quad .....(9)$$

where, C_a and D_a are solubility and diffusion coefficient of active agent in eluting solvent respectively and

ϵ and τ are porosity and tortuosity of the matrix respectively.

Higuchi equation can be modified for other geometries like cylinder and sphere[23]. When A --> C_p, Higuchi equation gives a result 11.3% smaller than the exact solution. Lee[25] has presented a simple analytical solution which is uniformly valid over all A/C_p values.

$$M_t = \frac{(1 + H)}{\sqrt{3H}} (C_p\sqrt{D_st}) \quad .....(10)$$

where, $H = 5(A/C_p) - 4 + \sqrt{(A/C_p)^2 - 1}$

1.6.2 Chemically controlled systems

In these systems the release of active agent is controlled by the rate of chemical reaction. The systems can be divided into two categories :

a) Bioerodible Systems,

b) Pendant Chain Systems.

1.6.2.1 Bioerodible systems

In these systems, the active agent is dispersed throughout the matrix and is released by diffusion from the polymer or released as the matrix is eroded, or by a combination of both[26-28]. Thus, the rate of release depends on the rate of the reaction which breaks down the matrix. Erosion of the polymer matrix could occur either by a) cleavage of the crosslinks or b) conversion of an insoluble polymer into soluble oligomers or c) conversion of initially insoluble polymer into a soluble polymer.

The erosion of the polymer matrix could be either i) bulk erosion or ii) surface erosion. In the bulk erosion, the erosion of the polymer takes place throughout the matrix simultaneously. The release under this condition is governed by diffusion as well as erosion. Therefore, these types of systems generally do not exhibit `zero order' kinetics.

In surface erosion, the cleavage of the polymer is restricted to the surface of the device and if the surface area of the device stays constant while it is eroding, the release of the agent will be `zero order', expressed by equation.

$$M_t = K_e C_o S t \qquad .....(11)$$

where, K_e is the erosion rate constant,

S is the surface area exposed to the environment and

C_o is the active agent loading in the erodible matrix.

As the surface area of the flat film or slab geometry does

not change as erosion occurs, the release rate of agent remains constant until the device ultimately disappears. But such type of zero order release is not possible for a spherical erodible device and the release decreases slowly with time.

1.6.2.2 Pendant chain systems

In these systems, the active agent is chemically linked to the polymer backbone through the pendant chain and is released by hydrolytic[29,30] or enzymatic cleavage[31]. Most common linkages are ester, anhydride and acetal[32]. The active agent itself can be attached directly to the polymer or it can be attached via a spacer group. The spacer group may be used to affect the rate of release and hydrophilicity of the system.

To achieve near constant release, the cleavage of active agent from the polymer must be the rate limiting step. If the rate of diffusion of the cleaving agent into the polymer matrix and the rate of diffusion of the active agent through the polymer matrix are much faster than the rate of cleavage, the release rate is limited by the chemical reaction. Thus, the release rate is constant only if the thermodynamic activity of the bound active agent is constant with time, and the cleaving agent (e.g. acid, base, enzyme) is present in a certain volume.

1.6.3 Solvent activated systems

In these systems, the active agent is dispersed in the polymer device and the permeation of the solvent brings about the release of active agent. The release could be either a) osmotically controlled or b) swelling controlled.

1.6.3.1 Osmotically controlled systems[33-35]

The simplest osmotic device consists of a core containing bioactive agent which is surrounded by a semipermeable polymer film or membrane with an orifice, for the delivery of the active agent. If placed in contact with water or an appropriate biological fluid, the fluid is transported through the membrane towards the core, resulting in release of equal volume of the active agent solution through the orifice. This solution is usually at saturation, although more dilute solutions may be used.

Three types of osmotically controlled devices have received attention in recent years. A mini osmotic pump consists of a layered membrane in the form of a tube and flow moderator, which is inserted into the system, after active agent loading. The second system consists of an elementary osmotic pump with delivery rate usually adjusted by varying the thickness of the semipermeable membrane. Third one is matrix type osmotically active system, where the active agent is uniformly suspended in a polymer.

However, such systems have not generally released active agent at zero order rates.

1.6.3.2 Swelling controlled systems

Swelling controlled systems describe those formulations, where the active agent release is actually controlled by the swelling phenomenon[36] by the relative position and velocity of the swelling interface[37,38]. Initially there is no diffusion of solute through the glassy polymer (B) (Fig.1.4) but when placed

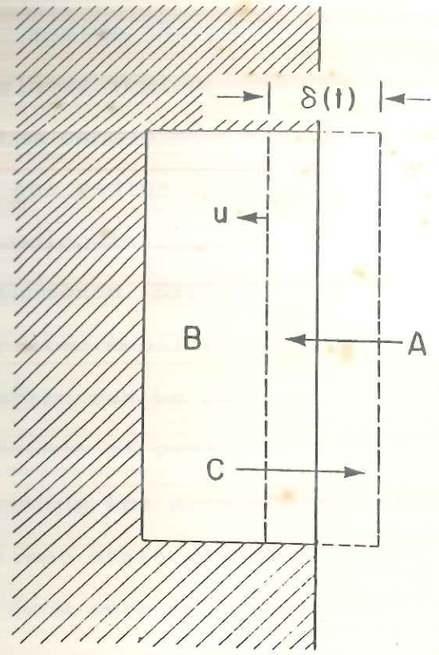

FIG. 1-4 : SWELLING CONTROLLED SYSTEM FOR THE RELEASE OF DRUGS. IT CONSISTS OF A POLYMER (B) CONTAINING A MOLECULARLY DISPERSED DRUG (C) AND PLACED IN CONTACT WITH A SWELLING AGENT (A).

into a suitable medium (A), molecules of penetrant begin to diffuse into the glassy region. Entrance of penetrant molecules in the glassy system causes stresses, which are then accommodated by an increase in the radius of gyration and end to end distance of the polymer molecule (Chapter III, Fig. 3.3). This is a relaxational phenomenon described by characteristic time, favoured due to greater mobility of the polymer chains. Increase in radius of gyration can be seen macroscopically as swelling. Thus, with the entrance of penetrant, two fronts are established; i.e. a front separating the glassy and rubbery state which moves inwards towards glassy state with velocity u and a front separating rubbery state from pure penetrant which moves outwards.

The swollen region has thickness which changes with time denoted by $\delta(t)$. The diffusion coefficient of the active agent (C) is much higher in the rubbery region than in the glassy region, so that as the polymer begins to swell, the active agent molecules begin to move out of the system by diffusion through the rubbery layer. The rate of diffusion of the active agent out of the system is dependant on macromolecular relaxation occurring in the polymer near the glass transition temperature and the rate of diffusion through the relaxed rubbery polymer[39,40]. Similar situation is observed in the active agent release from a hydrogel or hydrophilic polymer matrix. In swellable system, the penetrant can be a biological fluid, water or organic solvent which is thermodynamically compatible with the polymer, whereas hydrogels are water swollen crosslinked polymeric structures[41].

In the absence of crosslinks or molecular entanglements, the polymer will eventually dissolve. Dissolution of the polymer may be avoided if one works with semicrystalline, uncrosslinked or with amorphous, slightly crosslinked polymers. In this case the crystallites and crosslinks act as permanent junctions preventing dissolution. These systems are called swellable, nonerodible release systems. Despite the existence of permanent junctions, dissolution of the polymer may occur due to chemical degradation (such as hydrolysis) or due to biodegradation. In these systems, the active agent is originally dissolved or dispersed in polymer solution. Upon solvent evaporation, a solvent free glassy, polymeric matrix is obtained with active agent uniformly dispersed in it. Similar systems may be obtained by compression of particles or solvent free polymer and active agent, thus forming porous swellable systems or by physical entrapment by dispersing in polymer and then crosslinking the polymer. The problem of penetrant transport into the polymer and the associated problem of diffusional active agent release from the polymer is called Stefan or moving boundary problem[42] which arises due to the existence of moving surfaces separating the phases of the material. Lee[43] obtained the release rate equations from a swellable polymer slab containing dissolved or dispersed active agent where the release of active agent from hydrogel was interpreted in terms of time dependent solute diffusion coefficient which takes into account the time dependent, penetrant induced polymer relaxation.

Active agent release data from a glassy polymeric slab, under counter current simultaneous diffusion of a swelling agent, may be fitted to :

$$M_t/M\infty = k\ t^n \qquad .....(12)$$

as proposed by Ritger and Peppas[44] through physical models.

Sigot-Chicq and Peppas[45] have described a physical model for the transport behaviour of an active agent through porous swellable system. The active agent transport may be considered as the composite of the two mechanisms, diffusion in the pores and diffusion through the polymer proper. Diffusion in the pores is prominent at early times, before much swelling occurs, whereas the mechanism of diffusion through the polymer proper appears much later in the release process. For the diffusion of active agent in the pores, the release rate, $dM_{t,p}/dt$ may be expressed by a simple Fickian expression according to equation.

$$\frac{dM_{t,p}}{dt} = A_p D_{iw} \frac{\epsilon}{\tau} \frac{dc_i}{dx} \qquad .....(13)$$

where, D_{iw} is active agent diffusion coefficient through water (penetrant),

c_i is the concentration of dissolved active agent in penetrant,

x is position,

ϵ is the porosity (void fraction),

τ is the tortuosity, and

A_p is the available surface area for pore diffusion.

$A_p = \epsilon^{2/3} A$, where, A is the total surface area of a device

(system). Upon swelling of the polymer, additional active agent transport occurs through the swollen polymer proper. The release rate $dM_{t,s}/dt$ is given by equation

$$\frac{dM_{t,s}}{dt} = A_s D_{ip} \frac{dc_i}{dx} \qquad .....(14)$$

where, D_{ip} is the active agent diffusion coefficient through the swollen (or continuously swelling) polymer.

The use of dc_i/dx in equation (14) is the same gradient as in equation (13). A_s is the surface area for polymer diffusion, which may be expressed as:

$$A_s = (1 - \epsilon^{2/3})A \qquad .....(15)$$

The overall release rate is the summation of the two rate equations (13) and (14).

The importance of macromolecular relaxation in active agent diffusion is associated with two dimensionless numbers, the diffusional Deborah number De[39,40] and the swelling interface number S_W[18,39,42,46]. The ratio of the characteristic relaxation time λ to the characteristic diffusion time Θ is called the diffusional Deborah number :

$$D_e = \frac{\lambda}{\Theta} \qquad .....(16)$$

where, λ and Θ are function of temperature and penetrant.

Although macromolecular relaxations are associated with counter current diffusion of incorporated active agent, it is the relative mobility of the diffusing active agent with respect to the penetrating swelling agent that controls the mechanism of active agent release. This condition is analyzed by another

dimensionless swelling interface number S_W

$$S_W = u\delta/D_{s,s} \qquad .....(17)$$

where, u is the velocity of the penetrant front,

δ is the thickness of the swollen region, through which active agent diffusion occurs and

$D_{s,s}$ is the diffusion coefficient of the active agent in the swollen region.

Dimensionless Deborah number and swelling interface number may be used as a sufficient and necessary criterion for the selection of active agent/polymer/penetrant systems, which exhibit zero order release[42,47].

1.6.3.2a Swelling behaviour

An integral part of the swellable systems is their swelling behaviour in solvent, thermodynamically compatible with it, since during their use they must be brought in contact with the environmental fluid to yield final swollen rubbery structure. The degree to which the polymer will swell depends on the interactions between polymer and its environment.

The thermodynamic swelling force is counterbalanced by the retractive force of the crosslinked structure[48]. Equilibrium is attained in a particular solvent at a particular temperature, when the two forces become equal.

1.6.3.2b Structural characteristics

The parameter that describes the basic structure of a swellable system is the molecular weight between crosslinks, M_c[18,49] which defines the average molecular size between two

consecutive junctions regardless of the nature of those junctions. Additional parameters of importance in the structural analysis of hydrogels are the cross-link density and the effective number of crosslinks per original chain[49].

1.6.3.2c Choice of swellable polymers and their applications in controlled release formulations

Swelling controlled systems have received significant attention in the last three decades because of their exceptional promise in biomedical applications, especially hydrogels. The best approach for developing a swelling controlled system with desired characteristics is to correlate the macromolecular structure of the polymer with the swelling and mechanical characteristics desired.

One of the most widely used hydrogel is water swollen, cross-linked poly(2-hydroxylethyl methacrylate) (PHEMA) which was introduced as a biological material by Wichterle and Lim[50]. Other biocompatible hydrogels including polyacrylamide, copolymer of HEMA with acrylamide and methacrylamide have been evaluated for swelling and mechanical behaviour by Dusek and Janacek[51]. The extreme swelling behaviour of some PAM gels has been attributed to the hydrolysis of some of the acrylamide groups to acrylic acid.

For the polymers with ionizable groups, the degree of ionization and the nature of the medium surrounding the polymer are extremely important. Some variables which affect the final polymer behaviour are the pH of the polymerisation reaction[52],

the degree of ionization of the polymer[53,54] and the concentration of electrolyte in the swelling medium[55]. Poly (N-vinyl pyrrolidone) (PNVP) shows a very high water content at equilibrium swelling, while polymethyl methacrylate (PMMA) shows almost no swelling due to hydrophobic nature of methyl methacrylate (MMA). Copolymer of MMA and HEMA have a lower degree of swelling than pure PHEMA[56]. Effect of molecular weight, sample thickness and polymer composition on the swelling of and active agent transport in PMMA and P(HEMA-CO-MMA)[57] have been studied. Some examples of highly swollen hydrogels used in controlled drug delivery systems and other biological applications are cellulose derivatives, poly(vinyl alcohol) (PVA), PNVP and poly(ethylene glycol). Moderately and poorly swollen hydrogels are those of PHEMA and many of its derivatives. In order to achieve desired swelling properties one may copolymerise a basic hydrophilic monomer. Yasuda *et al*[58] have discussed swelling controlled release systems based on penetrant free crosslinked (PVA) where non Fickian active agent release with n as high as 0.76 was obtained. Possible modification of the solubility of the polymer may lead to a swelling controlled system with zero order release.

Knowledge of the swelling characteristics of a polymer is of utmost importance in biomedical and pharmaceutical applications, since the equilibrium degree of swelling influences the active agent diffusion coefficient through these hydrogels.

One of the earliest investigations with swelling controlled release system is attributed to Good[59] who studied the release of

tripelennamine hydrochloride from penetrant free, glassy, cross-linked sheets of poly(2-hydroxyethyl methacrylate) (PHEMA) and the kinetic study indicated zero order release.

Demonstration of the potential of swelling controlled systems to yield zero order release kinetic behaviour was offered by Hopfenberg and Hsu[36]. Sudan red IV dye was released from polystyrene in contact with n-hexane over a period of 60 h at constant rates. Use of the same technique for the release of various bioactive agents from ethylene-vinyl alcohol (EVA) copolymers into water did not produce zero order release[60], but a non-Fickian active agent release.

EVA copolymers have been used as carriers for release of bioactive agents, which are prepared by hydrolysis of ethylene vinyl acetate (EVAc) copolymers. Depending on the conditions of hydrolysis and the initial molar ratio of the two monomers in the copolymer, copolymers of varying hydrophilicity can be prepared. High or low temperature annealing has been used to introduce controlled degree of crystallinity as a means of controlling degree of hydrophilicity[61]. Other parameters affecting the equilibrium degree of swelling of these copolymers include the molecular weight, microstructure, degree of crosslinking and method of casting the films. Dynamic and equilibrium swelling studies of different EVA copolymers in water and electrolyte solutions have been presented by Hofenberg and his collaborators[46,62].

Gaeta et al[63] studied the release of lithium chloride -

(LiCl) from poly(ethylene-vinyl alcohol) copolymer. Initially, the release of lithium chloride was found to be controlled by nearly constant rate of absorption of water. At long times, the release lagged behind the water uptake, indicating that the release is governed by the diffusion process. It was observed that although the swelling increased with LiCl loading, the release rate remained unaltered.

Heller[64] developed a device for the release of insulin from pH sensitive poly(orthocarbonate). Here the pH sensitive polymer containing insulin is surrounded by a hydrogel containing glucose oxidase. When glucose diffuses into the device, gluconic acid produced within the hydrogel will decrease the pH, thus triggering the release of insulin from the polymer to the surrounding environment.

Similar studies were carried out by Ito *et al*[65]. Here insulin is in a membrane consisting of polyacrylic acid grafted porous cellulose film. At neutral pH in the absence of glucose, the carboxylate groups of polyacrylic acid which are negatively charged, make the polymer chains extended and close the pores of the membrane. Glucose oxidase catalyses the oxidation of glucose to gluconic acid and thus, protonates the carboxylic groups which make the graft chains coil and open the pores of the membrane to insulin.

With the plethora of monomers, polymers and preparation conditions available, it is possible to prepare a polymer with desired swelling behaviour for a variety of uses in controlled

release devices.

1.6.4 Magnetically controlled systems

In these systems, active agent and magnetic beads are uniformly dispersed within a polymer matrix. Upon exposure to aqueous medium, active agent is released in a fashion typical of diffusion controlled matrix system. However, upon exposure to an oscillating external magnetic field, active agent is released at a much higher rate.

Thus Langer and Hsieh[66] developed a magnetic controlled system that permits increased drug delivery rates on demand. In this case though the release in aqueous medium is diffusion controlled, upon exposure to an oscillating external magnetic field, the drug is released at upto thirty times higher rate. Although the mechanism responsible for magnetic modulation is unclear, it is thought that the beads cause alternating compression and expansion of the pores, thus facilitating the release.

This type of release pattern might be of value in the treatment of diseases such as diabetes in which constant rate insulin supplemented by increased rates before meals can be used to provide control of blood glucose. Magnetic systems may also be useful in birth control systems as a means of altering drug doses to correspond to the menstrual cycle.

REFERENCES

1. Kawal Dhari, Pesticides Information, XII(2) (1986) 6-19.
2. Langer, R., JMS-Rev. Macromol.Chem.Phys., C23(1) (1983) 61-126.
3. Controlled Release Technologies : Methods, Theory and Applications, CRC Press Florida Kydonieus A.F. (Ed.), Vol.I & II (1980).
4. Controlled Release Technology : Pharmaceutical Applications, Printed in U.S.A., Lee, P.I. and Good, W.R. (Ed.) (1987).
5. Medical Applications of Controlled Release, CRC Press Langer, R.S. and Wise, D.L., Vol.I (1984).
6. Insect Suppression with Controlled Release Pheromone Systems, CRC Press, Kydonieus, A.F. and Beroza, M., Vol.II (1982).
7. Controlled Release of Pesticides and Pharmaceuticals Plenum Press, New York and London, Lewis, D.H. (Ed) (1981).
8. Controlled Release Technology : Bioengineering Aspects, A Wiley-Interscience Publication of New York, Das, K.G. (Ed.) (1983).
9. Controlled Release Technologies : A Survey of Research and Commercial Applications, Elsevier Science Publishers Ltd., Duncan, R. and Seymour, L.W. (Eds) (1989).
10. Controlled Delivery of Crop-Protection Agents, Burgess Science Press, Basingstoke, Wilkins, R.M. (Ed.) (1990).
11. Controlled Release of Bioactive Materials Academic Press Baker, R. (Ed.) (1980).

12. Controlled Release-A Quantitative Treatment, Springer-Verlag, Berlin Heidelberg Fan, L.T., Singh, S.K. (1989).

13. Brannon-Peppas L., Polymer News 15 (6)(1990) 176-177.

14. Sudesh Kumar, Biodegradable Drug Delivery Systems, In : Biodegradabe Polymers Prospects and Progress, Marcel Dekker, Inc., New York and Basel (1987) 77-103.

15. Applied Bioactive Polymeric Materials, Plenum Press, New York and London, Gebelein, C.G., Carraher, C.E. Jr. and Foster V.R., (1988).

16. Rhine, W.D., Sukhatme, V., Hsieh, D.S.T. and Langer, R.S. Reference 11, 177-187.

17. Graham, N.B. and McNeill, M.E., Makromol.Chem.Macromol.Symp. 19 (1988) 255-273.

18. Korsmeyer, R.W. and Peppas, N.A., J.Mem.Sci., 9 (1981) 211-227.

19. Gander, B., Gurny, R., Doelker, E. and Peppas, N.A., Pharmaceutical Res. 6 (7) (1989) 578-584.

20. Fan, L.T., Sing, S.K. Reference 12, PP 20-44.

21. Kydoneius, A.F. Reference 3, Vol.I (1980) 129-174.

22. Fan, L.T., Singh, S.K. Reference 12, 49-50.

23. Roseman, T.J. and Cardarelli, N.F., Reference 3, Vol.I PP 21-41.

24. Higuchi, T., J.Pharm.Sci., 52 (1963) 1145.

25. Lee, P.I., J.Mem.Sci., 7 (1980) 255-275.

26. Heller, J., Pangburn, S.H. and Penhale, D.W. H., Reference 4, PP 172-187.

27. Heller, J. and Baker, R.W., Reference 11, PP 1-16.

28. Maa, Y.F. and Heller, J., J.Control.Rel., 15 (1990) 11-19.

29. Shah, S.S., Kulkarni, M.G. and Mashelkar, R.A., J.Appl. Polym. Sci., 41 (1990) 2437-2451.

30. Castellano, P.M., Bonvin, M.M., deBertorello, M.M. and Brinon, M.C., Polym. Bull., 26 (1991) 529-534.

31. Levenfeld, B. and Roman, J.S., Makromol.Chem., 192 (1991) 793-803.

32. Brannon Peppas, L., Polymers in Controlled Release, Polymer News, 15, No.11 (1990) 344-346.

33. Fan, L.T., Singh, S.K., Reference 12, PP 157-164.

34. Theeuwes, F. and Eckenhoff, B., Reference 11, PP 61-82.

35. Bindschaedler, C., Gurny, R. and Doelker, E., J.Control. Rel., 4 (1986) 203-212.

36. Hopfenberg, H.B. and Hsu, K.C., Polym.Engg.Sci., 18 (1978) 1186-1191.

37. Franson, N.M., Peppas, N.A., J.Appl.Polym.Sci., 28 (1983) 1299-1310.

38. Gostoli, C. and Sarti, G.C., Polym.Eng.Sci., 22 (1982) 1018-1026.

39. Raymond Davidson III, G.W. and Peppas, N.A., J.Control.Rel., 3 (1986) 259-271.

40. Raymond Davidson III, G.W. and Peppas, N.A., J.Control. Rel., 3 (1986) 243-258.

41. Brannon Peppas, L., Polymer News, 16, No.4 (1991) 114-116.

42. Peppas, N.A. and Franson, N.M., J.Poly.Sci.Polym.Phys.Ed., 21 (1983) 983-997.

43. Lee, P.I., In : Controlled Release Technology : Pharmceutical Application, ACS, Washington, D.C., Lee, P.I. and Good, W.R. (Eds) (1987) 71-83.

44. Ritger, P.L. and Peppas, N.A., J.Control.Rel.5 (1987) 37-42.

45. Segot-Chicq, S. and Peppas, N.A., J.Control.Rel., 3 (1986) 193-204.

46. Hopfenberg, H.B., Apicella, A., Saleeby, D.E., J.Mem.Sci., 8 (1981) 273-282.

47. Thomas, N.L. and Windle, A.H., Polymer, 23 (1982) 529.

48. Harrison, D.J.P., Rossyates, W., Johnson, J.F., J.M.S.- Rev. Macromol.Chem.Phys., C25 (4) (1985) 494-497.

49. Principles of Polymer Chemistry, Cornell University Press, Ithaca, New York, Flory, P.J., (1953) 576-584.

50. Wichterle, O. and Lim, D., Nature, 185 (1960) 117-119.

51. Dusek, K. and Janacek, J., J.Appl.Polym.Sci., 19 (1975) 3061.

52. Rajan, C.R., Srinivas, Y.S., Ponrathnam, S., Radhakrishnan, K., and Nayak, U.V., J.Poly.Sci., Polym.Lett., 25 (1987) 73.

53. Bednar, B., Morawetz, H. and Shafer, J.A., Macromolecules, 18 (1985) 1940.

54. Shieh, P.K. and Sivorinovsky, G., Polym.Prepr., 28(1) (1987) 215.

55. Kowbalnsky, M. and Zema, P., Macromolecules, 15 (1982) 788.

56. Franson, N.M. and Peppas, N.A., J.Appl.Polym.Sci., 28 (1983) 1299-1310.

57. Turner, D.T., Polymer, 28 (1987) 293.

58. Yasuda, H. and Lamaze, C.E., J.Macromol.Sci.Phys., B5 (1971) 111.

59. Good, W.R., In : Polymeric Delivery Systems (R. Kostelnik, Ed.) Gordon and Breach, New York, (1978) 139.

60. Hofenberg, H.B., Apicella, A. and Saleeby, D.E., J.Mem.Sci., 8 (1981) 273.

61. Yoshida, H., Tomizawa, K. and Kobayashi, Y., J.Appl.Polym. Sci., 24 (1979) 2277-2287.

62. Apicella, A. and Hopfenberg, H.B., J.Appl.Polym.Sci., 27 (1982) 1139.

63. Gaeta, S., Apicella, A. and Hopfenberg, H.B., J.Mem.Sci., 12 (1982) 195-205.

64. Heller, J., Chang, A.C., Rodd, G. and Grodsky, G.M., J. Control. Rel., 13 (1990) 295-302.

65. Ito, Y., Casolaro, M., Kono, K. and Imanishi, Y., J. Control. Rel., 10 (1989) 195-203.

66. Langer, R. Hsieh, D.S.T., Rhine, W. and Folkman, J., J.Mem.Sci., 7 (1980) 333-350.

CHAPTER - II

THE PRESENT INVESTIGATION

2.1. Starch and cellulose as encapsulating matrices

Advances in controlled release technology in recent years have been rapid because polymer science has become sophisticated enough to incorporate into polymers tailor-made properties required for each controlled release application. Currently, controlled release technology is a multi billion dollar industry involving dozens of applications in biological and other areas. Of these, major areas of application are pharmaceuticals, agrochemicals, veterinary products and industrial chemicals. There are many commercially available controlled release formulation (CRF) products in the market for pharmaceutical and veterinary applications. Thus, the field of CR pharmaceuticals and related areas has forged ahead followed by industrial chemicals. However, the CRF in agricultural applications is found to be lagging behind. This is mainly because increased cost for CR can be afforded for pharmaceuticals and veterinary drugs but not in agriculture. Thus, CR formulations in agriculture can have very little scope for sophisticated technology, no matter how effective it may be, unless it is reasonably cheap and can be applied on a large scale.

Thus, the factors governing agrochemical research and development are very different from those of pharmaceutical and veterinary research. This is partly due to the poor cash-return that most farmers expect per acre and also because of an understandable reluctance to experiment with new systems with the potential loss of a whole season's crop.

Inspite of the developments of many novel biologically active compounds, applied successfully in many different disciplines, it has become clear that significant improvements in their activities can be made by optimizing delivery. Hence, continued search for more effective and environment-friendly pesticide formulation based on CR technology is a desirable objective.

Evaluation of the potential application of controlled release in agriculture is currently a large and expanding area. A major component is the development of simple and relatively cheap formulations, that can be applied on a large scale to improve crop-yield based on agents giving protection against weeds, pests and other diseases as well as fertilisers designed to stimulate growth. For the purpose of convenience the CRF are divided according to applications concerned with the delivery of pesticides, herbicides, fertilizers and pheromones.

A large amount of work has been performed in the recent years on the development of sustained release herbicides and a large number of approaches are being investigated in search of the best solution to conventional application. Starch being an abundantly available, cheap biodegradable polymer with ability to be derivatized, has been reported as a CR matrix mainly for agrochemicals, such as pesticides, herbicides etc. Thus starch matrices such as starch xanthate[1-4], starch calcium adduct[5], starch borate[6,7] have been extensively used as encapsulating matrices for a number of pesticides. These CRF have shown

reduction in toxicity and prolongation of period of effectiveness compared to conventional formulations. A new technique of entrapment of herbicide in starch for spray application[8] by jet cooking of pearl starch[9] with varying amylose content for herbicide release is reported. Similarly, reports are there on chemical binding of pesticides to starch[10] and crosslinked amylose[11] for the preparation of CR formulations. Recent work of Shukla et al[12] on starch UF matrix [starch crosslinked by urea formaldehyde resin] for encapsulating carbofuran uses acidic conditions for the crosslinking reaction unlike the alkaline medium generally used.

Cellulose though similar in structure to starch has not been much utilized. Water soluble cellulose derivatives are found mainly in human application involving oral formulation in pharmaceutical drugs. Cellulose derivatives mainly used are cellulose esters and ethers, such as cellulose acetate[13], cellulose triacetate, ethyl cellulose[14] etc. Cellulose derivatives such as cellulose acetate, butyrate have increasing importance in the field of membrane science[15] due to the excellent physico-chemical properties exhibited by them. Use of cellulose esters and ethers in controlled release drug formulations, is of growing importance, because of hydrophilicity of the derivatives and non toxicity.

Dahl et al[16] have reported hydroxy propyl methyl cellulose as a rate controlling membrane in naproxen controlled release tablet formulation, where drug dissolution rate is proportional

to hydroxy propyl content. Release of phenyl propanalamine from pellet coated with ethyl cellulose was studied by Ozturk et al[17] who found that the release is mainly driven by osmotic pressure with minor contribution by diffusion through aqueous poree and solution/diffusion through the polymer membrane.

David et al[18] have studied the swelling characteristics of temperature sensitive hydrogels synthesised by chemical cross-linking of cellulose ether hydrogels. Cellulose ethers used were hydroxy propyl cellulose, methyl cellulose and hydroxy propyl methyl cellulose. From the study of gel properties, responsive gels can be readily created with desired properties from cellulose ether e.g. gel responding at body temperature, could be made from cellulose ether. Cellulose ethers are FDA approved for food and drug and can be readily utilised for pharmaceutical application unlike synthetic polymers. As the gel properties depend on crosslink density rather than chemical nature of the crosslinker, less toxic crosslinker (multifunctional carboxylic acids) could be used to create cellulose ether gels. Zia et al[19] reported biopharmaceutical evaluation of aspirin tablet dosage form made from ethyl cellulose to suppress the side effects of aspirin. This experimentally encapsulated aspirin tablet showed an excellent matching release profile to commercially available time release product prepared by direct compression using starch and talc as disintegrant and lubricant. Sheorey et al[20] developed a new technique for the encapsulation of water insoluble drugs [sulphadiazine] using ethyl cellulose.

Similarly, reports are there for chemical binding of pesticides to cellulose and also for crosslinked cellulose derivatives. Khue et al[21] studied the release of hydrocortisone and dexomethansone (antiinflammatory steroid) due to hydrolysis of carbonate linkage through which it is bound to the hydroxy propyl cellulose matrix.

Castellano et al[22] reported sulphonamide release from cellulose acetate membranes which were chemically modified by esterification with oxalyl chloride and was used as a hydrolytically labile spacer. Release of the drug occurred by the hydrolytic cleavage of the spacer drug linkage following zero order kinetics. Use of graft copolymers of cellulose in controlled release formulation is rarely reported. Thus, poly-(N-acryloyl glycine) grafted on porous cellulose membranes is reported to control the release of insulin[23].

There are very few examples of controlled release formulations for agrochemicals. Polymeric fungicide was reported by Mair et al[24] where pentachlorophenol was attached to cellulose via adipic acid as bridging group and release of pentachlorophenol occurred by cleavage of phenyl ester linkage.

In all these controlled release formulations, the first step involved is the preparation of cellulose derivatives which increases the cost due to synthesis, separation and purification steps involved in the preparation of cellulose derivatives. Also all these cellulose reactions are heterogeneous and depend upon the diffusion of reactant. In order to avoid cost problems in

derivatization and for making use of the cheap abundantly available and biodegradable material, direct use of cellulose, through standard procedure of viscose formation, is reported here. Intermediate viscose stage is used for the thorough dispersion of active agents. Though viscose formation is in alkaline condition, alkali labile pesticides can also be dispersed after neutralization of viscose. Thus, both alkali labile and alkali stable pesticides can be encapsulated with this matrix. Extensive study of the matrix carried out by encapsulation of model compounds has established its suitability for both water soluble and insoluble active agents.

Examination of prior literature reveals practically no work with the direct use of cellulose with in situ encapsulation of active agent.

2.2. Carbofuran : A candidate pesticide

Carbofuran [2,3 dihydro-2,2-dimethyl-7-benzo furanyl methyl carbamate; molecular weight : 221.3, m.p.: 153-154°C, v.p.: $2x10^{-5}$ mm of Hg at 33°C] was introduced in 1967 by the Agricultural Chemical Division of the FMC Corporation under the trade mark "Furadan".

Carbofuran is a broad spectrum systemic insecticide-nematicide and is known to be very effective against most soil and foliar pests such as the stem borer, leaf and plant hoppers etc. in the cultivation of rice; shoot fly in sorghum; nematodes in tobacco, ground nut and sugar cane; aphids and jassids in cotton, safflower and mustard. It has demonstrated excellent

bioefficacy for controlling several other pests in the cultivation of vegetables, banana, coffee etc. Carbofuran is classified as systemic carbamate pesticide.

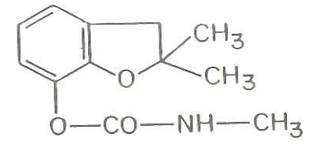

Although carbofuran proved to be highly effective during early 1970s, its use was limited there after presumably due to its break-down by chemical and microbial degradation[25] in the soil. The degradation of carbofuran in alkaline soil is largely chemical hydrolysis occurring at carbamate linkage yielding 2,3-dihydro 2,2-dimethyl-7-benzofuranol [equation (1)].

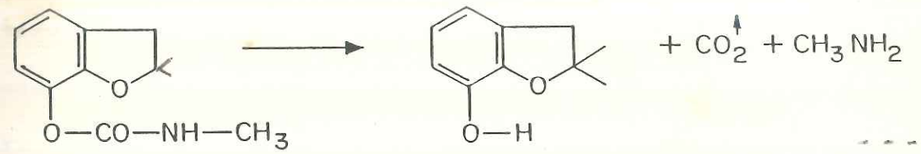

...(1)

while degradation in acid or near neutral soil is both chemical and biological. In microbial degradation, carbofuran is used as the source of both carbon and nitrogen. Thus presence of additional nitrogen source (nitrogen containing fertilizers) inhibits the degradation of carbofuran. There is complete decomposition of the ring moiety to CO_2 in soil and in microbial cultures. The rate of biodegradation depends on the rate and frequency of pesticide application, cropping system, chemical and physical characteristics of soil and the prevailing environmental

conditions. Rate of decomposition of carbofuran is faster in retreated soil than in untreated soil[26].

Bioassay studies showed that carbofuran (10 ppm) persisted with little or no loss in toxicity for three months in an acidic soil[27]. Carbofuran is found to be highly toxic to both insects and mammals and can cause adverse effects to nontarget[28] pests and environmental pollution such as poisoning of birds[29].

In India carbofuran is commercially available as 3% granules [FURADAN 3G] marketed by Rallis India Ltd., as soil broadcast formulation. A seed coat formulation containing 50% carbofuran (FURADAN 50 SP) has been withdrawn from use by Central Insecticide Board on account of its very high oral and inhalation toxicity.

Carbofuran thus appears to be an ideal candidate for encapsulation. Since, it is widely used in agriculture, in order to achieve safe handling with maximum output, inspite of its high toxicity, controlled release formulations were prepared which could circumvent some of the problems associated with the use of this pesticide.

2.2.1 Controlled release carbofuran formulations

There are very few reports in the literature on CR formulations of carbofuran. Physical controlled release formulations based on kraft lignin have performed well in insect control[30]. These formulations depend on the plasticization of the lignin with compatible pesticide or other material to form a matrix. Though crosslinked lignin gel can be used to increase the

range of pesticides that can be formulated with lignin, unmodified kraft lignin was used as a useful formulating agent for a number of pesticides such as the soil insecticide, carbofuran. Thus, monolithic granular formulations of carbofuran were prepared and their evaluation under conditions of tropical flooded rice showed extended duration of activity and increase in yield in rice cultivation[31]. Laboratory studies in static water indicated a diffusion controlled release rate with complete release within 40-60 days.

Similarly, better control than the commercial 3% granule was observed for CRF of pine kraft lignin-carbofuran with 15-45% active agent by weight, by Wilkins et al[32]. With broadcast application into the flood water, soil incorporation, and root zone injection, improvement in control of green leaf hoppers was noticed. The best lignin based formulation reduced level of tungro virus infection from 23% for conventional flowable carbofuran formulation to 1% at an application rate of 0.5 kg active agent/ha. At the same rate, the grain yield was increased from 3.56t/ha to 5.5t/ha using the controlled release formulation.

Studies conducted with EVA poly (ethylene co vinyl acetate) matrix showed that CR formulation can retain the activity of carbofuran even after 32 weeks[33]. Results with this formulation when compared to conventional Furadan for root zone application in rice plant showed similar level of carbofuran concentration in grain and straw for both formulations, while contamination of

paddy water and soil was substantially reduced (by 30-40%) in plots treated with EVA based CR formulation[34]. EVA matrix acts as a protective layer which prevents hydrolysis of carbofuran.

Evaluation of cellulose based (hydroxy ethyl cellulose crosslinked with melamine formaldehyde) formulation in rice paddy showed extended duration of carbofuran due to slower rate of release, with its level in water and plants, effective enough to protect the plant against insects[35]. Similarly seed coat using urea formaldehyde and starch xanthide carbofuran formulation showed better control of aphids and stem nematodes in field beans as observed from the yield[35].

2.3 The scope of the present investigation

In the present work, crosslinked cellulose has been studied as a biodegradable matrix for encapsulation of carbofuran, a systemic pesticide with high oral and contact toxicity. The direct use of cellulose (cotton pulp) is reported here with in situ conversion to viscose and encapsulation by crosslinking. The process is on similar lines to that of Shasha *et al*[1], on the encapsulation in starch xanthide matrix. Though the starch xanthide encapsulation process for agrochemicals and its bioefficacy has been studied in detail, very little is known about the mechanism of release of the agent from the matrix. Hence, comparative study of the encapsulation of carbofuran in cellulose and starch xanthide matrices was undertaken to investigate the effect of the matrix parameters like crosslink density, equilibrium degree of swelling, loading, crystallinity etc. on

the release rate. Experiments were carried out to clarify the effect of solubility of active agent on its release rate, by varying solubility of carbofuran by the variation in eluting media.

Since the controlled release formulations involved in this study consisted of granular particles of irregular shape and size, single particle release measurements were carried out to know the exact mechanism of release.

Effect of polymer composition, molecular weight and percentage crystallinity on release of caborfuran was studied by using cellulose from different sources and also by using agricultural wastes. Thus controlled release formulations (CRF) prepared using cotton pulp and wood pulp were found to have slower release due to retention of crystallinity after cross-linking whereas CRF prepared using Rice straw cellulose and Peanut shell cellulose showed comparatively faster release due to the complete conversion to amorphous structure on crosslinking. However, CRF prepared using agricultural wastes (Rice straw and Peanut shell powder) showed further increase in release due to the presence of amorphous lignin.

To gain further insight into the release mechanism, encapsulation of selected model organic compounds was carried out and the effect of physical state and solubility of the encapsulant on the swelling and release kinetics was studied.

Further modifications of the physical properties of cellulose matrix through graft copolymerisation with hydrophobic poly-

styrene and hydrophilic polyacrylamide branches were carried out and their effect on release of carbofuran was investigated.

Characterization of crosslinked starch, cellulose and of crosslinked graft copolymers of cellulose was studied by Solid State ^{13}C CP/MAS NMR. The spin-spin relaxation time (T_2), measured for crosslinked starch and cellulose was correlated with the swelling and release kinetics. Characterization of graft copolymers by FTIR and DTA provided proof of grafting for the cellulose graft copolymers. It has been established that the encapsulant is physically trapped in the network and no chemical bond formation occurs.

REFERENCES

1. Shasha, B.S., Doane, W.M. and Russel, C.R., J.Poly.Sci., Polym.Lett.Ed., 14 (1976) 417-420.
2. Doane, W.M., Shasha, B.S. and Russel, C.R., In : Controlled Release Pesticides, ACS Symp.Ser., 53, ACS Washington D.C., (1977) 74-83.
3. Stout, E.I., Shasha, B.S. and Doane, W.M., J.Appl.Poly.Sci., 24 (1979) 153-159.
4. Wing, R.E. and Otey, F.H., J.Polym.Sci., Polym.Chem.Ed., 21 (1983) 121-140.
5. Shasha, B.S., Trimnell, D. and Otey, F.H., J.Polym.Sci., Polym.Chem.Ed., 19 (1981) 1891-1899.
6. Shasha, B.S., Trimnell, D. and Otey, F.H., J.Appl.Polym.Sci. 29 (1984) 67-73.
7. Wing, R.E., Maiti, S. and Doane, W.M., J.Control.Rel., 5 (1987) 79-89.
8. Trimnell, D. and Shasha, B.S., J.Control.Rel. 7 (1988) 263-268.
9. Wing, R.E., Maiti, S. and Doane, W.M., J.Control.Rel., 7 (1988) 33-37.
10. McCormick, C.L. and Lichatowich, D.K., J.Polym.Sci., Polym.Lett. Ed., 17 (1979) 479-484.
11. Lenaerts, V., Dumoulin, Y. and Mateescu, M.A., J.Control. Rel., 15 (1991) 39-46.
12. Shukla, P.G., Rajagopalan, N., Bhaskar, C. and Sivaram, S., J.Control.Rel., 15 (1991) 153-165.

13. Bindschaedler, C., Gurny, R. and Doelker, E., J. Control. Rel., 4 (1986) 203-212.

14. Bhaller, H.L. and Shah, A.A., Indian Drugs, 28(9) (1991) 420-422.

15. Sourirajan, S. and Matsuura, T., Reverse Osmosis, Ultrafiltration Process Principles, N.R.C.C. Publ., No.24188 (1985) P-360.

16. Dahl, T.C., Calderwood, T., Bormeth, A., Trimble, K. and Piep meier E., J.Control.Rel., 14 (1990) 1-10.

17. Ozturk, A.G., Ozturk, S.S., Palsson, B.O., Wheatley, T.A. and Dressman J.B., J.Control.Rel., 14 (1990) 203-213.

18. Harsh, D.C. and Gehrke, S.H., J.Control.Rel., 17 (1991) 175-186.

19. Zia, H., Falamarzian, M., Raisi, A., Montaseri, H. and Needham, T.E., J.Micro.encap., 8(1) (1991) 21-28.

20. Sheorey, D.S., Sesha Sai, M. and Dorle, A.K., J.Micro.encap., 8 (1) (1991) 359-368.

21. Khue, N.V., Jung, L., Coupin, G. and Poindron, P., J.Polym. Sci.Polym.Chem., A 24 (1986) 359-373.

22. Castellano, P.M., Bonvin, M.M., deBertorello, M.M. and Brinon, M.C., Polym. Bull., 26 (1991) 529-534.

23. Barbucci, R., Casolaro, M. and Magnani, A., J.Control.Rel., 17 (1991) 79-88.

24. Mair, P., Bahadir, M. and Korte, F., J.Control.Rel., 5 (1988) 293-295.

25. Getzin, L.W., J.Environ.Entomol., 2 (1973) 461-467.

26. Felsot, A.S., Maddox, J.V. and Bruce, W., (Enhanced Microbial Degradation of Carbofuran in Soil with Histories of Furadan use) Bull.Environ.Contam.Toxicol., 26 (1981) 781.

27. Read, D.C., J.Econ.Entomol., 64 (1971) 800.

28. Somalik, J.D., Plant Diseases, 67(1) (1983) 28-31.

29. Stone, W.B. and Gradoni, P.B., North Environ.Sci., 4(3/4) (1985) 160-164.

30. Wilkins, R.M., In : Proc. of the 10th Int. Symp. on Controlled Release of Bioactive Materials, San Francisco CA, USA, (1983) 125-128.

31. Wilkins, R.M., Abstracts of 8th Int.Symp. on Controlled Release of Bioactive Materials, (1981) 72.

32. Wilkins, R.M., Batlerby, S., Heinrichs, E.A., Aquino, G.B. and Valencia, S.L., J.Econ.Entomol., 77 (1) (1984) 495-499.

33. Jamil, F.F., In : Proc. of 13th Int. Symp. on Controlled Release of Bioactive Materials, (1986) 238-239.

34. Bahadir, M. and Pfister, G., Chemosphere, 16(6) (1987) 1273-1279.

35. Schiffers, B.C., Dreze, P., Fraselle, J. and Gasia, M.C., In : Pesticides: Food and Environmental Implications, IAEA, Vienna (1988) 205-218.

CHAPTER - III

CELLULOSE XANTHIDE (CellX) AS AN ENCAPSULATING MATRIX : I COMPARISON WITH STARCH-XANTHIDE (StX) ON SWELLING AND RELEASE PROPERTIES

3.1 EXPERIMENTAL

3.1.1 Materials

. Corn starch granules : Obtained from Anil Starch Products Ltd., Ahmedabad.

. Cotton pulp : Purified cotton linter pulp processed in National Chemical laboratory, Pune.

. Carbon disulphide : Reagent grade obtained from S.D. Fine Chemicals which was distilled before use.

. Sodium hydroxide : Reagent grade.

. Methanol : Purified as spectral grade.

. Carbofuran : Received from Rallies India Ltd. as Technical grade which was purified by crystallization from acetone.

. Sulphuric acid : AR grade

. Hydrogen peroxide : 30% w/w

. Acetic acid : Glacial A.R. grade

3.1.2 Purification and analysis of carbofuran

3.1.2a Purification of carbofuran

150 g of technical grade carbofuran was dissolved in 1.0 L of acetone and the solution filtered through Whatman filter paper No.1 (flitted). The filtrate was added dropwise to 3.5 L of distilled water with stirring in a 5 L beaker. The carbofuran crystals that precipitated out, were separated by filter paper No.1 and dried overnight at room temperature. The carbofuran sample was further dried in an oven at 50-60^{o}C for 1.5 h. This procedure of dissolving and precipitating was repeated for a

second time to obtain purified carbofuran, m.p. 153°C (Literature[1] m.p. 153-154°C).

3.1.2b Elemental analysis of carbofuran :

Analysis Calcd. for $C_{12}H_{15}NO_3$ (221.3)

Calcd : C, 65.19%; H, 6.79%; N, 6.33%

Found : C, 65.28%; H, 7.02%; N, 5.96%.

3.1.2c Calibration of carbofuran by UV spectroscopy

Approximately 0.04 to 0.05 g of carbofuran was accurately weighed into a 100 ml volumetric flask and dissolved in spectral grade methanol and made upto the mark. From this stock solution, further dilutions were made with distilled water to provide carbofuran concentration ranging from 1 to 70 ppm. Carbofuran showed maximum absorbance at 278 nm (λmax) when scanned in the region of 200 to 400 nm in a UV spectrophotometer (Hitachi Model 220). Absorbances of a set of dilutions were noted at 278 nm. Plot of absorbance vs concentration was found to obey Lambert-Beer's law (Fig. 3.1). This was carried out in duplicate. Slope of this Lambert-Beer's plot was calculated by regression analysis and was found to be 0.01298. For getting the concentration of carbofuran in a given solution, absorption of that solution was noted at 278 nm and concentration was calculated by following formula:

Concentration of carbofuran in solution (ppm) = Absorbance/0.01298 .....(1)

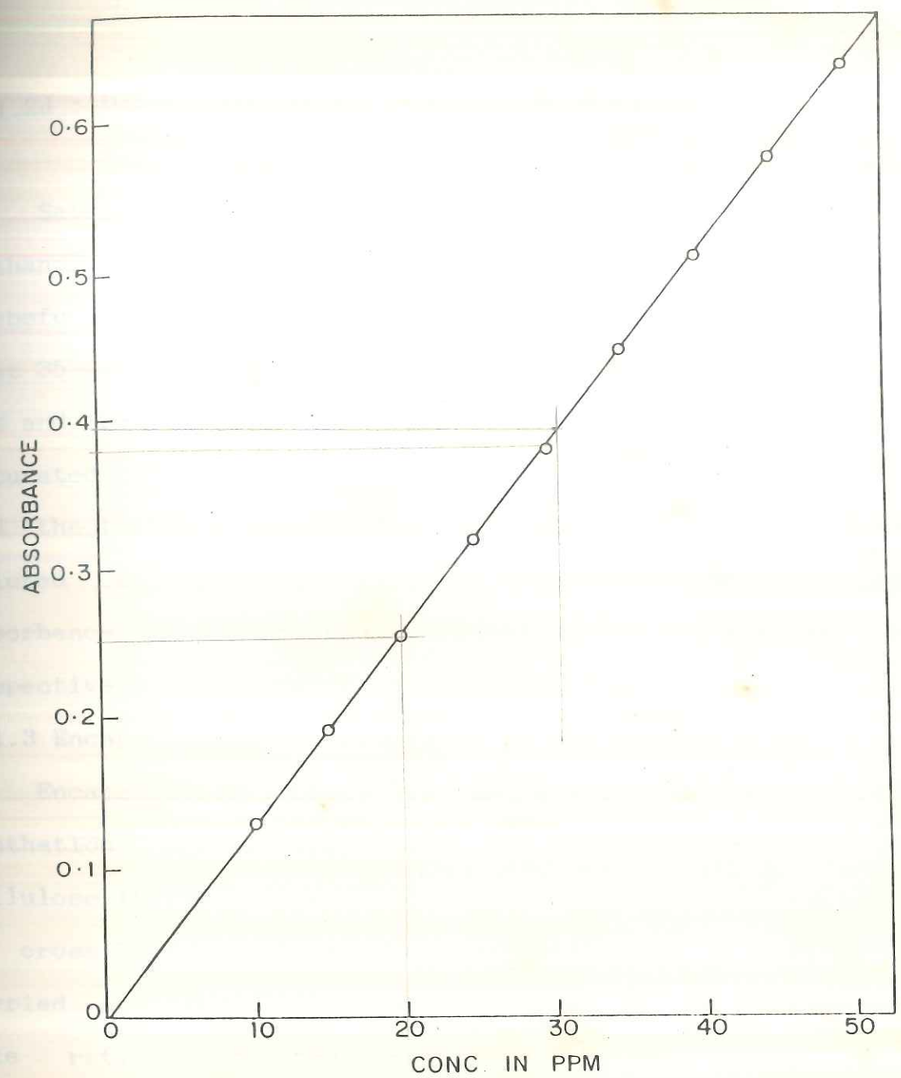

FIG. 3·1 : UV CALIBRATION CURVE OF CARBOFURAN

3.1.2d : Determination of solubility of carbofuran in different aqueous methanol solvent systems :

Saturated solutions of carbofuran in four different methanol-water solvent systems were prepared by adding excess carbofuran in the solvent system and shaking the mixture for 8-10 h at 35°C. These four solvent systems had 0% (water alone), 50%, 70% and 100% (methanol alone) methanol content (vol/vol). These saturated solutions were filtered through sintered crucible (G3) and the filtrate was diluted further so that the absorbance of diluted solution was in the acceptable range. From the absorbance (at 278 nm), solubility of carbofuran in the respective solvent system was calculated.

3.1.3 Encapsulation of carbofuran in StX and CellX matrices

Encapsulation procedure in starch involves gelation, xanthation and encapsulation by crosslinking whereas for cellulose it involves mercerization, xanthation and encapsulation by crosslinking. Xanthation of cellulose and starch were carried out under identical conditions and stoichiometry, the mole ratios of the reactants being 1:1.4:0.565 for cellulose/starch anhydroglucose unit, NaOH and CS_2 respectively.

A number of formulations of carbofuran encapsulated in StX/CellX matrix were prepared with different percentages of carbofuran loading, keeping the crosslink density constant i.e. using the same mole ratio of cell/st to carbon disulphide. Blank xanthides i.e. some formulations without an active agent (carbofuran) were also prepared (Table 3.1). Degree of cross-

linking (degree of xanthation) was computed by sulphur analysis (Table 3.4).

3.1.3a Encapsulation procedure in starch xanthide matrix Step 1&2 Gelation and xanthation :

Step 1 and 2 : Gelation and xanthation : 12 g (with correction for moisture) of starch was soaked in 110 ml of distilled water and treated with 4.5 g of carbon disulphide, followed by a solution of 2.66 g of sodium hydroxide in 40 ml of water with slow agitation to avoid loss of CS_2. The mixture was kept closed for 1 h at 30°C and an orange gelatinous mass of starch xanthate was obtained.

Step 3 : Encapsulation : The starch xanthate was neutralized to pH 7 with 5% acetic acid at 0-5°C. The required amount of carbofuran (4 g) was added in fine powdered form and thoroughly dispersed by agitation. An ice cold mixture of 6.5 ml H_2O_2 + 3 ml of concentrated H_2SO_4 was then added to the reaction mixture at 15°C with agitation, for effecting oxidative crosslinking and encapsulation. Thus, a granular precipitate was obtained after crosslinking. The final pH of the reaction mixture was 3 and temperature was 22°-25°C. The granular precipitate thus obtained was filtered with muslin cloth through buchner funnel. It was further neutralized to pH 7 with dilute NaOH solution and filtered, followed by two washings with cold water. It was wet sieved through No.5 mesh screen and dried in an air oven at 50° for 8-10 h. Mesh size of the particles used for swelling and release study was $\underline{-5+10}$ corresponding to particle size of 3.35 mm

to 1.70 mm.

3.1.3b Encapsulation procedure in cellulose xanthide matrix

Step 1 : Mercerization : 10 g of cotton pulp (with weight correction for moisture) was soaked in 18% NaOH solution for 90 min at 30°C. The pulp was squeezed out to remove the excess alkali to get a weight of 28 g of alkali cellulose.

Step 2 : Xanthation : Alkali cellulose obtained was shredded in a blender and transformed to a stoppered bottle having two outlets. The bottle was first evacuated by connecting to a vacuum pump and then 3.8 g of carbon disulphide was added through the other inlet and kept closed at 30° for 2 h. The xanthate formed was transferred to a reactor of 1 liter capacity and treated with 5.5 g of NaOH and sufficient water to get a total weight of 125 g of viscose solution containing 8% cellulose and 7% NaOH.

The viscose (cellulose xanthate) was stirred for 1 h so as to get homogenized and could be stored upto 3 days at 0-5°C before encapsulation. Nevertheless, to minimize the formation of by-products fresh batches were prepared as and when needed.

Step 3 : Encapsulation : The viscose was neutralized to pH 7 with 5% acetic acid at 0-5°C and sufficient quantity of carbofuran (3.34 g) was thoroughly dispersed in it. The temperature was raised to 15°C and then ice cold oxidizing mixture of 5.4 ml H_2O_2 (30%) and 5 ml of concentrated H_2SO_4 was added to get final pH of 3. The encapsulated product was obtained in the form of a rubbery mass. It was filtered, washed with dilute NaOH solution

to neutral pH and then with water. It was then wet sieved through mesh screen No.5 and dried for 8-10 h in air oven at 50°C.

Blank matrices were prepared in either case by the same procedure without adding carbofuran. Sieved portion of -5+10 mesh size corresponding to particle size of 3.35 mm to 1.70 mm was used for swelling and release measurements.

3.1.4 Analysis of CellX & StX samples

3.1.4a Moisture content

Moisture contents were determined at room temperature under vacuum over phosphorus pentoxide. Approximately 1 g of the sample was weighed accurately in a weighing bottle and kept in vacuum desiccator over P_2O_5 for 4 h. The sample bottle was then removed from desiccator, it was stoppered and weighed. This was repeated two times to get constant weight. Percentage moisture content was determined from the weight loss. Moisture content of sample No. $CellX_4$, $CellX_5$ and StX_3, StX_4 were determined along with that of starch and cellulose. Rest of the samples were dried in an air oven at 50°C for 8-10 h and all the samples were stored in vacuum desiccator over P_2O_5 and used as required.

3.1.4b Determination of carbofuran content in the sample

A known weight of the sample (~1.0 g) was refluxed in 50 ml of methanol for 4 h, cooled to room temperature and filtered through sintered glass crucible. Residue in crucible was washed with 20-30 ml of methanol. Filtrate and washings were transferred to 100 ml volumetric flask and diluted with methanol upto

the mark. From this 100 ml flask, 1.0 ml of solution was transferred to 25 ml volumetric flask and diluted upto the mark with distilled water. This last dilution was done in duplicate. The active agent content determination for a single experiment was repeated 4 to 5 times, and average was taken. From the absorbance of the diluted solution at 278 nm and using calibration slope, the carbofuran content in the sample was determined using following formula :

$$\% \text{ Carbofuran} = \frac{\text{Absorbance} \times 250}{0.01298 \times \text{wt. of sample (mg)}} \qquad \ldots\ldots(2)$$

3.1.4c Determination of percentage crystallinity

Percentage crystallinity was determined from the data obtained from X-ray diffractogram, using Philips X-ray unit (Philips Generator, PW 1730) and Nickel filtered Cu-kα radiations. Percentage crystallinity for original, mercerized and crosslinked cotton pulp was determined. Similarly, percentage crystallinity for original, gelatinised and crosslinked starch was also determined. Percentage crystallinity was determined from the diffractogram using area under the curve from 10, 2θ to 28, 2θ.

3.1.4d Sulphur content and degree of xanthation

Microanalysis of the blank xanthides was carried out for sulphur content and the degree of xanthation was calculated using the relation[2]:

$$DS = \frac{1.62 \times \% S}{64.12 - (0.75 \times \%S)} \qquad .....(3)$$

where, DS = Degree of substitution i.e. degree of xanthation.

3.1.4e Molecular weight between crosslinks

Estimation of sulphur content after crosslinking gives direct measure of the number of crosslinks and molecular weights between crosslinks.

The crosslinked cellulose xanthide involves structure as shown below.

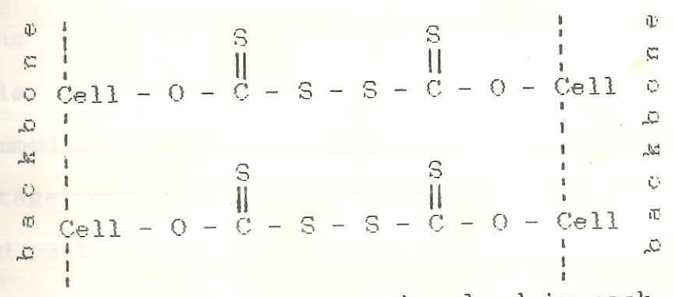

Thus, 4 sulphur atoms are involved in each crosslink. Thus, 128 g of sulphur corresponds to one crosslink. From sulphur analysis data of the crosslinked polymer we can calculate the molecular weight between crosslink as follows e.g. for $CellX_o$ sulphur content is 7.73% i.e.

7.73 g sulphur = 100 g polymer

Therefore, 128 g sulphur = 1656 g polymer

Thus, 1656 represents the molecular weight between the cross-link for $CellX_o$. Molecular weight of cotton pulp is 62,000 and the molecular weight between crosslink is (M_c) 1656 i.e. there are 37 crosslinks per mole of cellulose polymer. As degree

of polymerization (DP) is 388,there will be one crosslink after 10 units of anydroglucose units.

3.1.5 Swelling measurements

Since, the products are in the form of irregular particles (1.70 mm - 3.35 mm in size), the water uptake could only be measured gravimetrically. A series of stoppered weighing bottles containing known weights (~1.0 g) of the sample were treated with excess (20 ml) of water (or the appropriate swelling agent) at 35°C. The contents were gently stirred during first 1-2 h to prevent clumping. At the end of the required swelling time, it was quickly filtered through a glass sintered crucible, the swollen granules gently blotted with filter paper and immediately weighed in a stoppered weighing bottle. The percentage swelling was computed as parts of water uptake per hundred parts of dry sample (pph).

$$\text{Water uptake (pph)} = \frac{\text{wt. of swollen sample} - \text{initial wt. of sample}}{\text{initial wt. of sample}} \times 100 \quad \ldots\ldots(4)$$

The measurements were carried out in triplicate and an average value of water uptake was taken.

3.1.6 Release measurements

3.1.6a Bulk release

Release rate study of the encapsulated carbofuran samples in StX, CellX matrices was carried out under near perfect sink conditions by effective stirring of known weight of the sample in excess solvent, keeping the total carbofuran content at 5% of

its saturation solubility in the medium. Solubility of carbofuran in water at 35°C is 1200 ppm and maximum concentration of carbofuran in eluting medium allowed was to reach 50-60 ppm.

Sufficient quantity of the formulation was taken in 1 L R.B. flask fitted with a turbine stirrer and with 500 ml of the release medium measured into it and kept in a thermostatic bath maintained at 35 ± 0.5°C. The solution was stirred at a constant speed of 150 rpm and 10 ml aliquots of the medium were removed at periodic intervals for determining the carbofuran content by UV spectroscopy by measuring absorbance at 278 nm and equal volumes of the solvent replaced in the vessel to maintain the same overall volume. Thus the amount of carbofuran released from the formulations was monitored as a function of time. Three to four replications were carried out and for each time interval the average cumulative release was taken. The effect of solubility of carbofuran in eluting (release) medium on the release rate was studied by measuring release rate of StX_2/$CellX_2$ carbofuran formulations in four different aqueous methanol solvent systems. The solvent systems (release medium) used had 0% (water alone), 50%, 70% and 100% (methanol alone) methanol content and the release rate measurement experiments were carried out as described earlier.

3.1.6b Single particle release

Single particle release was carried out according to the procedure developed by Shukla et al[3]. In principle, it consisted of conducting the release experiments in a 10 mm quartz cell

mounted in the Hitachi 220 spectrophotometer and monitoring the absorbance at 278 nm at periodic intervals. A single particle of the sample (granule 3 to 4 mg wt) was kept in a stainless steel wire mesh boat submerged in water (3.5 ml) at the upper part of the cell which was not in the path of the beam and the solution was magnetically stirred from the bottom (Fig.3.2). The cell was kept covered with glass lid. By using a cell programmer, three replications could be carried out simultaneously and absorbance at 278 nm was printed out continuously at specific time intervals. Release experiments were carried out for a maximum of 8-10 h. This method was found to be useful for single particles containing carbofuran as it gives measurable absorbance over the release time studied. From the absorbances, amount of carbofuran released as a function of time was calculated. Single particle release study was carried out for $CellX_4$ Carbofuran and StX_4 Carbofuran formulations.

3.2 RESULTS AND DISCUSSION

3.2.1 Analysis of encapsulated samples

3.2.1a Efficiency of encapsulation

Table 3.1 describes the blank and encapsulated samples of CellX and StX, for % carbofuran content and efficiency of encapsulation. It is observed that for lower loading, efficiency of encapsulation is low for both CellX and StX matrices whereas for loading level above 15% onwards it is ranging approximately between 90 to 100%. Thus, for 5% loading efficiency of encapsulation is about 66 % and 73 % whereas for 10% loading it is 78

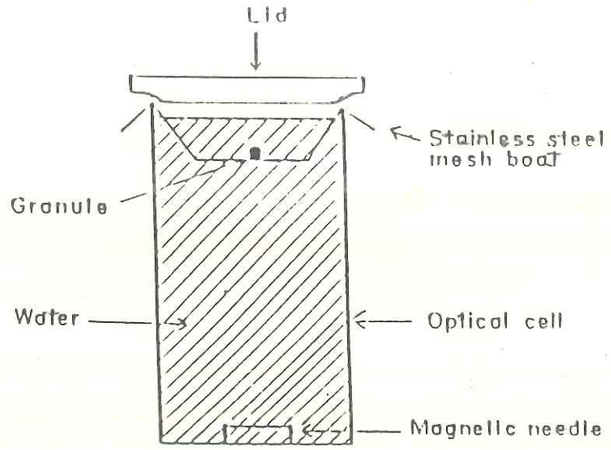

Size of Optical cell : 10 mm x 10mm x 45mm (ht.)

FIG.3·2.: SINGLE PARTICLE RELEASE SET-UP

TABLE 3.1

Description of Blank ($CellX_0$, StX_0) and Encapsulated samples of CellX* and StX**.

Sample code No.	Carbofuran used (g)	Carbofuran in the sample (%)	Efficiency of Encapsulation (%)	Yield (g)
$CellX_0$	-	-	-	11.00
$CellX_1$	0.91	5.2	66	11.60
$CellX_2$	1.67	10.6	78	12.30
$CellX_3$	2.06	14.4	90	12.85
$CellX_4$	3.81	24.7	95	14.61
$CellX_5$	4.23	26.8	95	15.00
StX_0	-	-	-	13.60
StX_1	1.15	5.8	73	14.44
StX_2	1.65	8.6	78	14.90
StX_3	4.00	20.5	95	18.55
StX_4	4.67	23.5	95	19.00

Blank - without carbofuran.

* For cellulose samples 10 g cotton pulp was used.

** For starch samples 12 g starch was used.

These samples were used making correction in weight for moisture content.

and 78% for CellX and StX respectively. The low efficiency at lower loading may be due to fact that large percentage of water is present in the system (~90%) at the time of encapsulation and carbofuran is lost in the filtrate.

3.2.1b Moisture content

Moisture content in free starch was usually 12% but the moisture content of the encapsulated StX was slightly less i.e. 7 to 11%. In case of cotton pulp the moisture content of 6 to 11% was increased to 11 to 12% in CellX (Table 3.2).

3.2.1c Carbofuran content

Encapsulated formulations of StX and CellX were checked for carbofuran content by refluxing in water, 50% aqueous methanol and methanol. It was observed that in water and 50% aqueous methanol, salts formed in neutralization of viscose and starch xanthate which were entrapped in encapsulation stage by cross-linking were extracted along with carbofuran and the reflux extract after filtration still remained turbid leading to erroneous results which did not match with the calculated values of carbofuran. After extraction of carbofuran in methanol for 4 h, extraction of the sample for 2nd and 3rd time did not show UV absorption at 278 nm i.e. carbofuran was completely extracted within 4 h (Table 3.3).

3.2.1d Structure of carbofuran in StX and CellX matrix

Microanalysis data, IR, proton NMR and ^{13}C CP/MAS. NMR of carbofuran extracted from StX and CellX matrix confirms that carbofuran does not undergo any chemical reaction during the

TABLE 3.2

Moisture Content in CellX and StX samples containing Carbofuran.

Sample code No.	Moisture Content (%)
$CellX_4$	11.6
$CellX_5$	11.6
StX_3	7.5
StX_4	10.5

TABLE 3.3

Carbofuran content in sample $CellX_4$ and StX_4 in different methanol-water refluxing solvent systems.

Methanol in refluxing solvent (%)	Carbofuran obtained (%)	
	$CellX_4$	StX_4
100	24.7	23.5
50	17.1	30.7
0 (water)	11.6	15.5

process of encapsulation but only gets physically entrapped within the crosslinked matrix which has been discussed in Chapter VII.

3.2.2 Swelling

Both the cellulose xanthide and starch xanthide encapsulation systems are monolithic devices with carbofuran being uniformly distributed in the polymer matrices. The matrices are hydrophilic and swellable in water. When placed in a thermodynamically compatible solvent (water), they undergo glass to gel transition resulting in change in the internal structure (macromolecular chain relaxation) and size (volume expansion); thus giving rise to a swelling controlled system considered in this work. The equilibrium swelling factor needs to be considered here. When an initially glassy hydrophilic polymer (crosslinked) is placed in contact with a thermodynamically compatible solvent (water), swelling occurs as the water molecules begin to penetrate by diffusion into the glass region. Thus, an opportunity for an increase in entropy is afforded in network polymer, also like a linear one when diluted by solvent due to polymer solvent interactions. However, complete mixing can not occur in polymer network. As the network is swollen by absorption of water (solvent), the chains between network junctions are required to assume elongated configurations[4] (Fig.3.3) and a force akin to the elastic retractive force in rubber, consequently develops in opposition to the swelling process. As swelling proceeds, this retractive force increases

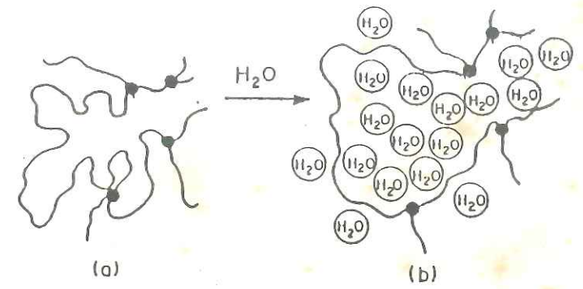

FIG. 3:3 : CHANGE OF THE DIMENSIONS OF MACRO-MOLECULAR CHAINS DUE TO THE SWELLING BY WATER, FROM THE UNPERTURBED STATE(a) TO THE SOLVATED STATE (b)

and the diluting force (entropy of dilution) decreases. Ultimately a state of equilibrium swelling is reached in which the entropy of dilution and the retractive forces are balanced[5]. The force of retraction in a stretched network structure depends also on the degree of crosslinking[6]. Thus the degree of swelling (or % swelling) observed at equilibrium in a good solvent invariably decreases with increasing degree of crosslinking. It also decreases with increase in the primary molecular weight[6].

Thus "Swelling controlled release systems" are based on the phenomenon that hydrophilic glassy polymers exhibit certain changes of their properties at their glass transition temperature (Tg). The penetrant refers to any low molecular weight species in the external medium which is thermodynamically compatible with polymer. In the presence of a penetrant (water), the glass transition temperature is lowered and the macromolecular chains relax to achieve a new thermodynamic state, i.e. the rubbery state. The term relaxation indicates the transition of polymer chains from glassy state to gel state. When water enters in the glassy polymer, it is slowly transformed into a rubbery system. Thus polymer undergoing chain relaxation due to absorption of penetrant commonly exhibits two distinct regions viz., unrelaxed glassy polymer region and a relaxed rubbery region, separated by a sharp boundary which moves inward into the glassy polymer as additional water is absorbed.

This change in state of the polymer occurs at a characteristic penetrant concentration of the polymer penetrant system.

Three basic classes of behaviour have been established.

Case I or Fickian diffusion behaviour is observed when the rate of transport or diffusion of the penetrant is much less than that of the relaxation process i.e. the kinetics of this phenomenon can be characterized by a single parameter diffusivity.

Case II transport is the other extreme in which transport of the penetrant through the gel region is very rapid compared with the relaxation process at the gel glassy polymer interface. Kinetics of case II transport can also be characterised by a single parameter - the velocity of the interface (and the equilibrium swelling factor if accompanied by volume expansion). At the end of the Case II transport process, a rapid increase in the penetrant sorption rate may sometimes be observed. In this situation, Case II transport is said to have evolved into Super Case II transport which is discussed in detail in Chapter V.

The last case is non-Fickian or anomalous transport of the penetrant which occurs when the diffusion and relaxation rates are comparable. As the penetrant diffuses into the polymer, rearrangement of the polymer chains does not take place instantaneously. Thus, the relaxation process influences the diffusive transport thereby giving rise to non-Fickian effects.

The three types of behaviour i.e. the mechanism of water transport, can be analysed by examination of the plots of water uptake as a function of time. If an active agent is homogeneously dispersed or dissolved in the polymer, its diffusion will

be controlled by the formation of the interface (sharp boundary) and the rubbery state behind the front. Again the active agent release can be characterized by the evaluation of the plot of fractional active agent release vs time. A simple way of analysing the water (penetrant) transport[7,8] and active agent release[9,10] is by the general equation[7]:

$$M_t/M_\infty = kt^n \qquad .....(5)$$

where, M_t/M_∞ is the fractional release of the agent at time t,

k is a constant characteristic of the active agent polymer system and

n is the diffusional exponent characteristic of the release mechanism.

Similarly, in case of penetrant transport M_t/M_∞ is the fractional uptake of the penetrant at time t, k_s is a constant characteristic of the system and n is an exponent characteristic of the mode of transport of the penetrant.

When analysing transport or release data for $M_t/M_\infty < 0.60$, the value of exponent n is a good indication of the transport or release mechanism. Thus, for a device of a slab geometry, a value of n of 0.5 denotes characteristic Fickian mechanism of $\sqrt{t}$ relationship and of 1.0, also known as 'zero order' indicates Case II transport. Values of n between 0.5 to 1.0 are treated as non-Fickian (anomalous) transport. In the case of devices of other shapes the values are 0.43 and 0.85 for a sphere and 0.45 and 0.89 for a cylinder respectively, as computed by Ritger and Peppas[7]. For polydisperse particulate system with which we are

at present dealing, it is not possible to compute the exact values fitting into these mechanisms. However, certain trends can be discerned. For example, for spherical particles of polydisperse distribution, Ritger and Peppas computed values of n as low as 0.3 and 0.45 for Fickian and Case II transport respectively. Further lowering of these values can be expected for a polydisperse system of irregular shape. Study of the release profiles of individual particles will however indicate the actual release mechanism. Statistical analysis is done by plotting log $M_t/M\infty$ vs log t. The 95% confidence level of n are also examined.

Cellulose, a naturally occurring biodegradable polysaccharide has been reported as encapsulating matrix for bioactive agent[11-13]. The direct use of cellulose is reported here with the <u>in situ</u> conversion to viscose and encapsulation by crosslinking, which is similar to that on the encapsulation in starch xanthide matrix[14-16]. Thus, xanthation of cellulose and starch were carried out under identical conditions and stoichiometry for comparison. StX and CellX matrices were studied in detail considering matrix properties and mechanism of release from these matrices. Hence, a comparative study of the encapsulation of carbofuran, a systemic broad spectrum, agricultural pesticide in cellulose and starch xanthide matrices was carried out for investigating the effect of matrix parameters such as degree of swelling, crystallinity, crosslink density, porosity etc.

3.2.3 Release of carbofuran

3.2.3a Crosslink density and molecular weight between crosslinks

Cellulose/starch xanthate undergoes oxidative crosslinking in the presence of oxidizing mixture H_2O_2/H_2SO_4, with the formation of the xanthide linkage.

$$P-O-\overset{\overset{S}{\|}}{C}-SNa \xrightarrow[H_2SO_4]{H_2O_2} P-O-\overset{\overset{S}{\|}}{C}-S-S-\overset{\overset{S}{\|}}{C}-O-P \qquad ...(6)$$

where, P = cellulose/starch.

Thus determination of sulphur content after crosslinking gives a direct measure of the number of crosslinks. The degree of xanthation can also be estimated by acidimetry[17].

Cellulose sodium xanthate is decomposed by mineral acids with the formation of cellulose and carbon disulphide according to following equation.

$$CS\begin{matrix}OP\\SNa\end{matrix} + H_2SO_4 = POH + NaHSO_4 + CS\begin{matrix}OH\\SH\end{matrix} \qquad .....(7)$$

The dithiocarbonic acid further decomposes as follows

$$CS\begin{matrix}\curvearrowright OH\\ S\text{-}H\ \curvearrowleft\end{matrix} = H_2O + CS_2\uparrow \qquad ..... (8)$$

The dithiocarbonic acid is stronger than organic acids of the type of acetic acid, and its salts are only slightly decomposed on treatment with such acids. The amount of sodium xanthate in a viscose solution was estimated by titrating

successively with N-acetic acid and N-sulphuric acid.

Though the sulphur content estimated by acidimetry were found to be same (DS-0.35) as the reactions were conducted under identical conditions, the sulphur content after crosslinking differed, the value for starch xanthide being 10.10% and that for cellulose xanthide being 7.73%, corresponding to DS values of 0.29 and 0.22 respectively (Table 3.4). Thus, starch is more crosslinked than cellulose. This is due to the regenerating tendency of cellulose under acidic conditions.

$$\text{Cell} - \text{O} - \overset{\overset{\text{S}}{\|}}{\text{C}} - \text{S} - \text{Na} \xrightarrow{\text{H}^+} \text{Cell} - \text{OH} + \text{CS}_2\uparrow \qquad \ldots\ldots(9)$$

Along with the crosslinked product there is regeneration of cellulose with evolution of CS_2 and hence decrease in sulphur content in cellulose xanthide. From the sulphur content the average molecular weight between crosslinks computed were 1267 for starch and 1656 for cellulose.

3.2.3b Percentage crystallinity

The encapsulation in cellulose involved mercerization (alkali treatment), viscose formation (xanthation) and cross-linking. The XRD data on percentage crystallisation obtained for all these stages is given in Table 3.5. Crystallinity of original cellulose (Cell) i.e. Cellulose I is reduced on mercerization. Cellulose I (natural form) is having parallel chains and H-bonded structure. Treatment with NaOH disrupts the H-bonded structure of cellulose I (thus reducing crystallinity) and swells the fiber, thereby enabling the chains to undergo a

TABLE 3.4

Sulphur analysis for blank xanthides ($CellX_0$ and StX_0).

Sample code No.	Sulphur (%)	Degree of xanthation		Molecular weight between crosslink (M_c)
		By acidimetry	From sulphur content	
$CellX_0$	7.73	0.35	0.22	1656
StX_0	10.10	0.35	0.29	1267

TABLE 3.5

Percentage crystallinity of cellulose and starch at different stages in the preparation of xanthide.

Sample	Crystallinity (%)			
	Original	Mercerised	Crosslinked	Xanthide swollen in water to equilibrium
Cellulose	57.4	47.3	36.5	38.1
Starch	39.5	-	complete amorphous	-

conformational change (antiparallel chains i.e. cellulose II). Hence, there is reduction in crystallinity. This mercerized cellulose (CellM) was used further for encapsulation and a further decrease in crystallinity was observed due to the introduction of S-S crosslink. Slight increase in crystallinity in the swollen cellulose xanthide may be due to distortion of chains on drying which is relaxed by wetting[18]. Thus crystallinity though reduced was retained even after crosslinking.

Starch with 39.6% crystallinity was converted to complete amorphous structure on xanthation and crosslinking, thus resulting in faster swelling and release than CellX.

3.2.3c Swelling studies

The percentage water uptake by dry polymer (blank i.e. without carbofuran-StX_0, $CellX_0$ and encapsulated with carbofuran-StX & CellX) with time was studied by checking the weight gain by dry polymer obtained after soaking at different intervals of time. The rate of water uptake was quite fast for both blank and encapsulated matrices, the time for reaching equilibrium swelling being in the range of 15-30 min. This is in contrast to the several hours taken by the starch UF matrices[3]. The presence of very large percentage of the less hydrophilic crosslinking component of UF resin could be the reason for the latter.

The swelling data (Table 3.6) for both StX_0, $CellX_0$ and StX_1, $CellX_1$ matrices indicate that the percentage swelling is nearly double for StX matrix as compared to CellX though the degree of crosslinking is higher for the former. This is due to

TABLE 3.6

Swelling data for blank ($CellX_0$, StX_0) and encapsulated ($CellX_1$[a] and StX_1[b]) samples.

Matrix system	Equilibrium swelling (%)	Time required to attain % equilibrium swelling (min)
$CellX_0$	66	15
$CellX_1$[a]	75	30
StX_0	131	30
StX_1[b]	141	30

a = Carbofuran content 5.2%

b = Carbofuran content 5.8%

the structural difference between the two molecules. The order in the highly branched amylopectin and relatively flexible six fold helix of amylose were completely disrupted by the-S-S- crosslinks leading to a completely amorphous structure having free hydroxyl groups and resulted in high water uptake. On the other hand the highly ordered cellulose chains which are almost linearly extended as a result of two fold helix, are only partially disrupted by-S-S-crosslinking, thus reducing its crystallinity and increasing its affinity to water, but not to the extent of starch. The swelling data of the blank and encapsulated matrices are of the same order. The absence of increased swelling in presence of encapsulant indicates that the matrices are nonporous and hence do not exhibit osmotic effect.

Thus, the penetration of water, though it exerts a force on the polymer chains causing them to rearrange, provides greater mobility for the polymer chains allowing them to respond to the stress exerted by penetrant. Thus the overall processes result in polymer relaxation. Each of these processes can be described by a characteristic time. Table 3.6 shows % equilibrium swelling and the time required to attain the same.

3.2.3d Effect of loading

CellX samples with five different loadings of carbofuran in the range of 5 to 27% were prepared and their percentage release with time was measured at 35°C in excess water under near perfect sink conditions. For comparison, StX samples with four different loadings of carbofuran in the range of 5 to 25% were also

prepared and their release was studied. The data was analysed by the generalised equation (5). The corresponding k and n values and the 95% confidence levels of the latter are given in Table 3.7 for CellX and in Table 3.8 for the StX system. Their % release vs time plot are given in Fig.3.4 and 3.5 respectively. For the CellX system, decrease in fractional release rate is observed with increase in loading in the entire range. A linear relationship between log % release and log % loadings is noticed (Fig. 3.6) with negative slope. This is a normal behaviour which is also noticed in the Higuchi derivation[19] for monolithic microporous slab, where the fraction released is shown to be proportional to $1/A^{1/2}$:

$$F_t = (2C_sD_st/Ah^2)^{1/2} \qquad .....(10)$$

where,

F_t - fraction released,

C_s - solubility of active agent in polymer matrix,

D_s - diffusion coefficient of active agent in the matrix,

A - concentration of active agent per unit volume in matrix phase,

h - thickness of slab.

C_s, D_s and h are fixed for a given system, therefore $F_t \propto t$ and $F_t \propto 1/A^{1/2}$.

Similar trend is also noticed with the StX system, though beyond 20%, the trend is reversed which can be seen from the half life values shown in Table 3.7 and 3.8. The faster release at 23.5% loading could be due to the development of porous structure

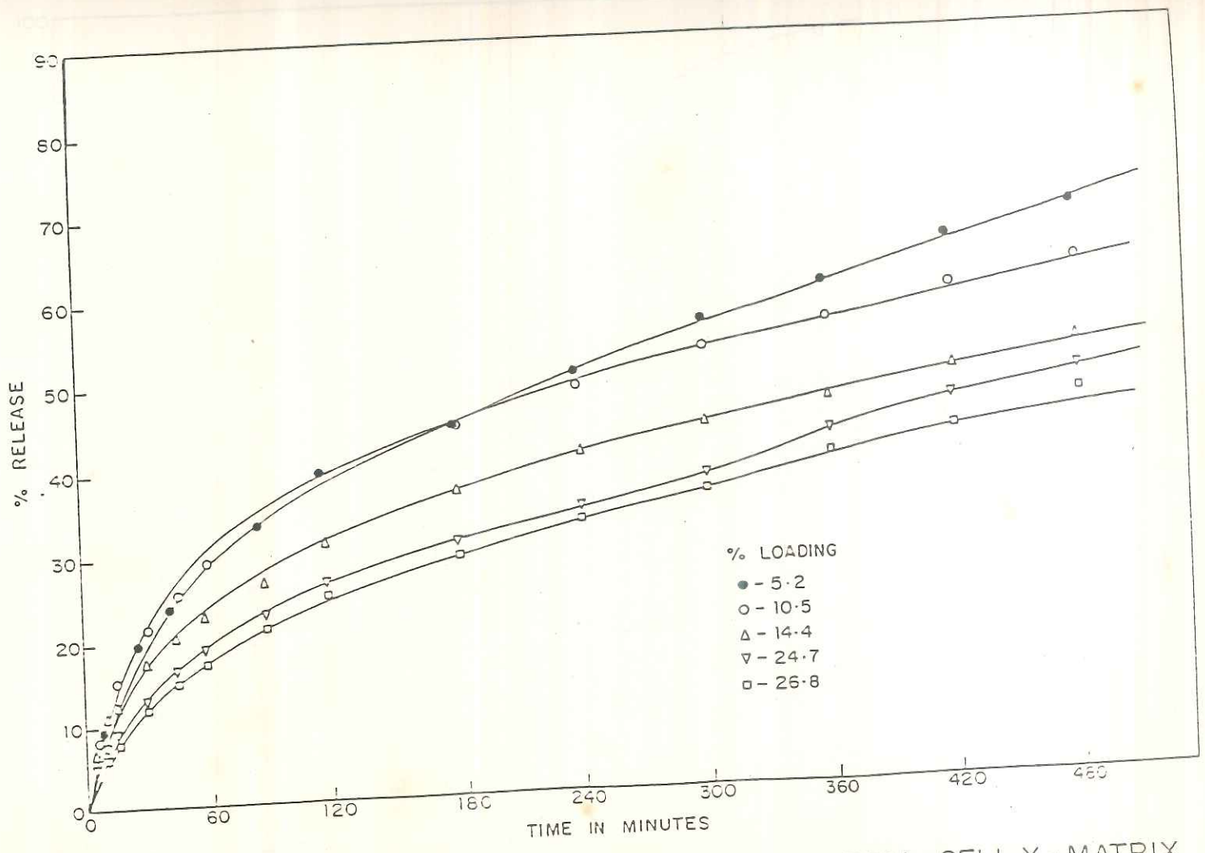

FIG. 3·4: RELEASE PROFILES OF CARBOFURAN FROM CELL X-MATRIX AT FIVE DIFFERENT LOADINGS

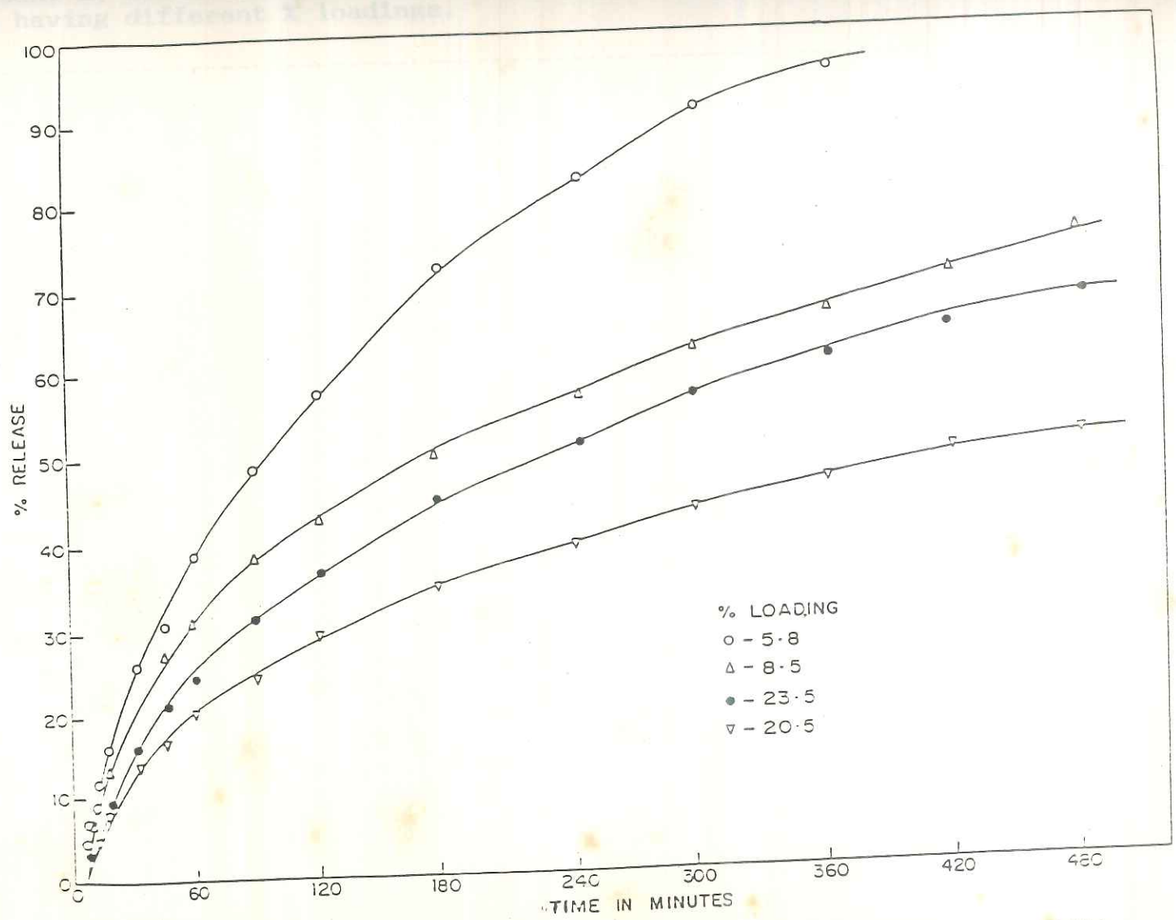

FIG. 3·5: RELEASE PROFILES OF CARBOFURAN FROM STX MATRIX AT FOUR DIFFERENT LOADINGS

TABLE 3.7

Release rate constant k, diffusional exponent n and half life values of CellX carbofuran sample having different % loadings.

Sample code No.	Carbofuran (%)	$k \times 10^2$ $(min)^{-n}$	n	95% confidence level for n		Half-life (min)	Correlation coefficient
				Upper limit	Lower limit		
$CellX_1$	5.2	2.97	0.53	0.56	0.49	240	0.998
$CellX_2$	10.6	4.51	0.44	0.46	0.41	258	0.995
$CellX_3$	14.4	3.78	0.43	0.44	0.42	430	0.998
$CellX_4$	24.7	2.44	0.52	0.54	0.49	524	0.999
$CellX_5$	26.8	1.98	0.49	0.50	0.48	562	0.997

TABLE 3.8

Release rate constant k, diffusional exponent n and half life values of StX carbofuran samples having different % loadings.

Sample code No.	% Carbofuran	k x 10^2 $(min)^{-n}$	n	95% Confidence level for n		Half-life (min)	Correlation coefficient
				Upper limit	Lower limit		
StX_1	5.8	2.69	0.64	0.67	0.61	94	0.998
StX_2	8.6	2.88	0.56	0.69	0.44	180	0.997
StX_3	20.5	1.73	0.57	0.61	0.54	450	0.996
StX_4	23.5	3.88	0.59	0.62	0.56	236	0.997

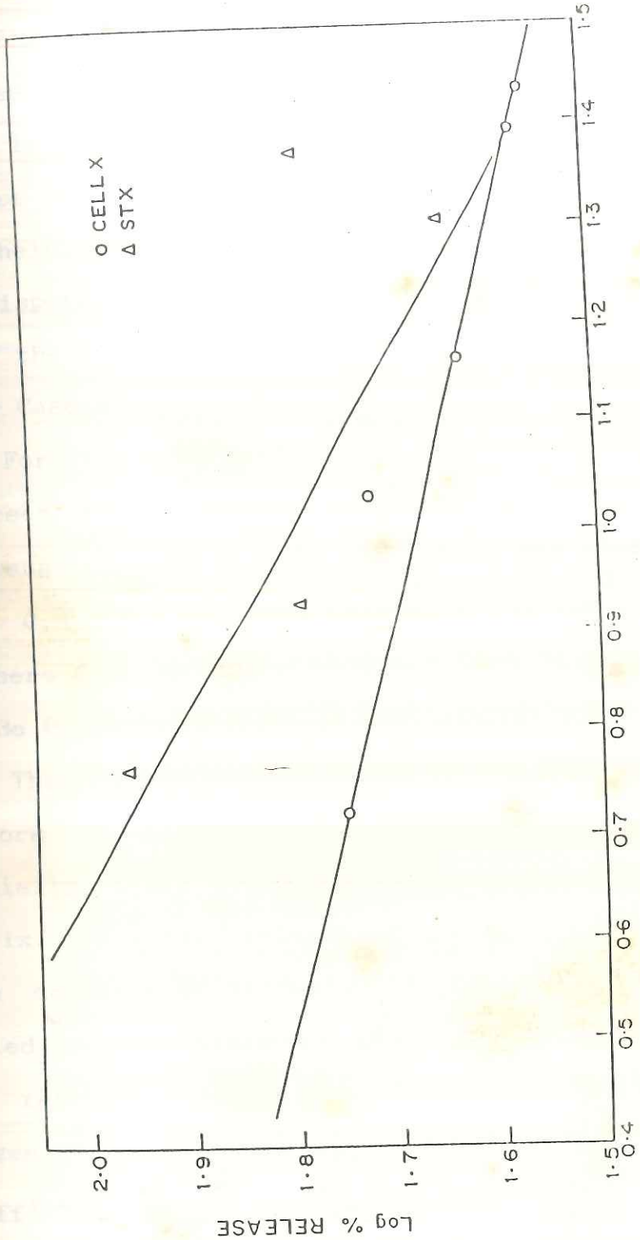

FIG. 3·6 : LOGARITHMIC PLOT OF % RELEASE vs % LOADING
AT t = 300 MINUTES FOR CELLX AND STX MATRICES

at high loadings.

For CellX system, the kinetic release constant k shows a decreasing trend with increase in loading whereas the n value which is characteristic of the overall mechanism of active agent release has no such trend. The n values range from 0.43 to 0.53 and their 95% confidence level vary from 0.41 to 0.56. For this polydisperse system of irregular shapes, these values indicate that the release mechanism could be anywhere from Anomalous to Super Case II.

For the StX system, the decreasing trend in k values is reversed at the maximum loading of 23.5%. The n values are in the range of 0.56 to 0.64 with their 95% confidence level varying from 0.44 to 0.69. The release mechanism could once again be anywhere from Anomalous to Super Case II.

3.2.3e Porosity

The release pattern for a porous matrix is governed by many factors as discussed by Koresmeyer *et al*[10]. The penetrant initially fills the pores and channels near the surface of the matrix. Initial release is controlled by the dissolution and then continuous diffusion of the agent through the penetrant filled pores, before the penetrant diffuses through the matrix and reaches to sufficient level and swells it. In the latter stages both the diffusion through the penetrant filled pores (D_{eff}) and through the swollen matrix (D_{ip}) play important roles. The effective diffusivity of agent, D_{eff} through the penetrant filled pores could be expressed according to equation :

$$D_{eff} = D_{is} \times \frac{\epsilon}{\tau} \qquad .....(11)$$

where,

D_{is} - diffusivity of the agent in the penetrant.

ϵ - porosity.

τ - tortuosity of the pore channels.

The value of D_{is} is directly related to the solubility of the agent in the penetrant as it is a measure of the thermodynamic interaction between the agent and the penetrant. D_{ip} i.e. the diffusivity of the agent through the swollen polymer, depends upon the physical structure of the polymer and is affected by properties such as the crosslink density and degree of crystallinity as well as the thermodynamic interaction between polymer and agent. Thus in principle a wide variation in solubility of the agent by varying the penetrant should correspondingly vary the release rate if the matrix is porous. In case of nonporous swellable system only diffusivity of the agent through swollen polymer assumes importance and thus release of the agent is not dependent on its solubility in the penetrant. As we have seen earlier by varying the % loading for CellX and StX that both matrices are non porous. while StX shows porosity beyond 20% loading. This was confirmed by varying the solubility of the agent.

In the present study mixtures of different proportions of methanol and water were used as penetrant with an 80 fold

variation in solubility of carbofuran in the mixture.

The formulations used were CellX with 10.6% of carbofuran i.e. $CellX_2$ and StX with 8.6% of carbofuran i.e. StX_2. Release profiles of these samples are shown in Fig.3.7 and 3.8 respectively. The data are presented together with the k and n values in Table 3.9 and 3.10.

Results show that neither of the products appears to be porous as the magnitude of increase in release is in no way comparable to those reported by Noren et al[20] and Shukla et al[3].

The release patterns for four different concentrations of methanol in water for CellX are shown in Fig. 3.7 and the k and n values are given in Table 3.9. It is observed that with increase in the solubility of active agent, though the initial release is higher, due to the release of carbofuran at the surface of controlled release formulation, prone to its higher solubility in methanol, the succeeding release is not significantly increased for 50 and 70% methanol.

With 100% methanol there is drastic reduction in release after the initial burst effect. Thus for CellX system (Table 3.9), the n values are in the region of 0.33 to 0.44 upto 70% methanol, indicating a partially or fully matrix controlled release mechanism. However, with 100% methanol, the value drops down to 0.10 indicating complete diffusion control as the matrix penetrant interaction is minimum. This also proves that the mechanism of transport of agent is through macromolecular chain relaxation of polymer in water and aqueous methanol. Thus

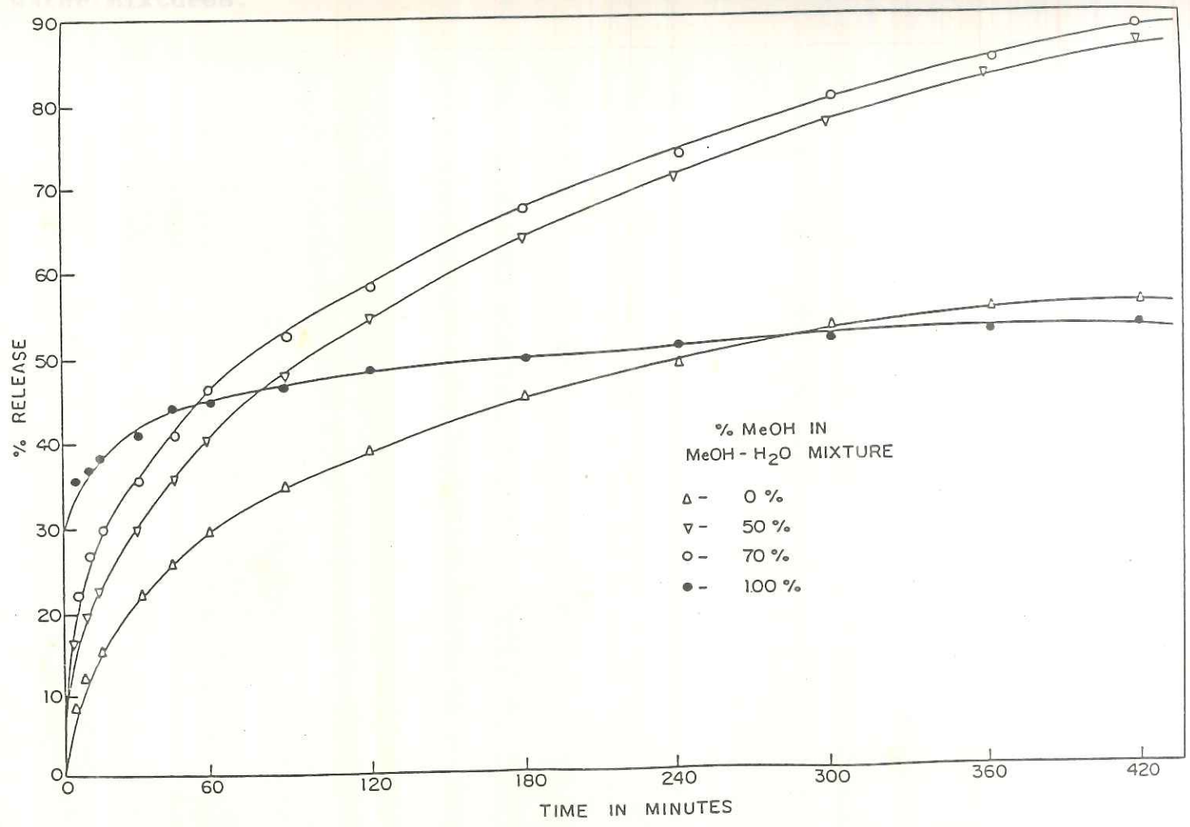

FIG. 3·7 : RELEASE PROFILES OF CARBOFURAN FROM CELLX MATRIX
(Sample No. CELLX2) IN DIFFERENT METHANOL WATER MIXTURES

TABLE 3.9

Release rate constant k, diffusional exponent n and half life values of CellX_2[a] in different methanol water mixtures.

Methanol in water (%)	Solubility of carbofuran x 10^{-3} (ppm)	k x 10^2 $(min)^{-n}$	n	95% confidence level for n		Half-life (min)	Correlation coefficient
				upper limit	lower limit		
0	1.20	4.51	0.44	0.46	0.41	258	0.996
50	10.00	8.08	0.40	0.41	0.38	93	0.999
70	27.00	11.92	0.33	0.34	0.32	79	0.999
100	100.00	28.64	0.10	0.11	0.09	215	0.997

a - Carbofuran content 10.6%

polymer penetrant interaction is negligible in 100% methanol and hence is governed by simple diffusion as shown by n values. From the k and n values we can observe that as solubility of carbofuran in the mixture increases, release rate constant k increases and n value decreases. Thus, for 100% methanol k value is highest whereas n value is lowest. Also the half life values of the carbofuran i.e. time required to release 50% of the carbofuran that is present in the sample is 215 min. Thus, the release in 100% methanol is slower than that in 50% and 70% methanol though only slighly increased than that in water.

For StX_2, the release profiles (Fig.3.8) show that there is increase in release, though not pronounced as you go from 0% methanol to 70%. In 100% methanol the release is further increased as seen from the k and n values (Table 3.10). Release rate constant k increases as solubility increases while n value decreases as k increases. With the StX matrix, the drop in n value to 0.17 from the region of 0.38 to 0.56 is not of the same magnitude as that in the $CellX_2$ indicating that matrix penetrant interaction is still existing and the overall release is also not reduced as seen from the half life value of release (22 min).

The variation in behaviour of the two matrices with variation in solubility of carbofuran can be explained from swelling data for the CellX and StX matrices in 70% and 100% methanol. Thus while varying the penetrant composition with the aim of varying the active agent solubility, the matrix penetrant interactions are also correspondingly altered which alters the

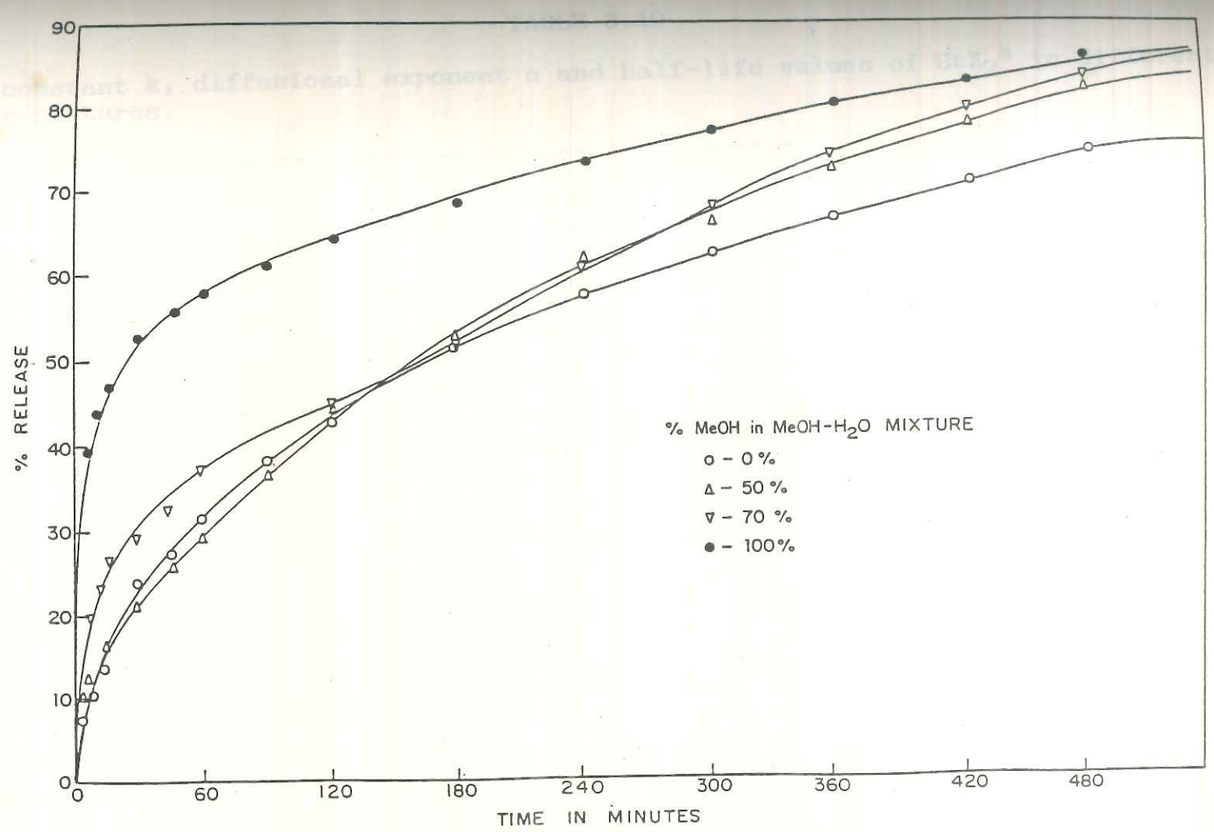

FIG. 3·8 : RELEASE PROFILES OF CARBOFURAN FROM STX MATRIX (Sample No. STX_2) IN DIFFERENT METHANOL WATER MIXTURES.

TABLE 3.10

Release rate constant k, diffusional exponent n and half-life values of StX_2[a] in different methanol water mixtures.

Methanol in water (%)	Solubility of carbofuran x 10^{-3} (ppm)	k x 10^2 $(min)^{-n}$	n	95% Confidence level for n		Half-life (min)	Correlation coefficient
				Upper limit	Lower limit		
0	1.20	2.88	0.56	0.69	0.44	180	0.996
50	10.00	3.85	0.49	0.53	0.46	158	0.995
70	27.00	7.42	0.38	0.43	0.34	163	0.992
100	100.00	29.70	0.17	0.18	0.16	22	0.996

a - Carbofuran content 8.6%

release kinetics. This is illustrated by the swelling data given in Table 3.11. The log log plot of k value against carbofuran solubility in different methanol water mixtures shows a linear relationship (Fig. 3.9).

As observed from effect of loading, StX matrix shows porous nature beyond 20% loading. Release profiles of StX_4 (23.5% carbofuran) were studied by varying the solubility of carbofuran using water and 100% methanol along with StX_2 (8.6% carbofuran) for comparison. The release is increased with increase in solubility. Release rate constant k and diffusional exponent n for StX_2 and StX_4 in water and 100% methanol are given in Table 3.12 for comparison. For StX_4 also the release rate constant k increases as solubility increases and n values range from 0.56 to 0.62 indicating partially or fully matrix controlled release. There is drop in n value to 0.25 for 100% methanol with its 95% confidence level ranging from 0.16 to 0.33. Fig.3.10 shows the comparison of release profiles for StX_2 and StX_4 in 100% methanol and in water. Release is observed to increase remarkably from 0% methanol to 100% methanol for StX_4 [23.5% carbofuran] by 80 fold increase in solubility than that for StX_2 (8.6% carbofuran). This proves the increase in porosity beyond 20% loading.

3.2.3f Single particle release

It is well known that in polydisperse multiparticulate system, the bulk release pattern will not be the same as that of the individual particles and the actual release mechanism can be delineated only from the latter. Dappert and Thies[21] (1978) were

TABLE 3.11

Swelling data for samples $CellX_2$[a] and StX_2[b].

Matrix	Penetrant	% Equilibrium Swelling	Time for Equilibrium Swelling (min)
$CellX_2$[a]	100% water	66	60
	70% aq. methanol	24	15
	100% methanol	14	2880
StX_2[b]	100% water	141	30
	70% aq.methanol	35	240
	100% methanol	6	480

a - carbofuran content 10.6%

b - carbofuran content 8.6%

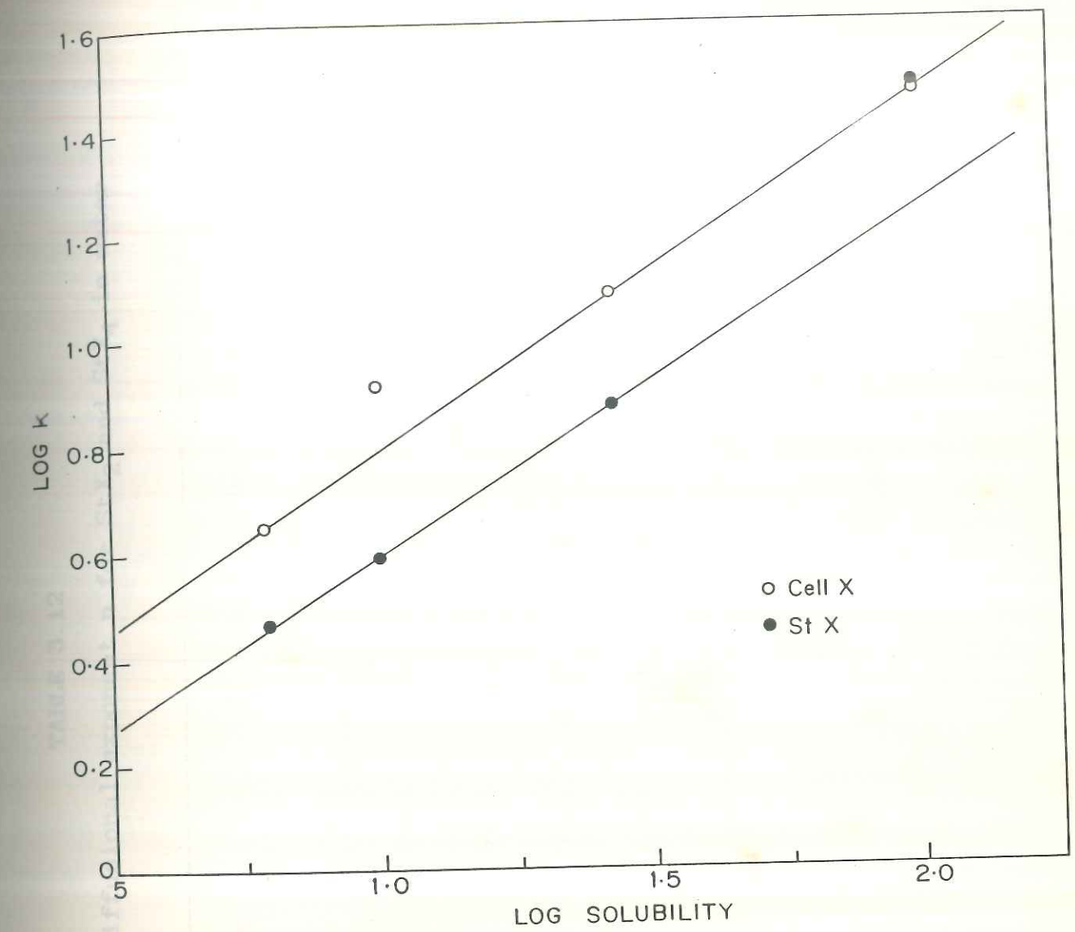

FIG. 3·9 : CORRELATION BETWEEN RELEASE RATE CONSTANT k DETERMINED IN DIFFERENT MEOH - H_2O MIXTURES AND SOLUBILITY OF CARBOFURAN IN THESE MIXTURES

TABLE 3.12

Release rate constant k and diffusional exponent n for StX_2 and StX_4 in water and 100% methanol.

Sample code No.	Solvent	Solubility of carbofuran x 10^{-3} (ppm)	k x 10^2 $(min)^{-n}$	n	95% Confidence level for n		Correlation coefficient
					Upper limit	Lower limit	
StX_2	Water	1.2	2.88	0.56	0.69	0.44	0.996
	Methanol	100	29.7	0.17	0.18	0.16	0.996
StX_4	Water	1.2	3.88	0.59	0.62	0.56	0.997
	Methanol	100	19.99	0.25	0.33	0.16	0.990

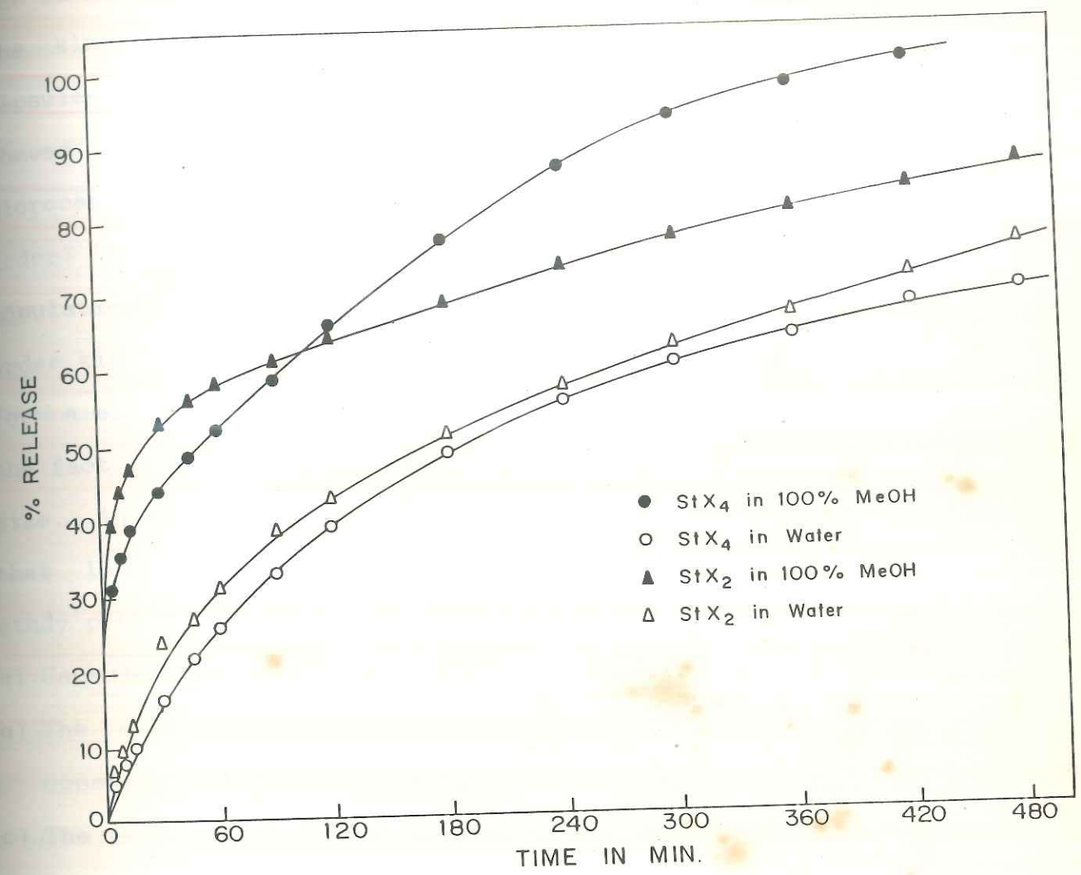

FIG. 3·10: RELEASE PROFILES OF CARBOFURAN FROM StX_2^a AND StX_4^b IN WATER AND 100 % METHANOL

a = CARBOFURAN CONTENT 8·6% , b = CARBOFURAN CONTENT 23·5 %

the first to propose an elegant and simple statistical model for the kinetics of release of heterogeneous populations of microcapsules based on the release behaviour of the individuals. They showed that every individual capsule from a population of microcapsules releases its active agent at a constant rate (zero order) but with different release rate constants. However, the population as a whole releases active agent according to first order kinetics. This difference in the kinetic order of release for a single capsule and that of a population, is attributed to the fact that individual capsules in a given population differ in size, initial active agent content, geometry and other factors that influence the release kinetics of a capsule. Thus their study postulated following general assumptions :

a) Capsules release their payload independent of each other.

b) The external concentration of material in the medium remains constant or under sink conditions.

c) The release functions of individual capsules in the ensembles have the same form and depend on a small number of physical parameters that vary from capsule to capsule.

Hoffman et al[22,23] studied the individual microcapsule release mechanism and observed similar first order release for population and zero order release for the individual and came to the conclusion that the overall release behaviour is not indicative of true release mechanism and the kinetic form of the cumulative release may be altered when the distribution profile of the population changes.

Further empirical investigation of single capsule release behaviour together with population release behaviour of the same capsules was carried out by Gross et al[24] under different physical conditions. The basic factors governing the distribution of parameters are t_∞ and M_∞, when capsules release their payload simultaneously into the same medium. Thus in a population of microcapsules, the individual capsules differ from each other basically due to two parameters M_∞ and t_∞. M_∞ is the initial active agent content (payload) of single capsule and t_∞ is the time required to release its complete payload. Thus with variation in size, the M_∞ and hence the t_∞ will vary. Other factor affecting the t_∞ is wall thickness. Also the defects in the capsule wall like pits and craters, accelerate the release resulting in shorter t_∞ values. For a population release where every individual capsule releases its active agent at constant rate, four types of possible release kinetics are possible, from the basic model developed by Gross et al[24] using different combinations of M_∞ and t_∞. These are zero order, first order, $\sqrt{t}$ order and apparent Hixon and Crowell release. Literature regarding the experimental evidences for the above theory are based on the study on depot devices (microcapsules) whereas Shukla et al[3] have studied single particle release for monolithic system under perfect sink condition. The same procedure has been followed here which has been described earlier.

The present system being both polydisperse and of irregular shape, the bulk kinetics so far reported could only indicate that

the release mechanism could be anywhere from "Anomalous to Super Case II". Ritger and Peppas have predicted n values in case of monodisperse system of spherical shape as 0.43 and 0.85 for Fickian and Case II transport respectively and the values in between for anomalous transport. For CellX carbofuran and StX carbofuran particulate system, assuming the particles to be spherical, we can expect values near about 0.43 and 0.85 respectively for corresponding mechanism of transport.

Single particle release study was conducted in triplicate with the $CellX_4$ system containing 24.7% carbofuran, choosing three particles of similar weight for comparison, though their size and shape may differ. Release profiles of carbofuran from single particles of $CellX_4$ sample carried out in triplicate are shown in Fig.3.11 and the log (% Release) vs log time plot for computing the k and n values are shown in Fig.3.12. Ignoring the initial burst effect (~5%) the latter linear part of the plot is taken for computing these values. Particulars about these particles and their k and n values are given in Table 3.13. Though the weights of the particles are chosen nearly similar, the particle shape and surface area are the variables which may affect the release rate. Despite the variation in weight and non uniform shape, both the k and n values are quite concordant. The maximum release obtained within 8-9 h was upto 30%. The release studies could not be extended further due to instrumental incapabilities. Initial burst effect is observed for initial 10 to 40 min giving about 4 to 5% release. Table 3.13 shows that

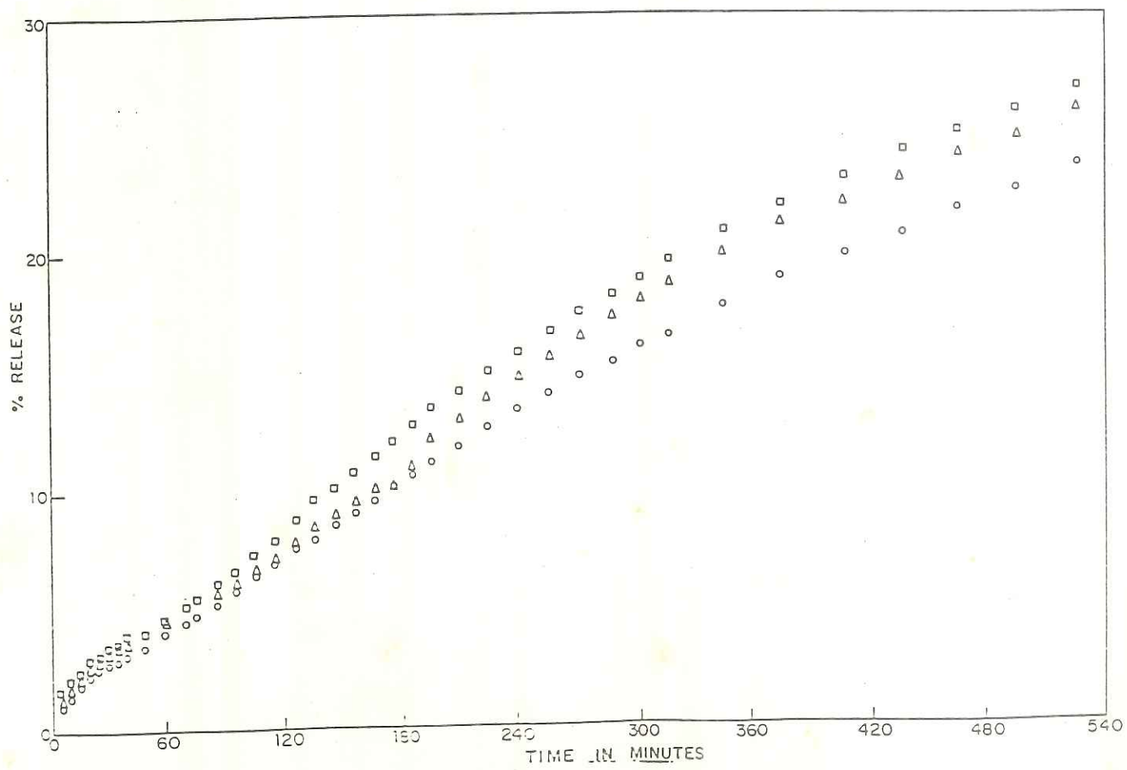

FIG. 3·11 : RELEASE PROFILES OF CARBOFURAN FROM SINGLE PARTICLES OF SAMPLE CELLX$_4$-RESULTS IN TRIPLICATE (CARBOFURAN CONTENT 24·7 %)

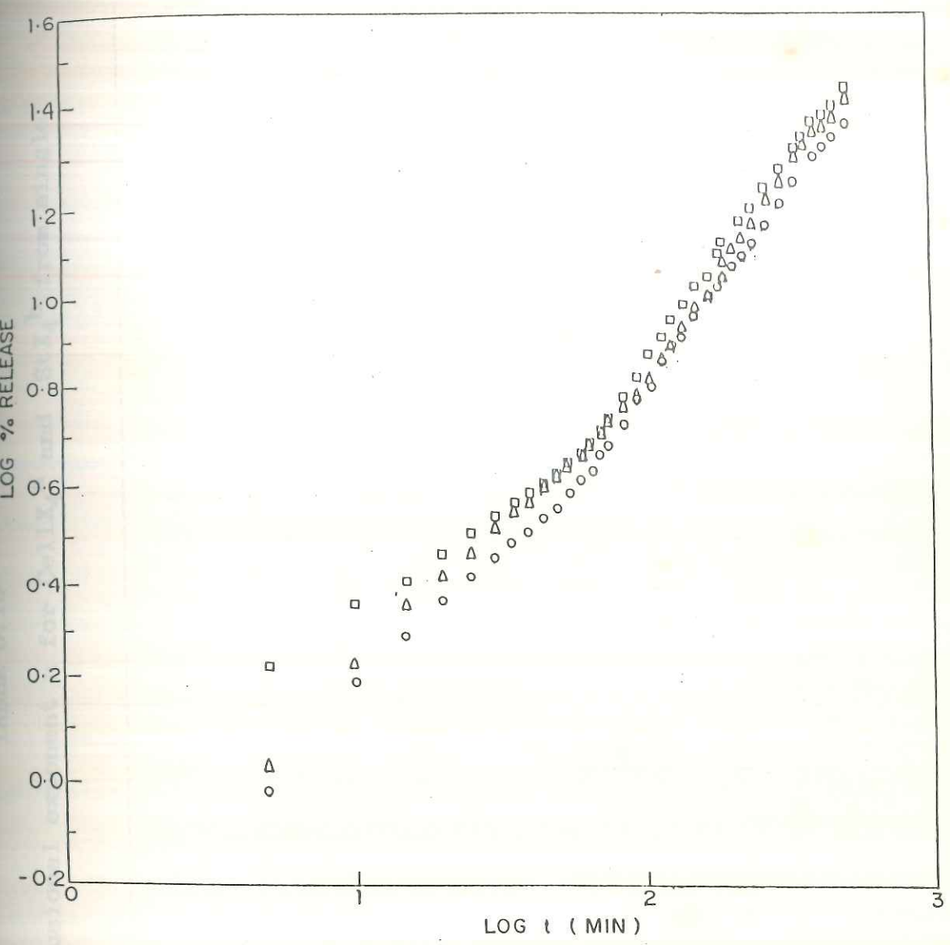

FIG. 3·12 : PLOT OF LOG (% Release) vs LOG t FOR SINGLE PARTICLES OF CELLX$_4$ CARBOFURAN SAMPLE - RESULTS IN TRIPLICATE (CARBOFURAN CONTENT 24·7 %)

TABLE 3.13

Release rate constant k and diffusional exponent n for $CellX_4$[a] and StX_4[b] from single particle release study.

Sample code No.		Sample weight (mg)	k x 10^3 $(min)^{-n}$	n	95% Confidence level for n		Correlation coefficient
					Upper limit	Lower limit	
$CellX_4$[a]	A	3.8	1.51	0.81	0.89	0.73	0.999
	B	3.9	1.65	0.81	0.89	0.74	0.968
	C	3.6	1.60	0.83	0.86	0.82	0.998
StX_4[b]	A	3.2	2.21	0.87	0.93	0.82	0.994
	B	3.4	2.82	0.82	0.85	0.79	0.998
	C	3.6	3.39	0.76	0.85	0.69	0.992

a = carbofuran content 24.7%

b = carbofuran content 23.5%

the n values are in the region 0.81 to 0.83 though their 95% confidence levels are 0.73 to 0.89. We can more or less safely conclude that the mechanism of release is case II as the n value is close to 0.85 computed for a sphere by Ritger and Peppas[7]. Thus, the release of carbofuran is mostly governed by matrix relaxation due to penetration by water. This is also supported by the very fast water uptake followed by a matrix relaxation at a much slower rate as shown by the agent release (Fig. 3.15). Similar results are obtained with the single particle release study of StX system as well, which is carried out as a comparative study. StX_4 system containing 23.5% of carbofuran was chosen for the single particle release study. The data are given in Table 3.13 and the % release vs time and log (% release) vs log time plot are given in Fig. 3.13 and 3.14. Here also ignoring the initial burst effect for 10 to 40 min giving about 4 to 5% release, the latter linear part of the plot was taken for computing the k and n values. Here the maximum release obtained within 8-9 h was upto 50%. There is slightly greater scatter in the k and n values with k values slightly higher than that of CellX system. Also the n values are in the region of 0.76 to 0.87 though their 95% confidence level are 0.69 to 0.93. The average n value is close to 0.82 indicating once again Case II mechanism.

Summing up the k and n values for multiparticle and single particle release system, for StX and CellX systems are given in Table 3.14 and the swelling and release profiles are given in

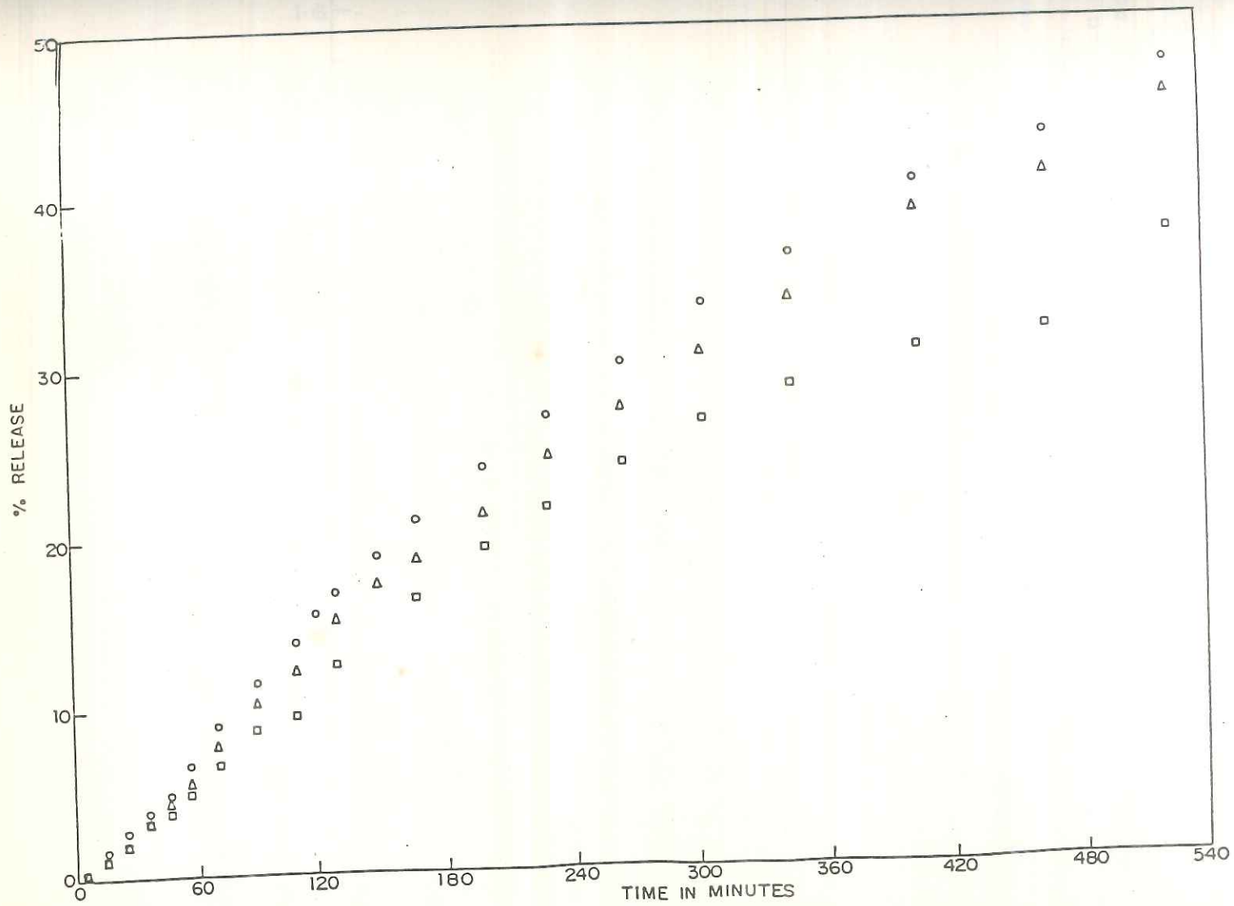

FIG. 3·13: RELEASE PROFILES OF CARBOFURAN FROM SINGLE PARTICLES OF SAMPLE STX_4 - RESULTS IN TRIPLICATE (CARBOFURAN CONTENT 23·5 %)

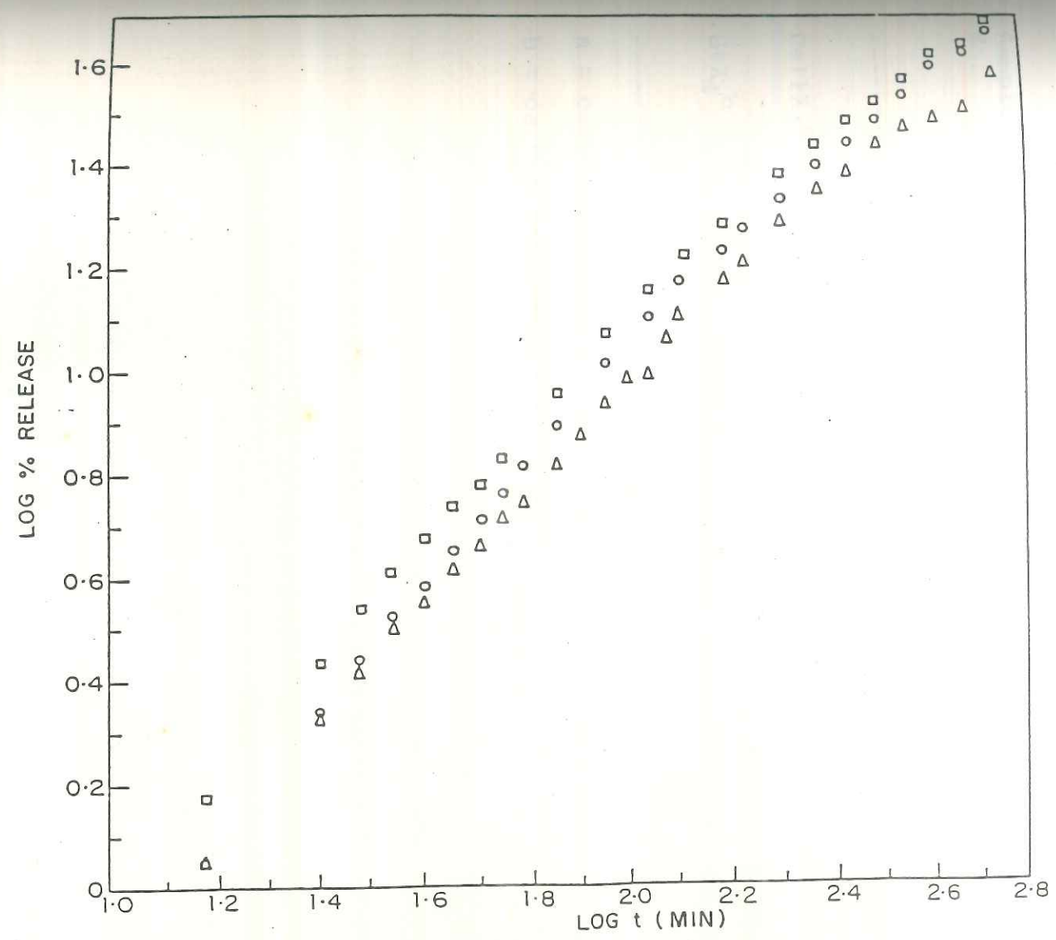

FIG.3·14: PLOT OF LOG (% Release) vs LOG t FOR SINGLE PARTICLES OF STX_4 CARBOFURAN SAMPLE-RESULTS IN TRIPLICATE (CARBOFURAN CONTENT 23·5 %)

TABLE 3.14

Release rate constant k and diffusional exponent n for $CellX_4$[a] and StX_4[b] from bulk release and single particle release study.

Sample No.	Multi particulate release system		Single particle release system	
	$k \times 10^2 (min)^{-n}$	n	$k \times 10^3 (min)^{-n}$	n
$CellX_4$[a]	2.44	0.52	1.58	0.82
StX_4[b]	3.88	0.59	2.80	0.82

a = carbofuran content - 24.7%

b = carbofuran content - 23.5%

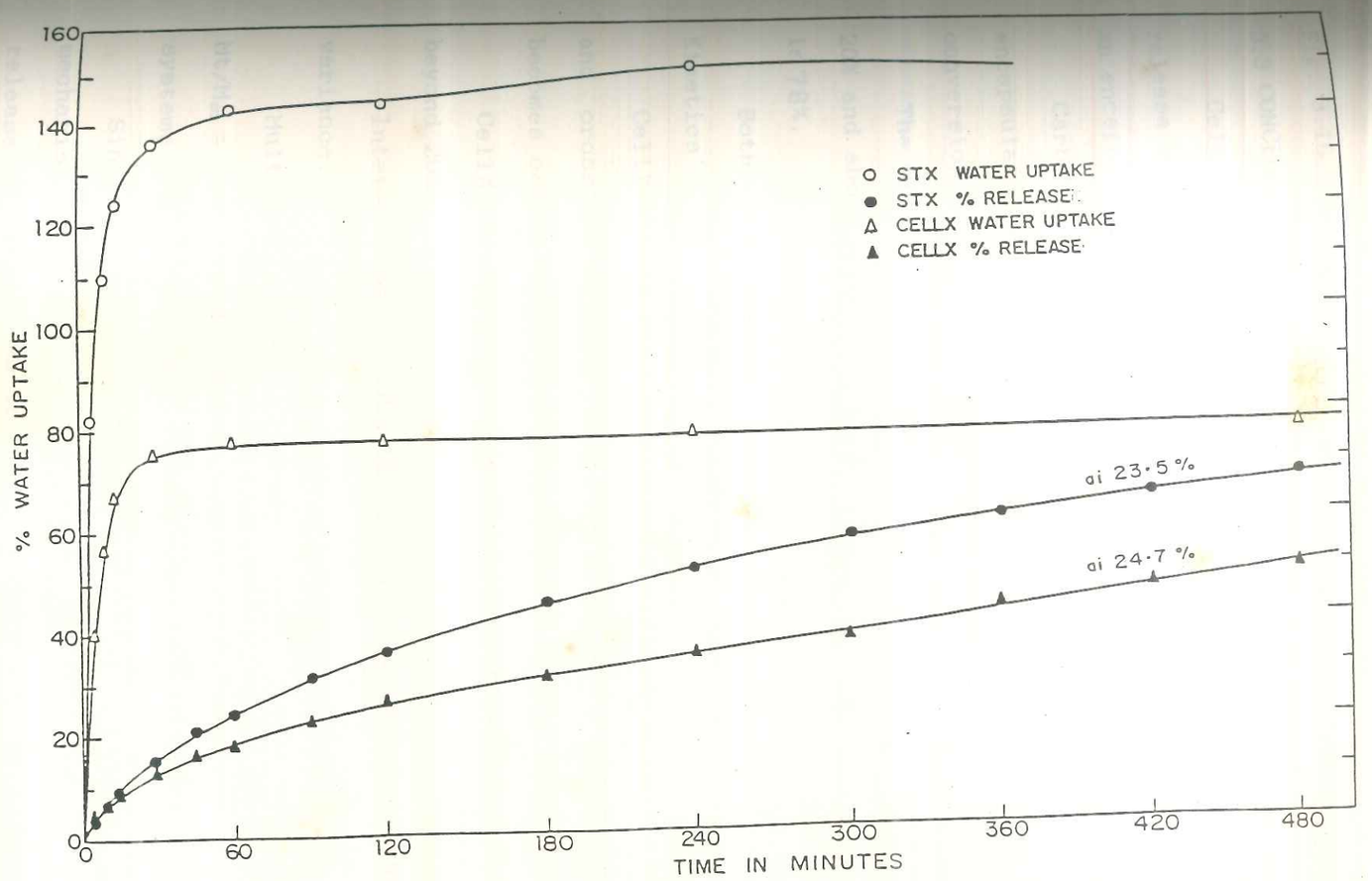

FIG. 3·15: PLOT OF % WATER UPTAKE vs TIME AND % RELEASE vs TIME FOR $CELLX_4^a$ AND STX_4^b SAMPLES

(a = CARBOFURAN CONTENT 24·7% ; b = CARBOFURAN CONTENT 23·5 %)

Fig. 3.15 for comparison.

3.3 CONCLUSIONS

Cellulose xanthide as an encapsulating matrix has comparable release properties to starch xanthide which is widely studied as an encapsulating matrix for agrochemicals.

Carbofuran, a broad spectrum pesticide, can be successfully encapsulated by the direct use of cellulose pulp with the in situ conversion to viscose and encapsulation by crosslinking.

The efficacy of encapsulation is almost 95 % for loadings of 20% and above while the efficacy of encapsulation for 10% loading is 78%.

Both the systems exhibit 'Swelling Controlled Release Kinetics'.

CellX matrix retains its crystallinity even after xanthation and crosslinking and hence has lower water uptake whereas StX becomes completely amorphous and swells more in water.

CellX forms a nonporous matrix whereas StX becomes porous beyond 20% loading.

Interactions of both the matrices with 100% methanol are at variance.

Multiparticulate release data analysed by equation $Mt/M_{\infty} = kt^{n}$ suggests that the release mechanism for both the systems can be anywhere from 'Anomalous' to Super Case II.

Single particle release studies confirm that release mechanism is Case II or zero order for both the systems i.e. the release of carbofuran is mostly governed by matrix relaxation due

to penetration by water.

As the products are in the granular form, they can be used as soil broadcast formulation.

Release kinetics of both the systems exhibit initial burst effect followed by a slower release profile.

REFERENCES

1. Cook, R.F., Analytical Methods for Pesticides and Plant Growth Regulators, Vol.VII (1973) 187-210.
2. Wing, R.E. and Otey, F.H., J.Polym.Sci. Polym.Chem.Ed., 21 (1983) 121-140.
3. Shukla, P.G., Rajagopalan, N., Bhaskar, C. and Sivaram, S., J.Control.Rel., 15 (1991) 153-166.
4. Davidson III, G.W.R. and Peppas, N.A., J.Control.Rel., 3 (1986) 259-271.
5. Harrison, D.J.P., Yates, W.R. and Johnson, J.F., J.Macromol. Sci. - Rev.Macromol.Chem.Phys., C 25(4) (1985) 481-549.
6. Flory, P.J., Principles of Polymer Chemistry, Cornell University Press, Ithaca, New York, (1953) 576-584.
7. Ritger, P.L. and Peppas, N.A., J.Control.Rel., 5 (1987) 37-42.
8. Franson, N.M. and Peppas, N.A., J.Appl.Polym.Sci., 28 (1983) 1299-1310.
9. Singh, S.K. and Fan, L.T., Biotechnol.Prog., 2(3) (1986) 145-156.
10. Korsmeyer, R.W., Gurny, R., Doelker E., Buri P and Peppas N.A., Int.J.Pharm., 15 (1983) 25-35.
11. Bindschaedler, C., Gurny, R. and Doelker, E., J.Control. Rel., 4 (1986) 203-212.
12. Babay, D., Hoffman, A. and Benita, S., Biomateriale, 9 (1988) 480.

13. Ozturk, A.G., Ozturk, S.S., Palsson, B.O., Wheatley, T.A. and Dressman, J.B., J.Control Rel., 14 (1990) 203-213.

14. Shasha, B.S., Doane, W.M., Russel, C.R., J.Polym.Sci., Polym.Lett.Ed., 14 (1976) 417-420.

15. Doane, W.M., Shasha, B.S. and Russel, C.R., In : Controlled Release Pesticides, ACS, Symp.Ser., 53, ACS, Washington D.C., Scher, H.B. (Ed.), (1977) 74-83.

16. Stout, E.I., Shasha, B.S., Doane, W.M., J.Appl.Polym.Sci., 24 (1979) 153-159.

17. Doree, C., In : Methods in Cellulose Chemistry, Whitefriars Press Ltd., London and Tonbridge, Doree, C., (1936) 254.

18. Hirai, A., Horii, F. and Kitamaru, R., J.Poly.Sci., Part C, Polym.Lett., 28 (1990) 357-361.

19. Kydonieus, A.F., In:Controlled Release Technologies: Methods, Theory and Application, CRC Press, Florida, Kydonieus A.F. (Ed), Vol.I (1980) 27.

20. Noren, G.K., Korpi, G.K. and England, G.J., J.Appl.Sci., 24 (1979) 2369.

21. Dappert, T. and Thies, C., J.Membr.Sci., 4 (1978) 99-113.

22. Hoffman, A., Donbrow, M., Cross, S.T., Benita, S. and Bahat, R., Int.J.Pharm., 29 (1986) 195-211.

23. Hoffman, A., Donbrow, M. and Benita, S., J.Pharm.Pharmacol., 38 (1986) 764-766.

24. Gross, S.T., Hoffman, A., Donbrow, M. and Benita, S., Int. J. Pharm., 29 (1986) 213-222.

CHAPTER - IV

CONTROLLED RELEASE CARBOFURAN FORMULATIONS USING CELLULOSE FROM DIFFERENT SOURCES AND AGRICULTURAL WASTES

4.1 EXPERIMENTAL

4.1.1 Materials

. Wood pulp : Processed in NCL (Soft would pulp by sulphite process)

. Rice straw cellulose : Bleached rice straw (prepared in laboratory).

. Peanut shell cellulose : Processed in NCL (Bleached Peanut shell cellulose water prehydrolysed sulphate pulp).

. Rice straw : Indian rice straw

. Peanut shell powder : Indian peanut shell ground to 50 mesh size.

. Sulphuric acid, Hydrochloric acid : L.R. grade

. Sodium hypochlorite : L.R. grade; SD Fine Chemicals Ltd.

. Rest of the chemicals are as described in Section 3.1.1.

4.1.2 Preparation of cellulose from rice straw (RS) and peanut shell powder (PNS)

Since peanut shell cellulose (PNSCell) was available, only rice straw cellulose (RSCell) was prepared in laboratory.

4.1.2a Preparation of RSCell as holocellulose from RS[1]

The term holocellulose is applied to the cellulose isolated from lignified material by chlorination. Sodium Hypochlorite method has proved to be convenient for the preparation of quantities of 200-300 g of cellulose in the laboratory and the product represents as closely as possible the cellulosic tissue of the plant freed from encrusting substances.

41 g of RS was weighed in a 2 L conical flask, followed by

450 ml of distilled water. It was heated to boil and then 5 ml of glacial acetic acid and 12 g of sodium hypochlorite were added to it in portions and at intervals with stirring for 3 h. At the end of 3 h, bleached straw obtained was filtered and washed till it was free from acid. The residue obtained was of Holocellulose and soluble part was lignin. Dry weight of Holocellulose obtained was 29.6 g, i.e. RS contained 72% Holocellulose and 28% lignin (Table 4.1).

4.1.3 Estimation of lignin content

4.1.3a Estimation of lignin in PNS

Lignin content in PNS was determined[1] using the procedure in which cellulose part is solubilised and lignin part remains insoluble and is determined gravimetrically. 2 g of the sample was weighed in a 1 L capacity beaker and treated with 60 ml of 72% sulphuric acid and 15 ml of 18% hydrochloric acid and kept as such at ambient conditions for 24 h. After this, 500 ml of water was added and the mixture was boiled for half an hour and then filtered and washed till it was free from acid and weighed. The residue obtained was lignin. The lignin content in PNS was found to be 36% (Table 4.1).

4.1.4 Analysis of RS, PNS and Cellulose derived from Wood pulp, RS and PNS

4.1.4a Percentage solubility in 18% alkali

Cellulose contains α, β and γ cellulose along with Pentosans. Mercerization involves soaking in 18% NaOH for 1.5 h. Only α cellulose is insoluble in 18% NaOH while other celluloses

along with pentosans etc. are soluble. Similarly some lignin part is soluble in 18% alkali. Since wood pulp (WPCell), RSCell, PNSCell, RS and PNS were used as such without further purification, weight correction was made for the alkali soluble part, before using it for mercerization and xanthation. Table 4.1 describes α cellulose content in WPCell, RSCell and PNSCell and soluble part in 18% NaOH. Similarly, it describes soluble part in 18% NaOH and lignin content in RS and PNS.

4.1.4b Determination of ash content and silica content in WPCell, RS and PNS

Ash contents were determined by combustion and silica contents were estimated by weight difference after volatilising of silica with a drop HF-H_2SO_4. Table 4.2 describes ash content and silica content.

4.1.4c Determination of molecular weight of WPCell, RSCell and PNSCell

Molecular weights of the celluloses from different sources were determined by intrinsic viscosity measurements. Here mercerized samples of cellulose were used after regeneration for viscosity determination, as the same were used further for xanthation and encapsulation. Cupriethylene diamine was used as a solvent for cellulose which was prepared according to Tappi standards[2] and molecular weights were determined by measuring intrinsic viscosity in 0.5 M cupriethylene diamine using a Ubbelohde dilution viscometer at $30^{o}C \pm 0.1^{o}C$. The relationship of Immergut *et al*[3] was used to calculate number average molecular

TABLE 4.1

Alkali solubility, ∝Cellulose content and percentage lignin in cellulose from different sources and agricultural wastes.

Cellulose	Solubility in 18% NaOH (%)	∝Cellulose (%)	Lignin (%)
WPCell	0.83	99.17	-
RSCell	30.80	69.20	-
PNSCell	11.70	88.30	-
RS	44.50	-	28
PNS	12.00	-	36

TABLE 4.2

Ash content and silica content in WPCell, RS and PNS.

Sample Cellulose type	Ash content (%)	Silica content (%)
WPCell	0.0344	0.0008
RS	22.52	6.69
PNS	2.12	0.23

weight.

$$[\eta] = KM^{a} \qquad .....(1)$$

where, K = 1.33 ml g^{-1} and a = 0.905

4.1.4d Determination of percentage crystallinity

Percentage crystallinity was determined from the data obtained from X-ray diffractogram as described in Section 3.1.4c. % Crystallinity for WPCell, RSCell and PNSCell and also for RS and PNS for the three stages, original, mercerized and crosslinked was determined.

4.1.5 Xanthation and encapsulation procedure

The encapsulation procedure involves three steps i.e. mercerization, xanthation and encapsulation. Since WPCell, RSCell, PNSCell and RS and PNS were used as such for mercerization and further for xanthation, alkali soluble part in 18% NaOH was used as a weight correction for mercerization. Percentage alkali soluble part is shown in Table 4.1.

Rest of the mercerization, xanthation and encapsulation procedure was carried out similar to that described in Chapter III (Section 3.1.3b). Description of CRF formulations of carbofuran and blank xanthides are shown in Table 4.3.

Blank xanthides and xanthides encapsulating carbofuran were dried in hot air oven at 50°C for 8 - 10 h and stored in vacuum desiccator over P_2O_5 and used for swelling and release measurements. Mesh size used was $\underline{-5+10}$, corresponding to particle size of 3.35 mm to 1.70 mm.

TABLE 4.3

Description of blank and encapsulated xanthides.

Cellulose type	Sample code No.	Yield in g xanthide		Carbofuran (%)		Encapsulation efficiency (%)
		Blank	Encap.	Calcd.	Found	
WPCell	$WPCellX_0$	11.10	-	-	-	-
	WPCellX	-	14.26	23.40	22.16	94
RSCell	$RSCellX_0$	11.20	-	-	-	-
	RSCellX	-	14.34	23.20	21.89	94
PNSCell	$PNSCellX_0$	11.20	-	-	-	-
	PNSCellX	-	14.07	23.16	20.40	86
RS	RSX_0	11.30	-	-	-	-
	RSX	-	14.35	23.26	21.25	91
PNS	$PNSX_0$	11.35	-	-	-	-
	PNSX	-	13.95	23.20	18.64	78

10 g pulp used for blank xanthide.

10 g pulp + 3.34 g carbofuran used for encapsulated formulations.

Blank - without carbofuran.

4.1.6 Analysis of the blank and encapsulated xanthides

4.1.6a Degree of xanthation

Microanalysis of the blank xanthides was carried out. Degree of xanthation was calculated from the sulphur content as described in Chapter III (Section 3.1.4d).

4.1.6b Molecular weight between crosslinks

The sulphur content obtained by microanalysis was used as direct measure of molecular weight between crosslinks. The calculations of molecular weight between crosslinks are described in Chapter III (Section 3.1.4e). % Sulphur content, degree of xanthation, molecular weight between crosslinks (M_c) are given in Table 4.4.

4.1.6c Determination of carbofuran content

Analysis of CRF of carbofuran prepared using WPCell, RSCell, PNSCell, RS and PNS was carried out for carbofuran content as described in Chapter III (Section 3.1.4b). Table 4.3 describes the carbofuran content.

4.1.7 Swelling and release measurements

Percentage water uptake by the dry polymers and release measurements at different intervals of time were carried out for encapsulated samples as described in Chapter III (Section 3.1.5 and 3.1.6).

4.2 RESULTS AND DISCUSSION

After standardization of encapsulation in cellulose xanthide using cotton pulp as an encapsulating matrix, the work was extended to encapsulation in cellulose from different sources and

agricultural wastes, using same level of carbofuran and keeping the carbon disulphide to polymer ratio constant as that used in cotton pulp.

Thus CRF of carbofuran were prepared using cellulose derived from wood pulp, RS and PNS. Similarly agricultural wastes such as RS and PNS were also used as an encapsulating matrix for carbofuran. Blank matrices without carbofuran were also prepared. Table 4.3 describes the blank xanthides, and xanthides encapsulating carbofuran.

4.2.1 Analysis of the blank xanthides

4.2.1a Percentage sulphur content

Table 4.4 shows data for the percentage sulphur content and degree of xanthation for $WPCellX_0$, $RSCellX_0$ and $PNSCellX_0$ (blank xanthides). It is observed that the sulphur content is more or less similar and the degree of xanthation is not much affected by the variation in source of the cellulose i.e. variation in crystallinity and molecular weight. However, wood pulp being highly crystalline, its sulphur percentage is slightly reduced.

4.2.1b Molecular weight between crosslinks

The sulphur content is directly used as a measure of molecular weight between crosslinks (M_c). Since sulphur percentage is more or less similar, M_c is not much differing (Table 4.4) as the reactions (xanthation and encapsulation) were carried out under identical conditions. However, the sulphur contents are less than theoretical due to the regenerating tendency of cellulose under acidic condition as discussed

TABLE 4.4

Percentage sulphur content, degree of xanthation, molecular weigh between crosslinks (M_c) and crystallinity for $RSCellX_0$, $PNSCellX_0$, and $WPCellX_0$.

Crosslinked Cellulose	Sulphur (%)	Degree of xanthation	Mol.wt. between crosslink (M_c)	Crystallinity
$RSCellX_0$	8.22	0.23	1557	amorphous
$PNSCellX_0$	8.36	0.23	1531	amorphous
$WPCellX_0$	7.90	0.22	1620	Retains parts of its crystallinity

TABLE 4.5

Percentage crystallinity at three different stages in xanthide preparation.

Cellulose type	Crystallinity (%)		
	Original	Mercerized	Crosslinked
Cell	57.4	47.3	36.5
WPCell	57.9	54.4	34.1
RSCell	28.9	32.2	Amorphous
PNSCell	45.8	34.8	Amorphous
RS	27.8	27.4	Amorphous
PNS	30.6	18.8	Amorphous

in Chapter III (Section 3.2.3a).

4.2.1c Percentage crystallinity

X-ray diffraction study was carried out for the original, mercerized and crosslinked cellulose and similarly, for agricultural wastes. Table 4.5 shows that like cotton pulp (Cell), in case of WPCell also there is retention of crystallinity on conversion to xanthide, whereas RSCell and PNSCell when converted to xanthide become totally amorphous. In case of RS and PNS as they contain lignin, the crystallinity observed is less than that of WPCell. Percentage crystallinity in case of RSCell on mercerization is not much affected but is in fact slightly increased due to the removal of non crystalline part that is soluble in 18% alkali. However, RS, PNS and the cellulose derived from them (i.e. RSCell and PNSCell) on crosslinking are converted to completely amorphous structure (Fig. 4.1).

4.2.2 Analysis of encapsulated xanthides

4.2.2a Efficiency of encapsulation

It is observed from Table 4.3 that the efficiency of encapsulation is about 80% to 94%; thus 86% for PNSCell, 91% for RS, 94% for both RSCell and WPCell whereas CR formulations using PNS show slightly less encapsulation efficiency i.e.78 %.

4.2.2b Analysis of the CR formulations for percentage loadings

Determination of carbofuran content in the encapsulating matrix was carried out as discussed in Chapter III (Section 3.1.3b). Repeated extraction of carbofuran from the matrix for second and third time does not show UV absorption for carbofuran

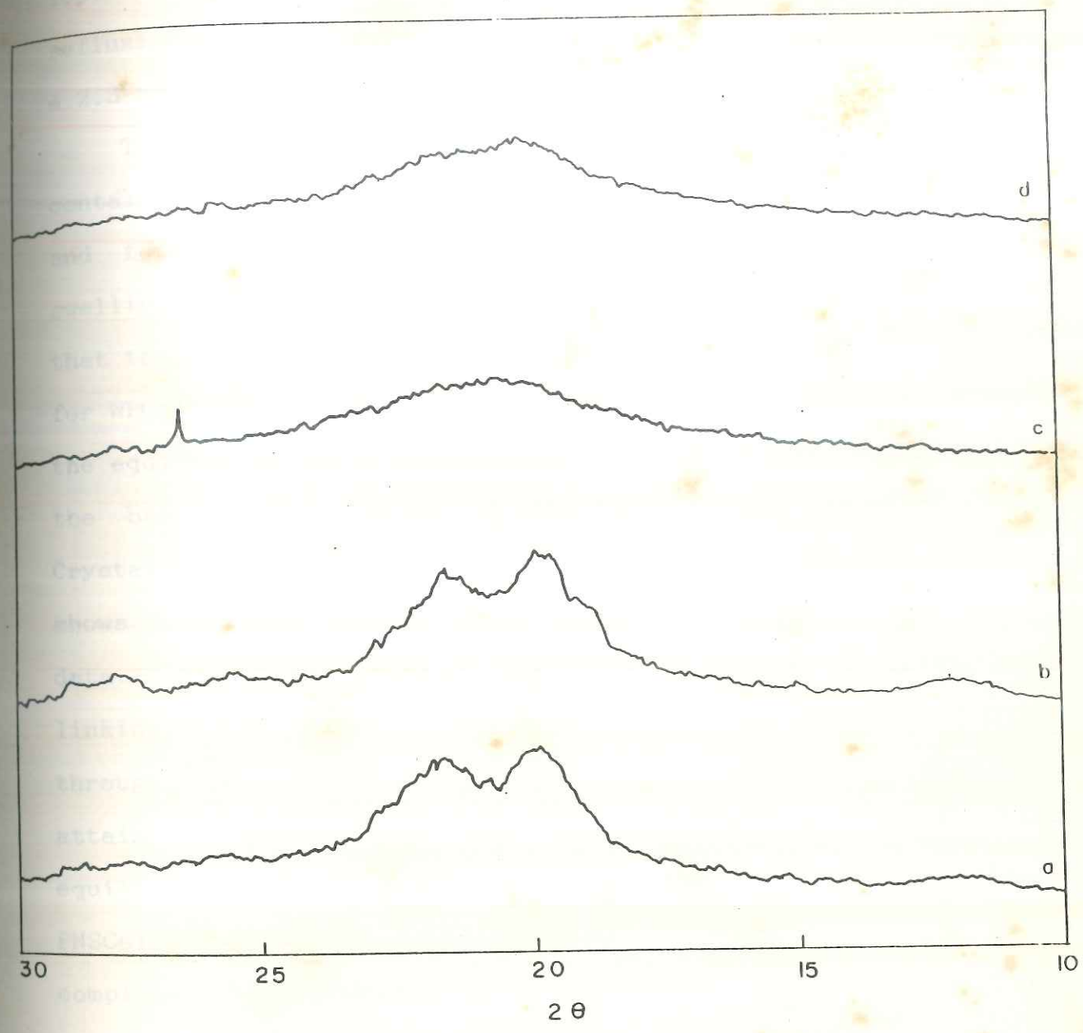

FIG. 4.1 : X-RAY DIFFRACTION PATTERN OF SAMPLES
ⓐ Cell X_0 ⓑ WPCell X_0 ⓒ RSCell X_0 ⓓ PNSCell X_0

i.e. carbofuran is completely extracted from the matrix by refluxing with methanol for 4 h.

4.2.3 Swelling studies

The percentage water uptake by dry polymer (xanthide containing carbofuran) was studied for WPCellX, RSCellX, PNSCellX and for RSX and PNSX. Table 4.6 shows percentage equilibrium swelling and time required to attain the same. It is observed that the percentage equilibrium swelling is more or less similar for WPCellX, RSCellX and PNSCellX but the time required to attain the equilibrium swelling is different. This can be explained on the basis of percentage crystallinity and molecular weight. Crystallinity affects the rate of swelling in water[4,5]. Table 4.7 shows molecular weight, crystallinity and equilibrium swelling data. As WPCellX retains its crystallinity even after cross-linking, more time is required for active agent to diffuse through the crystalline hydrogen bonded structure, finally to attain equilibrium as compared to the time required to attain equilibrium for totally amorphous structures of RSCellX and PNSCellX. However, RSCellX and PNSCellX though both are completely amorphous and their percentage equilibrium swelling is more or less similar, they differ in the time required for attaining equilibrium swelling. This can be explained on the basis of molecular weight of the starting polymer used for the matrix[6].

The correlation of the molecular weight of the starting polymer and crystallinity on equilibrium swelling and time

TABLE 4.6

Swelling data for CRF of carbofuran prepared using WPCell, RSCell, PNSCell and RS & PNS.

Cellulose type	Xanthide encapsulating carbofuran	Equilibrium swelling (%)	Time required for % equilibrium swelling (min)
WPCell	WCellX	69	1440
RSCell	RSCellX	69	120
PNSCell	PNSCellX	74	15
RS	RSX	103	480
PNS	PNSX	114	30

TABLE 4.7

Effect of molecular weight and crystallinity on equilibrium swelling.

Xanthide	Molecular wt. by viscosity ($\overline{M}_v$)	Crystallinity	Equilibrium swelling (%)	Time required to attain % equilibrium swelling (min)
WPCellX	45700	retained	69	1440
RSCellX	79940	Nil	69	120
PNSCellX	33000	Nil	74	15

required to attain the same is shown in Table 4.7. This can also be explained from Fig. 4.2. Thus for RSCellX, the time required to attain equilibrium swelling is 120 min due to its high molecular weight (80,000) as compared to PNSCellX which required only 15 min to attain equilibrium swelling due to its low molecular weight (33,000), thus allowing more intermolecular space for entrance of water as shown in Fig. 4.2. Polymer composition affects equilibrium degree of swelling[7,8]. RS and PNS being used as such, their lignin content affects the percentage equilibrium swelling and the time required to attain the same. Table 4.1 shows lignin content for RS and PNS. PNS with high lignin content of 36% required 30 min for attaining 114% equilibrium swelling, whereas RS with a lignin content of 28% required 480 min for 103% equilibrium swelling.

Thus percentage equilibrium swelling as well as time required to attain it depend on percentage crystallinity of the polymer used, molecular weight and also on the polymer composition, which in turn affect the carbofuran release from the matrix. Also the analysis of the RS and PNS for ash and silica content shows that RS contains more silica than PNS (Table 4.2) leading to less swelling of the RS formulations.

4.2.4 Release of carbofuran

As discussed in Chapter III, like cotton pulp and starch formulations, CRF of carbofuran prepared in this study are found to be swelling controlled[9,10], confirmed by interpretation of release kinetics through equation[11] :

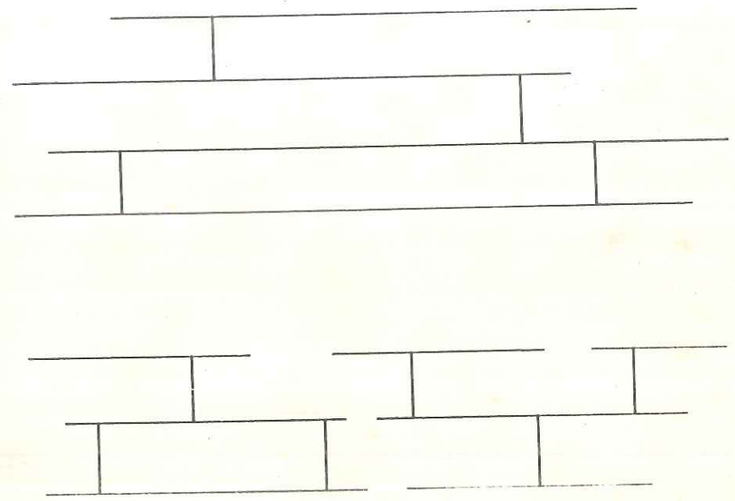

FIG. 4·2 : SCHEMATIC REPRESENTATION OF HIGH MOLECULAR WEIGHT AND LOW MOLECULAR WEIGHT CROSSLINKED POLYMER

$$M_t/M\infty = kt^n \qquad .....(2)$$

Hence, percentage equilibrium swelling is considered here. Also the release kinetics have shown that the release of carbofuran is affected by loading[12] level as well as matrix properties[13] such as crosslink density[4,14], crystallinity[5] porosity[15] etc. which affect the swelling properties of polymers (Chapter III).

In this study, since cellulose from different sources is used, matrix properties such as polymer molecular weight[6,7], polymer composition[7,8] and crystallinity[5,16] are considered which affect the swelling and hence release of carbofuran from the polymer as equilibrium degree of swelling of the polymer, is important in active agent diffusion[17].

The percentage release of carbofuran with time in water from samples WPCellX, RSCellX, PNSCellX, RSX and PNSX were evaluated spectroscopically under perfect sink condition at 35°C. The release profile of carbofuran from these samples are illustrated in Fig. 4.3. The data was analysed by the generalised equation (2) by Ritger and Peppas[11]. The results were plotted as log (% release) vs log t and the release profiles were governed by k and n. The k and n values and 95% confidence level of latter are given in Table 4.8. Not much correlation is found between k and n values. Thus WPCellX having sloweat release has k value of 1.5×10^{-2} with n value of 0.58 whereas RSCellX has k value of 5.0×10^{-2} with n value of 0.37, PNSCellX has k value of 3.6×10^{-2} with n value of 0.59, RSX has k value of 5.6×10^{-2} with n

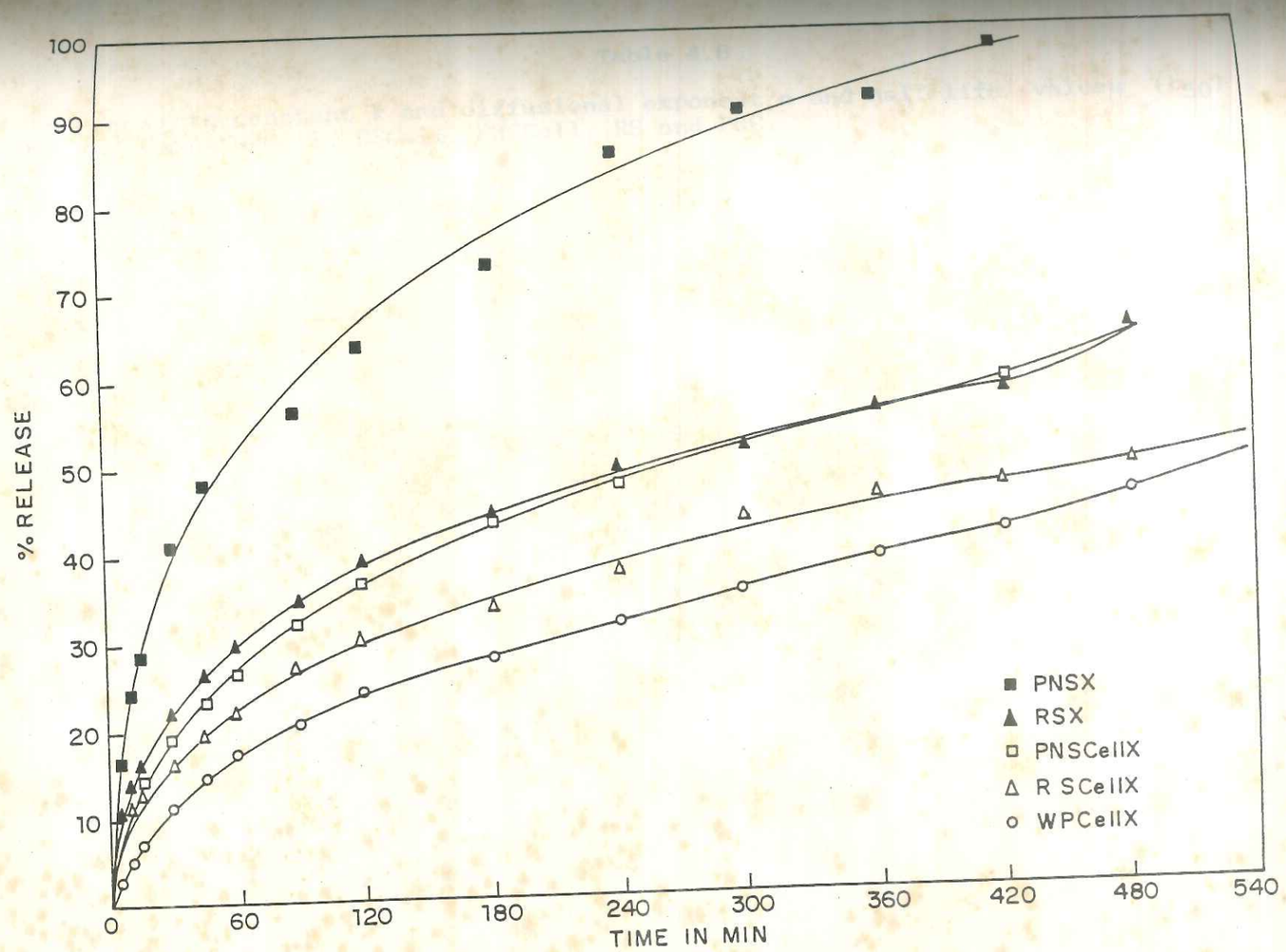

FIG. 4·3 : RELEASE PROFILES OF CARBOFURAN FROM SAMPLES WPCellX , PNSCellX , RSCELLX RSX AND PNSX.

Table 4.8

Release rate constant k and diffusional exponent n and half life values (t_{50}) for CRF using WPCell, RSCell, PNSCell, RS and PNS.

Cellulose	Sample	$kx10^2$ $(min)^{-n}$	n	95% Confidence		t_{50} (min)	Correlation coefficient
				Upper limit	Lower limit		
WPCell	WPCellX	1.50	0.58	0.59	0.54	562	0.998
RSCell	RSCellX	5.00	0.37	0.39	0.35	500	0.996
PNSCell	PNSCellX	3.61	0.59	0.67	0.50	280	0.999
RS	RSX	5.60	0.40	0.42	0.38	266	0.999
PNS	PNSX	8.70	0.44	0.46	0.43	54	0.998

value of 0.40 and PNSX has highest k value i.e. $8.7x10^{-2}$ with n value of 0.44. The 95% confidence level of n are ranging from 0.35 to 0.67. These values of diffusional exponents indicate that the release mechanism is any where between non-Fickian to Super Case II as observed in case of cellulose xanthide (cotton pulp) and starch xanthide. Slightly lower n values are observed for RSCellX and RSX than WPCellX, PNSCellX and PNSX. The n values for RSCellX from the 95% confidence level are ranging between 0.35 to 0.39 and for RSX between 0.38 to 0.42. The n values show that the release mechanism is any where between anomalous i.e. by diffusion of active agent through the polymer undergoing macromolecular relaxation to case II i.e. by macro-molecular relaxation (as stated by Ritger and Peppas for polydisperse spherical particles the n values can be 0.3 for Fickian and 0.43 for Case II and in multi particulate system of irregular shape and size these values can be further reduced).

Slightly higher n values are observed for WPCellX, PNSCellX and PNSX. The 95% confidence level of n for WPCellX, range from 0.54 to 0.59 and for PNSCellX and PNSX they are 0.50 to 0.67 and 0.43 to 0.46 respectively. Thus here also the release mechanism can be by macromolecular relaxation or by diffusion of active agent through the polymer undergoing macromolecular relaxation, but not by simple diffusion.

The k values vary from $1.50x10^{-2}$ to $8.7x10^{-2}$. The higher value of k is observed for PNSX containing high lignin content as compared to RSX, WPCellX, RSCellX and PNSCellX. Thus in case of

agricultural waste, due to presence of lignin content the release is faster than the rest. Taking into consideration equilibrium degree of swelling, RSX had lower percentage equilibrium swelling i.e. 103%, and the time required to attain it was 480 min due to lower content of amorphous lignin (28%) whereas PNSX required only 30 minutes to attain 114% equilibrium swelling which affected the release of carbofuran resulting in faster release of carbofuran than RSX. Thus percentage equilibrium swelling depends upon polymer composition (lignin content), as both matrices are converted to completely amorphous structure after crosslinking. Polymer composition affects the swelling and hence carbofuran release (Fig. 4.3).

Swelling and hence release of carbofuran is also affected by molecular weight of the polymer used. Thus for RSCellX and PNSCellX though the percentage equilibrium swelling is similar, the time required to attain equilibrium swelling is differing, which is 120 min for RSCellX which has high molecular weight (80,000) and 15 min for PNSCellX which has low molecular weight (33,000) leading to slow release of carbofuran from RSCellX than from PNSCellX.

WPCellX has the slowest release of carbofuran compared to RSCellX and PNSCellX which is also observed from the half life values for the release of carbofuran from these matrices (Table 4.8). WPCellX retains part of its crystallinity even after crosslinking like cotton pulp which affects the time required to attain equilibrium swelling, according to the

hypothesis of Graham and Rashid[16]. Similarly, Graham and McNeill[5] have reported that the presence of crystalline domains in the poly(ethylene glycol) based hydrogels influence the release of drug dissolved or dispersed in the polymer.

Percentage equilibrium swelling as well as time required to attain it in case of "Swelling Controlled System" depend upon matrix parameters such as crystallinity of the polymer used, molecular weight and polymer composition which in turn affects active agent diffusion through matrix and hence the release.

Thus the study reveals that the crystalline polymer (WPCell) has the slowest release in comparison to amorphous one. However, in amorphous polymer, the one with highest molecular weight (RSCell) is having slower release while in using agricultural wastes as an encapsulating matrix, the one (PNS) containing higher lignin content is having the faster release. However, the release mechanism is found to be the same.

4.3 CONCLUSIONS

Like cotton pulp, wood pulp also retains its part of crystallinity even after xanthation and crosslinking while RSCellX and PNSCellX are converted to completely amorphous structure. Thus WPCellX exhibits the slowest release compared to RSCellX and PNSCellX.

In case of RSCellX and PNSCellX, RSCell having higher molecular weight exhibits slower release than PNSCell.

In case of agricultural wastes (PNS) higher lignin increases the release.

Thus polymer crystallinity, molecular weight and composition affect the rate of release; however the release mechanism is unaffected.

REFERENCES

1. Doree, C., In : Methods in Cellulose Chemistry, Whitefriars Press Ltd., London Tonbridge, Doree C., (1936) 357-369.
2. Tappi Standards, T230 Su-66. Straus, F.L. and Levy, R.M., "Cupri-ethylene Diamine Disperse Viscosity of Cellulose", Paper Trade J. 114, No.3 (1942) 31-34.
3. Immergut, E.H., Ranby, B.G. and Mark, H.F., Ind.Eng.Chem., 45 (1953) 2483-2490.
4. Korsmeyer, R.W. and Peppas, N.A., J. Mem. Sci., 9 (1981) 211-227.
5. Graham, N.B., McNeill, M.E., Makromol.Chem., Macromol.Symp., 19 (1988) 255-273.
6. Flory, P.J., Principles of Polymer Chemistry Cornell University Press, Ithaca, New York (1953) 576-584.
7. Gander, B, Gurny, R., Doelker, E. and Peppas, N.A., J. Control. Rel., 5 (1988) 271-283.
8. Fransan, N.M. and Peppas, N.A., J.Appl.Polym.Sci., 28 (1983) 1299-1310.
9. Peppas, N.A. In : Recent advance in drug delivery systems, edited by James M. Anderson and Sung Wan Kim (Plenum Publishing Corporation (1984) 279-289.
10. Singh, S.K. and Fan, L.T., Biotech. Prog., 2(3) (1986) 145-156.
11. Ritger, P.L. and Peppas, N.A., J. Control. Rel., 5 (1987) 37-42.

12. Fong, J.W., Nazareno, J.P., Pearson, J.E. and Maulding, H.V., J. Control. Rel., 3 (1986) 119-130.

13. Bote, A.N., Nadkarni, V.M. and Rajgopalan, N., J. Control. Rel. (in press).

14. Lenaerts, V., Dumoulin, Y. and Mateescu, M.A., J. Control. Rel., 15 (1991) 39-46.

15. Noren, G.K., Korpi, G.K. and England, G.J., J.Appl.Polym. Sci., 24 (1979) 2369.

16. Graham, N.B., McNeill, M.E. and Rashid, A., J.Control.Rel., 2 (1985) 231-244.

17. Yasuda, H. and Lamaze, C.E., J.Macromol.Sci.Phys., B5(1) (1971) 111-134.

CHAPTER - V

ENCAPSULATION OF MODEL COMPOUNDS IN CELLULOSE XANTHIDE MATRIX

5.1 EXPERIMENTAL

5.1.1 Materials

. 4 Nitrophenol : Loba Chemie Ind.Ltd.

. Acetanilide : Loba Chemie Ind.Ltd.

. Dimethyl phthalate : Aldrich make.

. 3 Nitrotoluene : Sisco Research Laboratories Pvt.Ltd.

. Nitrobenzene : Indian Drug and Pharmaceutical Ltd.

. All other materials were same as described in Chapter III (Section 3.1.1).

5.1.2 Calibration of model compounds by UV spectroscopy

Standard calibrations of model compounds were carried out on UV spectrophotometer by a procedure described in Section 3.1.2c in order to estimate the amount of model compounds released and the percentage loading. The calibration curves (plots of absorbance vs concentration in ppm) were obtained at respective λmax of each compound. Slopes of these calibration curves were calculated by regression analysis and are given in Table 5.1. Concentration of compound in the solution was calculated by following formula :

$$\text{concentration (ppm)} = \text{Absorbance/slope} \qquad \ldots\ldots(1)$$

5.1.3 Encapsulation of model compounds

Encapsulation of all compounds was carried out as described in Chapter III (Section 3.1.3b). For liquid encapsulants the sieved product was dried in an air oven at 35°C and the dried $\underline{-5+10}$ mesh fraction was used for studies.

Table 5.1

λ max values and slopes of calibration curves for model compounds

Model Compound	λ max (nm)	Slope
Carbofuran	278	0.01298
Acetanilide	238	0.07485
4-Nitrophenol	317	0.06834
3-Nitrotoluene	272	0.0517
Nitrobenzene	267	0.0255
Dimethyl phthalate	276	0.00722

5.1.4 Analysis of the encapsulated samples

5.1.4a Percentage loading

The loading of encapsulant in the sample was determined as described in Chapter III (Section 3.1.4b).

5.1.4b Swelling and release measurements

Swelling and release measurements were carried out as described in Chapter III (Section 3.1.5 and 3.1.6a).

5.2 RESULTS AND DISCUSSION

Crosslinked cellulose was successfully used as a matrix for encapsulation of carbofuran. The release kinetics and mechanism of this system (CellX) are described in Chapter III (Section 3.2.3). To get further insight into the release mechanism, encapsulation of selected model organic compounds was carried out and the effect of physical state and solubility of the encapsulant on the swelling and release kinetics was studied.

5.2.1 Analysis of the encapsulated samples for percentage loading

5.2.1a Efficiency of encapsulation

Five model organic compounds were used along with carbofuran for comparison. Physical properties[1,2] of these model compounds are given in Table 5.2. All compounds were encapsulated in cellulose xanthide (using cotton pulp) matrix, with same level of crosslink density as described in Section 3.1.3b.

Controlled release formulations (CRF) using solid compounds (nitrophenol, acetanilide and carbofuran) were prepared with 10% w/w loadings. However, for nitrophenol, loading of 10% was possible only when a very large excess of the agent was taken.

Table 5.2

Physical properties of model compounds

Model compound	Nature	mp/bp (1 atm) (^{o}C)	Vapour pressure mm of Hg at 35^{o}C	Solubility in water at 25^{o}C (ppm)
Carbofuran	Solid	153.0	-	1000
Acetanilide	Solid	113.5	-	5400
4-Nitrophenol	Solid	114.0	-	16000
3-Nitrotoluene	Liquid	230.0	4.285×10^{-2}	500
Nitrobenzene	Liquid	211	5.486×10^{-3}	1900
Dimethyl phthalate	Liquid	282.0	2.625×10^{-4}	4300

The CRF prepared during the present study are listed in Table 5.3. Efficiency of encapsulation of the model compounds was compared with that of carbofuran. Efficiency of encapsulation of carbofuran (solubility 1200 ppm at 35°C) was about 78% for 10% active agent. However, for acetanilide with water solubility of 5400 ppm, efficiency of encapsulation was reduced to 40% whereas for nitrophenol having solubility of 16000 ppm, it was only 17%. This inverse relationship with solubility is due to the fact that a large percentage of water is present in the system (~90%) at the time of encapsulation and most of the soluble agent is lost in the filtrate. CRF using liquid compounds were also prepared with 10% w/w loadings and could not be loaded beyond 10%. With liquid encapsulants, maximum encapsulation achieved was 51% with dimethyl phthalate with solubility of 4300 ppm in water, whereas nitrobenzene (NB) and 3-nitrotoluene (3NT) had only 28% and 35% encapsulation efficiency with water solubility of 1900 and 500 ppm respectively. The comparatively lower encapsulation efficiency for liquid inspite of lower solubility appears to be related to their volatility[2] (see vapour pressure data in Table 5.2) rather than their solubility in water. Loss of agent during drying seems to be the deciding factor.

The liquid agent also has threshold degree of encapsulation (% active agent content) of ~10%. This seems to be the maximum holding capacity of the matrix beyond which the liquid is squeezed out. During the process of encapsulation, the last step involves the drying of rubbery swollen granules. In this step

Table 5.3

Description of CRF of Cellulose xanthide - Model compounds prepared in this study.

Expt. No.	Encapsulant	% Loading (w/w)		Encapsulation efficiency (%)
		Calculated	Obtained	
1.	Carbofuran	13.6	10.6	78
2.	Acetanilide	31.5	12.6	40
3.	4-Nitrophenol	61.9	10.5	17
4.	3-Nitrotoluene	19.6	6.9	35
5.	Nitrobenzene	37.0	10.8	28
6.	Dimethyl pthalate	22.9	10.1	51

considerable shrinking of the matrix takes place. Whereas the matrix can hold the solid encapsulant, a part of the liquid encapsulant is squeezed out of the matrix and gets evaporated during drying. Actually maximum loading obtained for 3NT was only 6.9% inspite of the attempts made to minimize evaporative losses.

5.2.1b Determination of active agent content in the CR formulations

Active agent content in CRF was determined by refluxing the samples in methanol for 4 h. As observed for cellulose xanthide carbofuran system, there was complete extraction of model compounds in methanol by refluxing for 4 h. Repeated extraction for second and third time did not show any increase in percentage loading.

5.2.2 Release of an encapsulant from swellable polymeric systems

Swelling study was conducted and percentage equilibrium swelling values were evaluated. Equilibrium swelling was reached within 60 min except for dimethyl pthalate. As described in Chapter III (Section 3.2.2), the penetrant uptake and release of an encapsulant from a swellable polymeric system can be analysed by the simple equations (2) and (3) respectively.

For penetrant uptake :

$$(M_t/M_\infty)_s = k_s t^n \qquad \ldots\ldots (2)$$

For release of an encapsulant :

$$M_t/M_\infty = kt^n \qquad \ldots\ldots (3)$$

Also a swellable system when placed in contact with

penetrant, undergoes macromolecular chain relaxation and volume expansion due to absorption of penetrant[3-6]. The three different types of transport mechanism (Fickian, anomalous and Case II) depending upon values of n have been discussed in Chapter III (Section 3.2.2). We will discuss now the 4th type of mechanism called super case II[7]. The value of n for a polydisperse system is difficult to compute as it will depend on the size and shape of the particles as well as the extent of polydispersity. A value as low as 0.45 for case II transport has been computed by Ritger and Peppas for a system of specific polydispersity and any value above this could be referred to as Super Case II. Further reduction in their values could be expected when dealing with a polydisperse system of irregular shapes as in the present case. Here the n values were found to be ranging between 0.79 to 1.03 respectively for nitrobenzene and 3_nitrotoluene which definitely indicate the Super Case II region.

Very few examples are available in the literature which describe the Super Case II transport[7] which is observed at the end of Case II in which gel-glassy interface moves inward at a constant velocity and controls the size of the Fickian wave ahead of this interface. The change in the mechanism of transport from Case II to Super Case II occurs when the Fickian waves advancing from both sides meet at the centre of the polymer. As a result, expansion forces are exerted by the outer swollen gel region on the glassy core. This causes the rapid increase in the concentration of penetrant in the highly stressed glassy core.

Thus Super Case II transport is also called accelerated Case II transport. When the interface velocity is relatively low, the Fickian wave extends far ahead of the moving boundary and Super Case II begins early in the swelling experiment. But when moving boundary advances rapidly as compared to Fickian diffusion into glassy core, Super Case II is observed later during the experiment. If these Fickian waves do not overlap then perfect Case II transport is observed until the end of experiment.

Thus when a swellable controlled release system containing active agent is brought in contact with solvent, thermodynamically compatible with the system, in addition to the swelling (i.e. sorption of solvent), the diffusion of active agent through swollen region (gel) to external medium also takes place (desorption of active agent). Super Case II release mechanism is reported to operate when the value of release exponent n is greater than 0.85 for spherical, 0.89 for cylindrical and 1.0 for thin film. For multiparticulate irregular shape system, these values can be as low as 0.45. Super Case II release of Sudan Red IV dye from polystyrene film in presence of n-hexane has been reported[8]. From the Arrhenius plot it was shown that the mechanism of n-hexane sorption in polystyrene film controls the observed kinetics of dye release.

For cellulose xanthide-carbofuran system consisting of irregular granules, the bulk release showed n values of 0.5 indicating the mechanism could be anomalous to Super Case II transport. Single particle release confirmed the mechanism to be

Case II giving n values in the range of 0.73 to 0.89.

5.2.3 Swelling studies

Swelling studies for the model compound encapsulated systems were carried out. Table 5.4 shows data for % equilibrium swelling and time required to attain it for different model compound encapsulated systems.

Nitrotoluene with lowest solubility is having the least percentage equilibrium swelling, whereas nitrobenzene and dimethylphthalate with higher solubility have increased percentage equilibrium swelling. However, the increase in percentage equilibrium swelling is not as pronounced as the increase in solubility. In case of solid encapsulants also, though the percentage equilibrium swelling is increased with increase in solubility, the increase is not much pronounced. Thus 4-nitrophenol having highest solubility in water (16000 ppm) showed higher percentage equilibrium swelling (71%) whereas carbofuran having lowest solubility showed lower equilibrium swelling (66%) though the time required to attain equilibrium was not differing.

5.2.4 Effect of encapsulant solubility

Results of the study of the effect of encapsulant solubility on release rate in eluting medium for solid encapsulants are shown in Fig. 5.1. Table 5.5 shows data for the k and n values. In Chapter III (Section 3.2.3e), the effect of encapsulant solubility on release rate was studied by changing the eluting medium i.e. by using different ratios of methanol water for

Table 5.4

Swelling data for CRF of model compounds using cellulose xanthide matrix.

Model compound	Solubility (ppm)	Equilibrium swelling (%)	Time required to attain % equilibrium swelling (min)
3-Nitrotoluene	500	54	60
Carbofuran	1200	66	60
Nitrobenzene	1900	67	60
Dimethyl phthalate	4300	67	120
Acetanilide	5400	69	60
Nitrophenol	16000	71	60

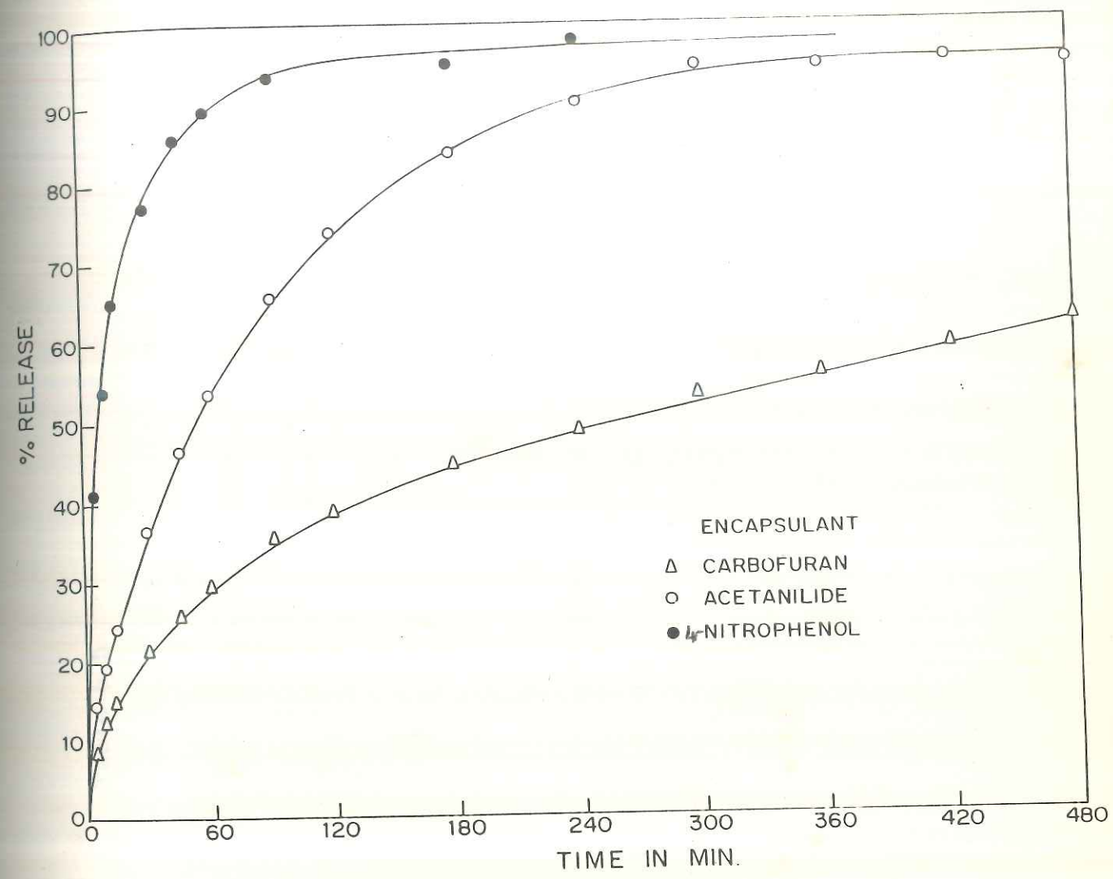

FIGURE 5·1 : RELEASE PROFILES OF Cell X SAMPLES CONTAINING SOLID ENCAPSULANT WITH 10% LOADING

Table 5.5

Release rate constant k, diffusional exponent n and half life values (t_{50}) of cellulose xanthide samples containing solids as encapsulants.

Model compound	Solubility (ppm)	Active agent (%)	k $\times 10^2$ $(min)^{-n}$	n	95% Confidence level of n		t_{50} (min)	Correlation coefficient
					Upper limit	Lower limit		
Carbofurn	1000	10.6	4.5	0.44	0.46	0.41	258	0.999
Acetanilide	5400	12.6	5.6	0.54	0.59	0.52	56	0.999
Nitrophenol	16000	10.5	27.0	0.29	0.35	0.24	8	0.998

cellulose xanthide carbofuran system and it was found that the matrix is non porous as the increase in release by increasing the solubility in the eluting medium though observed was not much pronounced. In the present study variation in solubility was effected by changing the encapsulant itself. Table 5.5 compares the release data of samples with solid encapsulants at ~10% loading. 4-nitrophenol having the highest water solubility showed faster release (t_{50}-8 min) compared to acetanilide (t_{50}-56 min) whereas carbofuran having the lowest solubility showed slower release (t_{50}-258 min) (Fig. 5.1). Similar results have been reported for release of drugs possessing different solubility from poly(2-hydroxyethyl methacrylate)[4] and release of triazine herbicides from Ca-Alginate gel formulations by Pfister et al[9].

Despite this similarity, it will be far fetched to conclude that agent solubility is the only factor governing the release pattern of the three solid agents studied. Fig. 5.1 clearly shows that there is a marked change in the pattern of the release profiles between nitrophenol and carbofuran, the former depicting greater influence of diffusion control. This is also exemplified by the n values obtained from the log (% release) vs log t plots (Fig. 5.2) which indicate the mechanism of transport. Both carbofuran and acetanilide having n values of 0.44 to 0.54 showed greater tendency towards anomalous, Case II or even Super Case II mechanism, where nitrophenol with n value of 0.29 was clearly in the Fickian region. Thus not only a change in rate but also a

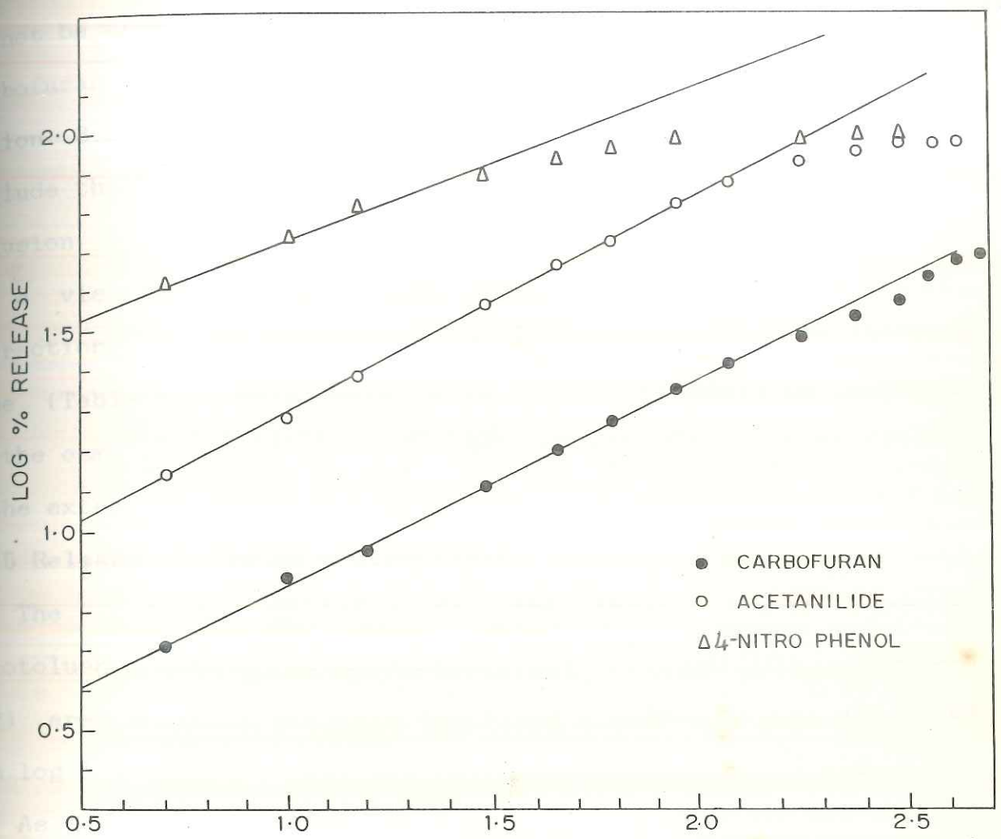

FIGURE 5·2: PLOT OF LOG (% RELEASE) vs LOG t FOR Cell X SAMPLE CONTAINING NITROPHENOL, ACETANILIDE AND CARBOFURAN

change in mechanism is taking place by using solid agents of different solubilities. Though a clearcut mechanism of release can not be established, either for nitrophenol or for acetanilide (carbofuran is shown to release by case II - see Chapter III, Section 3.2.3f), from these multiparticulate data, we can conclude that factors other than agent solubility, such as their diffusion coefficients in swollen matrix, their relative sizes vis a vis the macromolecular mesh and the agent — polymer interactions are also playing important roles. The increase in k value (Table 5.5) with increase in solubility could be ascribed to the osmotic effect which is also reflected to certain extent in the extent of swelling (Table 5.4).

5.2.5 Release of liquid encapsulants

The release profiles for the three liquid agents, nitrotoluene (3NT), nitrobenzene (NB) and dimethyl phthalate (DMP) are shown in Fig. 5.3 and k and n values were evaluated from log log plot of % release vs time (Table 5.6 and Fig. 5.4).

As in the case of solids, the release profile of the liquid with the highest solubility (DMP) shows a clear cut change in mechanism (Fig. 5.3) with a much greater Fickian component. The comparison however stops here since two of the three liquids show much greater trend towards Case II or Super Case II. The n values are 0.82 and 0.95 for 3NT and NB (a clear case of Super Case II) and 0.44 for DMP which could be anomalous. The values of n as high as 0.8 and above for 3NT and NB for a polydisperse system are rather inexplicable. They are rather high even for a

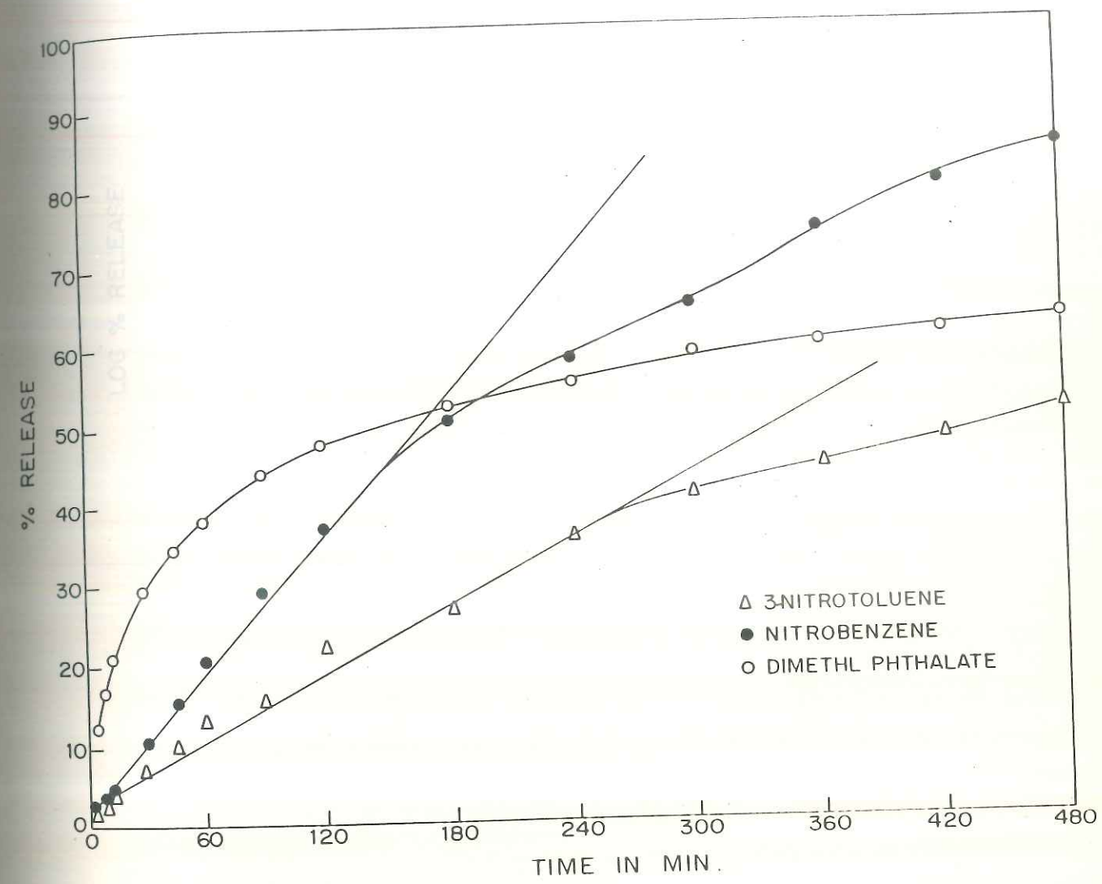

FIGURE 5·3 : RELEASE PROFILES OF Cell X SAMPLES CONTAINING LIQUID ENCAPSULANTS

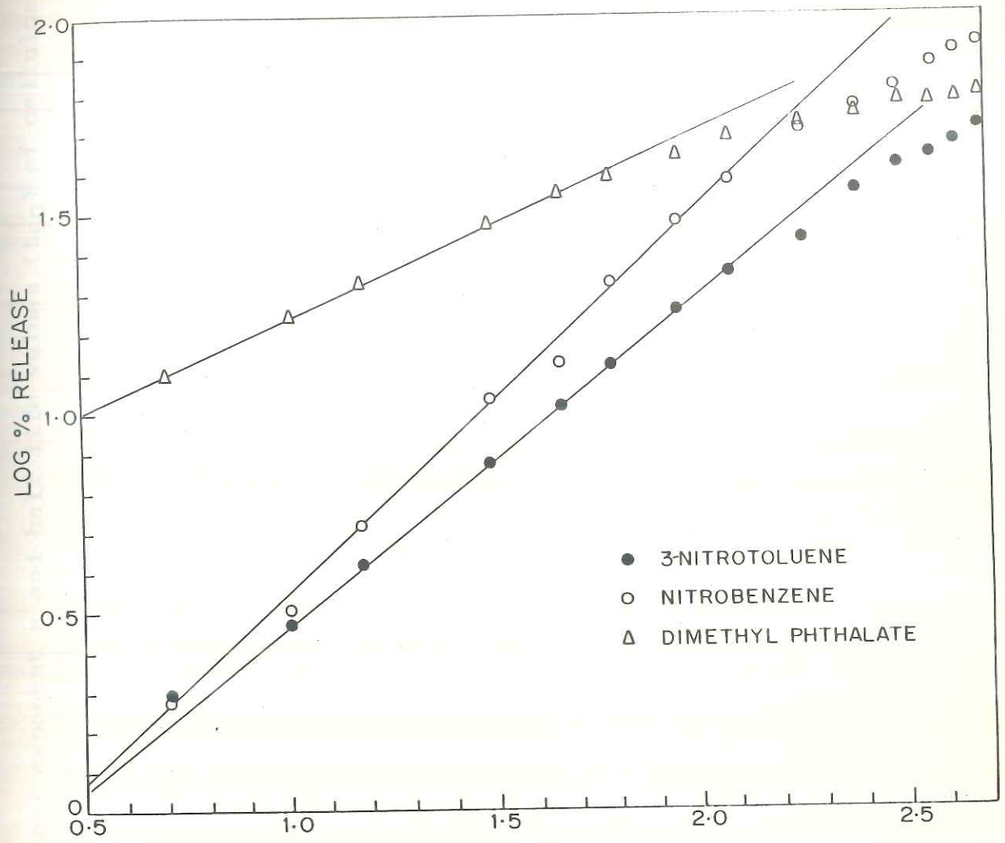

FIGURE 5·4: PLOT OF LOG (% RELEASE) vs LOG t FOR Cell X
SAMPLES CONTAINING 3NITROTOLUENE, NITROBENZENE
AND DIMETHYL PHTHALATE

Table 5.6

Release rate constant k, diffusional exponent n and half life values (t_{50}) of cellulose xanthide samples containing liquid encapsulants.

Model compound	Solubility (ppm)	Active agent (%)	k $\times 10^3$ $(min)^{-n}$	n	95% Confidence level of n		t_{50} (min)	Correlation coefficient
					Upper limit	Lower limit		
3-Nitrotoluene (Mol. Wt. 137)	500	6.9	4.6	0.82	0.84	0.79	465	0.999
Nitrobenzene (Mol. Wt. 123)	1900	10.8	4.11	0.95	1.03	0.86	224	0.999
Dimethyl Phthalate (Mol. Wt. 194)	4300	10.1	64.0	0.44	0.47	0.41	150	0.998

Super Case II mechanism. The release is almost linear upto 40% for both 3NT and NB. In addition, the two liquids also have k values more or less of the same order which are lower by a factor of 10 compared to the solids.

Both these factors such as the much lower release at near zero order indicate boundary layer effect which is overcome after 40% release. The lesser soluble liquids, 3NT and NB appear to be forming a hydrophobic film barrier at the interface of the device and the solvent medium. Transport across this barrier, being the slowest step, also becomes the rate determining step. Hence, for the two hydrophobic liquids 3NT and NB, factors such as their diffusion coefficients in swollen cellulose xanthide matrix and their partition coefficient between the water and swollen matrix become important. In case of 3NT, change of penetrant medium from water to 50% aqueous methanol (Fig. 5.5) does not alter the barrier mechanism. The rate of release is increased but the n value is still 1.0 indicating no change in mechanism (Table 5.7). The more hydrophilic dimethyl phthalate obviously does not form such a film barrier and behaves more like the solids with much higher k values and greater Fickian contribution in its release pattern.

5.3 CONCLUSIONS

The encapsulation efficiency of solid agents is inversely related to their solubilities in water with consequent extents of loss through the filtrate. Liquid agents have a threshold loading level of $\sim$ 10% beyond which the matrix is not able to hold them.

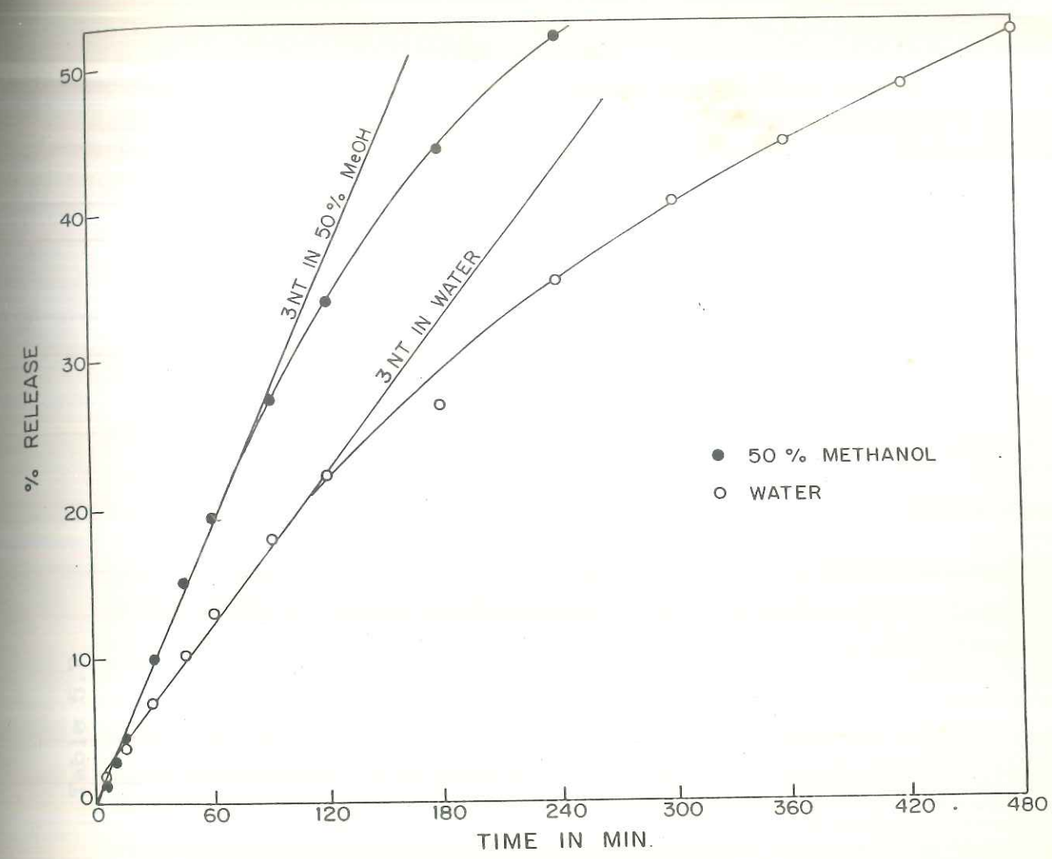

FIGURE 5·5 : RELEASE PROFILES OF CellX SAMPLES CONTAINING 3-NITROTOLUENE IN WATER AND 50% AQUEOUS METHANOL

Table 5.7

Release rate constant k, diffusional exponent n and half life values (t_{50}) of cellulose xanthide containing 3-nitrotoluene in water and in 50% aqueous methanol.

Agent solubility (ppm)	Penetrant	k $\times 10^3$ $(min)^{-n}$	n	95% Confidence level of n		t_{50} (min)	Correlation coefficient
				Upper limit	Lower limit		
500	Water	4.6	0.82	0.84	0.79	465	0.999
8530	50% MeOH	3.15	1.00	1.05	0.96	210	0.999

The excess of agent is squeezed out when the swollen mass shrinks during drying. The encapsulating efficiency of liquids is also dependent on the volatility, as loss of agent by evaporation during drying seems to be the deciding factor.

The extent of swelling of the matrix is somewhat increased with increase in solubility of the agent irrespective of its physical state which could be due to osmotic effect.

The kinetics and mechanism of release of the agent though dependent on their physical state and solubility, is not entirely governed by these two factors only.

Solid agents as a rule exhibit much faster release than the liquids of comparable solubilities. Carbofuran and acetanilide having lower solubilities exhibit anomalous to Super Case II release pattern, whereas nitrophenol with the highest solubility exhibits Fickian mechanism.

The more hydrophobic liquids 3NT and NB exhibit Super Case II release profiles which could be due to forming of a hydrophobic film barrier which controls the release rate.The more hydrophilic DMP however has an anomalous-Case II release profile.

Thus the release mechanism seems to be governed by many factors such as the diffusion coefficient of the agent in the swollen matrix, the agent polymer interactions, the partition coefficient of the agent between the swollen matrix and the eluting medium, their relative size vis a vis the macromolecular mesh etc. These factors to a certain extent are influenced by physical state and solubility of the agent.

REFERENCES

1. Lange's Handbook of Chemistry, John A Dean (Ed), 13th Edition (1985).
2. Boublik, T., Fried, V. and Hala, E., In: The Vapor Pressure of Pure Substances, Elsevier Scientific Publishing Company, Amsterdam (1973).
3. Gander, B., Gurny, R., Doelker, E. and Peppas, N.A., J. Control. Rel., 5 (1988) 271-283.
4. Robert, C.C.R., Buri, P.A. and Peppas, N.A., J. Control. Rel., 5 (1987) 151-157.
5. Singh, S.K. and Fan, L.T., Biotechnol. Prog. 2(3) (1986) 145-56.
6. Franson, N.M. and Peppas, N.A., J.Appl.Polym.Sci., 28 (1983) 299-1310.
7. Hopfenberg, H.B., J.Membr.Sci., 3 (1978) 215-230.
8. Hopfenberg, H.B. and Hsu, K.C., Polym. Engg. Sci., 18 (15) (1978) 1186-1191.
9. Pfister, G., Bahadir, M. and Korte, F., J. Control. Rel., 3 (1986) 229-233.

CHAPTER - VI

INCORPORATION AND RELEASE OF CARBOFURAN FROM MODIFIED CELLULOSE MATRIX

6.0 Modified cellulose for encapsulation of carbofuran

The chemical structure of cellulose can be changed in three ways :

a) by preparing a derivative, e.g. ester or ether;

b) by preparing a crosslinked cellulose i.e. a network structure; or

c) by preparing a branched cellulose i.e. a graft copolymer.

As we have studied the incorporation and release of carbofuran by dispersing carbofuran in cellulose xanthate and subsequently crosslinking to cellulose xanthide, incorporation and release of carbofuran using modified cellulose was carried out through graft copolymerization with vinyl monomer. Graft copolymerization is a novel method by which properties of (natural) polymers can be modified. Along with new forms of polymeric materials grafting of synthetic polymers on to cellulose produce materials of new properties intermediate between those of cellulose and synthetics[1,2], without destroying the crystallinity of cellulose[1,3].

Change in properties that can be brought about by grafting on to cellulose are hygroscopicity, water repellency, soil resistance, bactericidal properties, thermal stability etc[4-10].

Modification of cellulose was carried out by introduction of hydrophobic (polystyrene) and hydrophilic (polyacrylamide) branches on to cellulose backbone. Carbofuran was entrapped in the crosslinked graft copolymer (after xanthation) and its release was studied in relation to the factors such as polymer

composition, crystallinity, molecular weights and molecular weight distribution (MWD) of the grafted chains and grafting frequency. Effect of above factors on the swelling of the matrix which affects the diffusion and hence release of carbofuran through the matrix was also studied.

PART - I

Incorporation and Release of Carbofuran from Crosslinked, Cellulose Grafted with Polystyrene

6.1 EXPERIMENTAL

6.1.1 Materials

.Styrene, acrylonitrile: Styrene and acrylonitrile monomers were freed from inhibitor by washing with 8% solution of NaOH. Alkali was removed by repeated washing with distilled water. Monomer was then dried over anhydrous calcium chloride overnight, distilled under vacuum and stored in refrigerator.

. Ceric ammonium nitrate: A.R. grade, Qualigens

. Nitric acid : A.R. grade

. Sulphuric acid : A.R. grade

. Benzene, chloroform : distilled and used.

. Acetic anhydride : A.R. grade from S.D. Fine Chem.Ltd.

. Initiator solution : A 0.1 M solution of initiator was prepared by dissolving the required amount of ceric ammonium nitrate $[Ce(NH_4)_2(NO_3)_6]$ in 1 M nitric acid[11]. This stock solution was diluted to the required concentration just before use. The stock solution stored for more than three days was discarded and fresh solution was prepared, as the stock solution is reported to lose activity after 4 days[12].

All other materials used were same as described in Chapter III (Section 3.1.1).

6.1.2 Grafting procedure

Grafting was carried out according to Ref. 11 with a few variations such as application of pretreatment technique[12] to cotton pulp. 8 g of cotton pulp with moisture correction was preswollen for 30 min with 200 ml of water in a three neck

R.B. flask. 20 ml of styrene was added to the pulp and the contents were stirred vigorously in nitrogen atmosphere for 15 min to facilitate styrene diffusion into cellulose. The reaction flask was then kept in thermostat at 65.5°C. After adequate purging with nitrogen, initiator solution was added [dissolve 1.0852 g of Ceric ammonium nitrate (CAN) in 200 ml of water containing 1.3 ml of conc. nitric acid]. Nitrogen was bubbled throughout reaction period of 4 h. After completion of reaction, graft copolymer along with homopolymer was filtered and dried at 50°C for 8-10 h.

Grafting experiments were conducted, both without acrylonitrile (AN) and in the presence of small amount of AN monomer[13] (1 and 2.5 ml) (Table 6.1).

Above grafting procedure is mentioned for 0.005 M initiator (CAN) concentration. In the light of preliminary trials conducted, grafting was carried out under nitrogen, by varying the conditions in order to get variation in grafting frequency as follows :

1. At the initiator concentrations of 0.004 M and 0.005 M respectively for 4 h at 65.5°C keeping the monomer to cotton ratio (2:1) constant.
2. At the initiator concentration of 0.005 M, for 4 h at 70°C, with other variables being constant.

6.1.3 Isolation of homopolymer

The grafted pulp was extracted with benzene in soxhlet apparatus (for 15 - 20 h) till no more polystyrene is extracted

and then dried at 50°C for 5-6 h and weighed. The grafted pulp, after removal of homopolymer was used for xanthation and further encapsulation.

6.1.4 Hydrolysis of graft copolymer and isolation of grafted polystyrene chains

Separation of grafted branches from cellulose backbone was carried out by acetolysis [12]. The hydrolysis was carried out in a 300 ml R.B. flask with ground glass joint stoppers. Thus 2 g of graft copolymers was swollen in N,N-dimethylformamide and then transferred to the flask containing the hydrolysis mixture. The mixture consisted of 70 ml of acetic anhydride, 70 ml of benzene and 12 ml of H_2SO_4 (72%). The reaction flask was kept stirred at 60°C for 72 h. After completion of the reaction the sample was precipitated in methanol, filtered, redissolved in chloroform and again reprecipitated with methanol for 3-4 times. Isolated polystyrene was dried under vacuum at 60°C.

6.2. Characterisation of the graft copolymer

6.2.1a Percentage grafting

Percentage grafting was calculated as follows :

$$\text{Graft } \%(G) = \frac{W_2 - W_1}{W_1} \times 100 \qquad \ldots\ldots(1)$$

where, W_1 is the weight of the pulp taken and

W_2 is the weight of the grafted pulp after extraction of homopolymer.

6.2.1b Molecular weight determination by viscosity

The viscosity of cellulose was determined in cupriethylene-diamine solution at $30^{o}\pm0.1^{o}C$. The viscosity average molecular weights were calculated using correlation (2) as described in Chapter IV (Section 4.1.4c).

$$[\eta] = 1.33 \times 10^{-4} M^{0.905} \quad \ldots\ldots (2)$$

The viscosity of polystyrene separated from the graft copolymers was determined in chloroform at $30^{o}\pm0.1^{o}C$ utilizing an Ubbelohde viscometer. The viscosity average molecular weights were calculated from the intrinsic viscosity $[\eta]$ on the basis of relation[14] :

$$[\eta] = 4.9 \times 10^{-5} M^{0.794} \quad \ldots\ldots (3)$$

6.2.1c Molecular weight distribution (MWD) determination by gel permeation chromatography (GPC)

Molecular weight distribution (MWD) ($\bar{M}_w/\bar{M}_n$) of polystyrene separated from SgCell determined by Waters GPC II using columns 10^6, 10^5, 10^4, 10^3, 500x2 and 100x2, $A^{o}\mu$ styragel and RI detector. Freshly distilled and dried tetrahydrofuran (THF) was used as eluent at ambient temperature.

6.2.1d Grafting frequency

Grafting frequency i.e. chains of polystyrene (Pst) per chain of cellulose was calculated from the data such as weight % of polystyrene and cellulose in the graft copolymer and their molecular weights determined by viscosity, using the following formula :

$$\text{Graft freq.} = \frac{\%\ \text{Pst in the graft copolymer}}{\%\ \text{cellulose in the graft copolymer}} \times \frac{\bar{M}_n \text{ of cellulose}}{\bar{M}_n \text{ of polystyrene}} \quad \ldots\ldots(4)$$

Percentage of polystyrene in the graft copolymer was calculated using formula :

$$\%\text{Pst} = \frac{W_2 - W_1}{W_2} \times 100 \quad \ldots\ldots(5)$$

subtracting %Pst from 100, percentage cellulose in the graft copolymer was obtained.

6.2.2 Techniques used for characterization of the graft copolymer (SgCell)

6.2.2a FTIR Spectrophotometry

FTIR spectra of SgCell and blends of cellulose and separated grafted Pst were taken on Perkin Elmer FTIR Spectrophotometer.

KBr pellets of the samples of cellulose, SgCell and of the blend using cellulose and separated styrene from SgCell were prepared by thorough mixing of 300 mg KBr with 1 mg of sample (finely ground under liq. nitrogen) and pressing at room temperature under vacuum (0.1 mm of Hg) at 13000 pounds pressure for 7 min. Blank KBr pellets, without any sample were also prepared.

6.2.2b ^{13}C NMR

Structural characterization of SgCell was carried out using solid state ^{13}C CP/MAS NMR and is described in Chapter VII.

6.2.2c Thermogravimetric analysis

Thermogravimetric analysis was made using a Netzsch STA 409 thermogravimetric analyser (TGA), under nitrogen atmosphere. The

heating rate used was 5°C min^{-1} and the temperature was measured by a Pt-Pt Rh (10%) thermocouple.

6.2.2d X-ray diffraction study

X-ray diffraction study of SgCell was carried out for the three stages viz., original, mercerized and crosslinked.

6.3 Preparation of CR formulations of carbofuran using SgCell

Of the various graft copolymers prepared, three graft copolymers with varying grafting frequency were selected and used for the preparation of CRF of carbofuran.

CR formulations of carbofuran using SgCell were prepared through steps such as mercerization, xanthation and encapsulation through crosslinking as described in Chapter III (Section 3.1.3b). Blank xanthides without carbofuran were also prepared.

6.3.1 Analysis of the blank (without carbofuran i.e. $SgCellX_0$) and encapsulated (with carbofuran i.e. SgCellX) graft copolymer xanthides

6.3.1a Sulphur analysis and degree of xanthation

The $SgCellX_0$ prepared using grafted pulp of different grafting frequency were checked for degree of xanthation. Since only cellulose part takes part in xanthation and crosslinking, % sulphur contents obtained for $SgCellX_0$ were assigned to the cellulose moiety for computing the degree of xanthation using equation as described in Chapter III (Section 3.1.4d).

6.3.1b Molecular weight between crosslinks

The percentage sulphur content assigned to cellulose part alone was used directly for the determination of molecular weight

between crosslinks as described in Chapter III (Section 3.1.4e).

6.3.1c Moisture content

The $SgCellX_0$ and CRF samples of carbofuran prepared using graft copolymer xanthides (SgCellX) were dried for 5-6 h at 50°C and stored in vacuum desiccator over phosphorous pentoxide and used when required.

6.3.1d Determination of carbofuran content

Determination of carbofuran content in SgCellX prepared using grafted pulp of different grafting frequency was carried out as described in Chapter III (Section 3.1.4b). Extraction with methanol for the 2nd and 3rd time did not show any absorbance at λ_{max} 278 nm for carbofuran i.e. carbofuran was completely extracted from the samples within 4 h.

6.4 RESULTS AND DISCUSSION

Release rate study of carbofuran from crosslinked SgCell was carried out. The influence of the introduction of hydrophobic groups (polystyrene) through graft copolymerization was investigated. Grafting provides a means of modifying cotton without much altering its desirable characteristics. Ceric ion initiation of graft copolymerisation on to polysaccharides being the most promising and practical method was used for grafting of styrene on to cellulose.

Of the common, vinyl monomers such as methyl acrylate (MA), methyl methacrylate (MMA), acrylonitrile (AN), vinyl acetate (VA) and styrene, styrene is the least reactive and no grafting occurs with styrene below 60°C[15]. Haung and Chandramouli[12] obtained

higher grafting by pretreatment of pulp with water. It has been shown in several publications that the rate of copolymerization for monomer mixtures are higher than the rates of polymerization for monomers alone (synergistic effect)[13]. Therefore an even more economical grafting process may result from employing the synergistic effect, induced by the addition of a small amount of another monomer to the reaction system.

6.4.1 Mechanism of initiation by ceric ion

The mechanism of initiation by ceric ion has been discussed in detail by several workers[16-18]. The mechanism has been reported to be a free radical process which involves the formation of a ceric cellulose complex and subsequent disproportionation of the complex, resulting in the formation of free radicals on the cellulose molecule. Graft polymerization reaction with vinyl monomers is then initiated at these radical sites (as described in Scheme 1).

6.4.2 Reaction conditions affecting grafting

6.4.2a Pretreatment technique

Before starting graft copolymerization reaction, pretreatment technique[12] was applied to aid the diffusion of styrene into cellulose resulting in the availability of large amount of monomer for grafting.

6.4.2b Synergistic effect

Along with styrene monomer small amount of acrylonitrile (1 and 2.5 ml) was added in order to increase grafting efficiency of styrene through synergistic effect. Experiments carried

SCHEME I : MECHANISM OF CERIC ION INITIATION OF GRAFT COPOLYMERIZATION ON TO CELLULOSE

RADICAL FORMATION :

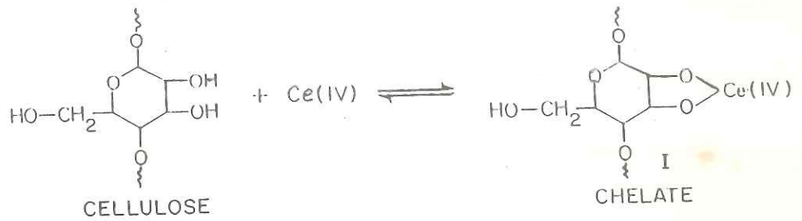

CELLULOSE

CHELATE

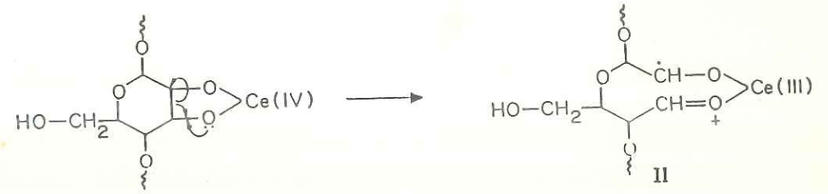

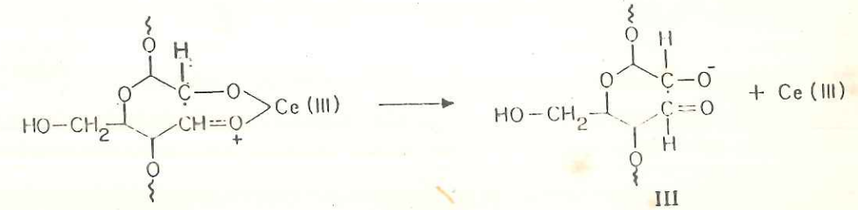

GRAFT POLYMERIZATION:

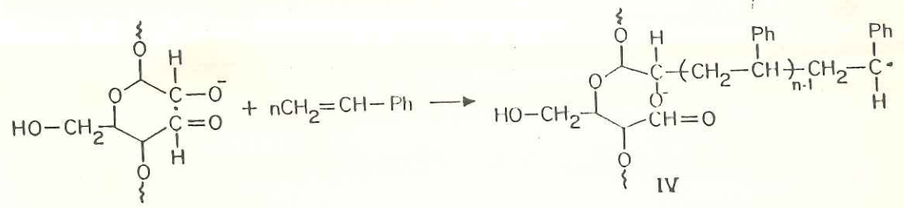

RADICAL TERMINATION:

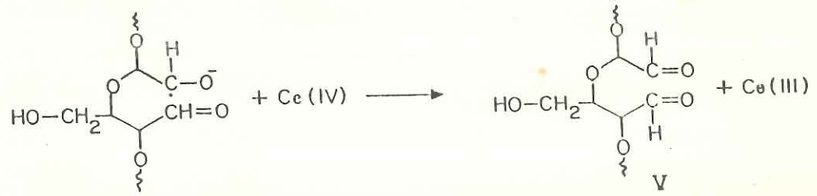

out using two different proportions of AN used and their grafting efficiency (graft yields) are shown in Table 6.1. It is observed that at higher AN content, the grafting efficiency is increased. The weight of the grafted styrene polymer was obtained by the weight difference in graft copolymer (extracted with solvent to remove the homopolymer) and the starting cellulose (cotton pulp) used.

$$\text{Grafting efficiency} = \frac{W_2 - W_1}{W_3} \times 100 \qquad \text{.....(6)}$$

where, W_3 = styrene monomer used for graft copolymerization.

6.4.2c Reaction variables

The dependence of ceric ion initiated vinyl graft copolymerization on factors such as concentration of initiator and monomer, grafting time, temperature etc., has been widely reported. Since two variables were used in this study, effect of these variables i.e. initiator concentration and temperature on % grafting, grafting frequency and chain lengh was considered. Percentage grafting and grafting frequency was found to increase with increasing initiator concentration from 0.004 M to 0.005M (for $SgCell_{10}$ and $SgCell_{11}$ respectively) with other reaction conditions (temperature, time and monomer concentration) being the same (constant). However, at the initiator concentration of 0.005 M with further increase in temperature to 70°C, it was observed that though the % grafting is not much affected, the grafting frequency is reduced, thus increasing the molecular weights of the grafted chains.

Table 6.1

Synergistic effect in the preparation of SgCell*.

Sr. No.	Expt. No.	Weight of pulp (g)	Acrylonitrile used (ml)	Polystyrene grafted in g by weight difference	Graft yield (%)
1.	$SgCell_1$	4.0	0.0	1.46	16.04
2.	$SgCell_2$	4.0	1.0	2.03	22.33
3.	$SgCell_3$	4.0	2.5	5.13	56.93

* SgCell = Styrene grafted to cellulose.

Table 6.2

Abbreviations of cotton pulp and SgCell used in the preparation of CRF of carbofuran.

Sample	Original	Mercerized	Crosslinked	
			Blank	Encapsulated
Cotton pulp	Cell	Cell M	$CellX_0$	$CellX_4$
Styrene grafted to cellulose Expt.No.7	$SgCell_7$	SgCell M_7	$SgCellX_{07}$	$SgCellX_7$
Expt. No. 10	$SgCell_{10}$	SgCell M_{10}	$SgCellX_{010}$	$SgCellX_{10}$
Expt. No. 11	$SgCell_{11}$	SgCell M_{11}	$SgCellX_{011}$	$SgCellX_{11}$

Generally the degree of polymerization is decreased while the grafting frequency is increased, whereas % grafting and grafting frequency is generally increased with initiator concentration and then level off[12,19]. However,it was observed that grafting frequency was maximum at 0.005 M Ceric ion concentration and decreased at the same concentration with further increase in temperature. Thus, grafting frequency was found to decrease at 0.005 M Ceric ion concentration and 70°C temperature. As expected there should be increased number of free radical sites for graft copolymerization of vinyl monomer with increase in initiator concentration. However, with increase in temperature there is a decrease in reactive sites and hence decrease in grafting frequency, due to the instability of the initiator, particularly CAN , at elevated temperature[20]. At elevated temperature there is increased rate of oxidative termination[20], compared to graft copolymerization, leading to more rapid formation of aldehydes from the free radicals produced, by H - abstraction[20] as outlined below :

$$- \dot{C}HOH \longrightarrow - \overset{H}{\overset{|}{C}} = O + H$$

Also the changes in grafting with temperature are due to a variety of temperature dependent factors such as diffusion, adsorption of monomer in to the substrate and changes in the rates of initiation, propagation, termination and homopolymerization. As free radical sites on cellulose substrate are reduced due to oxidative termination while monomer concentration remains

the same, less grafting frequency and increased molecular weights of the grafted chains result.

6.4.3 Characterization of the separated grafts of polystyrene

6.4.3a Solubility, molecular weight and molecular weight distribution (MWD) of the grafted polystyrene branches

Isolation of grafted polystyrene branches was carried out by hydrolysing the cellulose part of SgCell to soluble products. To study molecular weight and MWD of the grafted polystyrene branches, SgCell was acetolysed to hydrolyze the cellulose backbone.

Polystyrene, thus separated, was dried and weighed in order to get weight % of polystyrene grafted on to cellulose (Table 6.3). Also the isolated polystyrene was checked for its solubility. It was found that the polystyrene thus separated from cellulose is partially soluble in toluene even after prolonged stirring and warming, but completely soluble in chloroform which suggest that these separated branches are more polar than polystyrene. It may be due to possible sulfonation of polystyrene during hydrolysis of cellulose[21] and due to glucose end residues retained even after hydrolysis.

The FTIR spectra of the separated polystyrene shows some glucose end group. Thus presence of glucose end groups may be the reason for insolubility of polystyrene in toluene. The FTIR spectrum of styrene separated from SgCell is illustrated in Fig. 6.1 which shows OH band at 3500 cm^{-1}, may be from glucose end residue. Molecular weight determined by viscosity method

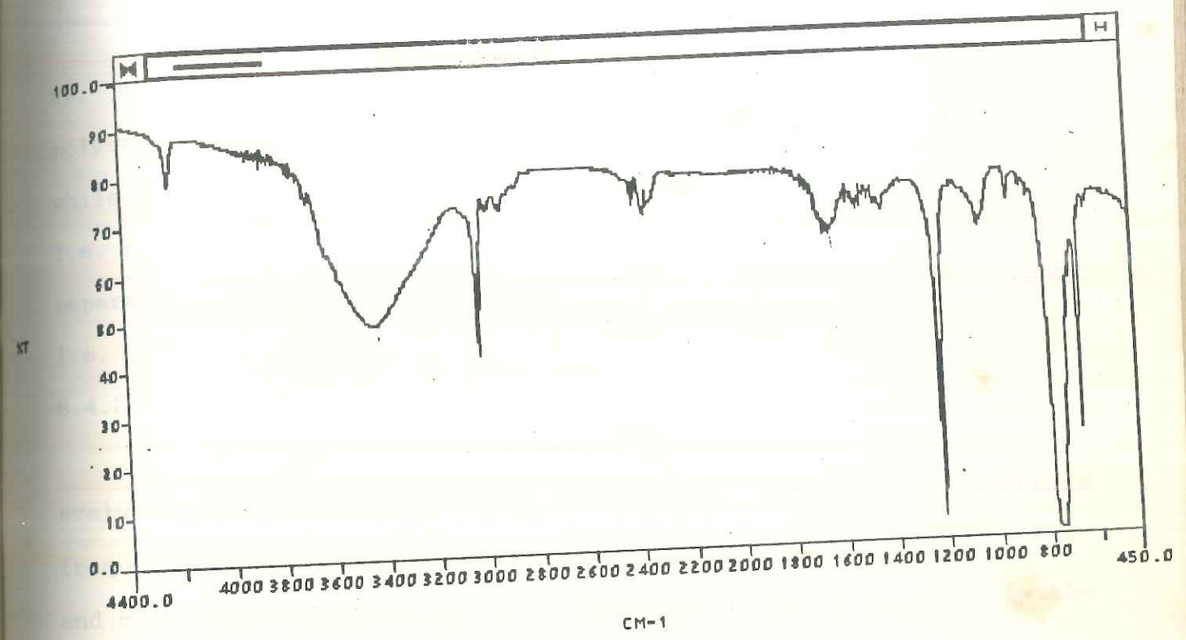

FIG. 6·1 : FTIR SPECTRA OF POLYSTYRENE SEPERATED FROM $SgCell_7$ BY ACETOLYSIS.

shows good correlation with grafting frequency (Table 6.3). Though the molecular weights of $SgCell_{10}$ and $SgCell_{11}$ are not much differing, with further decrease in grafting frequency molecular weight is found to increase in $SgCell_7$.

Table 6.3 shows % Pst in graft copolymer, grafting frequency, molecular weights and MWD of separated polystyrene. Thus polystyrene separated from $SgCell_{11}$ has dispersity index of 2.26 while polystyrene from $SgCell_{10}$ has dispersity index of 2.28 i.e. both the values are not much differing. However, polystyrene separated from $SgCell_7$ has dispersity index slightly higher i.e. 3.27.

6.4.3b Grafting frequency

Molecular weights of the separated polystyrene samples were evaluated from the values of intrinsic viscosity. Grafting frequencies calculated, from percentage Pst in the graft copolymer and molecular weight data (determined by viscosity), were of the order of 0.01 to 0.08 polystyrene branches per cellulose chain.

6.4.3c Site of branch attachment

With many of the methods used for the preparation of cellulose graft copolymers, the branches are attached to the oxygen atoms of one of the three hydroxyl groups on the anhydrogluclose unit. In other cases, such as where grafting occurs through hydrogen abstraction, the branches are attached to one of the three carbon atoms bearing hydroxyl groups. Thus grafted synthetic polymer may be bound at carbon C_2 or C_3 along the cellulose chain or a portion of the synthetic polymer may be

Table 6.3

Percentage polystyrene in SgCell and properties of polystyrene separated from SgCell by acetolysis.

Sample No.	Polystyrene (%)	Grafting frequency	$\overline{M}_v \times 10^{-6}$	MWD	$\overline{M}_n \times 10^{-5}$	$\overline{M}_w \times 10^{-6}$
$SgCell_7$	37.09	0.017	2.00	3.27	7.0	2.3
$SgCell_{10}$	30.04	0.044	0.60	2.23	2.3	0.5
$SgCell_{11}$	40.91	0.072	0.59	2.25	8.7	1.9

$\overline{M}_v$ = Viscosity average molecular weight.
$\overline{M}_n$ = Number average molecular weight.
$\overline{M}_w$ = Weight average molecular weight.
MWD = Molecular weight distribution.

Table 6.4

Thermal properties of polystyrene*(Pst), $SgCell_{11}$ and blend of cotton pulp (cell) and Pst.

Sample	IDT	T_{max} (°C)			Endotherm
	(°C)	T_{1max}	T_{2max}	T_{3max}	(°C)
Cell	293	363	-	-	-
Pst from $SgCell_{11}$	309	368	431	558	431
Cell+Pst 6:4 (Blend)	298	374	452	-	431
$SgCell_{11}$	282	358	405	-	405

* Polystyrene grafts separated from $SgCell_{11}$ by acetolysis.
IDT = Initial decomposition temperature.
T_{max} = Temperature for maximum weight loss.

linked at the hemi acetal group at the end of cellulose chain[22-24]. Thus it would seem that the structure of graft copolymer consist of a mixture of block type and graft type structure.

6.4.4 Proof of grafting

6.4.4a Solvent extraction

Graft copolymers containing homopolymer were soxhlet extracted using benzene (solvent for styrene), for several hours (about 15-20 h) till no more polymer is extracted. Thus the gain in weight of starting cellulose (cotton pulp) after extraction accounts for the polystyrene that is grafted on to cellulose.

6.4.4b Swelling behaviour in solvent

The graft copolymers were swelled in chloroform and benzene, but not soluble, thereby showing the presence of polystyrene branches on to the cellulose backbone. Also insolubility of the graft copolymer in cupriethylene diamine confirms the presence of polystyrene branches on cellulose backbone.

6.4.4c FTIR Spectroscopy

Presence of band at 1600 cm^{-1} confirms the presence of polystyrene in the graft copolymer (Fig. 6.2). However, the mixture of cellulose and polystyrene if taken in the same proportion as that of graft copolymer also shows the polystyrene band at same frequency. There is no shift in frequency on chemical bonding through graft copolymerization. Thus the proof for chemically bound polystyrene in the graft copolymer can be

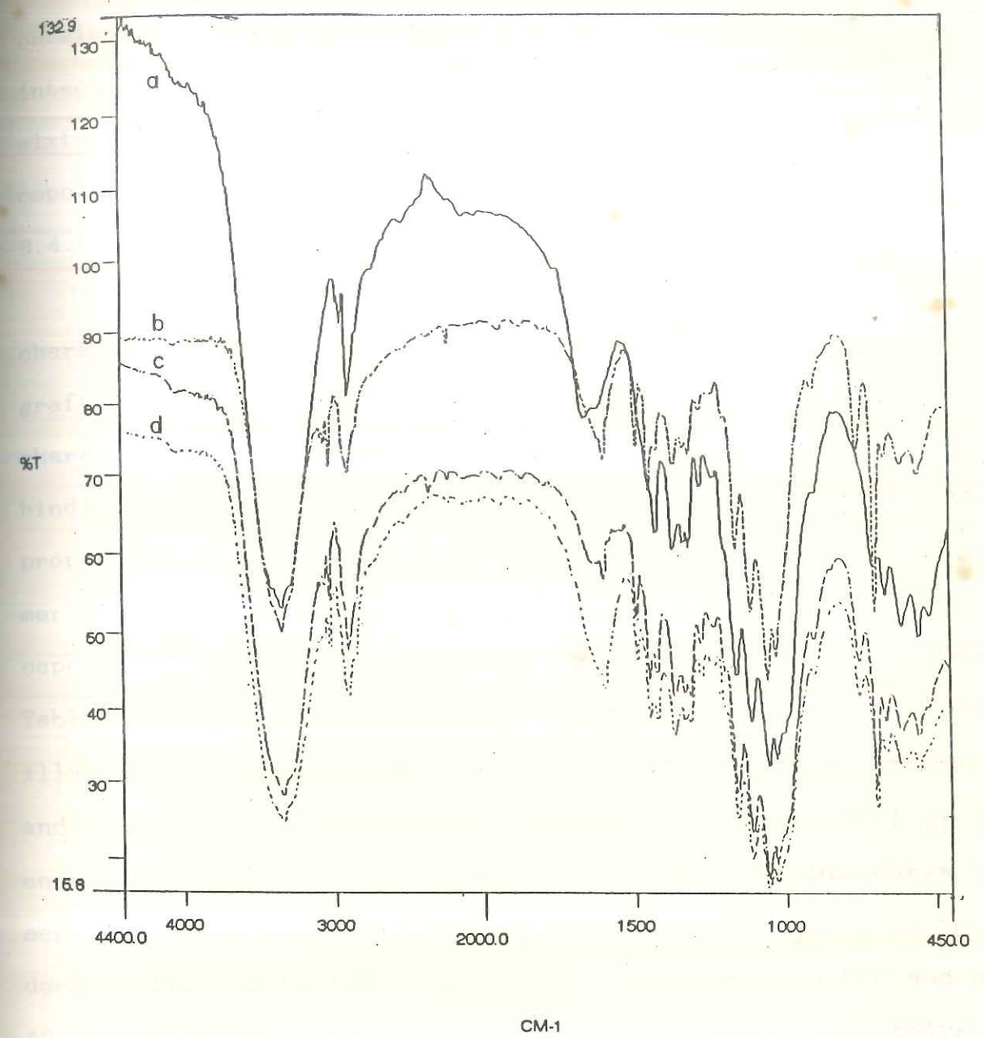

FIG. 6·2 : FTIR SPECTRA OF CELLULOSE AND GRAFT COPOLYMERS OF CELLULOSE a) Cell , b) $SgCell_7$, c) $SgCell_{10}$, d) $SgCell_{11}$

obtained by change in intensity of absorbance[25]. The absorbance intensity in graft copolymer was less than that of a physical mixture taken in the same proportions as that of graft copolymer (Fig. 6.3).

6.4.4d Thermogravimetric and differential thermal analysis (DTA)

Endotherm or exotherm observed in DTA thermogram is a characteristic of that particular polymer and when the polymer is grafted on a preformed polymer, changes the position of that characteristic endotherm or exotherm which proves the chemical bindinge of that polymer on preformed polymer[26]. The thermal properties of the polystyrene (Pst) separated from graft copolymer $SgCell_{11}$ and of blend of cellulose (cotton pulp) and the separated Pst were studied and the results are summerised in Table 6.4. The TGA thermograms of the respective samples are illustrated in Fig. 6.4. DTA study of the blend of cotton pulp and Pst in the proportion 6:4 as that in $SgCell_{11}$ shows endotherm at 431°C which is also observed in the DTA curve of Pst separated from $SgCell_{11}$. Thermal study of $SgCell_{11}$ shows two step decomposition with IDT at 282°C and endotherm at 405°C and not at 431°C. The absence of endotherm at 431°C proves that polystyrene is chemically bound to cellulose.

6.4.5 Characterization of the graft copolymers

6.4.5a Structural characterization of the graft copolymer

Structural characterization of the graft copolymer (SgCell) was carried out by FTIR and solid state ^{13}C NMR spectroscopy. Characterization of graft copolymer by FTIR is described in

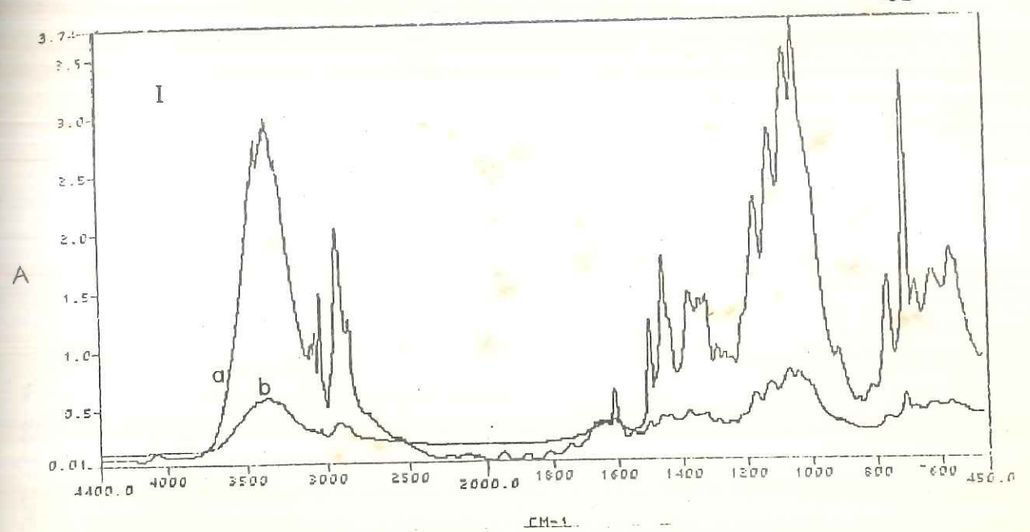

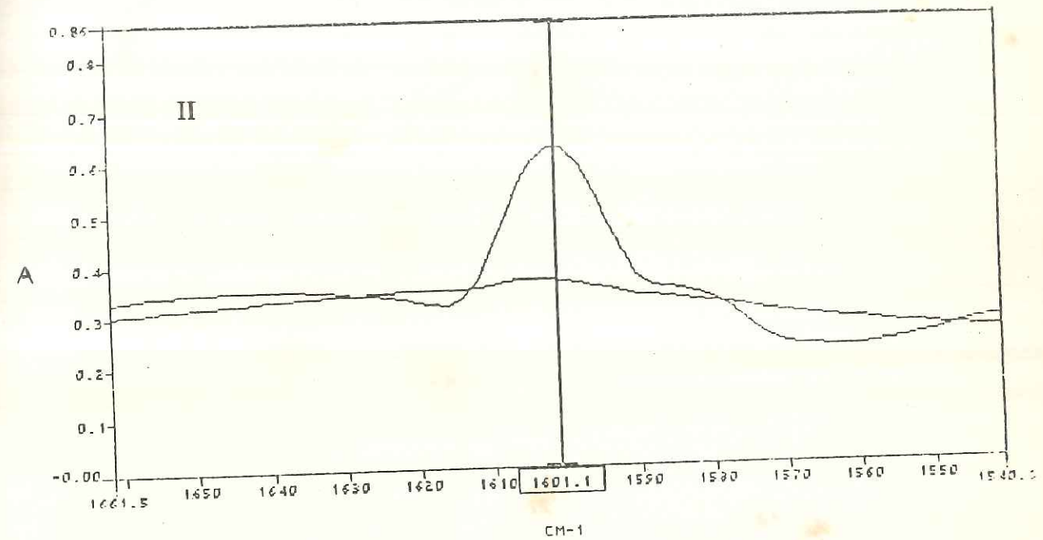

FIG. 6·3: I) FTIR SPECTRA OF (a) BLEND OF CELLULOSE + Pst (POLYSTYRENE SEPERATED FROM $SgCell_{II}$) AND (b) OF $SgCell_{II}$

II) FTIR SPECTRA OF THE SAME, POLYSTYRENE REGION EXPANDED

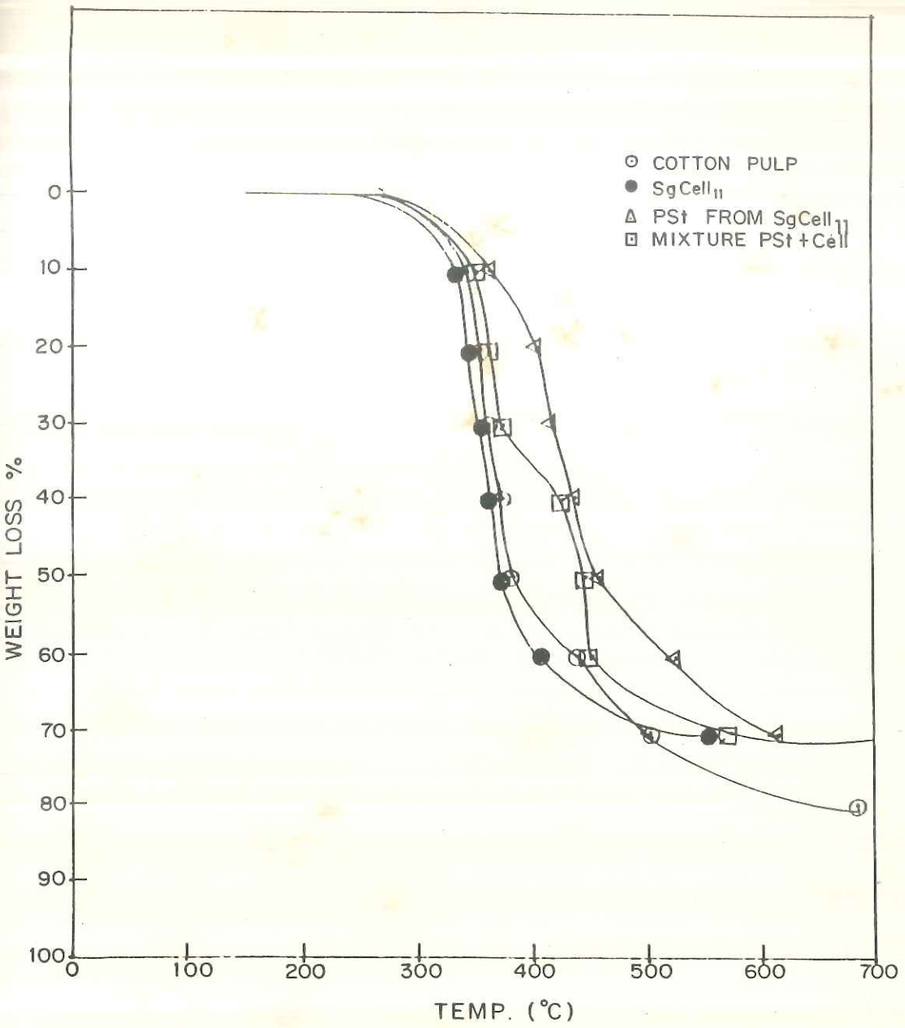

FIG. 6·4 : TGA CURVES OF COTTON PULP , $SgCell_{11}$, POLY-STYRENE FROM $SgCell_{11}$ AND MIXTURE OF PSt + COTTON PULP

Section 6.4.4c as a proof of grafting.

Structural characterization of the SgCell was studied by solid state ^{13}C CP/MAS NMR spectroscopy and is described in Chapter VII.

6.4.5b Characterization of the graft copolymer by thermal stability

As mercerized graft copolymer pulp (SgCellM) was used further for xanthation and encapsulation, the thermal behaviour of the SgCellM was studied. Also the thermal behaviour of cotton pulp (cell) and mercerized cotton pulp (CellM) was studied for comparison (Table 6.5). The TGA curves of Cell and CellM are illustrated in Fig. 6.5. Thermal decomposition of cell takes place in two distinct stages. In the first stage, most of the decomposition of cellulose takes place in the temperture range of 260°C-400°C. During the second stage undecomposed cellulose and other impurities are lost above 400°C. The DTA thermogram of CellM shows sharp endotherm at 328°C and decrease in thermal stability i.e. IDT and Tmax values are lowered (Table 6.5). During mercerization cellulose I is converted to cellulose II, having more amorphous nature resulting in more free hydroxyl content which decrease the thermal stability.

The thermal study of SgCell M shows increase in T_2^{max} values due to grafting of styrene on to cellulose (Table 6.5). The TGA curves of CellM and SgCellM are illustrated in Fig. 6.6. The grafting frequencies and Tmax values of the SgCellM in comparison with CellM are given in Table 6.6. It has been

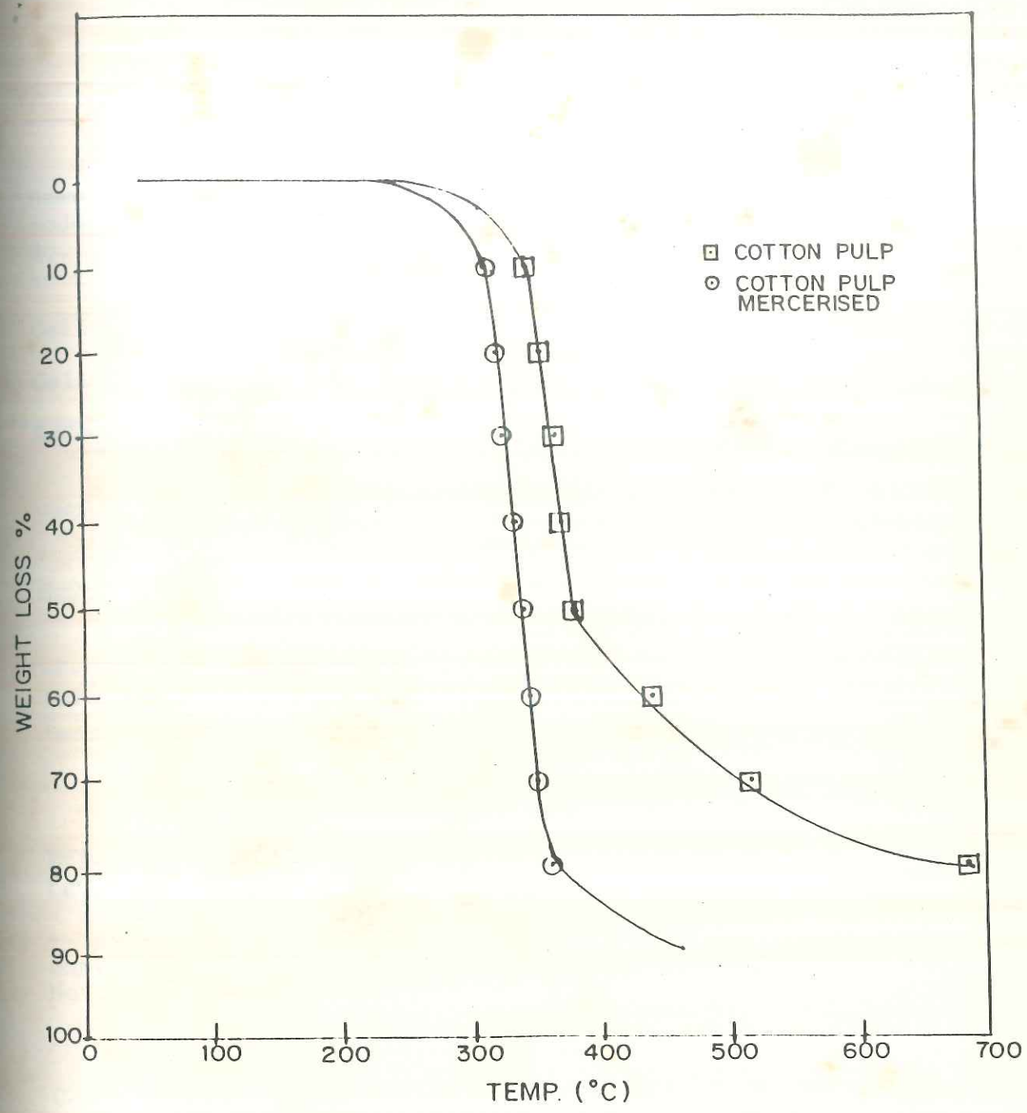

FIG. 6·5 : TGA CURVES OF COTTON PULP AND MERCERISED COTTON PULP

Table 6.5

Thermal properties of Cell, CellM and SgCellM

Sample code No.	IDT (°C)	T_{max}(°C)		Endo-therm (°C)	10% loss (°C)	Total loss (%)	Residue (%)
		T_{1max}	T_{2max}				
Cell	293	363	-	-	331	81	19
Cell M	273	338	-	328	317	80	20
$SgCellM_7$	306, 386	360	418	349, 413	328	89	11
$SgCellM_{10}$	331	361	431	358, 421	342	74	26
$SgCellM_{11}$	273, 392	370	438	349, 433	339	87	13

IDT = Initial decomposition temperature.
T_{max} = Temperature for maximum weight loss.

Table 6.6

Effect of grafting frequency on the thermal properties of SgCellM.

Sample No.	Grafting frequency	IDT (°C)	T_{max}(°C)	
			T_{1max}	T_{2max}
CellM	-	273	338	-
$SgCellM_7$	0.0167	306,386	360	418
$SgCellM_{10}$	0.0435	331	361	431
$SgCellM_{11}$	0.0717	273,392	370	438

IDT = Initial decomposition temperature.
T_{max} = Temperature for maximum weight loss.

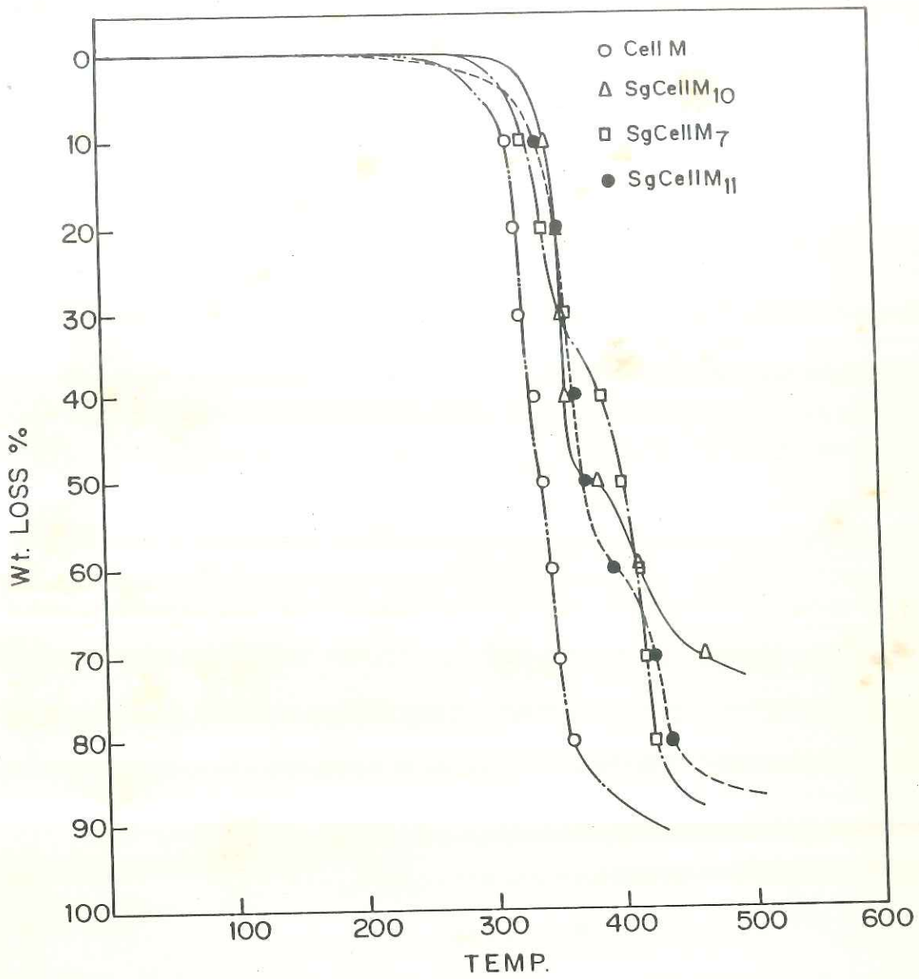

FIG. 6·6 : TGA CURVES OF SAMPLES Cell M , SgCell M_7 , SgCell M_{10} AND SgCell M_{11}

observed from the results that the T_2max values are increased as grafting frequency is increased.

Thermal stability of blends of cellulose and Pst (separated from the graft copolymer $SgCell_{11}$) and Pst are summerised in Table 6.4 and are described in Section 6.4.4d, as a proof of grafting.

The TGA thermogram of Pst shows three step decomposition pattern (Fig. 6.4). The first step starts from 309°C which may be due to destruction of pyranosic rings of the glucose residues that are present at the end of styrene polymer. The second decomposition step starts from 405 °C which may be due to the decomposition of polystyrene backbone unite ($-CH_2-CH-$). The third step decomposition starts from 431°C, which may be due to complete decomposition of aromatic rings. The DTA curves show endotherm at 431°C which is the characteristic of the separated polystyrene.

6.4.5c Crystallinity

The percentage crystallinity data for cotton pulp (cell) and SgCell after mercerization and crosslinking is summarised in Table 6.7. As grafting on to cellulose takes place in more accessible i.e. amorphous region, the crystalline part of cellulose remains unaffected. Thus crystallinity of cellulose is unaffected or slightly reduced. However, the addition of amorphous polymer will reduce the percentage crystallinity quantitatively.

It is observed that crystallinity of cotton pulp is only

Table 6.7

Percentage crystallinity of Cell and SgCell at three different stages in the xanthide preparation.

Sample	Crystallinity (%)		
	Original	Mercerized	Crosslinked
Cell	57.4	47.3	36.5
$SgCell_7$	33.9	29.0	22.9
$SgCell_{10}$	46.6	42.6	26.9
$SgCell_{11}$	46.0	40.1	28.0

Table 6.8

Different blank and encapsulated xanthides prepared using SgCell.

Sample code No.	Xanthide[a] yield (g)	Encapsulated[b] xanthide yield (g)	Carbofuran (%)		Efficiency of encapsulation(%)
			Calcd.	Actual	
$SgCell_7$	5.43	6.61	24.08	17.80	70
$SgCell_{10}$	5.49	6.60	23.62	16.80	66
$SgCell_{11}$	5.27	6.70	24.03	21.37	86

[a] Blank xanthides (without carbofuran) were prepared using 5 g of SgCell.

[b] Carbofuran encapsulated xanthides were prepared using 5 g of SgCell and 1.67 g of carbofuran.

Table 6.7

Percentage crystallinity of Cell and SgCell at three different stages in the xanthide preparation.

Sample	Crystallinity (%)		
	Original	Mercerized	Crosslinked
Cell	57.4	47.3	36.5
$SgCell_7$	33.9	29.0	22.9
$SgCell_{10}$	46.6	42.6	26.9
$SgCell_{11}$	46.0	40.1	28.0

Table 6.8

Different blank and encapsulated xanthides prepared using SgCell.

Sample code No.	Xanthide[a] yield (g)	Encapsulated[b] xanthide yield (g)	Carbofuran (%)		Efficiency of encapsulation(%)
			Calcd.	Actual	
$SgCell_7$	5.43	6.61	24.08	17.80	70
$SgCell_{10}$	5.49	6.60	23.62	16.80	66
$SgCell_{11}$	5.27	6.70	24.03	21.37	86

[a] Blank xanthides (without carbofuran) were prepared using 5 g of SgCell.

[b] Carbofuran encapsulated xanthides were prepared using 5 g of SgCell and 1.67 g of carbofuran.

slightly reduced on grafting but it is further reduced, on mercerization and crosslinking. Fig. 6.7 shows the X-ray diffraction pattern of original, mercerized and crosslinked SgCell.

The percentage crystallinity in $SgCell_7$ is low as compared to the other two $SgCell_{10}$ and $SgCell_{11}$. This may be due to high molecular weight styrene branches with less grafting frequency in $SgCell_7$ as compared to $SgCell_{10}$ and $SgCell_{11}$.

6.4.6 Characterization of graft copolymer xanthides ($SgCellX_0$) and encapsulated graft copolymer xanthides (SgCellX)

6.4.6a Efficiency of encapsulation

Table 6.8 describes different blank and encapsulated formulations along with carbofuran content and efficiency of encapsulation. It is observed that the percentage of carbofuran in these formulations is less than that in cotton pulp and efficiency of encapsulation is reduced to 66 to 86% .

6.4.6b Sulphur coutent and degree of xanthation

The blank graft copolymer xanthides were analysed for sulphur content. Since only cellulose moiety takes part in xanthation and crosslinking, the sulphur content (%) obtained for $SgCellX_0$ were calculated for the cellulose xanthide part and compared with cellulose xanthide ($CellX_0$) prepared using cotton pulp. It is observed from Table 6.9 that the sulphur contents are not much differing inspite of the presence of hydrophobic polystyrene branches. Only sulphur content of the $SgCellX_{10}$ is slightly higher giving lower value of molecular weight between

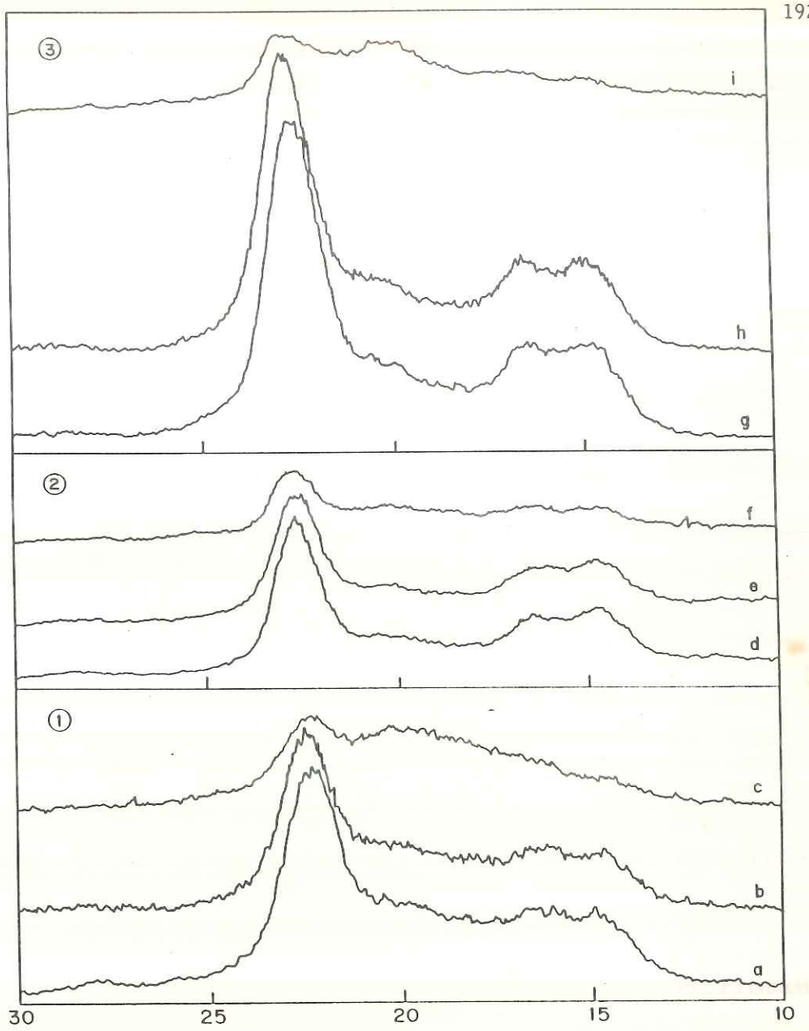

FIG. 6·7 : X RAY DIFFRACTION PATTERN OF SAMPLES

① a) $SgCellI_7$ b) $SgCellIM_7$ c) $SgCellIX_{07}$

② a) $SgCellI_{10}$ b) $SgCellIM_{10}$ c) $SgCellIX_{010}$

③ a) $SgCellI_{11}$ b) $SgCellIM_{11}$ c) $SgCellIX_{011}$

Table 6.9

Sulphur analysis for samples $CellX_0$ and $SgCellX_0$ (converted to cellulose xanthide part).

Experiment No.	Sulphur (%)	Degree of xanthation	M_c
$CellX_0$	7.73	0.22	1657
$SgCellX_{07}$	6.65	0.18	1924
$SgCellX_{010}$	8.74	0.25	1465
$SgCellX_{011}$	7.41	0.21	1727

Table 6.10

Effect of grafting frequency on equilibrium swelling.

Expt. No.	Grafting frequency	Equilibrium swelling (%)	Time required to attain % equilibrium swelling (min)
$SgCellX_7$	0.0167	134	120
$SgCellX_{10}$	0.0435	124	120
$SgCellX_{11}$	0.0717	106	1440
$CellX_4$	-	59	60

crosslinks.

6.4.7 Swelling studies

Table 6.10 shows data for swelling of encapsulated samples prepared using SgCellX with different grafting frequencies. Thus $SgCellX_{11}$ with highest grafting frequency of 0.0717 i.e. 0.0717 polystyrene branches per cellulose chain, has the lowest % equilibrium swelling (106%) and the time required to attain the same is more (1440 min). Whereas $SgCellX_7$ with lowest grafting frequency is having the highest % equilibrium swelling (134%) and the time required to attain it is 120 min. In case of $SgCellX_{10}$ it has % grafting frequency of 0.0435 with intermediate equilibrium swelling between $SgCell_7$ and $SgCell_{11}$ and the time required to attain it is 120 min. However, as compared to encapsulated formulation with cotton pulp, these equilibrium swelling values are higher inspite of the introduction of hydrophobic groups.

In graft copolymer there is change in packing density and chain torsional mobility due to presence of grafted branches. The cellulose chains go away from each other due to grafting. Therefore, coheshive forces of attraction between neighbouring cellulose chains through hydrogen bonding is reduced and free volume is increased which allows penetration of water thus leading to increased % equilibrium swelling than cellulose xanthide itself inspite of the presence of hydrophobic styrene branches. However, with increase in grafting frequency, the % equilibrium swelling is reduced whereas with low grafting frequency, long chains of polystyrene lead to more free volume

resulting in increase in % equilibrium swelling as shown in $SgCell_7$ (Table 6.10).

6.4.8 Release of carbofuran

The graft copolymer samples with different grafting frequencies were selected and further used for xanthation and encapsulation of carbofuran. Release of carbofuran was analysed by the generalized equation $M_t/M_\infty = kt^n$. The three different types of transport mechanism Fickian, anomalous and case II depending on values of n are discussed in Chapter III (Section 3.2.2).

Release profiles of carbofuran from $SgCell_{7,10}$ and 11 are shown in Fig. 6.8. It is observed that release of carbofuran from $SgCell_{11}$ is slow while that from $SgCell_7$ is fast. We have already discussed that the release of carbofuran is dependent on percentage equilbrium swelling which in turn depends on grafting frequency. $SgCell_{11}$ with highest grafting frequency has more short chains of polystyrene. Thus, greater coverage of cellulose backbone is possible which affects the percentage equilibrium swelling leading to slow release of carbofuran. In case of $SgCellX_7$, grafting frequency being less, it has less coverage of cellulose backbone. Hence the long chains of polystyrene lead to increase in free volume and more percentage equilibrium swelling resulting in faster release of carbofuran. $SgCellX_{10}$ with grafting frequency in between the two shows percentage equilibrium swelling and release curve in between the two.

Thus it may be concluded that the grafting frequency mainly

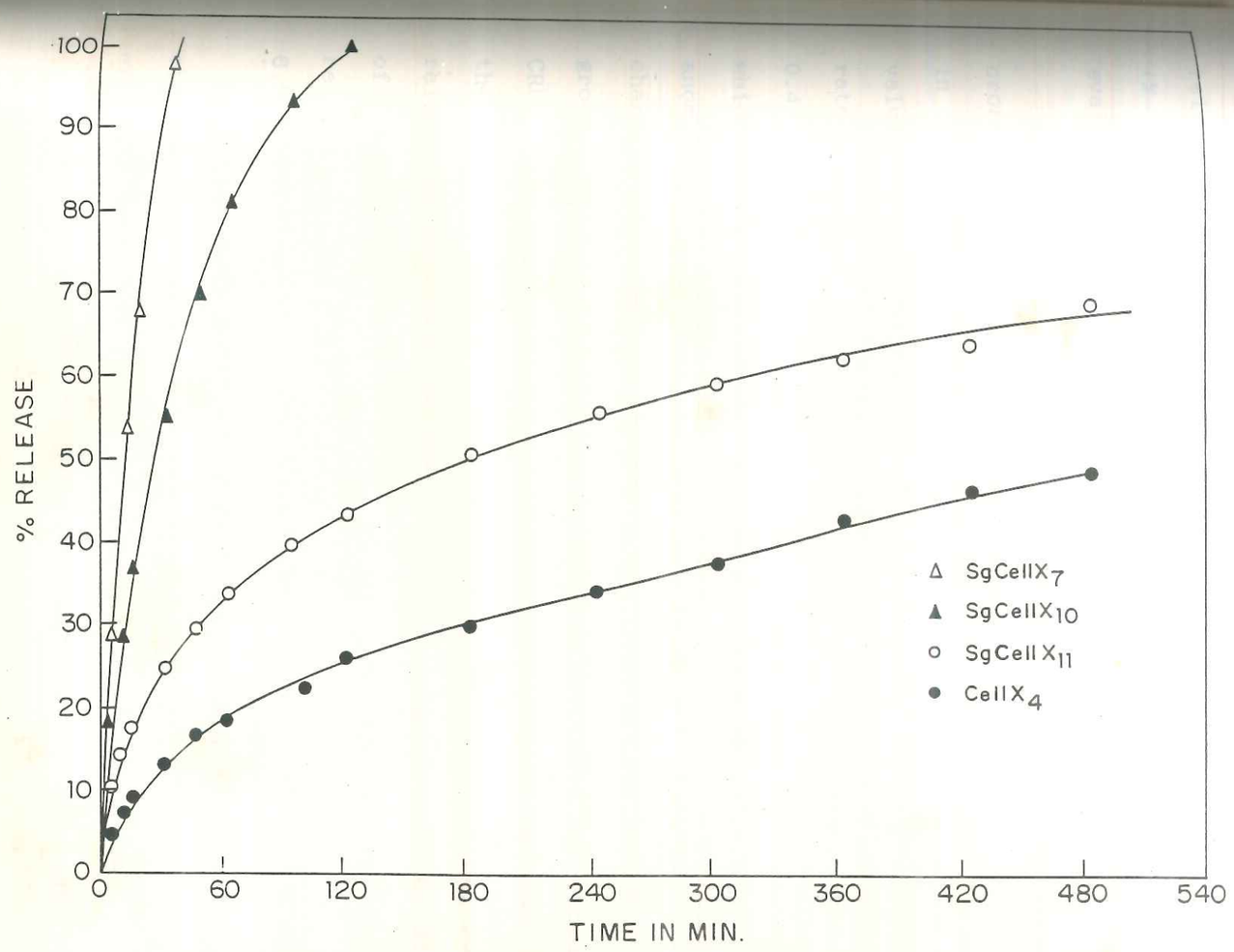

FIG. 6·8 : RELESE PROFILES OF CARBOFURAN FROM C R F SAMPLES $SgCellX_7$, $SgCellX_{10}$, $SgCellX_{11}$ AND $CellX_4$

determines the extent of hydrophobicity and extent of swelling rather than chain length or extent of grafting.

In order to know the effect of matrix modification on release mechanism, the release data were plotted as log (% release) vs log t. From these plots k and n values were evaluated.

The release profiles for the CRF of carbofuran using crosslinked SgCell are governed by k and n values and are given in Table 6.11. It has been observed from the results that n values are increased as release is increased and also release rate constant is increased. Though n values are varying from 0.41 to 0.58, their 95% confidence level vary from 0.39 to 0.67 which indicates that the release mechanism is ranging in between anomalous and Super Case II, but it is not Fickian. Thus by changing the matrix property by introduction of hydrophobic groups, release is not slowed down but increased as compared to CRF using ungrafted cotton pulp. Mechanism of release remains the same in both i.e. in grafted and ungrafted cotton pulp and release is governed by macromolecular relaxation or by diffusion of carbofuran through the polymer undergoing macromolecular relaxation.

6.5 CONCLUSIONS

Cotton pulp modified by graft copolymerization with styrene can be used as a matrix for encapsulation of carbofuran. The efficacy of encapsulation is less than that in cotton pulp.

Data for percentage equilibrium swelling and time required

Table 6.11

Release rate constant and diffusional exponent n for CRF of carbofuran prepared using crosslinked SgCell.

Expt. No.	k x 10^2 $(min)^{-n}$	n	95% Confidence level of n		Half life (min)	Correlation coefficient
			Upper limit	Lower limit		
$SgCellX_7$	13.96	0.58	0.67	0.49	8	0.999
$SgCellX_{10}$	8.63	0.53	0.59	0.48	28	0.995
$SgCellX_{11}$	5.89	0.41	0.43	0.39	155	0.996

to attain equilibrium swelling show that percentage equilibrium swelling is more than that in cotton pulp though hydrophobic groups are introduced. This is due to increase in free volume due to branched structure in graft copolymer.

The percentage equilibrium swelling is reduced with increase in grafting frequency. Crystallinity is retained even after xanthation.

Release data analysed by equation $M_t/M\infty = kt^n$ suggests that release mechanism is ranging between anomalous and Super Case II but not Fickian i.e. similar to cotton pulp. Thus the release mechanism has remained the same even after changing the matrix property.

RERERENCES

1. Iwakura, Y., Kurosaki, T., Uno, K. and Imai, Y., J. Polym. Sci., C4 (1964) 673.
2. Dasgupta, S., J.Polym.Sci. C37 (1972) 333.
3. Toda, T., J.Polym. Sci., 58 (1962) 411.
4. Maeda, H., Suzuki, H., Yamauchi, A. and Sakimae, A., Bio. chem. Biotech., 17 (1975) 119.
5. Demint, R.J., Arthur, J.C.Jr., Markezich, A.R. and McSherry, W.F., Text.Res.J., 32 (1962) 918.
6. Negishi, M., Nakamura, Y., Kakinuma, T. and Iizuka, Y., J. Appl. Polym.Sci., 9 (1965) 2227.
7. Kulkarni, A.Y. and Mehta, P.C., Textile Res.J., 32 (1962) 701.
8. Hayakawa, K. and Yamakita, H., J.Appl.Polym. Sci., 21 (1977) 665.
9. Kaizerman, S., Mino, G. and Meinhold, L.F., Textile Res.J., 32 (1962) 136.
10. Wegner, J. and Patat, F., J. Polym. Sci. Polym. Symp., 31 (1971) 121.
11. Thejappa, N. and Pandey, S.N., Indian J.Text.Res., 5 (1980) 109-113.
12. Huang, R.Y.M. and Chandramouli, P., J. Appl. Polym. Sci., 12 (1968) 2549.
13. Kokta, B.V. and Valade, T.L., Tappi, 55(3) (1972) 366-369.
14. Polymer Hand Book, Brandrup, J. and Immergut, E.H., (Ed) Wiley-Interscience Publication (1975).

15. Hebeish, A. and Mehta, P.C., Cellul. Chem. Tech., 3 (1969) 469.

16. Immergut, E.H., In : Encylopaedia of Polymer Science and Technology, Vol. 3, Interscience Publishers, New York, London, Sydney Edited by Mark, H.F., Gaylord, N.G. and Bikales, N.M. (1965) 245.

17. Mino, G. and Kaizerman, S., J. Polym. Sci., 31 (1956) 242.

18. McDowall, D.J., Gupta, B.S. and Stannett, V.T., In : Prog. Polym.Sci., Pergamon Press, Oxford, New York, Jenkins, A.D. and Stannett, V.T. (Ed) Vol. 10 (1984) 1-16.

19. Huang, R.Y.M. and Chandramouli, P., J. Polym. Sci., A 1, 7 (1969) 1393-1405.

20. Hebeish, A. and Mehta, P.C., J. Appl. Polym. Sci., Vol. 12 (1968) 1625-1647.

21. Guthrie, J.T., Huglin, M.B. and Philips, G.O., J. Appl. Polym. Sci., 15 (1971) 1033-1035.

22. Imai, Y., Masuhara, E. and Iwakura, Y., J. Polym. Sci. Part B, 8 (1970) 75-79.

23. Doba, T., Rodehed, C. and Ranby, B., Macromolecules, 17 (1984) 2512-2519.

24. Iwakura, Y., Kurosaki, T. and Imai, Y., J. Polym. Sci., 3 (1965) 1185-1193.

25. Imrisova, D. and Maryska, S., J. Appl. Polym. Sci., 11 (1967) 901-907.

26. Arthur, J.C.Jr. and Demint, R.J., Text. Res. J., 31 (1961) 988.

PART - II

Incorporation and Release of Carbofuran from Crosslinked, Cellulose Grafted with Polyacrylamide

6.6 EXPERIMENTAL

6.6.1 Materials

. Acrylamide : Recrystallized from acetone m.p. 84.5°C

. Ceric ammonium nitrate : A.R. grade from Qualigens

. Nitric acid : L.R. grade

. Sulphuric acid : L.R. grade

. Acetone : distilled

. Rest of the materials were same as described in Chapter III Section 3.1.1.

6.6.2. Grafting procedure

The procedure[1] described below typifies the synthesis of a graft copolymer at 3% monomer concentration, 0.02% initiator concentration and 0.75% cotton pulp. Reaction temperature was 25°C and final pH was approximately 1.8.

Cotton pulp 5.25 g (corrected for moisture content) was introduced into a reaction vessel of 750 ml capacity, three neck R.B. flask together with 320 ml of water and homogenized by stirring for 1 h. The reaction flask was adjusted in thermostatic water bath at 25°C. A solution of 21 g of acrylamide in 320 ml of water was added and the system was purged with a vigorous stream of nitrogen (this was continued throughout the reaction period). After 30 minutes a solution of 0.140 g of ceric ammonium nitrate in 20 ml of 1M nitric acid was added through the dropping funnel, and the funnel was rinsed with 140 ml of water. This made a final volume of 700 ml in the liquid phase. The reaction was continued for 3 h and was stopped by

filtration of the diluted pulp suspension. From the filtrate which was a viscous fluid, polyacrylamide (PAM) homopolymer was isolated from the viscous filtrate in the following manner.

6.6.3 Isolation of homopolymer

The pulp cake recovered was stirred into a large quantity of hot water and washed for at least 2 h by vigorous stirring and filtered. The remaining homopolymer was removed from the pulp by soxhlet extraction with water in Soxhlet for 48 h till no more PAM was extracted. The PAM obtained was separated by precipitation from the aqueous solution by the addition of methanol as follows :

An aliquot of the above filtrate (soxhlet extract) was diluted to about 4-6 times of its initial volume and ethanol was added drop by drop with vigorous stirring. As the saturation point was approached, the rate of addition was reduced to avoid sudden precipitation of PAM in the form of a heavy gel containing large quantities of occluded water. Due to the low rate of addition, small flakes were obtained which could easily be dried to constant weight. After complete precipitation, an excess of ethanol was added and the precipitate left overnight in its mother liquor. PAM was then collected on a sintered glass crucible, washed with ethanol, and dried at 50^{o}C under vacuum to constant weight. PAM is hygroscopic and hence was stored in a vacuum desiccator over phosphorous pentoxide.

6.6.4 Characterization of the graft copolymer (AmgCell).

6.6.4a PAM content

The graft copolymer (polyacrylamide grafted to cellulose i.e. AmgCell) obtained after complete removal of homopolymer was dried under vacuum at 50°C for 5-6 h and stored in vacuum desiccator over phosphorous pentoxide. The weight difference between the AmgCell (after homopolymer extraction) and the starting cellulose accounts for the weight added due to polyacrylamide grafts on to cellulose backbone. The percentage PAM in AmgCell can be calculated using the formula.

$$\% \text{ PAM} = \frac{\text{wt. of AmgCell} - \text{wt. of cellulose used}}{\text{wt. of AmgCell}} \times 100$$

The PAM content (%) was also determined by elemental analysis of the product obtained for nitrogen. PAM content (%) in the AmgCell by gain in weight and by N analysis are described in Table 6.6.1.

6.6.4b FTIR Spectroscopy

The FTIR spectra of AmgCell and blend of cellulose and PAM (extracted homopolymer) were scanned. KBr pellets of the samples were prepared as described in Section 6.2.2a.

6.6.4c X-ray diffraction study

The X-ray diffraction study was carried out for the determination of crystallinity (%) at the three stages viz., original, mercerized and crosslinked form of AmgCell in the process of encapsulation.

6.6.4d Solid state ^{13}C CP/MAS NMR

Structural characterization of AmgCell was carried out using solid state ^{13}C CP/MAS NMR spectroscopy which is described in Chapter VII (Section 7.3.5a).

6.6.4e Thermogravimetric analysis

Thermogravimetric analysis (TGA) was carried out as described in Section 6.2.6. Thermogravimetric analysis (TGA), derivative thermogravimetry (DTG) and differential thermal analysis (DTA) for AmgCell, mercerized AmgCell (i.e. AmgCellM) and PAM homopolymer was carried out.

6.6.5 Preparation of CRF of carbofuran using AmgCell

Encapsulation of carbofuran in the xanthide matrix involves mercerization, xanthation and encapsulation. As the polyacrylamide grafted cotton pulp was subjected to mercerization, PAM was partly hydrolysed to polyacrylic acid due to high concentration of sodium hydroxide used in mercerization. This mercerized graft copolymer (AmgCellM) was further used for xanthation and encapsulation. Therefore, the CR formulations of carbofuran prepared using $AmgCell_1$ and $AmgCell_2$ (polyacrylamide grafted to cotton pulp Expt. No.1 and 2) consist of partly hydrolysed polyacrylmide branches i.e. copolymer of polyacrylamide and polyacrylic acid. Encapsulation was carried out as described in Chapter III (Section 3.1.3b).

Blank xanthides using $AmgCell_1$ and $AmgCell_2$ were also prepared without using any encapsulant (carbofuran).

6.6.6 Characterization of the blank ($AmgCellX_0$) and encapsulated graft copolymer xanthides (AmgCellX)

6.6.6a Sulphur content

Blank xanthides $AmgCellX_{01}$ and $AmgCellX_{02}$ prepared using acrylamide grafted pulp $AmgCell_1$, $AmgCell_2$ respectively were analysed for sulphur content by elemental analysis.

6.6.6b Degree of xanthation

The sulphur content obtained for $AmgCellX_{01}$ and $AmgCellX_{02}$, were converted to cellulose part and degree of xanthation of the cellulose part alone was calculated using equation as described in Chapter III (Section 3.1.4d).

6.6.6c Molecular weight between crosslinks

Sulphur content was used as direct measure of molecular weight between crosslinks for the cellulose backbone of the graft copolymer xanthides (Chpater III, Section 3.1.4e).

6.6.6d Analysis of the AmgCellX

Analysis of AmgCellX for moisture content and carbofuran content, and swelling and release measurements was carried out as described in Chapter III (Section 3.1.4a & b, 3.1.5, and 3.1.6a respectively).

6.7 RESULTS AND DISCUSSION

Release rate study of carbofuran from cellulose xanthide matrix modified by introduction of hydrophilic groups through graft copolymerization on to cellulose was undertaken with a view to study the influence of grafting. Major part of the work done in this field i.e. grafting on to cellulose has been concerned

with imparting hydrophobicity to the substrate, obtained by the graft copolymerization of acrylonitrile, acrylic ester and styrene. On the other hand, interesting aspects are also associated with increased hydrophilicity. One means of increasing the hydrophilic character of cellulose is by the incorporation of PAM.

Various monomers, such as acrylamide (Am),acrylonitrile (AN) and certain esters of acrylic and methacrylic acid, have been successfully grafted on to cellulosic materials using Ce IV ion catalyst[2-7]. Kaizerman et al[8] have polymerized AN, Am and methyl acrylate (MA) within the fiber of cotton and viscose rayons. Schwab et al[2] studied the graft polymerization of Am, AN and methylmethylacrylate (MMA), ethylacrylate (EA) and styrene on to paper using Ce IV ion process and the reactivity of the monomer for the graft copolymerization was found to be as follows:

Ethylacrylate > methyl methacrylate > acrylonitrile > acrylamide > styrene.

These investigators also reported an optimum temp.of 25-40°C for grafting initiated by Ceric ammonium nitrate for acrylamide beyond which the amount of graft formed rapidly decreased.

Yields of graft copolymer and homopolymer are influenced by different factors such as initiator concentration, pH of the medium, monomer concentration and period of reaction.

The copolymer produced may be graft or block type. Polymerization may be effected helically, starting from

hemiacetal end group of the cellulose and proceeding along the backbone. Strong hydrogen bonds exist between the OH groups of the cellulose and $CO-NH_2$ groups of the polyacrylamide and PAM shell is formed[1].

Cellulose being a highly crystalline polymer, equilibrium swelling is much less due to the strongly hydrogen bonded crystalline structure leading to slow release of carbofuran as the crystallinity is retained even after xanthation and crosslinking. By grafting, the inter and intra molecular hydrogen bonds in cellulose are replaced by $CO-NH_2$ groups of the PAM. Thus the hydrophilicity is increased which affects the swelling and release of carbofuran.

6.7.1 Analysis of the graft copolymer (AmgCell)

6.7.1a Percentage PAM content

Analysis of AmgCell for PAM content (%) was carried out by gain in weight of the starting cellulose used and also by estimations of nitrogen content of AmgCell. It has been observed from Table 6.6.1 that the percentage PAM content in AmgCell carried out by gain in weight are almost similar with the percentage PAM content calculated from N content.

6.7.2 Proof of grafting

6.7.2a Solvent extraction

Graft copolymer containing homopolymer was soxhlet extracted using water as solvent for PAM extraction for 3 days, till no more polyacrylamide was extracted. The gain in weight after extraction accounts for the polyacrylamide that is grafted on to

Table 6.6.1

Description of the graft copolymers (AmgCell) prepared alongwith % PAM content in the graft copolymer

Expt. No.	Cotton pulp (Cell) used (g)	PAM content in AmgCell by gain in weight (g)	PAM in AmgCell by gain in weight (%)	PAM in AmgCell by N analysis (%)
$AmgCell_1$	5.25	2.07	28.3	28.6
$AmgCell_2$	5.25	3.58	40.5	38.1

Reaction time - 3 h for $AmgCell_1$,
5 h for $AmgCell_2$

Table 6.6.2

Thermal behaviour of samples Cell, PAM_2, blend of Cell + PAM_2 and $AmgCell_2$

Sample code No.	IDT (°C)	T_{max} (°C)		Endotherm (°C)
		T_{1max}	T_{2max}	
Cell	293	363	-	-
PAM_2	267,354	306	391	295,370
Cell+PAM_2 (6:4)	265	379	-	293
$AmgCell_2$	289	375	-	278 not prominent

IDT = Initial decomposition temperature.
T_{max} = Temperature for maximum weight loss.

cellulose.

6.7.2b Swelling behaviour

The graft copolymer swelled in water indicating the presence of PAM branches on cellulose backbone.

6.7.2c Solubility in solvent

Evidence for real grafting was obtained by comparing the solution behaviour of the graft copolymer with the physical mixture of the two.

Dissolution of the graft copolymer (AmgCell) in cuprietheylene diamine and addition of non solvent (acid) for cellulose, revealed the existence of graft copolymer. When mixture of cellulose and polyacrylamide (PAM) with ratio of cellulose to PAM similar to that in the graft copolymer, was taken, weight of precipitate obtained after addition of acid was of cellulose only and IR spectrum of the acid precipitated part showed no PAM. However, with graft copolymer,it was completely precipitated, fully accounting for both starting cellulose and the grafted PAM though the conditions were same as in physical mixture.

6.7.2d FTIR spectra

The presence of band at 1675 and 1634 cm^{-1} in FTIR spectra confirms the presence of PAM (Fig. 6.6.1). The mixture of cellulose and polyacrylamide taken in the same proportion as that of $AmgCell_2$ (cellulose to polyacrylamide ratio 6:4) using PAM from extracted homopolymer shows amide carbonyl at the same frequency. Comparison of the IR spectra of $AmgCell_2$ and the mixture of cellulose and PAM taken in proportion as that in

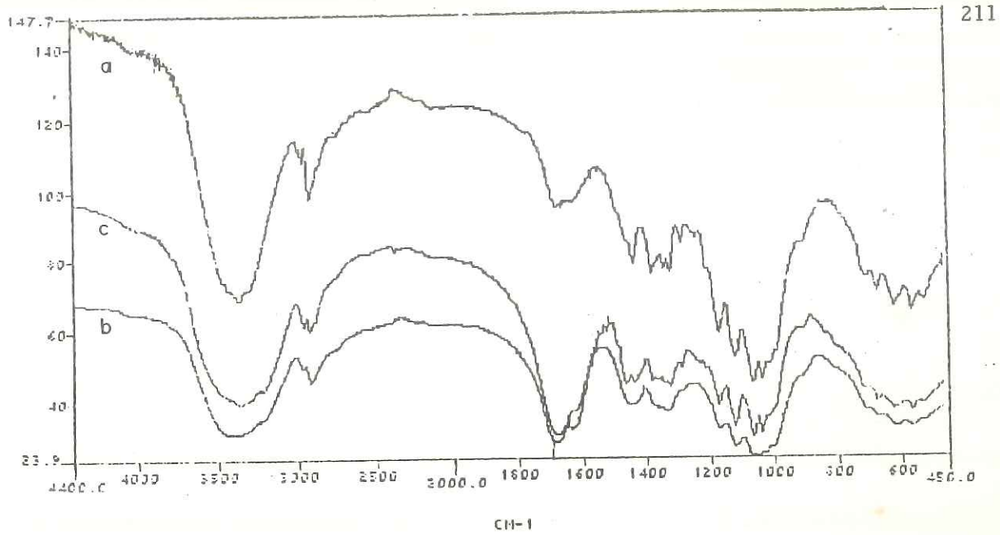

FIG. 6·6·1 : FTIR SPECTRA OF SAMPLES , a) Cell , b) $AmgCell_1$ AND c) $AmgCell_2$

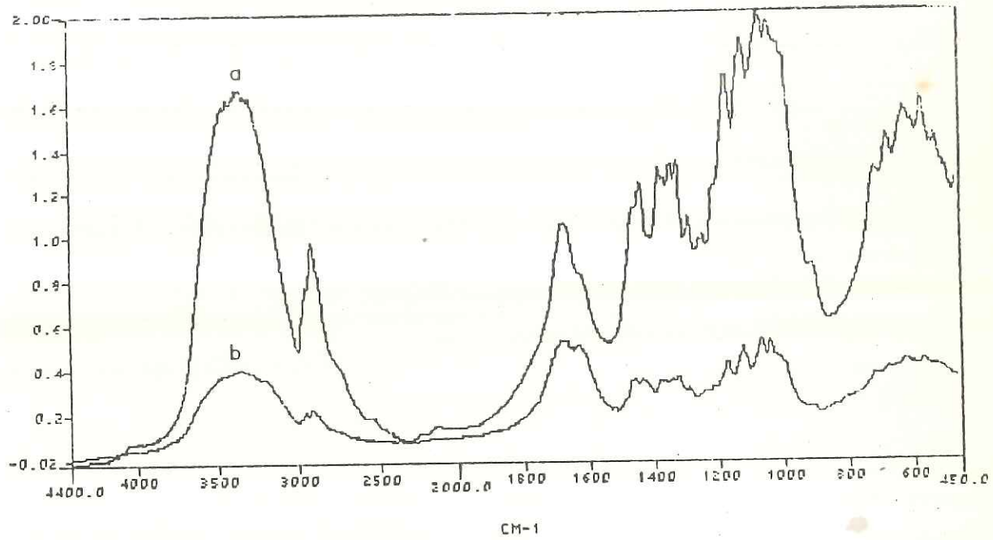

FIG. 6·6·2 : FTIR ABSORPTION SPECTRA OF SAMPLES

a) BLEND OF CELLULOSE + PAM (Extracted homopolymer from $AmgCell_2$) AND b) OF $AmgCell_2$

$AmgCell_2$ shows (Fig. 6.6.2) that the absorption intensity in $AmgCell_2$ was less than that in the physical mixture. The reduction in absorption intensity is a proof for chemically bonded PAM on to cellulose backbone. The band at 1675 cm^{-1} corresponds to amide carbonyl and 1634 cm^{-1} corresponds to NH_2 deformation. Hydroxyl group of cellulose is generally observed at 3400-3200 cm^{-1} due to polymeric association of hydrogen bonding. In AmgCell it is at 3400 cm^{-1}. The shift in frequency is due to cleavage of hydroxyl hydrogen bonding in cellulose chains and new hydrogen bonding between hydroxyl of cellulose and $-CO-NH_2$ of polyacrylamide is formed.

6.7.2e Thermal analysis

Thermal properties of homopolymer, PAM_2 (homopolymer extracted from $AmgCell_2$) and its blends with cellulose are summarised in Table 6.6.2. Blend of cellulose with PAM_2, taken in the proportion as that in $AmgCell_2$ shows endotherm at 293°C which is a characteristic of PAM_2, as it is observed in the DTA curve of PAM_2 but found to be absent in $AmgCell_2$. Thus the absence of characteristic endotherm in $AmgCell_2$ proves that polyacrylamide is chemically bound to cellulose. The TGA curves of cellulose, PAM_2, $AmgCell_2$, blend of cellulose and PAM_2 are illustrated in Fig. 6.6.3.

6.7.3 Characterization of AmgCell

6.7.3a Thermal stability

The thermal stability of cellulose (cotton pulp), its graft copolymers and extracted homopolymers was studied by thermo-

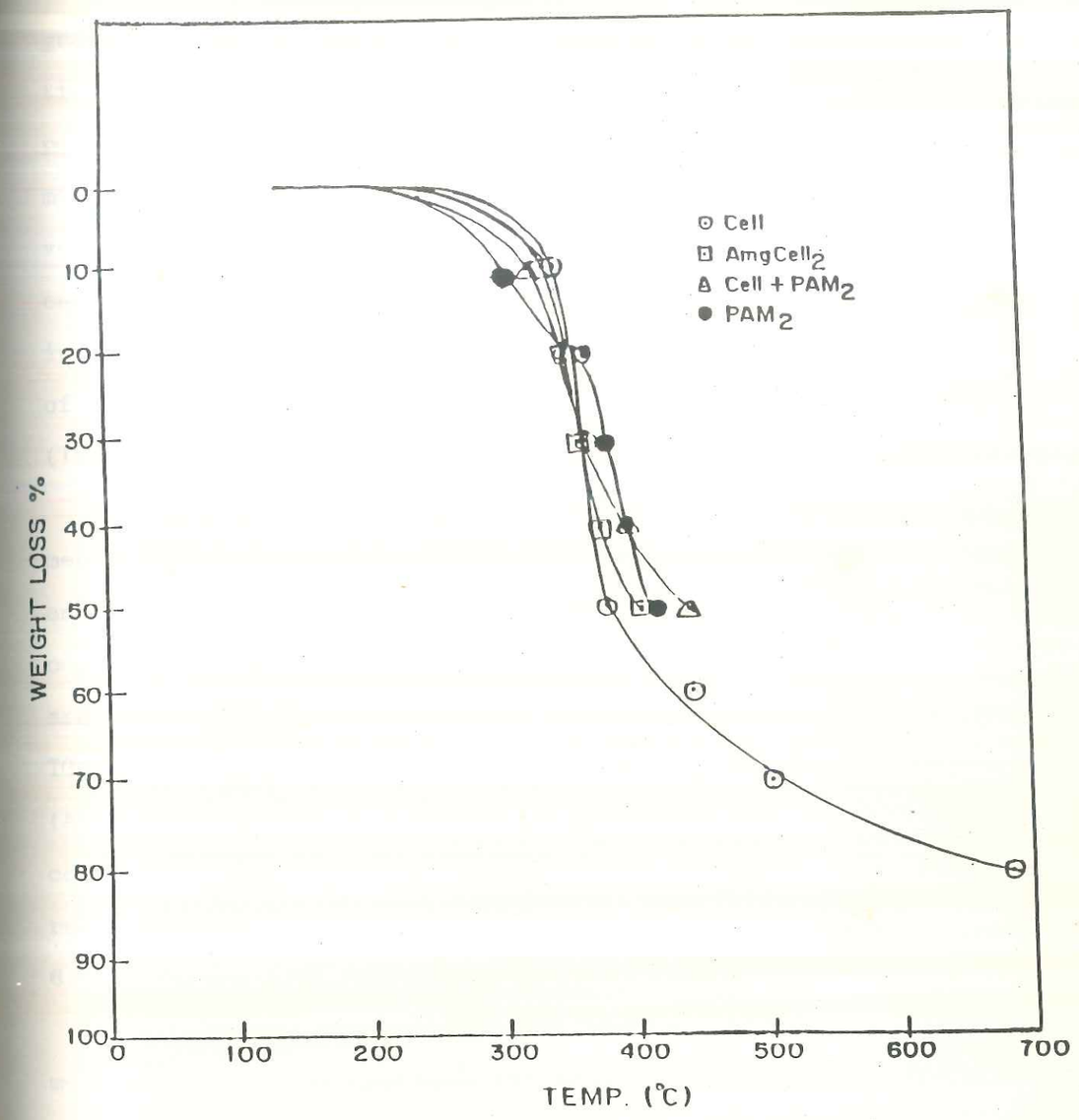

FIG. 6·6·3: TGA CURVES OF CELLULOSE, $AmgCell_2$, Cell + PAM_2 AND PAM_2

gravimetry (TG), derivative thermogravimetry (DTG) and differential thermal analysis (DTA). The thermal properties of these polymers are summarised in Table 6.6.3. It is observed that the mercerized cellulose shows low thermal stability with low T_{max} values. Also the thermal stability of polyacrylamide grafted cellulose is not much affected by grafting PAM on it or increasing the PAM content as compared to the thermal stability of cotton pulp as seen from the initial decomposition temperature (IDT).

Similarly, the thermal stability of mercerized graft copolymer (AmgCellM) is lower than that of mercerized cotton (CellM) and is increased with increase in the PAM content in the graft copolymer (as seen from the IDT and 10% loss). The T_{max} values are lower in case of mercerized graft copolymers. The respective TGA curves for cotton pulp (Cell), its graft copolymers (AmgCell), mercerized cotton pulp (CellM) and mercerized graft copolymer (AmgCellM) are illustrated in Fig. 6.6.4 and 6.6.5 respectively.

6.7.3b Percentage crystallinity

Percentage crystallinity of the pulp after grafting is not much affected. Percentage crystallinity for Cell and AmgCell at three different stages viz., original, mercerized and cross-linked, are given in Table 6.6.4 and the X-ray dffraction are illustrated in Fig. 6.6.6. As grafting was carried out in the aqueous medium and since the intercrystalline swelling of cellulose by water occurs predominantly in the accessible or

Table 6.6.3

Thermal behaviour of samples Cell, CellM, AmgCell, AmgCellM and PAM (homopolymer).

Expt. No.	IDT (°C)	T_{max} (°C)		Endotherm (°C)	10% loss (°C)	Total loss (%)	% Residue
		T_{1max}	T_{2max}				
Cell	293	363	-	-	331	81	19
$AmgCell_1$	296	382	-	310,382	340	79	21
$AmgCell_2$	289	376	-	278	344	74	26
PAM_1	233	262	344	256,338	273	78	22
PAM_2	267	306	391	295,370	306	76	24
CellM	273	338	-	328	317	80	20
$AmgCellM_1$	205	329	-	249,340,450	263	70	30
$AmgCellM_2$	256	328	-	267	289	70	30

IDT = Initial decomposition temperature.

T_{max} = Temperature for maximum weight loss.

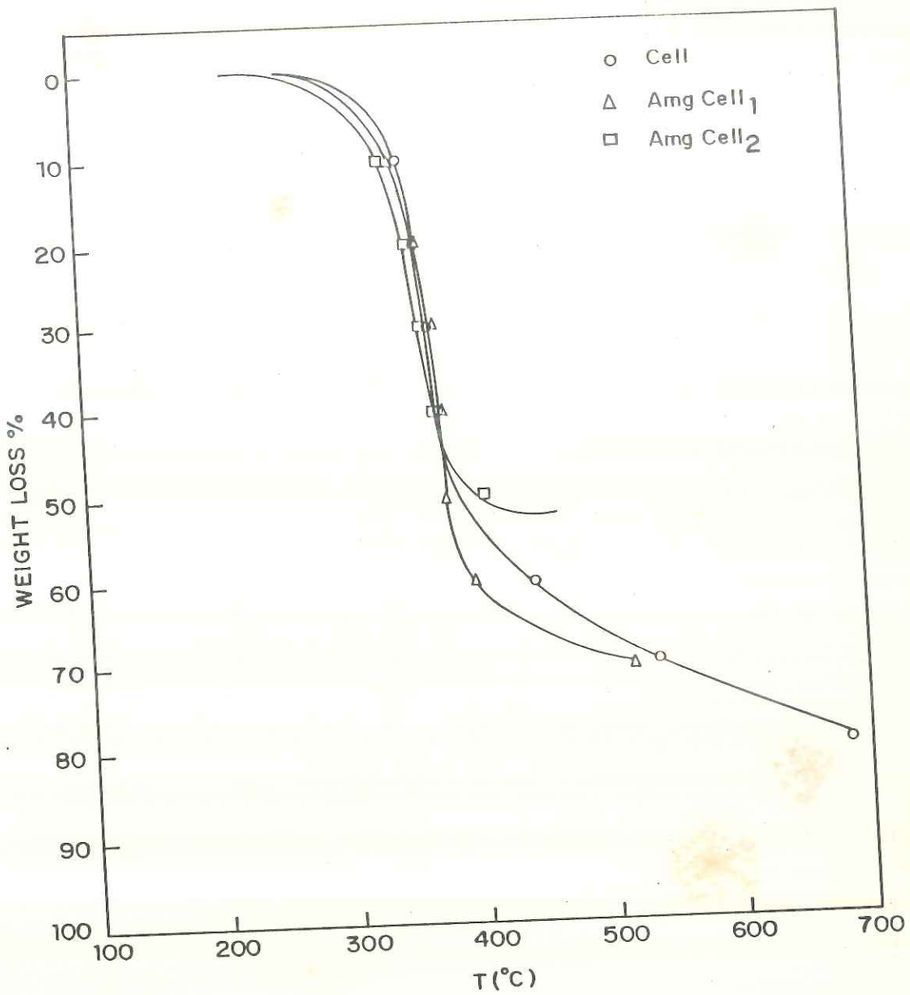

FIG.6·64: TGA CURVES OF SAMPLES CELLUOSE, Amg $Cell_1$ Amg $Cell_2$.

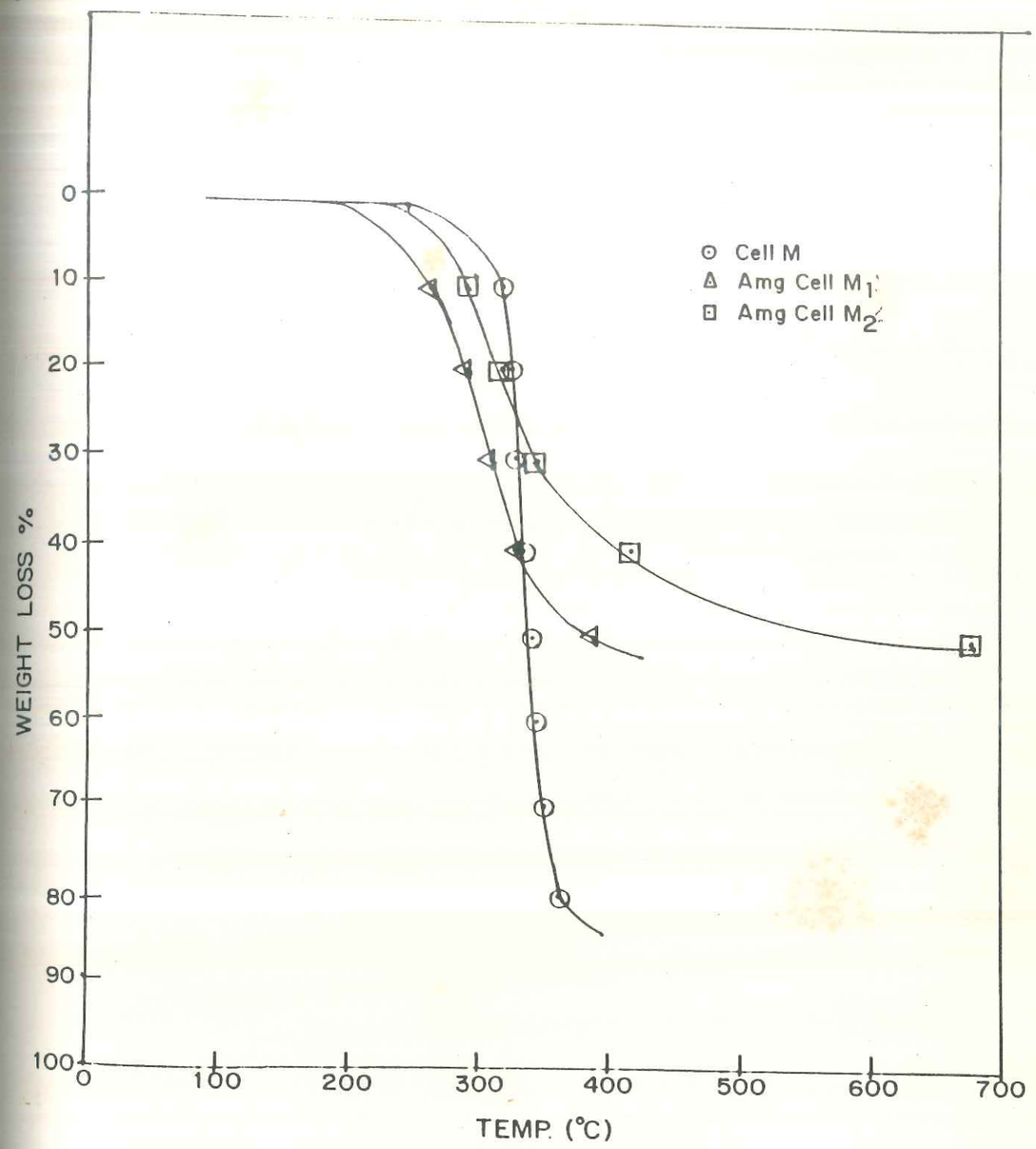

FIG. 6·6·5 : TGA CURVES OF MERCERISED CELLULOSE , AmgCell M_1 AND AmgCell M_2.

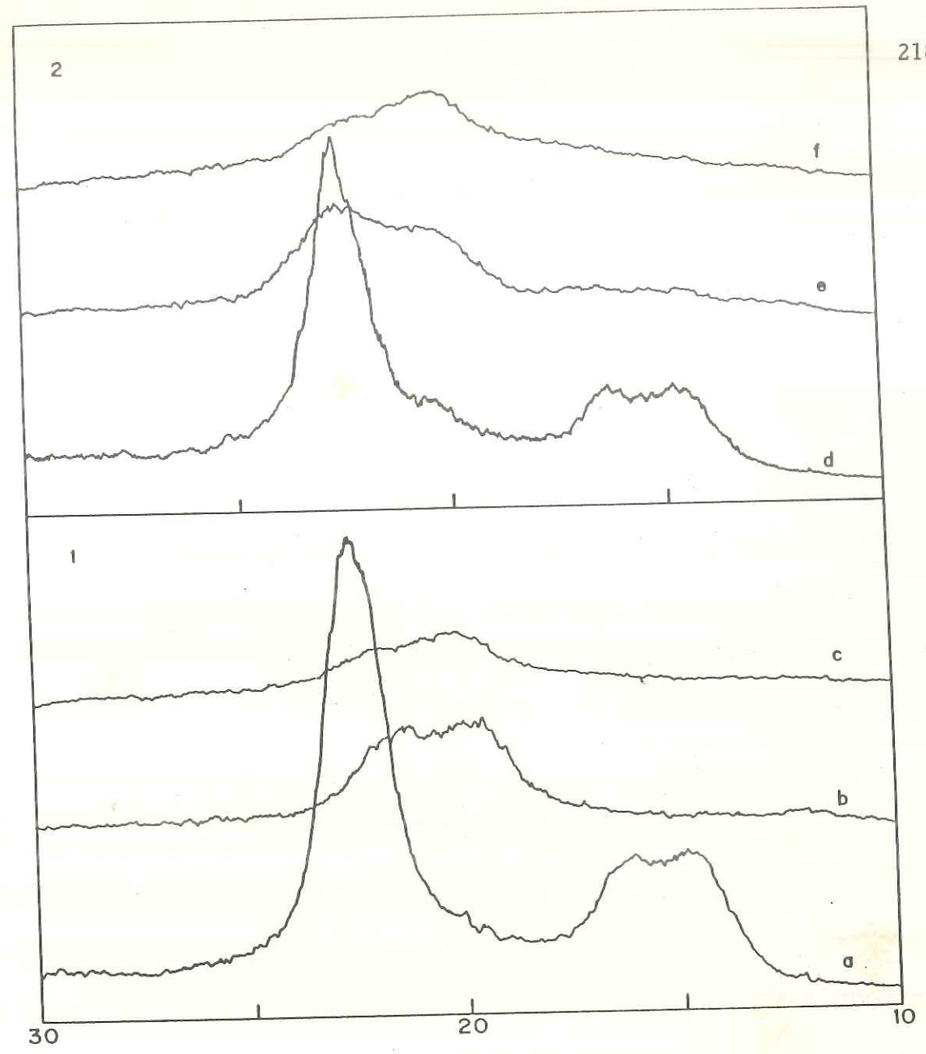

FIG. 6·6·6 : X-RAY DIFFRACTION PATTERNS OF SAMPLES
1) (a) $AmgCell_1$ (b) $AmgCellM_1$ (c) $AmgCellX_{O1}$
2) (d) $AmgCell_2$ (e) $AmgCellM_2$ (f) $AmgCellX_{O2}$

Table 6.6.4

Percentage crystallinity of samples Cell, $AmgCell_1$ and $AmgCell_2$ at the three different stages in the xanthide preparation.

Sample code No.	Crystallinity (%)		
	Original	Mercerized	Crosslinked xanthide
Cell	57.4	47.3	36.5
$AmgCell_1$	44.3	34.3	22.4
$AmgCell_2$	39.7	30.6	20.4

Table 6.6.5

Description of blank and encapsulated xanthides prepared using graft copolymer ($AmgCell_1$ and $AmgCell_2$)

Expt. code No.	Yield in (g)	Carbofuran (%)		Efficiency of encapsulation (%)
		Calculated	Obtained	
$AmgCellX_{o1}$	5.16	-	-	-
$AmgCellX_1$	6.67	24.4	22.6	90
$AmgCellX_{o2}$	5.20	-	-	-
$AmgCellX_2$	6.71	24.3	22.5	90

$AmgCellX_o$ (blank without carbofuran) prepared using 5 g of AmgCell.

AmgCellX (encapsulated with carbofuran) prepared using 5 g of AmgCell and 1.67 g of carbofuran.

amoprhous region of cellulose, the diffusion and therefore grafting of monomers is probably restricted to these regions. Thus, though the fibrous structure is changed, the fine structure of cellulose is practically unaltered. The decrease in crystallinity observed is due to quantitative addition of amorphous polymer (PAM). However, mercerization carried out prior to xanthation, reduces percentage crystallinity due to conversion of cellulose I to cellulose II and after crosslinking to xanthide, it is further reduced.

6.7.3c Structural characterization

Structural characterization of the AmgCell, AmgCellM and that of carbofuran dispersed in the xanthide matrix (AmgCellX), determined by solid state ^{13}C NMR is described in Chapter VII (Section 7.3.5a and 7.3.5b).

6.7.4 Analysis of the Blank and Encapsulated graft copolymer xanthides

6.7.4a Efficiency of encapsulation

Blank and encapsulated graft copolymer xanthides along with carbofuran content are described in Table 6.6.5. Efficiency of encapsulation is 90%.

6.7.4b Analysis of the blank xanthides for sulphur content

Sulphur content of $AmgCellX_{01}$ and $AmgCellX_{02}$ were found less than $SgCellX_0$ (styrenes grafted cellulose xanthides). However, with increase in PAM content, sulphur content is increased. Table 6.6.6 shows data for sulphur content, dégree of xanthation, and molecular weight between crosslinks in comparison to

Table 6.6.6

Effect of PAM content on sulphur analysis.

Expt. code No.	PAM content (%)	Sulphur (%)	Degree of xanthation	M_c
$CellX_0^*$	-	7.73	0.215	1657
$AmgCellX_{01}$	28.00	2.61	0.095	3544
$AmgCellX_{02}$	40.90	3.27	0.160	2175

* - Cellulose xanthide prepared using cotton pulp.

Table 6.6.7

Polyacrylamide (PAM) and polyacrylic acid (PAA) content in AmgCell at different stages in the xanthide preparation.

Sample code No.	N content by micro-analysis (%)	PAM content based on N (%)	PAA content by difference (%)	PAA by titration of xanthide (%)
$AmgCell_1$	5.63	28.60	-	-
$AmgCellM_1$	2.80	14.40	14.20	-
$AmgCellX_{01}$	1.91	9.82	-	7.50
$AmgCell_2$	7.52	38.10	-	-
$AmgCellM_2$	3.71	18.82	19.30	-
$AmgCellX_{02}$	2.70	13.89	-	8.10

cellulose xanthide ($CellX_0$). Degree of xanthation is 0.095 and 0.16 and molecular weight between crosslinks are found to be 3549 and 2175 for $AmgCellX_{01}$ and $AmgCellX_{02}$ respectively. Thus there is one crosslink after ten anhydroglucose units in cellulose xanthide ($CellX_0$) whereas in acrylamide graft copolymer of cellulose there is one crosslink after every twenty second anhydroglucose units in $AmgCellX_{01}$ and there is one crosslink after every thirteenth anhydroglucose unit in $AmgCellX_{02}$ i.e. Xanthide structure of AmgCell is less compact than $cellX_0$.

6.7.4c Polyacrylic acid content

Encapsulation procedure involves mercerization step as described in Chapter III (Section 3.1.3b). The PAM grafts of the $AmgCell_1$ and $AmgCell_2$ when subjected to mercerization before xanthation gets partly hydrolysed to polyacrylic acid. The FTIR spectra of mercerized AmgCell (AmgCellM) shows a band at 1700 cm^{-1} which corresponds to carbonyl stretching vibrations of acid group and 1610 cm^{-1} corresponds to carboxylate anion stretching (Fig. 6.6.7).

From elemental analysis of the AmgCellM for N, acrylic acid content was calculated by difference in PAM content of the original and mercerized (AmgCell and AmgCellM) graft copolymer. Acrylic acid content in graft copolymer xanthide ($AmgCellX_0$) was estimated by titration. The polyacrylamide and polyacrylic acid content in original, mercerized and crosslinked form are described in Table 6.6.7.

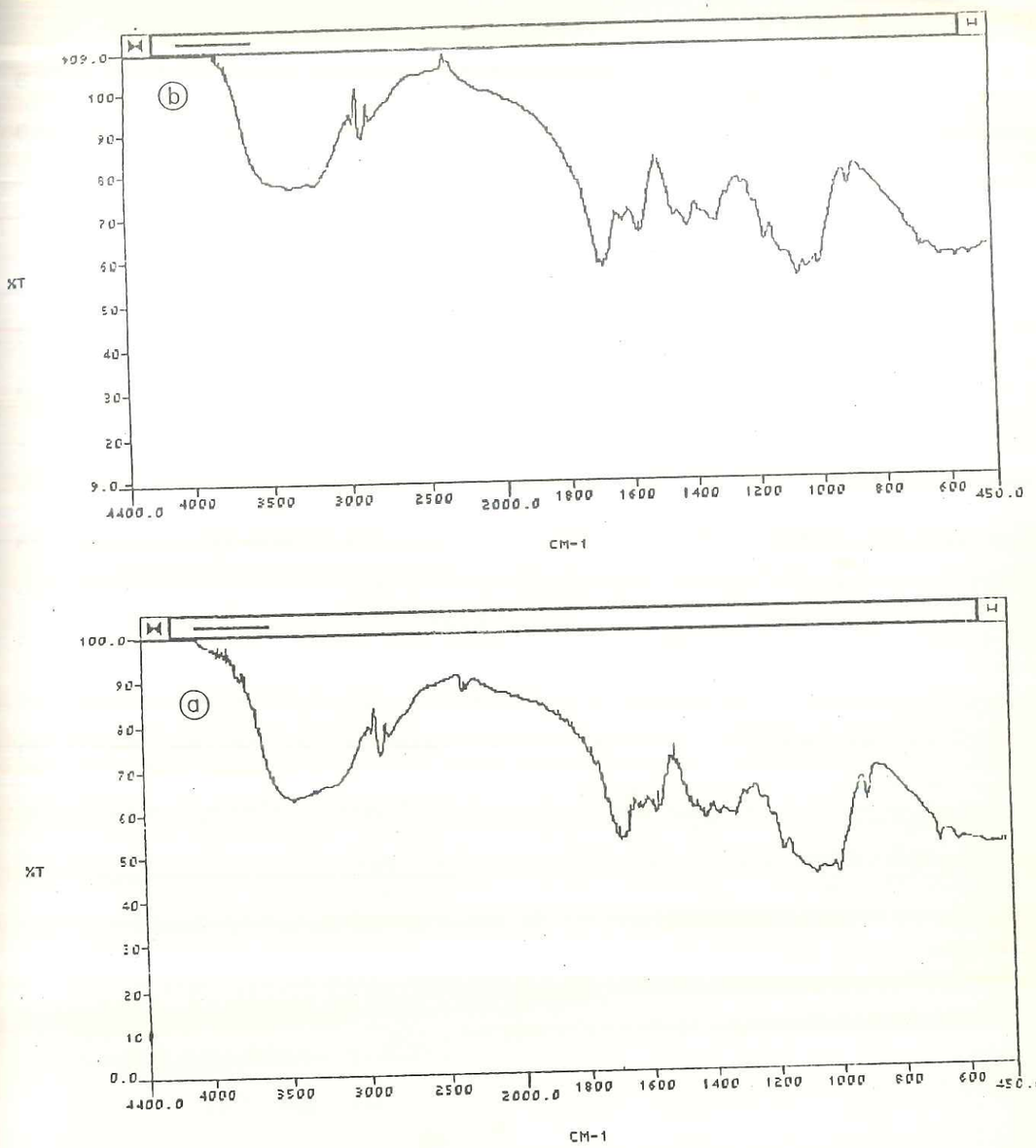

FIG. 6·6·7 : FTIR SPECTRA OF SAMPLES (a) AmgCellM$_1$ AND (b) AmgCellM$_2$

6.7.5 Swelling and release studies

6.7.5a Swelling studies

Percentage of water uptake by dry polymer with time was studied. Effect of sulphur content, polyacrylamide content and crystallinity on the percentage equilibrium swelling is described in Table 6.6.8. It is oberved that due to the presence of grafted hydrophilic PAM branches, percentage equilibrium swelling in AmgCell is three times more than that in cotton pulp. There is some difference between the extent of swelling between $AmgCellX_1$ and $AmgCellX_2$ (188 and 200%) which contain 28.0% and 40.9% of grafting (PAM%) respectively. The higher grafted $AmgCellX_2$ shows greater swelling and faster release. The sulphur content which is a measure of crosslinking and the percentage grafting which is a measure of hydrophilicity should have opposite effects on the degree of swelling and the t_{50} values reported reflect the net result of the two opposing factors.

6.7.5b Release of carbofuran

AmgCellX, a monolithic device with carbofuran being uniformly dispersed in the matrix when placed in thermodynamically compatible solvent (water), undergo glass to gel transition resulting in macromolecular chain relaxation and volume expansion. Thus the relaxation is facilitated by the presence of penetrant molecules, allowing the polymer chain greater mobility. The swollen or rubbery region of the polymer sample has a thickness which changes with time and finally equilibrium is attained. The diffusion coefficient of the active agent is

Table 6.6.8

Effect of sulphur content[a], PAM content[b] and crystallinity on swelling and half life values.

Expt. code No.	PAM content (%)	Sulphur (%)	Crystallinity (%)	Equilibrium swelling (%)	Time required to attain % equilibrium swelling (min)	Half life (min)
$CellX_4$	-	7.73	36.50	59	60	521
$AmgCellX_1$	9.82	3.61	22.40	188	2880	293
$AmgCellX_2$	13.89	5.88	20.40	200	1440	151

[a] - Sulphur content obtained for AmgCellX are converted to cellulose xanthide part.

[b] - PAM contents in the $AmgCellX_0$ (i.e. in crosslinked graft copolymer).

Table 6.6.9

Release rate constant k, diffusional exponent n and half life values of samples $CellX_4$, $AmgCellX_1$ and $AmgCellX_2$.

Expt. No.	Carbofuran (%)	k x 10^2 (min^{-n})	n	95% Confidence level of n		Half life (min)	Corr. coeff
				Upper limit	Lower limit		
$CellX_4$	24.7	2.4	0.52	0.54	0.49	521	0.999
$AmgCellX_1$	22.6	2.7	0.50	0.56	0.44	293	0.995
$AmgCellX_2$	22.5	3.4	0.53	0.55	0.50	151	0.998

generally much higher in the rubbery region than in the glassy region so that as the polymer begins to swell, active agent begins to move out of the system by diffusion through the rubbery layer. Rate of diffusion of the active agent out of the system is dependent both on the rate of penetrant uptake by the system and rate of diffusion of the agent through the rubbery layer. Besides the rate of penetrant uptake the diffusion coefficient of active agent in the rubbery region is affected by their partition coefficient between the water and swollen polymer phase and the relative size of the active agent and the macromolecular mesh i.e. crosslink density[9], which in this case is dependent on sulphur percentage and hence on the molecular weight between the crosslinks.

Thus as we have already discussed, the equilibrium water uptake was found to be directly related to the polyacrylamide content and degree of crosslinking. As degree of crosslinking is increased, crystallinity is reduced which also affects the rate of swelling in water[10].

Thus swelling in water, crystallinity and active agent partitioning in the polymer matrix and eluting medium (water), affects release of carbofuran, from fully swollen CR formulations using crosslinked AmgCell. Release profiles of carbofuran from CRF prepared using cotton pulp (Cell) and AmgCell are shown in Fig. 6.6.8 and it is observed that as the acrylamide content is increased, release is also increased. Release data for samples $AmgCellX_1$ and $AmgCellX_2$ along with $CellX_4$ were plotted as

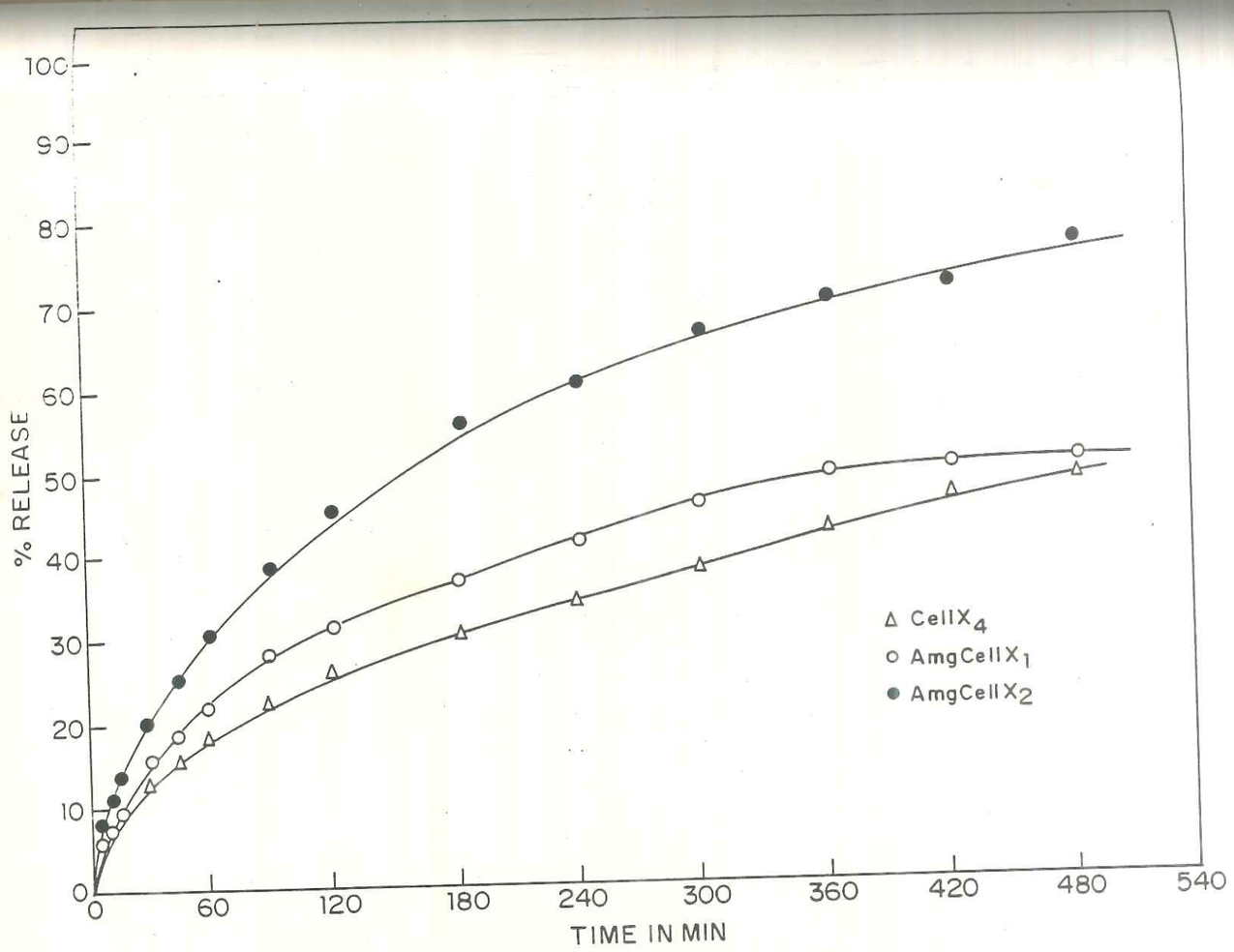

FIG. 6·6·8: RELEASE PROFILES OF CARBOFURAN FROM CRF SAMPLES AmgCellX$_1$, AmgCellX$_2$, AND CellX$_4$.

log (% release) vs log t. Table 6.6.9 shows k and n values evaluated from these plots.

The results depict linear portion upto 60% release over the period upto 360 to 420 minutes. The major release profile is governed by the k and n values. From the comparison of k and n values of $AmgCellX_1$ and $AmgCellX_2$ with $CellX_4$, it is observed that release rate constant k is only slightly increased as release is increased as a result of increase in polyacrylamide content. From the n values we can see that introduction of hydrophilic content had no effect on transport mechanism (release mechanism) and n values remained more or less the same. However, from the 95% confidence level of n i.e. upper and lower limit, it is observed that n values range from 0.44 to 0.56, indicating that the mechanism of release could be anomalous to Super Case II but not Fickian. Thus release mechanism is unaffected even after introduction of hydrophilic polymeric chain on cellulose backbone and release is governed by macromolecular chain relaxation or by diffusion of carbofuran through the polymer undergoing macromolecular chain relaxation.

6.7.6 CONCLUSIONS

Carbofuran, a broad spectrum pesticide can be successfully encapsulated by a similar procedure in both crosslinked cotton pulp and crosslinked, cotton pulp grafted with polyacrylamide matrices. The efficacy of encapsulation is 90%. The product is in the granular form and can be used as soil broad cast formulations. The encapsulation procedure involves the merceriza-

tion step which is required for activating the pulp before xanthation. Mercerization of AmgCell causes partial hydrolysis of the polyacrylamide branches to polyacrylic acid. Thus the graft copolymer xanthide encapsulating carbofuran contains copolymer of acrylamide and acrylic acid.

CRF of carbofuran using cotton pulp behaves like a normal crosslinked swellable hydrophilic polymer in both its water uptake and its active agent release properties. However, retention of high crystallinity even after crosslinking resulted in slower release.

Increase in release is observed by introduction of hydrophilic acrylamide branches on to cellulose. However, the increase observed compared to styrene grafted polymer is less though retention of crystallinity is observed in both the cases even after crosslinking.

Swelling and release studies show increase in swelling and release with increase in the hydrophilic content.

Increase in release is observed by increasing crosslinking and PAM content which reduces the crystallinity.

Release data analysed by equation $M_t/M_\infty = kt^n$ suggests that the release mechanism can be anomalous to Super Case II but not Fickian.

6.9 Comparison of the CRF of carbofuran prepared using SgCell and AmgCell with CRF of carbofuran prepared using cotton pulp with respect to swelling and release.

The swelling and release kinetics of CRF prepared using crosslinked SgCell and AmgCell (SgCellX and AmgCellX) shows that both these formulations have faster release than the CRF prepared using crosslink cotton pulp (CellX).

SgCellX shows faster release of carbofuran than CellX, inspite of the presence of hydrophobic styrene branches on the cellulose backbone. As the polystyrene branches are hydrophobic in nature their interactions with the cellulose backbone are repulsive in nature leading to more free volume for penetration of water and hence shows greater degree of equilibrium swelling than CellX. This results in faster release of carbofuran as the active agent is less tightly bound by the matrix (graft copolymer xanthide). SgCell shows less efficiency of encapsulation than cotton pulp and AmgCell. In case of CRF of carbofuran prepared using AmgCell, release of carbofuran is faster than that of cotton pulp but slower than SgCell formulations. Polyacrylamide branches being hydrophilic in nature they surround the cellulose backbone helically due to the hydrogen bonding between cellulose hydroxyl and $CO\text{-}NH_2$ groups of PAM. Thus inspite of cleavage of cellulose (-O-H---O-) hydrogen bonding new $-O\text{-}H\text{-}NH_2-$ hydrogen bonding is formed. Thus the PAM being hydrophilic and polar in nature, the interactions between cellulose backbone and PAM are attractive which bind the active agent (carbofuran), though the

degree of equilibrium swelling is more than that in SgCell. This resulted in faster release of carbofuran from CRF using PAM grafted cotton pulp xanthide (AmgCellX) than using only cotton pulp xanthide. However, the release is slower than CRF prepared using styrene grafted one (SgCellX).

Summing up, grafting on to cellulose backbone whether with a hydrophobic or a hydrophilic polymer leads to increase in agent release. Surprisingly the increase is more with the hydrophobic polymer graft.

REFERENCES

1. Neimo, L. and Sihtola, H., Papper och. Tra. No. 6 (1965) 369-379.
2. Schwab, E., Stannett, V. and Herman, J.J., Tappi 44(4) (1961) 251-256.
3. Richards, G.N. and White, E.F.T., J. Poly. Sci. Part C, No.4 (1963) 1251-1260.
4. Vasuda, H., Wray, J.A. and Stannett, V., J. Polym. Sci. C2, (1963) 387-402.
5. Kamogawa, H. and Sekiya, T., Text. Res. J., 31, 7 (1961) 585-591.
6. Vitta, S.B., Stahel, E.P. and Stannett, V.T., J. Appl. Polym. Sci., 38 (1980) 503-510.
7. Vitta, S.B., Stahel, E.P. and Stannett, V.T., J. Macromol. Sci. Chem., A(22) 5-7 (1985) 579-590.
8. Kaizerman, S., Mino, G., Meinhold, F., Textile Res. J., 32, (1962) 136.
9. Korsmeyer, R.W. and Peppas, N.A., J. Mem. Sci., 9 (1981) 211-227.
10. Graham, N.B. and McNeill, M.E., Makromol. Chem., Macromol. Symp., 19, (1988) 255-273.

CHAPTER - VII

CHARACTERIZATION OF CRF OF CARBOFURAN PREPARED FROM MODIFIED STARCH AND CELLULOSE MATRICES, BY ^{13}C CP/MAS NMR SPECTROSCOPY

7.1 INTRODUCTION

Structural characterization of polymers is very essential to understand their behavior on which their properties are dependent. Crosslinked polymers are difficult to characterize due to their insolubility and infusibility. However, it is highly essential to characterize crosslinked polymers because crosslinking of polymers has tremendously extended their range of practical utility, since the end use properties depend critically on the extent of cure. The crosslinks have major role in affecting the physical properties of polymeric materials.

The chemical analysis of the structure of crosslinked polymer network is complex in nature and can not be studied by solution techniques using usual physical and chemical methods because of limited solubility. Various approaches have been used to understand these systems.

The crosslinked network can be characterized by studying the physical and chemical property changes that have occurred in the elastomers. The physical properties, that are usually evaluated are: (a) modulus, (b) ultimate tensile properties, (c) swelling, (d) glass transition temperature and (e) mechanical properties. An estimate of the effective degree of crosslinking of the network can be calculated from the measured physical properties and with appropriate empirical equations. Even though these techniques have been well developed to a high degree of sophistication, they do not provide an absolute means of characterizing the network structure of polymer.

Various spectroscopic methods, viz., UV, IR, X-ray and Raman which are direct methods for chemical characterization, have been employed with limited success.

The development of high resolution solid state ^{13}C NMR has provided a means for studying solid interactable polymeric systems. Combining the techniques of dipolar decoupling (DD), cross-polarisation (CP) and magic angle sample spinning (MASS), high resolution carbon -13 solid state spectrum of the rigid crosslinked polymeric structure is obtainable.

The spectral parameters measured include chemical shifts, absorption line width, spin-lattice and spin-spin relaxation times. Except chemical shifts, other measurements are associated with the molecular motions of polymer chains which are hindered by inter molecular couplings such as physical entanglements and/or chemical crosslinks.

The use of solid state NMR for characterizing polymers have been well documented in the form of books[1,2] and reviews[3,4].

Before going further into the application of these measurements to crosslinked polymers, it is worthwhile to discuss briefly the NMR phenomenon and the concept of molecular relaxation.

7.1.1 NMR phenomenon and relaxation

Certain types of nuclei like protons, carbon - 13 and fluorine - 19 when placed in strong magnetic field B_0, can absorb electromagnetic radiation in the radiofrequency range. The precise frequencies at which the spin active nuclei resonate

can be picked up and displayed by instrument called Nuclear Magnetic Resonance (NMR) spectrometers.

Thus spin active nuclei when placed in a magnetic field, orient themselves with respect to the direction of magnetic field. Thus two orientations are possible for a proton, α and β spin states which differ in energy. It is this energy difference that can be supplied by the radiofrequency (also called Larmor frequency) radiation allowing the nuclear spins to change their state (Fig. 7.1a and Fig. 7.1b). The energy difference between the two spin states can be given by

$$E = h\nu \qquad .....(1)$$

where, h is Planck's constant and

ν is a frequency of electromagnetic radiation.

A well known relationship between Larmor frequency with applied magnetic field can be obtained by

$$\nu = \frac{\gamma}{2\pi} B_0 \qquad .....(2)$$

where, $\gamma/2\pi$ is the proportionality constant,

γ is the magnetogyric ratio of the nucleus.

In Boltzman distribution a mathematical expression links the population of different energy levels to the energy difference between them.

$$N_2/N_1 = 1 - (\Delta E/kT) \qquad .....(3)$$

where, N_2 and N_1 are the populations of the upper and lower energy levels,

ΔE is the difference between the energy levels,

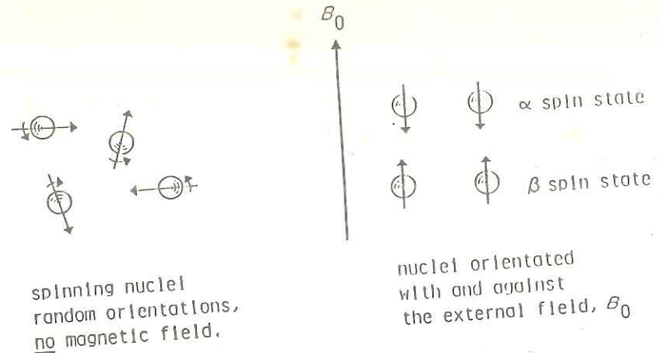

FIG. 7·1a : NUCLEAR SPIN

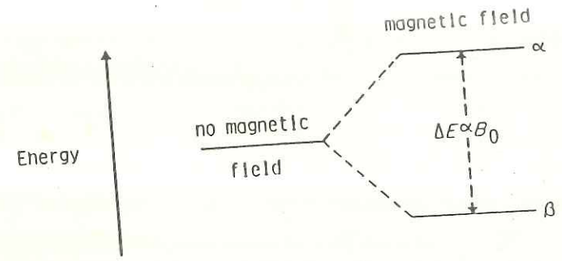

FIG. 7·1b : ENERGY DESCRIPTION OF THE NMR PHENOMENA

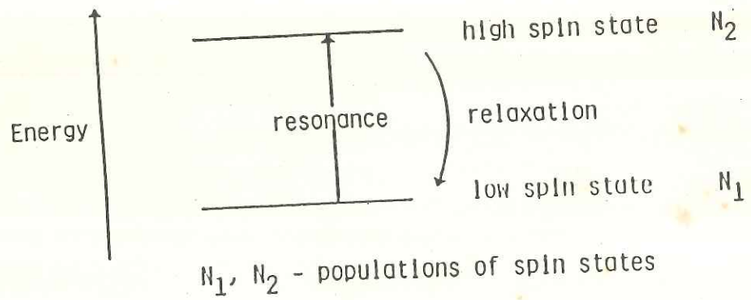

FIG. 7·1c : RESONANCE AND RELAXATION

k is the Boltzmann constant and

T is absolute temperature.

ΔE for spin states (ground and excited state) is so small that N_2/N_1 is almost unity.

Thus even in highest magnetic field, separation of energy levels is very small and even in absence of radio frequency magnetic field, there is rapid transfer of spins from lower to the upper state and vice versa. An equilibrium population distribution is attained within a few seconds after B_0 is applied. In the presence of field B_1 (r-f magnetic field) there will be net transfer of spins from lower to upper energy state. But again equilibrium will be reestablished by relaxing upper level spins to lower level. Thus a spin active nucleus in a magnetic field can be excited from its lower spin state to a higher spin state by radio frequency radiation of its Larmor frequency. This is the phenomenon of resonance. However, having been excited, the spin active nucleus must lose that extra energy if it is to return to the lower spin state. The means whereby this energy is lost are known as relaxation (Fig. 7.1c).

The relaxation occurs by two types of mechanisms namely spin-lattice relaxation and spin-spin relaxation. The former is a process by which the spin system attains equilibrium from non-equilibrium state by transfer of energy from the spin system to rest of the assembly of molecules referred as lattice. Spin-lattice relaxation is characterized by time T_1. The latter involves the relaxation from upper to lower energy state by

interaction between adjacent spin active nucleus. This type of relaxation is characterized by time T_2.

In case of polymers, spin-lattice relaxation time (T_1) is determined by high frequency short range motions of polymer chains while spin-spin relaxation time (T_2) is determined by low frequency long range motions of polymer chains.

The advent of solid state NMR spectroscopy has enabled direct measurements with solid samples, which have reduced mobility and hence an ineffective removal or averaging of various nuclear spin interactions. The liquid samples have substantial molecular mobility as a result of which the nuclear spin interactions are averaged (or removed by micro Brownian molecular motions). As far as the polymers are concerned, it is more relevant to consider the solid state ^{13}C NMR spectroscopy.

Solid samples give rise to broader NMR lines due to reduced mobility and hence ineffective averaging of various nuclear spin interactions. The dominant source of broadening of ^{13}C lines in solids is ^{13}C-^{1}H heteronuclear dipolar interactions, ^{13}C-^{13}C dipolar interactions being of relative unimportance because of the low natural abundance of ^{13}C nuclei (1.1%). Removal of ^{13}C-^{1}H dipolar broadening is accomplished by coherent averaging via strong irradiation (decoupling) at the proton resonance frequency which results in individual carbon resonance subject to residual broadening by chemical shift anisotropy (CSA). In solution an average chemical shift is observed due to rapid tumbling of the molecules whereas in solid state the chemical

shift for a given nucleus depends upon the molecular orientation with respect to the applied magnetic field. Removal of the broadening due to CSA is optimally accomplished by mechanically rotating the sample about an axis inclined at the magic angle (54.7^{o}) relative to the applied magnetic field. This gives rise to the single isotropic shift value, the same net result as for the random motion of the molecules. The result of magic angle spinning (MAS) is coherent averaging of the shielding anisotropy, in combination with proton irradiation; this produces in principle, a ^{13}C spectrum in which each magnetically distinct carbon appears as a narrowed single resonance at a frequency characteristic of the isotropic chemical shift for the solid state. Sensitivity enhancement is achieved by cross polarisation (CP). In solid state experiment, the polarization of low γ nuclei are altered by exploiting the dipolar coupling to high γ nuclei. This experiment is known as cross polarisation. The combined cross polarisation, dipolar decoupling sequence may be applied to a sample that is spinning at the magic angle to give what is commonly called a CP/MAS experiment and has found wide application in study of polymers because it allows the generation of high resolution ^{13}C spectra of insoluble material.

7.1.2 Application of NMR spectroscopy in crosslinked polymers

Synthetic polymers were the first polymer samples to be studied by solid state NMR techniques. The relationship between changes in crosslink density and relaxation properties of polymers was first studied by Gutowsky et al[5]. With the use of

absorption line widths as well as spin-lattice relaxation times, they showed that in vulcanization of natural rubber with sulphur, the crosslinking does occur at higher sulphur content and the reaction rate is favoured by sulphur ring forming mechanism.

Patterson and Koenig[6] have described the changes in the structure of natural rubber and cis polybutadiene using solid state ^{13}C NMR. At least four different methyl groups have been detected in the crosslinking of natural rubber by dicumyl-peroxide, which indicates that there is simple combination of allylic free radical in the curing process. Detection of presence of quaternary aliphatic carbons suggests double bond migration. Polybutadiene showed only methine and methylene carbons in the crosslinked network with a small amount of methyl end groups. The increase in line width of the highly crosslinked elastomers observed is in part due to static dipolar interactions between carbons and protons and chemical shift dispersions.

Cholli et al[7] studied Carbon-13 NMR spectra for cured epoxy polymers. The diglycidyl ether of bisphenol- A (DGEBA) was cured with dimethyl benzylamine (DMBA) and spectra were obtained at various cure times. During the reaction the decrease of resonance or intensity due to the epoxy ring and increase in oxymethylene carbon was noticed.

The structure of acetylene-terminated polyamide resins were studied by Sefcik et al[8] using magic angle spinning solid state ^{13}C NMR. It was found that the acetylene bond resonance at 84 ppm decreased with increase in curing. Thus the NMR technique

absorption line widths as well as spin-lattice relaxation times, they showed that in vulcanization of natural rubber with sulphur, the crosslinking does occur at higher sulphur content and the reaction rate is favoured by sulphur ring forming mechanism.

Patterson and Koenig[6] have described the changes in the structure of natural rubber and cis polybutadiene using solid state ^{13}C NMR. At least four different methyl groups have been detected in the crosslinking of natural rubber by dicumyl-peroxide, which indicates that there is simple combination of allylic free radical in the curing process. Detection of presence of quaternary aliphatic carbons suggests double bond migration. Polybutadiene showed only methine and methylene carbons in the crosslinked network with a small amount of methyl end groups. The increase in line width of the highly crosslinked elastomers observed is in part due to static dipolar interactions between carbons and protons and chemical shift dispersions.

Cholli et al[7] studied Carbon-13 NMR spectra for cured epoxy polymers. The diglycidyl ether of bisphenol- A (DGEBA) was cured with dimethyl benzylamine (DMBA) and spectra were obtained at various cure times. During the reaction the decrease of resonance or intensity due to the epoxy ring and increase in oxymethylene carbon was noticed.

The structure of acetylene-terminated polyamide resins were studied by Sefcik et al[8] using magic angle spinning solid state ^{13}C NMR. It was found that the acetylene bond resonance at 84 ppm decreased with increase in curing. Thus the NMR technique

was shown to be useful for studying the progress of a curing reaction.

Similarly, polychloromethyl styrene crosslinked by divinyl benzene was analyzed qualitatively and it was found that line width increases with increase in crosslink density[9].

Studies on radiation induced crosslinking at different radiation doses have also been reported by Charlesby *et al*[10]. They showed that solubility method only detects a permanent crosslinked network whereas T_2 measurements are sensitive to the presence of a network formed from both corsslinks and/or entanglements. When $1/T_2$ was plotted against radiation dose (r), a linear relationship was obtained with an intercept on dose axis. This intercept was fairly close to the virtual dose (re) for unirradiated sample. Virtual dose (re) represents the dose necessary to produce a density of crosslinks equivalent to that of intrinsic entanglement density.

Solid state NMR has thus proved to be a powerful tool for the study of structure of crosslinked polymers. In the course of present investigation ^{13}C CP/MAS NMR technique was employed to elucidate the structure of crosslinked starch and cellulose and also of crosslinked graft copolymers of cellulose.

7.1.3 Structure of starch and cellulose

7.1.3.1 Structure of starch

Starch, the natural polysaccharide, contains two components namely amylopectin and amylose. Amylose consists of (1-4) αD glucose units, while amylopectin consists of (1-4) αD glucans

grafted to the linear molecule by a single (1-6) linkages at intervals of twenty units or so (Fig. 7.2). Cereal starch contains amylopectin as a major component while tuber starch contains amylose as a major component.

X-ray diffraction pattern[11] shows A and B type for cereal and tuber starches depending upon origin. Imberty et al have studied these A[12] and B[13] type starches and concluded that the unit cell in A type contains twelve glucose residues located in two left handed parallel-stranded double helices packed in a parallel fashion with six residues per strand of the double helix and maltotriose as the asymmetric unit. The unit cell in B type starch consist of maltobiose repeat unit. This is also confirmed by NMR. Thus ^{13}C NMR for A and B starch, gives rise to triplet and doublet respectively for C_1 carbon. Therefore, A and B type have similar molecular conformations, which differ only with respect to the packing of the helical chains. In type A the close packing of double helix, one double helix surrounded by six neighbours and interstrand stabilization within double helix is achieved by extensive hydrogen bonding.

Extensive work has been carried out on the structural study of amylose polymorphs by CP/MAS ^{13}C NMR spectroscopy and X-ray analysis[12-14].

Structural characterization of the monosaccharide unit αD glucan and βD glucan has also been carried out by Parfondry and Perlin[15] along with their modified forms by ^{13}C NMR spectroscopy. The chemical shift displacements for C_1 and C_4 carbon (i.e.

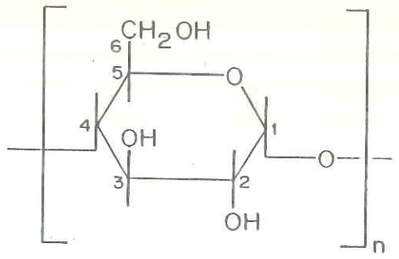

AMYLOSE

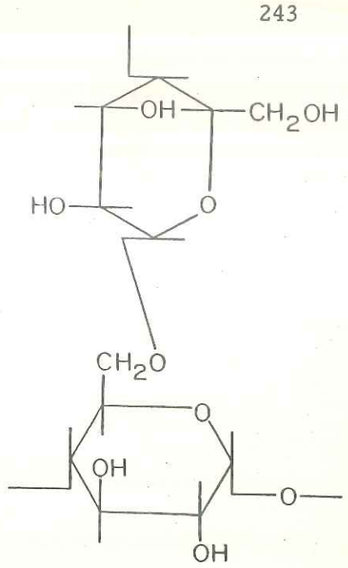

AMYLOPECTIN

AMYLOSE AND AMYLOPECTIN COMPONENTS OF STARCH

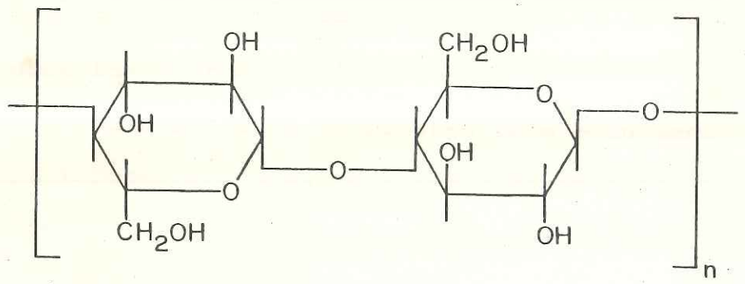

CELLULOSE

FIG. 7·2 : STRUCTURE OF STARCH AND CELLULOSE

carbons involved in glycosidic linkages) are related to amorphous and crystalline materials along with substantial conformational changes. Hence, amorphous structure corresponds to a single chain whereas the crystalline structure corresponds to a double helical conformation. This was shown by the study of starch and related compounds through high resolution ^{13}C CP/MAS NMR spectroscopy by Gidley et al[16].

7.1.3.2 Structure of cellulose

Cellulose a major constituent of plant cell wall is $\beta(1-4)$ linked polymer of anhydroglucose and, has well established structure.

It is known to exist in four distinct polymorphs as revealed by solid state ^{13}C NMR on the basis of differing chemical shifts[17]. Of the most common are cellulose I and cellulose II. Cellulose I is the naturally occurring form, its fibrillar dimensions and degree of crystallinity (60% to 90%) differ depending upon the source. Cellulose II is the usual polymorph obtained when cellulose is precipitated from solution, although mercerized cellulose (produced in a solid state transformation by treatment with sodium hydroxide) also has cellulose II features. The crystal structure of cellulose revealed a parallel chain packing for cellulose I while cellulose II is believed to adopt an antiparallel chain arrangement[18].

7.1.3.2a Cellulose I

Native cellulose (Cellulose I) is often heterogeneous containing highly ordered or crystalline component, the one

buried inside the fibril and disordered region which is believed to be material on the surface of crystallities.

Highly ordered crystalline region gives rise to sharp peak, whereas the material on the surface or disordered region gives rise to broad peak in their NMR spectrum. The ^{13}C signals from more ordered region appear as well resolved peaks. The splittings for carbon have been interpreted as direct evidence for the presence of two types of glycosidic linkages and suggest an alternation of inequivalent glycosidic linkages along the chain[19] (Fig. 7.2).

The native cellulose can be classified into two groups viz., cotton ramie type and bacterial valonia type[20,21] which are referred to as I_a and I_b, respectively. The appearance of the narrower peaks in the cellulose I spectrum is governed by the origin of the sample (e.g. Valonia cellulose, bacterial, cotton etc.). Multiplicities have been observed particularly in the resonance arising from C_1, C_2, and C_6. The relative intensities of the components of these multiplets are sample dependent.

Two different interpretations have been proposed to account for the variations in the spectra of native cellulose. The more ordered component of native cellulose is composed of two forms $I\alpha$ and $I\beta$[22] of two crystal forms as shown by X-ray diffraction. It is made up of varying amounts of two types of material that are characterized either by eight chain unit cell or a two chain unit cell. Thus, peaks due to C_1 and C_4 in the ^{13}C NMR spectrum of a given sample of native cellulose would arise from a linear

combination of 1:1:2 multiplet due to the eight chain cell material and a 1:1 multiplet due to the two chain material. In crystal, cellulose forms almost linear two fold helical structure.

7.1.3.2b Cellulose II

Natural form of cellulose (parallel chains) exists in a metastable state and can be transformed irreversibly to the more stable form (antiparallel form) by mercerization[17,18]. The biosynthetic apparatus consists of closely packed structure which produces many cellulose chains simultaneously in close proximity to each other. As these chains are spread out in a parallel arrangement, they form interchain hydrogen bonds, thereby becoming trapped in a metastable state with a high activation energy preventing them from achieving the more stable antiparallel arrangement. The transformation from a parallel to an antiparallel arrangement during mercerization may be occurring by a mechanism shown in Fig. 7.3. Treatment with NaOH would disrupt the H-bonds of cellulose I and swell the fiber, thereby enabling the chains to undergo a conformational change. Long antiparallel chains can support the chain fold indicated in Fig. 7.3. In the swollen state, the activation energy for the transformation would be lowered and chains could then take on their more stable antiparallel arrangements[18].

X-ray diffraction and solid state ^{13}C NMR of highly crystalline and pure cellulose polymorphs have revealed the difference between cellulose I and cellulose II. In solid state ^{13}C NMR

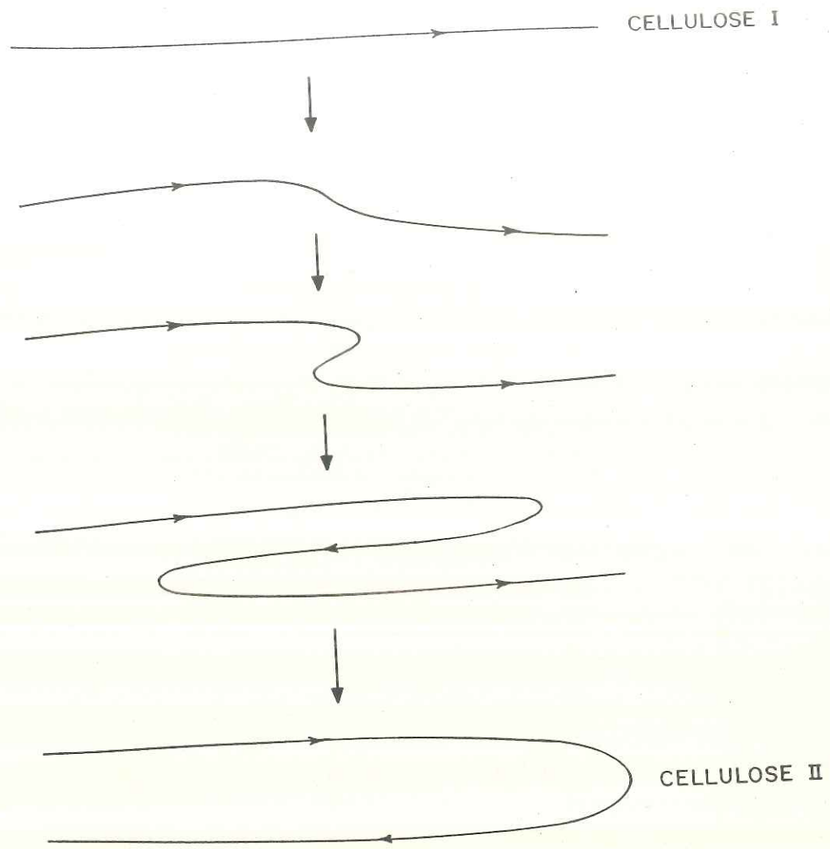

FIG. 7·3 : SCHEMATIC REPRESENTATION OF SUCCESSIVE STAGES OF THE TRANSFORMATION FROM A PARALLEL TO AN ANTIPARALLEL ARRANGEMENTS OF CELLULOSE CHAINS DURING MERCERIZATION

the difference appears in the form of chemical shifts of C_4 and C_6. Some conformational transformations or crystalline packing influences of C_4 and C_6 in anhydroglucose units are likely to cause these chemical shift differences between cellulose polymorphs[23] and the transformations of X-ray diffraction patterns[18].

7.2 EXPERIMENTAL

7.2.1 Materials

Samples of crosslinked cellulose and starch (CellX and StX) were used for the NMR analysis along with their original (Cell and St) and mercerized and gelatinized forms (CellM and StG). Similarly, crosslinked graft copolymers of cellulose alongwith their original and mercerized forms were used. Dried granules of mesh size (crosslinked samples) -5+10 were ground in an analytical mill and a fraction of -100+170 was generally used for NMR analysis.

Purified carbofuran as described in Chapter III (Section 3.1.2a) was used. Similarly, carbofuran extracted from samples $CellX_4$ and StX_4 was redissolved in acetone and precipitated in distilled water. This precipitated carbofuran was separated from water by filtration and dried in oven at 50° to a constant weight. The samples used for NMR studies are listed in Table 7.1.

7.2.2 Measurements

^{13}C CP/MAS NMR measurements were carried out on a Bruker MSL-300 NMR spectrometer operating at 75.5 MHz for carbon. The samples were placed in a 7 mm cylindrical zirconia rotor and spun

Table 7.1

Details of samples used for NMR analysis.

Sr.No.	Sample designation	Description
1.	St	Starch
2.	StG	Gelatinized starch
3.	StX_C	Starch xanthide with carbofuran
4.	StX_O	Starch xanthide without carbofuran
5.	Cell	Cellulose (cotton pulp)
6.	CellM	Mercerized cellulose
7.	$CellX_O$	Cellulose xanthide without carbofuran
8.	$CellX_C$	Cellulose xanthide with carbofuran
9.	CF	Pure carbofuran
10.	CF-E	Carbofuran extracted from matrix.
11.	AmgCell	Acrylamide grafted to cellulose
12.	AmgCellM	Mercerized AmgCell
13.	AmgCellX	Crosslinked AmgCell
14.	SgCell	Styrene grafted to cellulose
15.	SgCellM	Mercerized SgCell
16.	SgCellX	Crosslinked SgCell

at 3 to 4 kHz. The Hartman Hahn match condition was adjusted using admantane and was maintained at 50 kHz. The chemical shifts were referred to the admantane CH taken as 38.7 ppm.

The spin-spin relaxation time (T_2) for the samples Cell, CellX_0, St and StX_0 have been calculated from the ^{13}C line width data which have been obtained by the deconvolution of the ^{13}C CP/MAS NMR spectra using a Bruker utility programme, LINESIM T_2 was calculated using the equation :

$$LW = \frac{1}{\pi T_2} \quad \text{or} \quad T_2 = \frac{1}{\pi LW} \qquad .....(4)$$

7.3 RESULTS AND DISCUSSION

7.3.1 Structure of pure, gelatinized starch and crosslinked starch

7.3.1a Structure of pure and gelatinized starch (St and StG)

The ^{13}C CP/MAS spectra of St and StG starch are shown in Fig. 7.4a and Fig. 7.4b. The chemical shifts assignments are based on previous findings[24,25] and are shown in Table 7.2.

The C_1 carbon of St being directly attached to two oxygen atoms resonates at relatively lower field (102.5 ppm) than the other five. The nature of this peak is generally used to characterize starch obtained from different sources. The C_1 peak in Fig. 7.4a did not show any characteristic splitting of a highly crystalline sample. This itself clearly indicated that the native maize starch used in this study consists of crystalline and amorphous forms. However, deconvolution of the

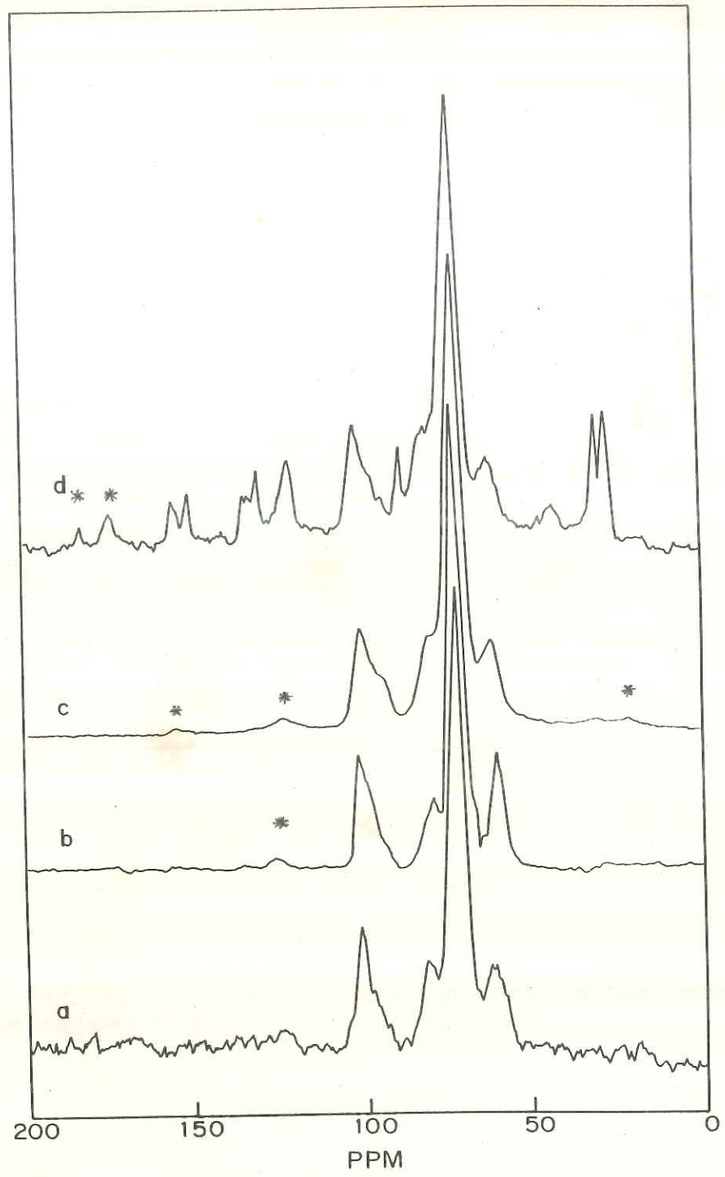

FIGURE 7·4: ^{13}C CP/MAS NMR SPECTRA OF SAMPLES
a) St , b) StG , c) StX_O , d) StX_C
* SIDE BAND

Table 7.2

^{13}C NMR chemical shifts of samples St, StG, StX_O and StX_C.

Sr.No.	Sample	C_1	$C_{2,3,5}$	C_4	C_6
1.	St	102.5 100.5 98.7 94.7	74.2 71.9 70.4 -	80.8 - - -	61.4 - - -
2.	StG	102.2	72.1	81.6	61.6
3.	StX_O	102.2	74.0 72.1 70.9	81.2 -	61.4 -
4.	StX_C	102.7	72.7	82.0	61.8 61.6

Table 7.3

Spin relaxation time, T_2 (μs) of starch carbons for pure starch and crosslinked starch

Sample	C_1	C_4	$C_{2,3,5}$	C_6
St	1837	834	1220, 2849, 1701	1216
StX_O	1013	726	1334, 1497, 1181	960

experimental spectrum unambiguously showed its multi-component nature, especially for the C_1 carbon. The components had chemical shift of 102.5, 100.5, 98.7 and 94.7 ppm. This can also be seen from the ^{13}C CP/MAS spectra of St (broken line) and StX_0 in Fig. 7.6 where 50 to 110 ppm region is expanded. The sharp peak at 100.5 ppm is due to the crystalline component of the C_1 while down field shoulder at 102.5 ppm and the broad upfield signals at 100 to 95 ppm are assigned to amorphous component in native maize starch. The crystalline part arises from amylopectin and amorphous regions from branch point of amylopectin and long chains of linear amylose. The X-ray diffraction pattern shown in Fig. 7.5a also confirm the presence of crystalline and amorphous nature of maize starch. As seen from Fig. 7.6, carbons C_2, C_3 and C_5 resonate in the range 65 - 78 ppm. The peak at 80.8 ppm is due to C_4 carbon which provides direct evidence for the presence of glycosidic linkages[24]. C_6 carbon appears at 61.4 ppm. Amorphous nature of starch makes the peaks broad with poor resolution of individual carbon resonance.

The ^{13}C CP/MAS spectrum obtained for StG (Fig. 7.4b) is similar to that of St except for the nature of C_1. The C_1 of StG shows a broad peak at 102.2 ppm which is due to its amorphous nature. Thus, there is loss of crystallinity during the process of gelatinization, which is supported by XRD (Fig. 7.5b).

7.3.1b Structure of crosslinked starch (starch xanthide StX_0)

The ^{13}C CP/MAS NMR spectrum of StX_0 is shown in Fig. 7.4c

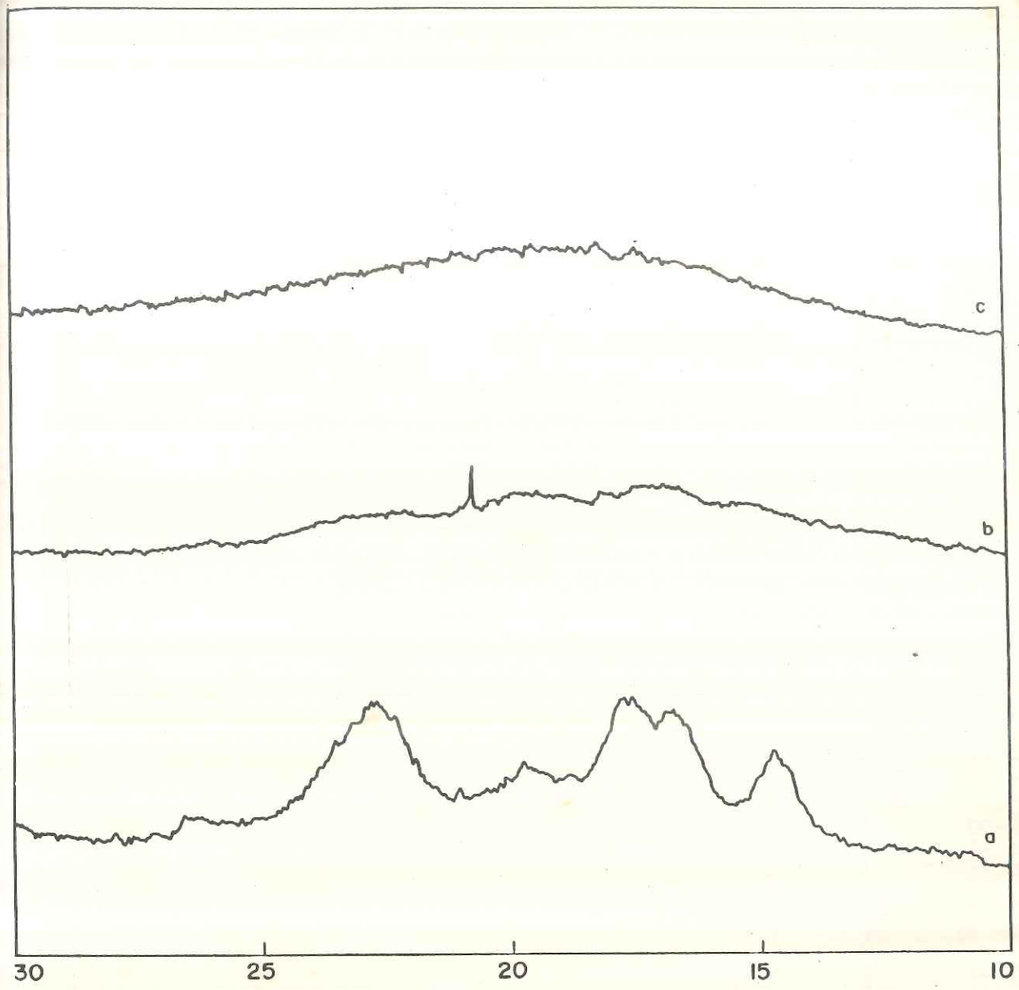

FIG. 7.5 : X-RAY DIFFRACTION PATTERNS OF SAMPLES a) St b) StG c) StX_0

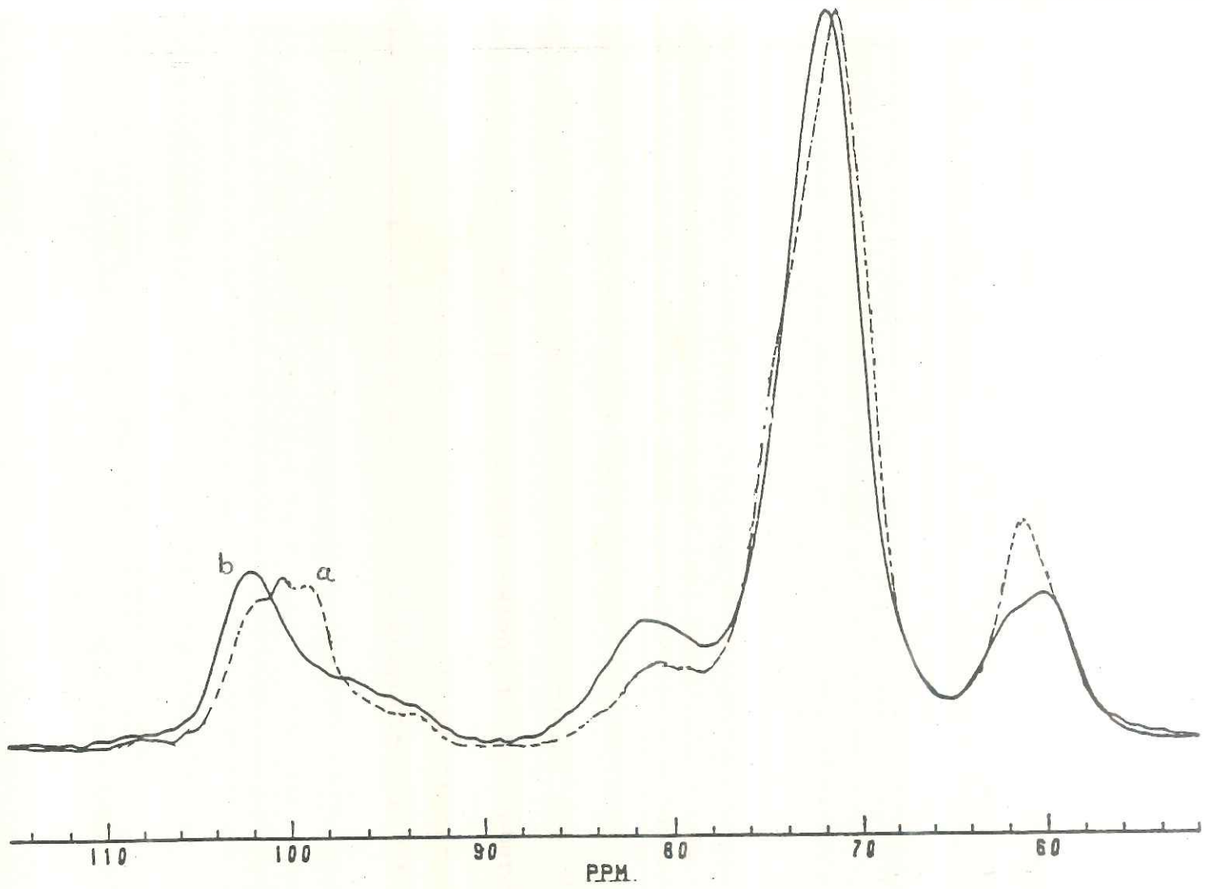

FIG. 7·6 : COMPARISON OF ^{13}C NMR SPECTRA OF SAMPLES a) St AND b) StX_o (50 TO 110 REGION EXPANDED)

and the assignments of chemical shifts are given in Table 7.2. In order to differentiate the spinning side bands from the ^{13}C signals, the CP/MAS spectral data were collected at two spinning speeds (3.01 KH_z and 4.0 KH_z). The differentiation is based on the fact that the spinning side bands shift their position with respect to the spinning speed whereas a real peak does not shift the position. The absence of sharp C_1 peak in the region of 102 ppm demonstrated the crosslinked nature of the modified starch. The complete conversion of native maize starch into an amorphous form of starch is due to S-S crosslink in starch xanthide. This is expected as the sulphur crosslinks completely rupture the hydrogen bonded six fold double helical structure and convert the polymer into a random coil structure. This is also evident from the nature of C_4 signal at 81.2 ppm and also a broad peak at 61.4 ppm for C_6. The nature of the changes induced in the ^{13}C CP/MAS NMR spectrum upon crosslinking can be clearly seen in Fig. 7.6 which depicts the 112 to 52 ppm region of the starch (broken line) and the crosslinked one (StX_0). The amorphous nature of the crosslinked polymer was further supported by the XRD data (Fig. 7.5c).

A comparison of Fig. 7.4 (a,b, and c) and the data presented in Table 7.2 shows that the chemical shifts obtained upon gelatinization (Fig. 7.4b) and oxidative crosslinking (Fig. 7.4c) are more or less similar to that of starch itself except for the broadening of the peaks. For example, the signal at 102.5 ppm for C_1 transforms from a multiplet to a broad singlet with

upfield shoulder. It can also be noted that the C_4 signal at 80.8 ppm in pure starch gets broadened after gelatinization and almost merged into the broadened signal of carbon $C_{2,3,5}$. The sharp C_6 peak in pure starch at 61.4 ppm also broadened on gelatinization while crosslinking broadened it further to an extent that it appeared as a hump at the base of $C_{2,3,5}$ signal. It is known that during gelatinization, intra and inter-helical hydrogen bonds get ruptured causing dissociation of double helices and disturbing the closely packed ordered double helical structure. The broadening of the C_1 resonance is due to the opening of double helical structure to random coil. This is also supported by T_2 (spin-spin relaxation time) calculated from the line width data (Table 7.3). T_2 calculated for C_6 carbon of starch was 1216 μs whereas T_2 for the same carbon on crosslinking was 960 μs.

The reduction in T_2 values can be attributed to the restricted motion of polymer chains due to crosslinking. The conversion of pure starch to crosslinked one is accompanied by a complete conversion of crystalline structure to amorphous one which is manifested as reduction in spin-spin relaxation time (T_2) and hence as broadening of the peaks. A similar result was also reported by Shukla et al[26] in their study of crosslinking of starch with urea formaldehyde (UF) resin. They observed an increase in line width and reduction in spin-spin relaxation time with increase in UF to starch ratio.

7.3.2 Structure of native, mercerized and crosslinked cellulose

7.3.2a Structure of native cellulose

The ^{13}C CP/MAS spectra of native (Cell) and mercerized cellulose (CellM) are comparatively illustrated in Fig. 7.7 along with the spectra obtained on oxidative crosslinking ($CellX_O$) and that encapsulating carbofuran ($CellX_C$). ^{13}C CP/MAS spectra of cellulose I (Cell) is reminiscent of previously published cellulose spectra[20,27,28]. The peak at 105 ppm is assigned to the C_1 anomeric carbon which resonates at down field than the corresponding starch carbon due to equatorial position. The signals in the region of 70-80 ppm are assigned to the C_2, C_3 and C_5 carbons of cellulose. The sharper resonance at 88 ppm and the broader resonance at 83 ppm are assignable to C_4 and the narrower peak at 64.7 and broader peak at 62 ppm, may be due to C_6 resonances. The narrower peaks are arising from the highly ordered environment and broad peaks from the less ordered environment.

7.3.2b Structure of mercerized cellulose

In transformation of cellulose I to Cellulose II, a clear difference in the chemical shift of C_1, C_4 and C_6 is observed (Table 7.4). Fig. 7.7b shows ^{13}C NMR spectrum of CellM. It is known that in conversion of cellulose I to cellulose II, the linearly extended two fold hydrogen bonded structure is destroyed which is also supported by X-ray diffraction study (Fig. 7.8b). Thus, C_1 appears at 106.6 and 104.8 ppm as a doublet. The $C_{2,3,5}$ appears at 74.6 ppm, C_4 appears at 87.8, 85.6 and 85.0 ppm and C_6

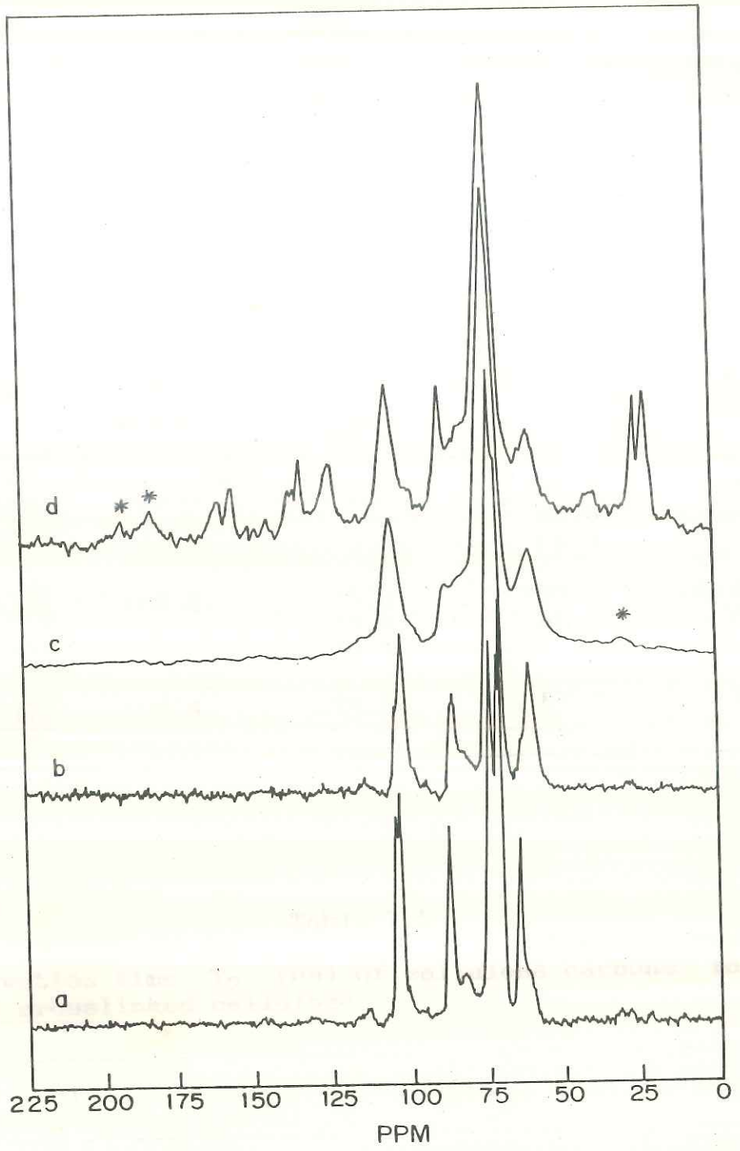

FIGURE 7·7: ^{13}C CP/MAS NMR SPECTRA OF SAMPLES
a) Cell , b) Cell M , c) Cell X_o , d) Cell X_c
* SIDE BAND

Table 7.4

^{13}C NMR chemical shifts of cellulose mercerized cellulose and crosslinked cellulose

Sr.No.	Sample	C_1	$C_{2,3,5}$	C_4	C_6
1.	Cell	105.0 103.6	74.1 71.5 70.7	88.3 83.0	64.7 62.0
2.	CellM	106.6 104.8	74.6	87.8 85.6 85.0	62.6
3.	$CellX_O$	104.4	75.5 73.9 72.3	87.2 82.1	61.9 59.9
4.	$CellX_C$	104.4	74.5	87.2	62.3

Table 7.5

Spin relaxation time, T_2 (μs) of cellulose carbons for native and crosslinked cellulose

Sample No.	C_1	C_4	$C_{2,3,5}$	C_6
Cell	3198	2186, 937	1697, 2349, 2920	2420
$CellX_O$	1269	1502, 737	1641, 2173, 1912	1766

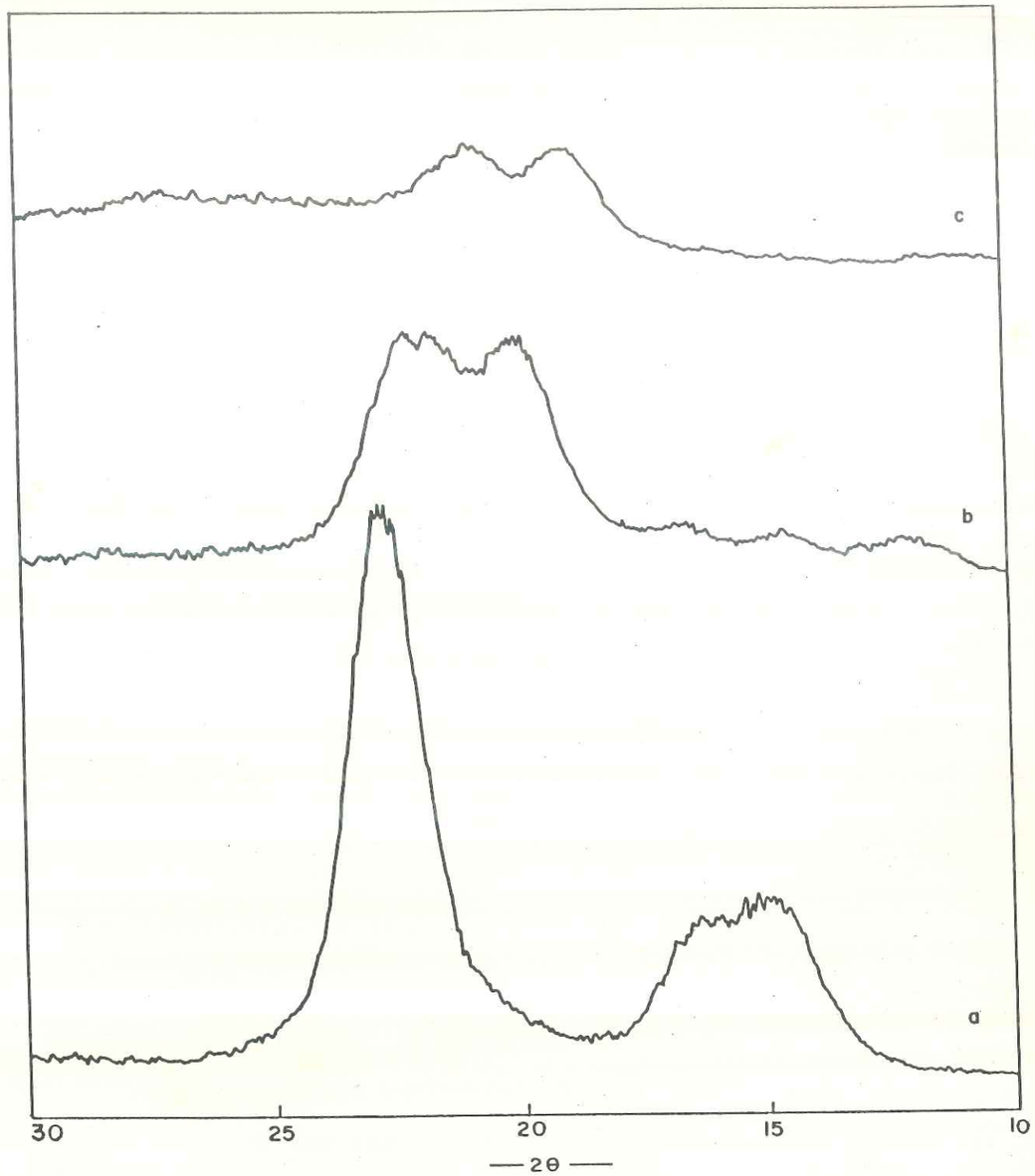

FIG. 7.8 : X-RAY DIFFRACTION PATTERNS OF SAMPLES

a) Cell b) Cell M c) Cell X_0

appears at 62.6 ppm. The peaks are not much broadened though reduction in crystallinity is observed in XRD, in the conversion of cellulose I to cellulose II.

7.3.2c Structure of crosslinked cellulose

^{13}C CP/MAS NMR spectrum of $CellX_0$ is shown in Fig. 7.7c. The assignments of chemical shifts are given in Table 7.4. From the spectra, it is observed that sharp peaks in Cell that are broadened to a small extent in CellM, are further broadened on crosslinking. This can be explained in terms of an increase in the amorphous nature of $CellX_0$ or reduction in crystallinity as observed by X-ray diffractogram (Fig. 7.8c). A comparison of the 112 to 52 ppm region of the ^{13}C CP/MAS spectrum of Cell (broken line) with that of $CellX_0$ is presented in Fig. 7.9 to show the nature of changes in the spectral data on crosslinking. In general a broadening of all the ^{13}C resonances are apparent as evident from the figure.

The broadening of the ring carbons and C_6 carbon is caused by the cleavage of hydrogen bonded double helical structure due to sulphur crosslinks. This is also supported by the T_2 data which showed a reduction on crosslinking. The T_2 calculated for Cell was 2420 μs for the C_6 carbon peak whereas the T_2 of the same carbon peak on crosslinking was 1766 μs. Similar increase in line width was also observed by O'Donnell and Whittaker[29] for ethylene propylene copolymer swollen with $CDCl_3$ after irradiation, where the intensities of the original resonance decreased with increasing radiation dose.

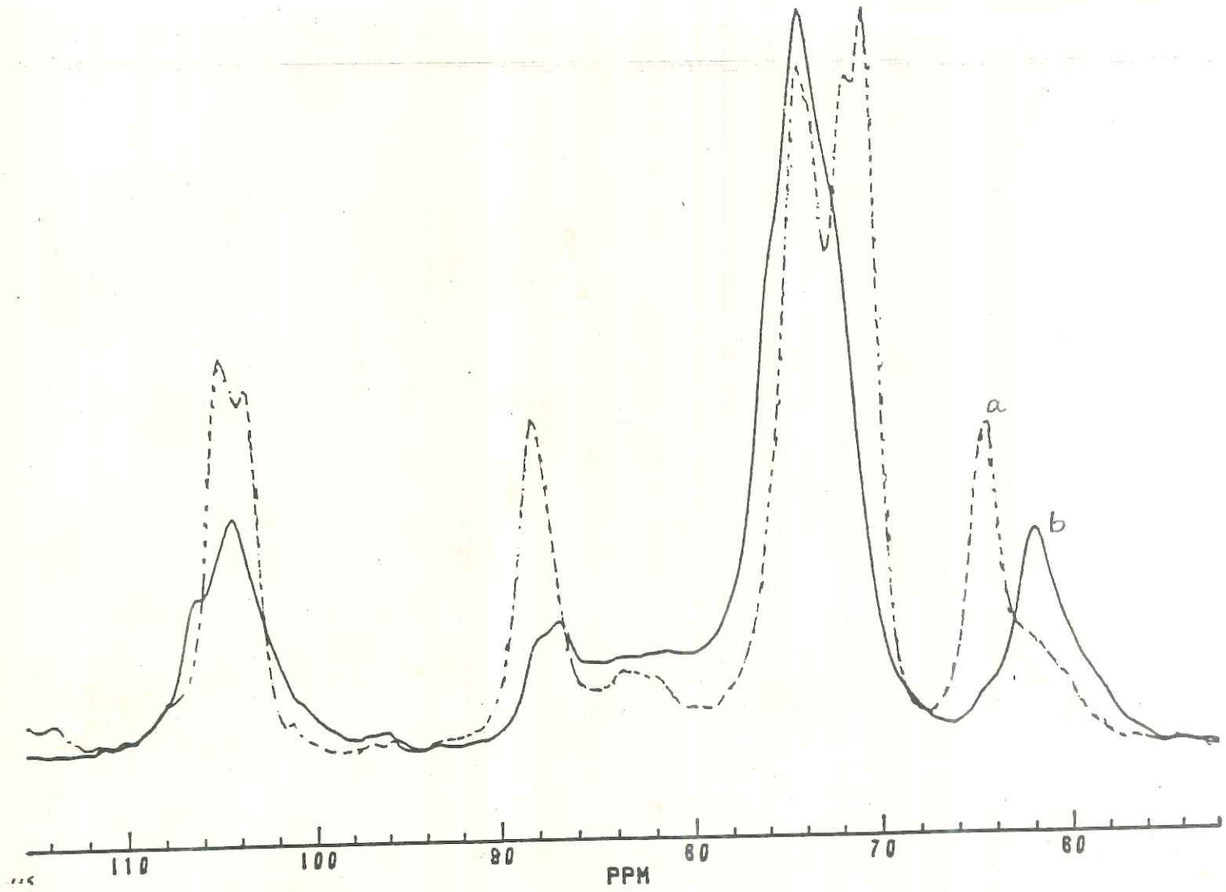

FIG. 7·9 : COMPARISON OF ^{13}C NMR SPECTRA OF SAMPLES a) Cell AND b) Cell X_0
(50 TO 110 PPM REGION EXPANDED)

Thus, line broadening and spin-spin relaxation time unambiguously proves the presence of crosslinking in the polymer which is further supported by XRD data and swelling studies (Chapter III, Section 3.2.3b and 3.2.3c). From the comparison of the NMR spectrum of crosslinked starch and cellulose, (Fig. 7.6 and 7.9), it is noticed that the increase in line width is more pronounced in starch than in cellulose which is also supported by XRD. From the X-ray diffraction pattern (Fig. 7.5 and 7.8) it is observed that on crosslinking, starch is converted completely into an amorphous structure whereas there is some retention of crytallinity or ordered structure on crosslinking of cellulose. This affects the swelling and release of carbofuran from these crosslinked matrices. Though sulphur content and hence crosslink density is more in crosslinked starch than the crosslinked cellulose, the latter shows slower release (Fig. 3.15 in Chapter III) than the former. This is due to the retention of some crystallinity in the crosslinked cellulose.

7.3.3 Structure of carbofuran inside CellX and StX matrices

7.3.3a Analysis of pure and extracted carbofuran

Microanalysis of pure carbofuran (CF) and extracted carbofuran from the CellX and StX matrices (CF-E) showed similar results.

Pure cabofuran (CF)

C : 65.28% (65.19); H : 7.02% (6.79); N: 5.96 (6.33).

Extracted carbofuran (CF-E)

C : 65.38% (65.19); H : 6.88% (6.79); N : 6.16% (6.33).

The ^{1}H NMR spectra of CF and CFE from CellX and StX are shown in Fig. 7.10. The CF-E shows the same NMR spectrum as that of pure carbofuran. The FTIR spectra of CF and CF-E from CellX and StX matrices are shown in Fig. 7.11. Again the CF-E shows the same FTIR spectrum as that of CF.

7.3.3b ^{13}C NMR of pure carbofuran and carbofuran entrapped in CellX and StX matrices

The ^{13}C NMR spectra of carbofuran in solution ($CDCl_3$) and in solid state are illustrated in Fig. 7.12. The assignments of chemical shifts are given in Table 7.6.

The ^{13}C NMR spectrum of $CellX_C$ and StX_C (i.e. cellulose and starch xanthide containing carbofuran, Fig. 7.7d and 7.4d) shows all peaks observed in the blank matrices (i.e. $CellX_0$ and StX_0) and peaks due to carbofuran (Fig. 7.7c, 7.4c, 7.12 and Table 7.7).

Peaks at 28, 30, 43 ppm are due to methyl 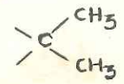 , methyl ($NH-CH_3$) and $-CH_2-$ respectively. Peak at 88 ppm corresponds to quaternary carbon attached to oxygen. Broad multiplets between 120 to 134 ppm are due to aromatic carbons.

Thus, microanalysis, ^{1}H NMR, FTIR and ^{13}C NMR results clearly indicate that the structure of carbofuran is not affected during the process of encapsulation and carbofuran is only physically entrapped in the CellX and StX matrices.

7.3.4 Relationship between NMR measurements and swelling and release kinetics data

In chapter III, we have seen that the water uptake by a

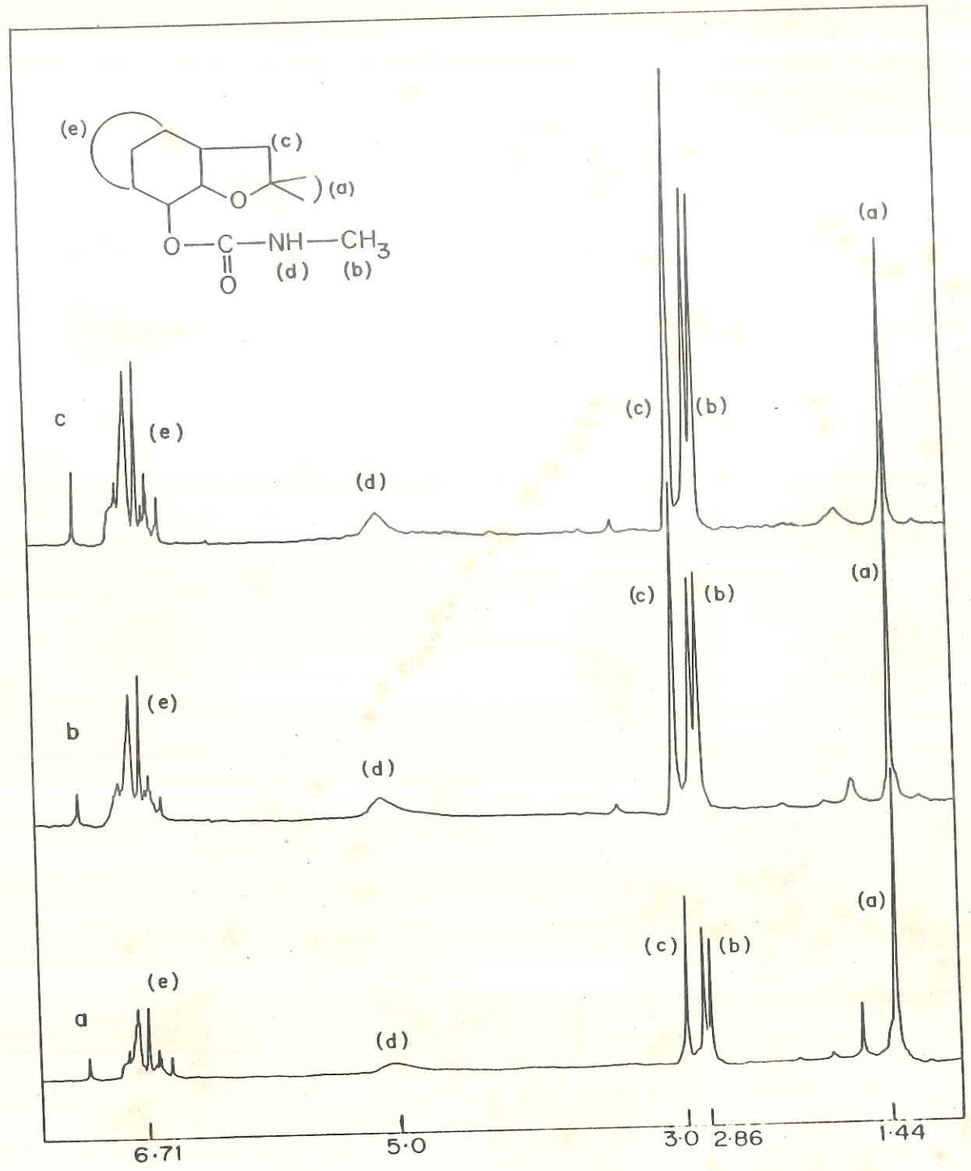

FIGURE 7·10: ^{1}H NMR SPECTRA OF CARBOFURAN (a) AND EXTRACTED CARBOFURAN FROM STARCH (b) AND CELLULOSE (c) MATRICES

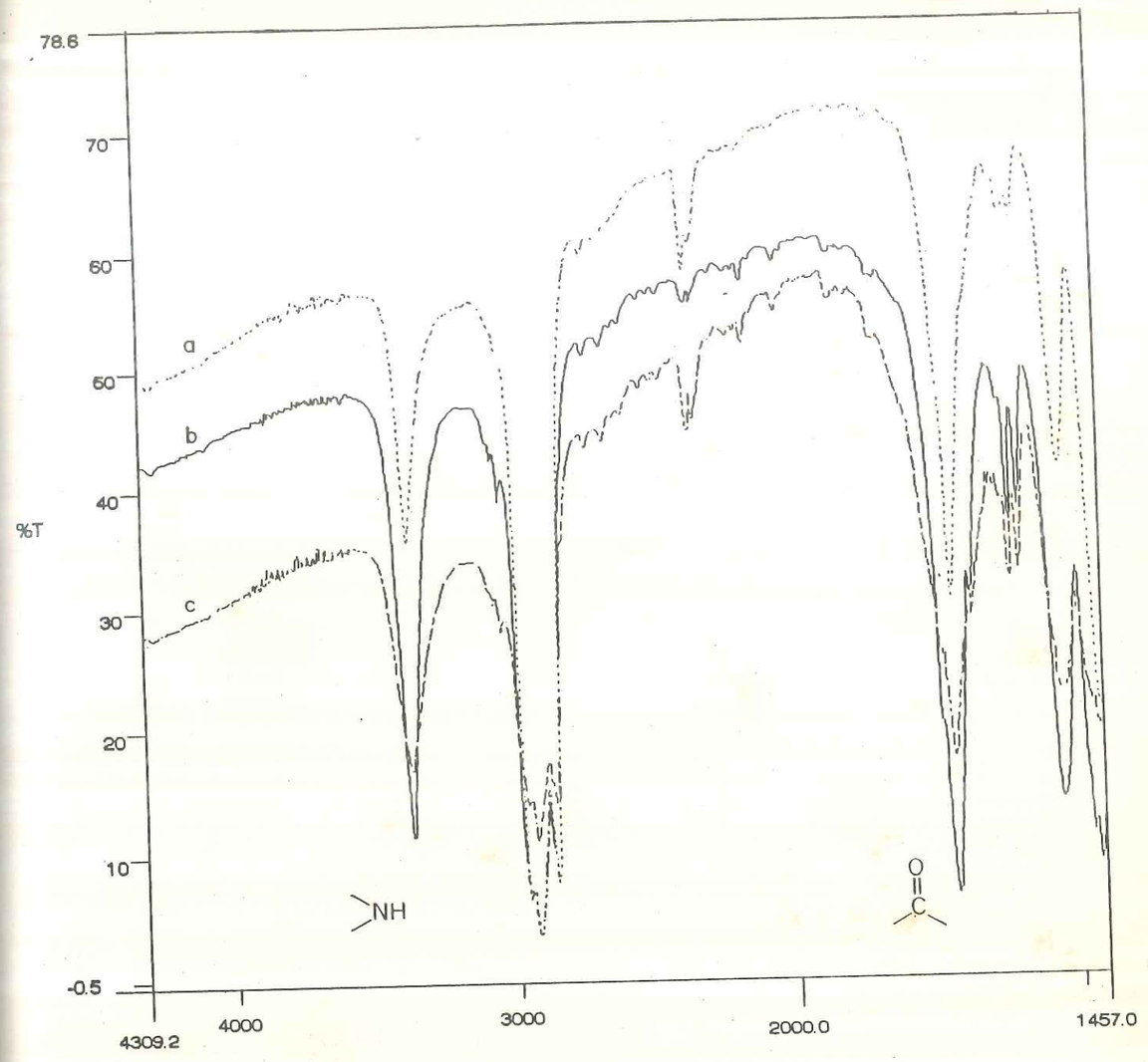

FIG. 7.11 : FTIR SPECTRA OF CARBOFURAN (a) AND EXTRACTED CARBOFURAN FROM CELLULOSE (b) AND STARCH (c) MATRICES.

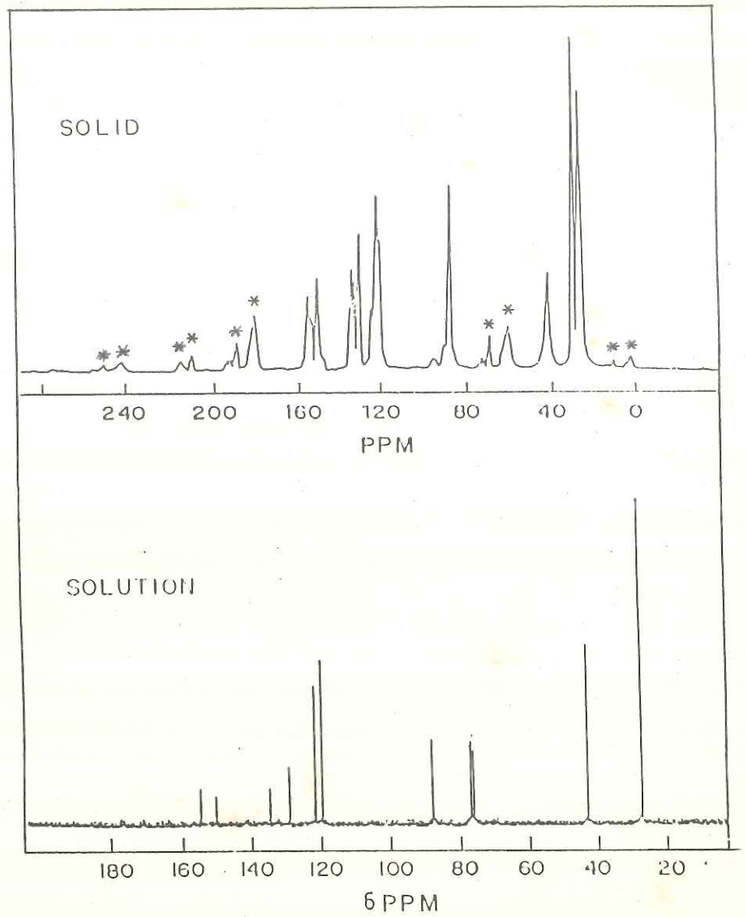

FIG. 7·12 ^{13}C NMR SPECTRA OF CARBOFURAN

* SIDE BAND

Table 7.6

^{13}C NMR chemical shifts of carbofuran in solution and solid state.

Carbon atom (^{13}C) of carbofuran	^{13}C NMR Chemical shifts (ppm)	
	Solution	Solid
$-CH_3$	27.5	28.1
$-NHCH_3$	27.9	30.0
$-CH_2$	42.9	43.1
C-O-(-carbon attached to O)	87.9	87.5
Aromatic carbons		
C-7,5 and C-F	119-122	120-122
C-6,4 and C-F	130-134	132-134
C=O	154	150-154

Table 7.7

^{13}C NMR chemical shifts of $CellX_O$ and StX_O, carbofuran and $CellX_C$ and StX_C (containing carbofuran)

Carbon atoms ^{13}C	^{13}C NMR Chemical shifts (ppm)				
	$CellX_O$	StX_O	Carbofuran	$CellX_C$	StX_C
<u>of Starch/Cellulose</u>					
C_1	104.6	102.1	-	104.4	102.3, 102.6
$C_{2,3,5}$	74.5	72.6	-	74.4	72.7
C_4	87.0	81.2	-	87.2	82.0
C_6	62.3	61.9	-	62.3	61.9, 61.6
<u>of Carbofuran</u>					
CH_3			28.1	27.7	27.8
$NHCH_3$			30.0	30.4	30.4
CH_2			43.1	43.0	43.0
C-O (carbon) attached to O			87.5	88.4	88.5
Aromatic carbons			120-134	122-131	122-131
C=O			150-154	150-155	150-155

glassy polymer and release of an active agent from this polymer can be analyzed by generalized equations :

$(M_t/M\infty)_s = k_s t^n$ and $M_t/M\infty = kt^n$

respectively. In CellX and StX systems, the release of carbofuran is mostly governed by matrix relaxation due to penetration by water. This is also supported by the very fast water uptake followed by a matrix relaxation at a much slower rate as shown by agent release (Fig. 3.15). Release kinetics has proved the mechanism of release to be non Fickian or anomalous to Case II in bulk release, whereas single particle release proved it to be by Super Case II.

Case II mechanism is observed when release of active agent is governed by relaxation of polymer chains at the gel glassy interface.

Thus swelling and release properties of both the matrices are intrinsically related to the molecular motions occurring within a crosslinked polymeric matrix. The number of crosslinks or entanglements affect the molecular motions of the polymer chains considerably and the resulting low frequency, long range motions.

In starch and cellulose xanthide though the crosslink density was expected to be constant at the same level of carbon disulphide, values obtained differed due to the regenerating tendency of cellulose. Thus cellulose had less crosslink density than starch as reflected in the retention of its crystallinity after crosslinking in the former case whereas the latter was

completely amorphous (supported by XRD). This was also noticed from the swelling and release study which can be correlated to the NMR line width and hence to T_2 values. It was indeed seen, by deconvolution of the ^{13}C NMR spectra, that the line width measured for the crosslinked starch was more than that of crosslinked cellulose for the same carbon. For example, the C_6 carbon had a line width of 180.3 Hz and 331.6 Hz for crosslinked cellulose and crosslinked starch, respectively. The effect of this difference was also reflected in the equilibrium swelling studies of these two crosslinked systems. The swelling of starch system was almost double than that of the cellulose system. This results in a slower release of carbofuran from cellulose than from starch (Fig. 3.15, Chapter III). However, n values remain more or less constant for both matrices indicating that the release mechanism was unaffected.

The molecular motions of starch and cellulose carbons as a function of crosslinking were studied by T_2 measurements which clearly showed a reduction as the crosslink density was increased.

7.3.5 Structural characterization of graft copolymers by ^{13}C solid state NMR

7.3.5a Structural characterization of polyacrylamide grafted cellulose (AmgCell)

^{13}C chemical shifts for mercerized cotton pulp and mercerized polyacrylamide grafted cotton pulp (CellM and $AmgCellM_2$) are presented in Table 7.8. It is observed that the

Table 7.8

^{13}C chemical shifts of samples CellM, PAM, $AmgCellM_2$ and Amg $CellX_2$.

Carbon atom	CellM	PAM	$AmgCellM_2$	$AmgCellX_2$
of Cellulose				
C_1	106.6,104.8		105.1	105.0
$C_{2,3,5}$	74.6		74.5	74.5
C_4	87.8, 85.6		88.3	-
C_6	62.6		62.4	62.4
of Polyacrylamide				
$-CH_2$		41.6	37.9	36.7
-CH-		-	44.3	43.0
$-CO-NH_2$		179.6	-	179.0
$-COO^-$		-	183.5	183.5

Table 7.9

^{13}C Chemical shift of samples $AmgCellX_2$ and CF for carbofuan carbon

Carbon atom	Pure carbofuran	$AmgCellX_2$
CH_3	28.1	28.0
$NHCH_3$	30.0	30.6
$-CH_2-$	43.1	43.2
-C-O	87.5	88.1
Aromatic carbon	120-134	122-135
C=O	150-154	150-155

difference in chemical shift is not apparent as the density of grafting is small. In other words, the intensities of the signals of the anhydroglucose units where the polyacrylamide is grafted, are too weak to be differentiated from the noise level. Thus, C_1 peak appeared at 106.6 and 104.8 ppm in CellM whereas C_1 of $AmgCellM_2$ appeared at 105.1 ppm and carbon $C_{2,3,5}$, C_4 and C_6 were not much differing in chemical shift.

Comparison of ^{13}C NMR spectra of PAM with that of $AmgCellM_2$ is shown in Fig. 7.13a and c. PAM spectrum shows peak corresponding to methylene, methine and amide carbon. Peak at 25 to 50 ppm corresponds to methylene and methine carbon whereas peak at 179.6 corresponds to amide carbon. ^{13}C NMR of $AmgCellM_2$ shows peak for methylene and methine carbon at 37.9 and 44.3 ppm. The amide carbon observed at 179.6 ppm in PAM is in the range of 177 to 190 ppm in $AmgCellM_2$, corresponding to both amide and acid peak. On treatment of AmgCell with NaOH in the mercerization step, the polyacrylamide branches are likely to get hydrolyzed to polyacrylic acid. The peak obtained at 183.5 corresponds to the one expected for poly(sodium acrylate) as the sample used for NMR study was obtained by washing with water till alkali free after mercerization and drying.

Further comparison of these two spectra with $AmgCellX_2$ (crosslinked cellulose grafted with acrylamide containing carbofuran) showed two peaks in the carbonyl region, one corresponding to amide CO from polyacrylamide at 179.9 ppm and

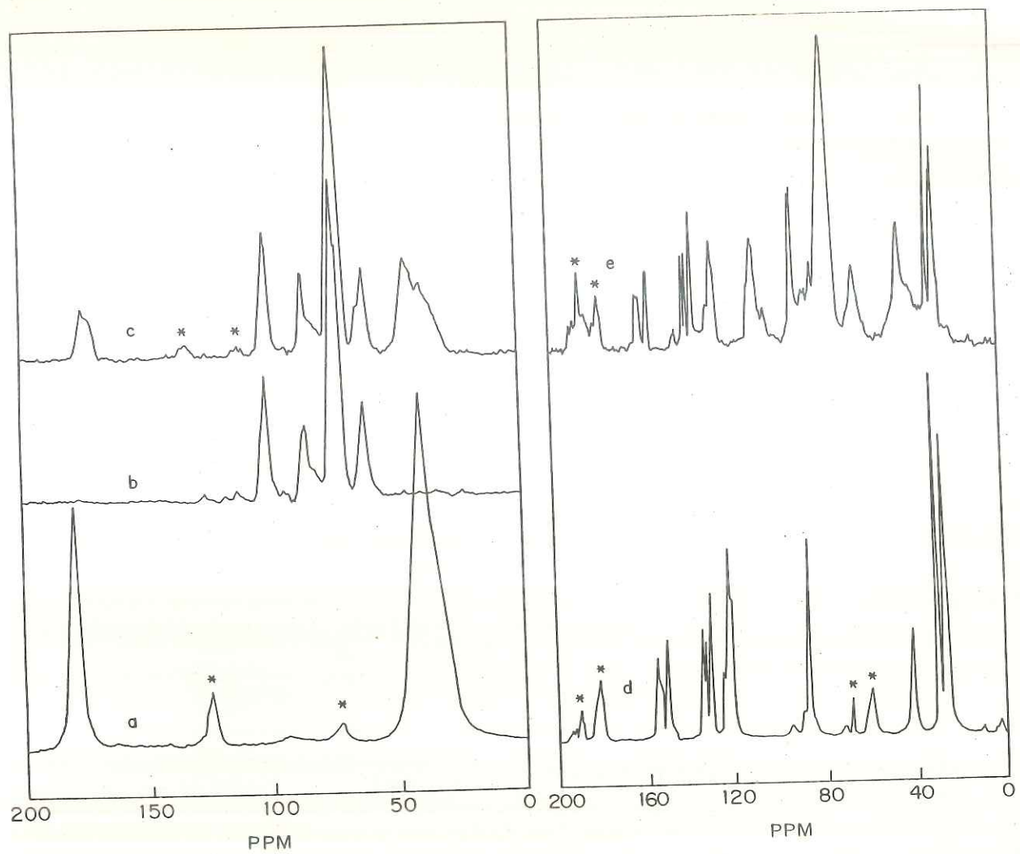

FIG. 7·13 : ^{13}C CP/MAS NMR SPECTRA OF SAMPLES (a) PAM , (b) Cell M , (c) AmgCellM_2, (d) CARBOFURAN , (e) AmgCellX_2

* SIDE BANDS

the other corresponding to acidic group, $COO^{-}Na^{+}$ formed during mercerization at 183.5 ppm (Table 7.8, Fig. 7.13c). Thus ^{13}C NMR provides a structural characterization for the grafted polyacrylamide chains on to cellulose backbone, which is also supported by FTIR, where reduction in absorption intensity due to grafting was observed (Chapter VI, Section 6.7.2d) and by DTA study (Chapter VI, Section 6.7.2e).

7.3.5b Structure of carbofuran inside the encapsulating matrix (AmgCellX)

The chemical shifts corresponding to pure carbofuran (CF) are compared to that of chemical shifts of carbofuran entrapped in the graft copolymer xanthide, $AmgCellX_2$. It is observed from Table 7.9 that the chemical shifts for the entrapped carbofuran are exactly matching with that of pure carbofuran, which provides a proof for the physical trapping of carbofuran inside graft copolymer xanthide matrix.

7.3.5c Structural characterization of styrene grafted cellulose

The ^{13}C chemical shifts for CellM, polystyrene (Pst) and mercerized styrene grafted cellulose ($SgCellM_7$, $SgCellM_{11}$ and $SgCellM_{10}$) are presented in Table 7.10. Comparison of ring carbons of CellM with SgCellM shows that chemical shift of carbons C_1, C_4 and $C_{2,3,5}$ are almost same in CellM and SgCellM. C_6 peak of CellM is found to be deshielded in SgCellM.

Comparison of ^{13}C chemical shifts of Pst with SgCellM shows that all peaks corresponding to Pst are observed in SgCellM (Table 7.10 and Fig. 7.14).

Table 7.10

^{13}C NMR chemical shifts of samples CellM, $SgCellM_7$, $SgCellM_{11}$, $SgCellM_{10}$ and Pst.

Carbon atom	CellM	Pst	$SgCellM_7$	$SgCellM_{11}$	$SgCellM_{10}$
of Cellulose					
C_1	106.7 104.8	- -	105.1 104.8	105.1 103.9	105.5 104.1
$C_{2,3,5}$	74.6	-	74.5	74.3 71.2	74.8 71.4
C_4	87.8 85.6	- -	88.7 -	88.5 -	88.6 -
C_6	62.6	-	65.2	64.9	65.2
of Styrene					
$-CH_2/CH$	-	41.7	41.0	40.0	40.4
Epso carbon	-	147.1	144.9	146.4	146.0
Aromatic		128.0	127.5	126.0	128.0

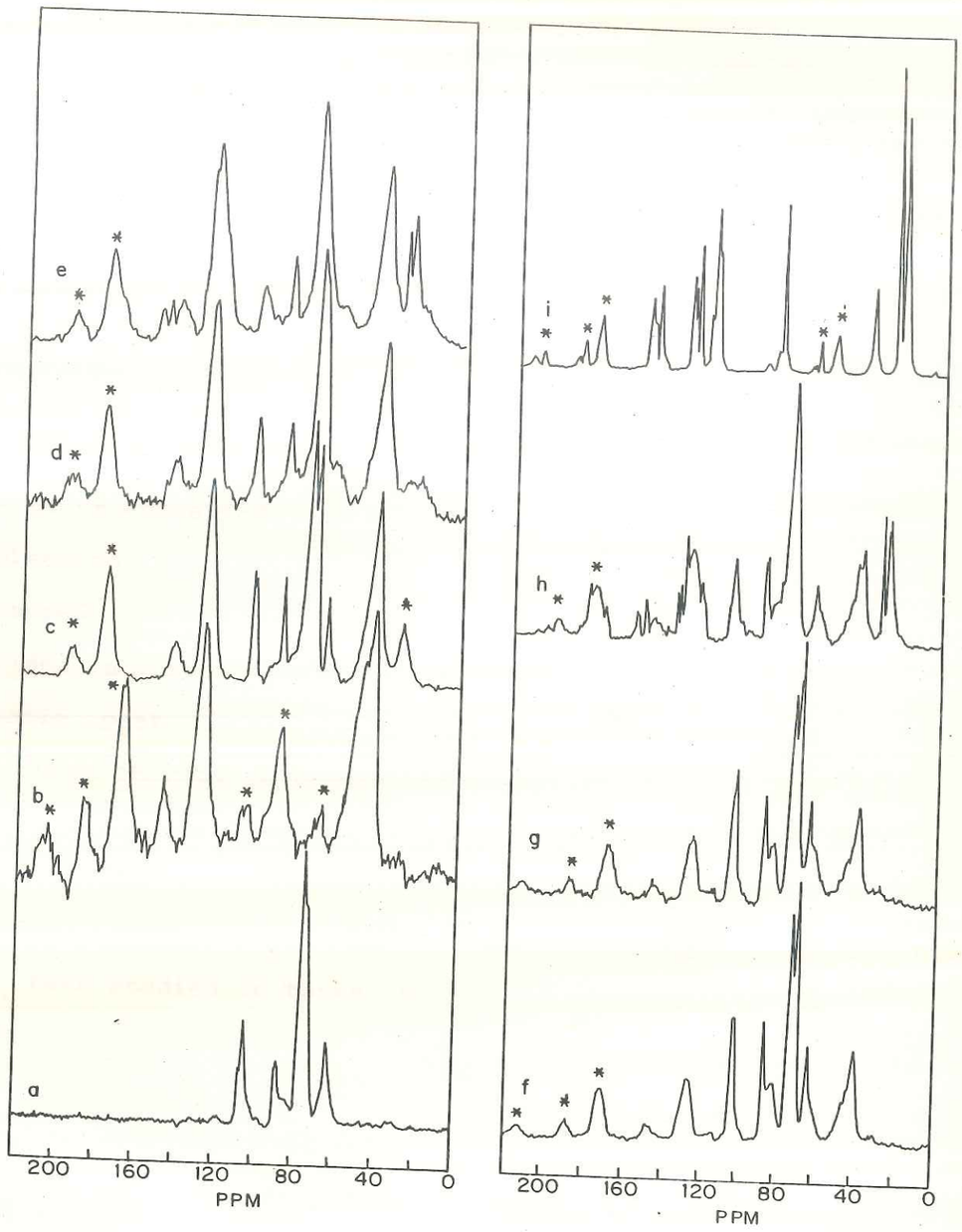

FIG. 7·14 : ^{13}C NMR SPECTRA OF THE SAMPLES
a) Cell M , b) Pst , c) $SgCell_7$, d) $SgCellM_7$, e) $SgCellX_7$,
f) $SgCell_{11}$, g) $SgCellM_{11}$, h) $SgCellX_{11}$, i) CARBOFURAN.
* SIDE BANDS

Thus, solid state ^{13}C NMR spectra confirms presence of polystyrene grafts on cellulose backbone which is again supported by DTA study and by FTIR wherein a reduction in absorption intensity was noticed (Chapter VI, Section 6.4.4d and 6.4.4c respectively).

7.3.5d Structure of carbofuran inside encapsulating matrix (SgCellX)

The chemical shifts corresponding to CF were compared to that of CF entrapped in the graft copolymer xanthide SgCellX. It is observed from the Table 7.11 that the chemical shifts for the entrapped carbofuran are exactly matching with that of CF which provides a proof for the physical trapping of carbofuran. Aromatic peak of styrene is merged into the aromatic peak of carbofuran thereby increasing the complex nature of the aromatic region of the spectrum.

7.4 CONCLUSIONS

^{13}C CP/MAS NMR spectra of crosslinked starch and cellulose have been studied in terms of chemical shift displacement, line width and T_2 measurements. Pure starch loses its crystallinity and is converted to completely amorphous structure upon gelatinization and crosslinking which is evidenced by the disappearance of multiplicity of anomeric carbon of starch, increase in line width of ring carbons and C_6 carbon and also by reduction in spin-spin relaxation time, T_2. Cellulose retains, parts of its crystallinity upon mercerization and crosslinking as seen by the disappearance of C_1 multiplicities. However, the

Table 7.11

^{13}C chemcial shift of pure carbofuran and that enclosed in graft copolymer (SgCellX).

Carbon atom ^{13}C	^{13}C Chemical shift (ppm)		
	Pure Carbofuran	$SgCellX_7$	$SgCellX_{11}$
CH_3	28.1	27.4	28.0
$NHCH_3$	30.0	30.5	30.5
$-CH_2-$	43.1	41.0	42.6
-C-O	87.5	88.6	88.9
Quaternary carbon attached to O.			
Aromatic carbon	120-134	127.9	122-135
-C=O	150-154	150-155	150-156

broadening of peaks after crosslinking (increase in line width and reduction in T_2) is less than that of starch, supported by XRD, swelling and release kinetics.

Equilibrium swelling is more than double in starch than that of cellulose due to complete conversion to amorphous structure. Release of carbofuran from these matrices is governed by relaxation of polymeric chains which are hindered due to crosslinking.

In the process of encapsulation, carbofuran does not undergo any chemical reaction but gets physically entrapped.

^{13}C CP/MAS NMR spectra of crosslinked graft copolymers of cellulose have been studied in terms of chemical shifts which prove the presence of polyacrylamide and polystyrene structures in the graft copolymers.

Comparison of spectra of carbofuran with spectra of carbofuran encapsulated within crosslinked starch, cellulose and crosslinked graft copolymers of cellulose show that carbofuran does not undergo any chemical reaction but gets physically entrapped.

REFRRENCES

1. High Resolution NMR Spectroscopy of Synthetic Polymers in Bulk, VCH Publishers. Deerfield, F.L. Komoroski (Ed) (1986).
2. Characterization of Highly Crosslinked Polymers, ACS Symp. Ser. 243, ACS, Washington, D.C., Labana, S.S. and Dickie, R.A. (Eds) (1984).
3. Harrison, D.J.P., Yates, W.R. and Johnson, J.F., J.Macromol. Chem. Phys., C 25(4) (1985) 481-549.
4. Andreis, M. and Koenig, J.L., Adv. Polym. Sci., 70 (1989) 69.
5. Gutowsky, H.S., Saika, A., Takeda, M. and Woessmer, D.E., J. Chem. Phys., 27 (1957) 534-542.
6. Patterson, D.J. and Koenig, J.L., Ref. 2, pp 211-230.
7. Cholli, A. and Ritchey, W.M., Ref. 2, pp 233-238.
8. Sefcik, M.D., Stejskal, E.O., Mckay, R.A. and Schaefer, J., Macromolecules, 12 (1979) 423-425.
9. Ford, W.T. and Balakrishnan, T., Macromol., 14 (1981) 284-288.
10. Charlesby, A.& Folland, R., Polymer, 20 (1979) 211-214.
11. Wu, H.C.H. and Sarko, A., Carbohydr. Res., 61 (1978) 7-25.
12. Imberty, A., Chanzy, H. and Perez, S., J. Mol. Biol., 201 (1988) 365-378.
13. Imberty, A. and Perez, S., Biopolymers, 27 (1988) 1205-1221.
14. Horii, F., Yamamoto, H., Hirai, A. and Kitamaru, R., Carbohydr. Res. 160 (1987) 29-40.

15. Parfondry, A. and Perlin, A.S., Carbohydr. Res., 57 (1977) 39-49.

16. Gidley, M.J., and Bociek, S.M., J. Am. Chem. Soc., 107 (1985) 7040-7044.

17. Isogai, A., Usuda, M., Kato, T., Uryu, T. and Atalla, R.H., Macromolecules, 22 (1989) 3168-3172.

18. Simon, I., Glaser, L., Scheraga, H.A. and John Manley, R. St., Macromolecules, 21 (1988) 990-918.

19. Fyfe, C.A., Dudley, R.L., Stephenson, P.J., Deslandes, Y., Hamer, G.K. and Marchessault, R.H., J.Macromol.Sci., -Rev. Macromol. Chem. Phys., C 23(2) (1983) 187-216.

20. Earl, W.L. and VanderHart, D.L., Macromolecules, 14 (1981) 570-574.

21. Horii, F., Hirai, A. and Kitamaru, R., Macromolecules, 20 (1987) 2117-2120.

22. VanderHart, D.L. and Atalla, R.H., Macromolecules, 17 (1984) 1465-1472.

23. Dudley, R.L., Fyfe, C.A., Stephenson, P.J., Deslandes, Y., Hamer, G.K. and Marchessault, R.H., J. Am. Chem. Soc., 105 (1983) 2469-2472.

24. Dais, P. and Perlin, A.S., Carbohydr. Res., 100 (1982) 103-116.

25. O'Donnell, D.J., Ackerman, J.J.H. and Maciel, G.E., J. Agric. Food Chem., 29 (1981) 514.

26. Shukla, P.G., Sivaram, S. and Mohanty, B., Macromolecules, 25 (1992) 2746-2751.

27. Atalla, R.H., Gast, J.C., Sindorf, D.W., Bartuska, V.J., and Maciel, G.E., J. Am. Chem. Soc., 102 (1980) 3249-3251.

28. Earl, W.L. and VanderHart, D.L., J. Am. Chem. Soc., 102 (1980) 3251.

29. O'Donnell, J.H. and Whittaker, A.K., Brit. Polym. J., 17 (1985) 51.

ABSTRACT

A novel encapsulating matrix for pesticides, based on cheap, readily available, biodegradable natural polymer, cellulose, was studied during this investigation. Carbofuran, a broad spectrum carbamate pesticide was chosen as a candidate for encapsulation. Granular encapsulated carbofuran formulations were prepared using crosslinked cellulose (cellulose xanthide) and compared with starch xanthide which is already known as an encapsulating matrix. Effect of the matrix parameters, such as crosslink density, loading level, porosity etc., on the swelling of the matrix and release of carbofuran was studied for both the matrices. The release kinetics was found to conform to "Swelling Controlled Release System" and the data were interpreted in terms of the generalized equation $M_t/M_\infty = kt^n$. Both the matrices (cellulose and starch) showed inverse relationship between rate of release and loading level. However, in case of starch at higher loading level (beyond 20%) it was reversed due to increase in porosity. This was confirmed by studying release rates by changing the eluting medium so as to change the solubility of carbofuran in it. A novel single particle release measurement was carried out to understand the exact release mechaniem, as ensemble kinetics is inconclusive. Thus, the mechanism of transport was established to be case II.

Similarly, matrix parameters like polymer composition, molecular weight and crystallinity which affect the swelling of the matrix and release of carbofuran were studied by preparation of CRF of carbofuran using cellulose from different sources and

agricultural wastes.

The influence of physical state and solubility of encapsulant on the rate and mechanism of release and swelling of the crosslinked cellulose matrix was studied by encapsulating model organic compounds. Solid agents exhibited much faster release than the liquids of comparable solubilities. Model compounds with the highest solubility exhibited Fickian mechanism whereas model compounds with lower solubilities exhibited anomalous to Super Case II release pattern. The more hydrophobic liquids showed Super Case II release profiles which could be due to forming of hydrophobic film barrier, which controls the release rate. The more hydrophilic liquid however, had an anomalous-Case II release profile. Thus the release mechanism seemed to be governed by many factors such as the diffusion coefficient of the agent in the swollen matrix, the active agent-polymer interactions, the partition coefficient of the agent between the swollen matrix and the eluting medium, their relative size vis a vis the macromolecular mesh etc. These factors to a certain extent are influenced by physical state and solubility of the agent.

Modification of the physical properties of the cellulose matrix was carried out by grafting hydrophobic and hydrophilic polymeric chains on to cellulose backbone. Thus polystyrene and polyacrylamide graft-copolymer of cellulose of varying grafting frequency were prepared and their effect on swelling and release of carbofuran was studied. Grafting frequency was found to be the deciding factor which affected the swelling and release of

carbofuran. Interestingly both the hydrophobic polystyrene and the hydrophilic polyacrylamide grafts tended to enhance the agent release though for different reasons.

The release study carried out for the CRF of carbofuran prepared so far, exhibited that, though the release rate is changed, the release mechanism remained the same.

Structural characterization of the crosslinked starch, cellulose and graft-copolymers of cellulose was carried out through ^{13}C CP/MAS NMR spectroscopy. Line width and spin-spin relaxation data (T_2) proved the crosslinked structure of cellulose xanthide and starch xanthide. This was supported by XRD where reduction in crystallinity of cellulose and complete conversion to amorphous structure in starch on crosslinking was observed. Characterization of the graft-copolymers of cellulose was studied by ^{13}C CP/MAS NMR, FTIR and DTA. ^{13}C CP/MAS shows signals corresponding to grafted polymer (polystyrene and polyacrylamide) whereas FTIR and DTA provide proof of grafting for the graft-copolymers.

LIST OF PUBLICATIONS

1. Cellulose xanthide (CellX) as an encapsulating matrix I. comparison with starch xanthide (StX) on swelling and release properties.

   A.N. Bote, N. Rajagopalan and V.M. Nadkarni,
   J.Contr.Release (1993) (Communicated).

2. Study of polymer crystallinity and composition in connection with swelling and release of carbofuran from CRF prepared using cellulose from different sources and agricultural waste.

   A.N. Bote, N. Rajagopalan, P.G. Sharma and V.M. Nadkarni,
   J. Appl. Polym. Sci. (1993) (to be communicated).

3. Influence of solubility and physical state of encapsulant on rate and mechanism of release from swellable cellulose xanthide matrix.

   A.N. Bote, N. Rajagopalan and V.M. Nadkarni,
   Int. J. of Pharmaecutics, (1993) (to be communicated).